

Electronic Theses and Dissertations, 2004-2019

2014

A Continuous Hydrologic Model Structure for Applications at Multiple Time Scales

Jonathan Griffen
University of Central Florida

 Part of the [Engineering Commons](#), and the [Water Resource Management Commons](#)
Find similar works at: <https://stars.library.ucf.edu/etd>
University of Central Florida Libraries <http://library.ucf.edu>

This Masters Thesis (Open Access) is brought to you for free and open access by STARS. It has been accepted for inclusion in Electronic Theses and Dissertations, 2004-2019 by an authorized administrator of STARS. For more information, please contact STARS@ucf.edu.

STARS Citation

Griffen, Jonathan, "A Continuous Hydrologic Model Structure for Applications at Multiple Time Scales" (2014). *Electronic Theses and Dissertations, 2004-2019*. 4504.
<https://stars.library.ucf.edu/etd/4504>

A CONTINUOUS HYDROLOGIC MODEL STRUCTURE FOR APPLICATIONS AT
MULTIPLE TIME SCALES

by

JONATHAN GRIFFEN
B.S. University of Central Florida, 2012

A thesis submitted in partial fulfillment of the requirements
for the degree of Master of Science
in the Department of Civil, Environmental, and Construction Engineering
in the College of Engineering and Computer Science
at the University of Central Florida
Orlando, Florida

Spring Term
2014

Major Professor: Dingbao Wang

© 2014 Jonathan Griffen

ABSTRACT

There are many different controlling factors on the partitioning of rainfall into runoff. However, the influence of each of these controls varies across different temporal scales. Consequently, numerous water balance models have been developed in the literature for application across various time scales. These models are usually developed for a particular time scale so that the controls with the greatest influence on rainfall partitioning are captured. For example, the SCS curve number method was developed to simulate direct runoff at the event scale; the “abcd” model was developed as a monthly water balance model; and the Budyko model was developed for long-term water balance. More recently, the proportionality hypothesis, which traces its origins from the SCS curve number method, has been identified as the commonality between these three hydrologic models, suggesting that this hypothesis may be the unifying principle of hydrologic models across various time scales.

The objective of this thesis is to develop a conceptual hydrologic model structure for continuous simulations for multiple time scales. The developed model is applicable to daily, monthly, and annual time scales.

Direct runoff is computed by a proportionality relationship in the SCS curve number method. In the “abcd” model, evapotranspiration and storage at the end of each time period are computed by a proportionality relationship, however evapotranspiration is computed based on an exponential relationship of storage and potential evapotranspiration while base flow is computed

based on a linear reservoir model. In the Budyko model, runoff and evapotranspiration are computed by a proportionality relationship.

The primary difference with the proposed model in this thesis in comparison with the other three water balance models is the application of the proportionality hypothesis to the partitioning of surface runoff and continuing abstraction as well as the partitioning of continuing evapotranspiration and subsurface flow.

The proposed model structure is implemented in Matlab. The developed model includes six parameters, which are estimated for 71 case study catchments in the United States using a genetic algorithm. The model performances at the daily, monthly and annual time scales are evaluated during calibration and validation periods, and compared with the “abcd” model and a Budyko-type model developed for multiple time scales.

Evaluation of the models shows that the proposed model performs better or comparable to the other models at all time scales.

I dedicate this thesis to my family.

ACKNOWLEDGMENTS

I want to thank my advisor, Dr. Dingbao Wang for the incredible support he has given throughout the development of this thesis. I have really benefited from the time spent working with him and have learned so much.

I also want to thank Dr. Stephen Medeiros and Dr. Andrew O'Reilly for serving on my thesis committee and for their insightful comments that have helped improved the quality of this thesis.

TABLE OF CONTENTS

LIST OF FIGURES	xiii
LIST OF TABLES	xxi
CHAPTER 1: INTRODUCTION.....	1
1.1 The Proportionality Hypothesis	5
1.2 The Hydrologic Cycle and Hydrologic Processes.....	6
CHAPTER 2: LITERATURE REVIEW	9
2.1 Introduction	9
2.1.1 History of Water Balance Models.....	10
2.1.2 Water Balance Modeling Methods	13
2.1.3 Number of Parameters	14
2.2 Summary of Models	15
2.2.1 Climate and Model Performance	16
2.3 Thornthwaite and Mather Model.....	17
2.3.1 $T\alpha$ Variant of the Thornthwaite and Mather Model	19
2.4 Palmer Model	21
2.5 Thomas “abcd” Model	23

2.5.1	Abcd-type Budyko model	26
2.6	SCS Curve Number Method	27
2.7	SWB Model.....	29
2.8	Vandewiele Model	33
2.9	GR2M Model	36
2.10	Dynamic Water Balance Model	39
2.11	Equity Model	44
CHAPTER 3: METHODOLOGY		47
3.1	Data	47
3.1.1	MOPEX Data Set.....	47
3.1.2	Evapotranspiration and Potential Evapotranspiration Data Set	51
3.2	Test Statistics (Performance Metrics)	53
3.3	Optimization Methodology	54
3.4	Problems Encountered in Hydrologic Modeling.....	55
3.4.1	Effect of Temporal Lumping on Data Quality.....	55
3.4.2	Regional Groundwater Flow	57
3.4.3	Saturation Excess vs. Infiltration Excess	58
3.4.4	Fluctuating Groundwater Table	58

3.5	Model Calibration and Validation.....	59
3.5.1	Model Assumptions	61
3.6	Development of the Proposed Model.....	61
3.6.1	Initial Model Stage.....	62
3.6.2	Correcting the Second Proportionality Relationship	66
3.6.3	Modifications to the Expression of Evapotranspiration.....	72
3.6.4	Modifications of Subsurface Runoff and Evapotranspiration Processes	77
3.6.5	Additional Model Structure Changes.....	84
3.6.6	Modifications to Model 14.....	90
3.6.7	Model Selection	94
3.6.8	Model 21	96
3.6.9	Final Model (Proposed Model).....	98
CHAPTER 4: RESULTS AND DISCUSSION.....		111
4.1	Analysis of the Proposed Model Parameters.....	112
4.2	Analysis of the Proposed Model at One Catchment in Florida.....	120
4.2.1	Modeled vs. Actual Evapotranspiration.....	123
4.2.2	Initial and Continuing Evapotranspiration.....	126
4.2.3	Runoff Processes.....	130

4.2.4	Simulated vs. Observed Runoff	135
4.2.5	Soil Moisture Levels	140
4.3	Summary of Model Performance for the Proposed Model	144
4.4	Comparison between Models	147
4.4.1	Full-Record Calibration Results	150
4.4.2	Half-Record Calibration Results.....	156
4.4.3	Validation Results.....	162
4.5	Second Model Calibration and Validation Method.....	168
4.5.1	Half-Record Calibration Results (Second Calibration Method).....	170
4.5.2	Validation Results (Second Calibration Method).....	176
4.6	Additional Discussion	182
CHAPTER 5: SUMMARY AND CONCLUSIONS		183
CHAPTER 6: ADDITIONAL DISCUSSION.....		194
6.1	Six Poorly Performing Catchments.....	194
6.2	The Equity Equation vs. the “abcd” Model.....	204
APPENDIX A: PERFORMANCE RESULTS FOR EACH CATCHMENT		206
A.1	Full-Record Calibration Results for Each Catchment.....	207
A.1.1	Daily Time Scale.....	207

A.1.2	Monthly Time Scale.....	210
A.1.3	Annual Time Scale.....	213
A.2	Calibration and Validation Results for Each Catchment	216
A.2.1	Daily Time Scale.....	216
A.2.2	Monthly Time Scale.....	219
A.2.3	Annual Time Scale.....	222
A.3	Second Calibration and Validation Results for Each Catchment.....	225
A.3.1	Daily Time Scale.....	225
A.3.2	Monthly Time Scale.....	228
A.3.3	Annual Time Scale.....	231
APPENDIX B: MATLAB CODE FOR CALIBRATION AND VALIDATION.....		234
B.1	Master Script for Calibration	238
B.2	Model Function for the abcd Model (First Calibration Method).....	241
B.3	Model Function for the abcd Model (Second Calibration Method).....	244
B.4	Master Script for Validation (First Calibration Method)	247
B.5	Master Script for Validation (Second Calibration Method).....	255
B.6	Script for the abcd Model (Validation based on the First Calibration Method)	263
B.7	Script for the abcd Model (Validation based on the Second Calibration Method).....	265

REFERENCES 267

LIST OF FIGURES

Figure 2.1. Thornthwaite and Mather Model.....	19
Figure 2.2. $T\alpha$ -variant of the Thornthwaite and Mather Model.	20
Figure 2.3. Palmer Model.	22
Figure 2.4. Thomas (1981) abcd Model.....	26
Figure 2.5. Model of the Curve Number Method.	29
Figure 2.6. SWB Model.	33
Figure 2.7. Vandewiele Model.....	36
Figure 2.8. GR2M Model.....	39
Figure 2.9. Dynamic Water Balance (DWB) Model.	44
Figure 2.10. The Equity Model.....	46
Figure 3.1. Selected Catchments for Analysis of the Proposed Model Structure.....	50
Figure 3.2. Aridity Index ($Ep/P - \Delta S$) for 71 MOPEX catchments.....	51
Figure 3.3. Catchment 07261000.....	57
Figure 3.4. Initial Model Structure of the Proposed Model.....	65
Figure 3.5. MOPEX catchment in Pennsylvania (01574000) used for testing the initial model structures.	72
Figure 3.6. Four MOPEX watersheds chosen for initial model evaluation.	74
Figure 3.7. NSE for Models 2 through 15.	83
Figure 3.8. NSE Values from the Best Models Illustrated in Figure 3.7.....	84

Figure 3.9. Model 16.....	85
Figure 3.10. Model 17.....	87
Figure 3.11. Performance of Models 14, 16, 17, and 19.....	90
Figure 3.12. Performance of Model 14 Variations for 55 Catchments.....	93
Figure 3.13. Performance of Model 14 and 19 Variations.	96
Figure 3.14. Stage 1 of the Final Model Structure.....	99
Figure 3.15. Stage 2 of the Final Model Structure.....	101
Figure 3.16. Stage 3 of the Final Model Structure.....	103
Figure 3.17. Stage 4 of the Final Model Structure.....	105
Figure 3.18. Stage 5 of the Final Model Structure.....	106
Figure 3.19. Stage 6 of the Final Model Structure.....	107
Figure 3.20. Stage 7 of the Final Model Structure.....	109
Figure 3.21. Final Model Structure.....	110
Figure 4.1. Relationships between the Maximum Capacity of the First Soil Moisture Reservoir, $S1_{max}$, of the Proposed Model at Different Time Scales for the Full-Record Calibration Stage.	114
Figure 4.2. Relationships between the Maximum Capacity of the Second Soil Moisture Reservoir, $S2_{max}$, of the Proposed Model at Different Time Scales for the Full-Record Calibration Stage.....	115
Figure 4.3. Relationships between Parameter $k1$ of the Proposed Model at Different Time Scales for the Full-Record Calibration Stage.....	116

Figure 4.4. Relationships between Parameter k_2 of the Proposed Model at Different Time Scales for the Full-Record Calibration Stage.....	117
Figure 4.5. Relationships between Parameter k_3 of the Proposed Model at Different Time Scales for the Full-Record Calibration Stage.....	119
Figure 4.6. Relationships between Parameter k_5 of the Proposed Model at Different Time Scales for the Full-Record Calibration Stage.....	120
Figure 4.7. Topographic Map of Florida MOPEX Catchment (02296750).	122
Figure 4.8. Modeled Daily Evapotranspiration vs. Observed Daily Evapotranspiration from 1/25/1983 to 12/31/2003 at the Florida Catchment.	124
Figure 4.9. Modeled Monthly Evapotranspiration vs. Observed Monthly Evapotranspiration from 1/1985 to 12/2003 at the Florida Catchment.....	125
Figure 4.10. Modeled Annual Evapotranspiration vs. Observed Annual Evapotranspiration from 1/1/1983 to 12/31/2003 at the Florida Catchment.	126
Figure 4.11. Modeled Daily Initial Evapotranspiration and Continuing Evapotranspiration for 1994 at the Florida Catchment.....	128
Figure 4.12. Modeled Monthly Initial Evapotranspiration and Continuing Evapotranspiration for 1994 through 1995 at the Florida Catchment.	129
Figure 4.13. Modeled Annual Initial Evapotranspiration and Continuing Evapotranspiration for 1986 through 2003 at the Florida Catchment.	130
Figure 4.14. Time Series of Daily Surface Runoff, Interflow, and Baseflow during 1994 for the Florida Catchment.....	133

Figure 4.15. Time Series of Monthly Surface Runoff, Interflow, and Baseflow from 1994 to 1995 for the Florida Catchment.	134
Figure 4.16. Time Series of Annual Surface Runoff, Interflow, and Baseflow from 1986 to 2003 for the Florida Catchment.	135
Figure 4.17. Daily Observed Runoff and Modeled Runoff for the Proposed Model at the Florida Catchment.	137
Figure 4.18. Monthly Observed Runoff and Modeled Runoff for the Proposed Model at the Florida Catchment.	138
Figure 4.19. Annual Observed Runoff and Modeled Runoff for the Proposed Model at the Florida Catchment.	139
Figure 4.20. Daily Simulations during 1994 of Soil Moisture Storage at the End of the Day for the Upper and Lower Soil Moisture Layers.	141
Figure 4.21. Monthly Simulations from January 1994 to December 1995 of the Soil Moisture Storage at the End of the Month for the Upper and Lower Soil Moisture Layers.	142
Figure 4.22. Annual Simulations from 1986 to 2003 of the Soil Moisture Storage at the End of the Year for the Upper and Lower Soil Moisture Layers.	143
Figure 4.23. NSE Values for the Proposed Model at the Daily Time Scale during the Full-Record Calibration Stage.	145
Figure 4.24. NSE Values for the Proposed Model at the Monthly Time Scale during the Full-Record Calibration Stage.	146

Figure 4.25. NSE Values for the Proposed Model at the Annual Time Scale during the Full-Record Calibration Stage.	147
Figure 4.26. Comparison of the Performance of the Proposed Model vs. the abcd Model during the Full-Record Calibration Stage at the Daily Time Scale.	151
Figure 4.27. Comparison of the Performance of the Proposed Model vs. the Zhang Model during the Full-Record Calibration Stage at the Daily Time Scale.	152
Figure 4.28. Comparison of the Performance of the Proposed Model vs. the abcd Model during the Full-Record Calibration Stage at the Monthly Time Scale.	153
Figure 4.29. Comparison of the Performance of the Proposed Model vs. the Zhang Model during the Full-Record Calibration Stage at the Monthly Time Scale.	154
Figure 4.30. Comparison of the Performance of the Proposed Model vs. the abcd Model during the Full-Record Calibration Stage at the Annual Time Scale.	155
Figure 4.31. Comparison of the Performance of the Proposed Model vs. the Zhang Model during the Full-Record Calibration Stage at the Annual Time Scale.	156
Figure 4.32. Comparison of the Performance of the Proposed Model vs. the abcd Model during the Half-Record Calibration Stage at the Daily Time Scale.	157
Figure 4.33. Comparison of the Performance of the Proposed Model vs. the Zhang Model during the Half-Record Calibration Stage at the Daily Time Scale.	158
Figure 4.34. Comparison of the Performance of the Proposed Model vs. the abcd Model during the Half-Record Calibration Stage at the Monthly Time Scale.	159

Figure 4.35. Comparison of the Performance of the Proposed Model vs. the Zhang Model during the Half-Record Calibration Stage at the Monthly Time Scale.	160
Figure 4.36. Comparison of the Performance of the Proposed Model vs. the abcd Model during the Half-Record Calibration Stage at the Annual Time Scale.	161
Figure 4.37. Comparison of the Performance of the Proposed Model vs. the Zhang Model during the Half-Record Calibration Stage at the Annual Time Scale.	162
Figure 4.38. Comparison of the Performance of the Proposed Model vs. the abcd Model during the Validation Stage at the Daily Time Scale.	163
Figure 4.39. Comparison of the Performance of the Proposed Model vs. the Zhang Model during the Validation Stage at the Daily Time Scale.	164
Figure 4.40. Comparison of the Performance of the Proposed Model vs. the abcd Model during the Validation Stage at the Monthly Time Scale.	165
Figure 4.41. Comparison of the Performance of the Proposed Model vs. the Zhang Model during the Validation Stage at the Monthly Time Scale.	166
Figure 4.42. Comparison of the Performance of the Proposed Model vs. the abcd Model during the Validation Stage at the Annual Time Scale.	167
Figure 4.43. Comparison of the Performance of the Proposed Model vs. the Zhang Model during the Validation Stage at the Annual Time Scale.	168
Figure 4.44. Comparison of the Performance of the Proposed Model vs. the abcd Model during the Half-Record Calibration Stage (Second Calibration Method) at the Daily Time Scale.	171

Figure 4.45. Comparison of the Performance of the Proposed Model vs. the Zhang Model during the Half-Record Calibration Stage (Second Calibration Method) at the Daily Time Scale. 172

Figure 4.46. Comparison of the Performance of the Proposed Model vs. the abcd Model during the Half-Record Calibration Stage (Second Calibration Method) at the Monthly Time Scale. . 173

Figure 4.47. Comparison of the Performance of the Proposed Model vs. the Zhang Model during the Half-Record Calibration Stage (Second Calibration Method) at the Monthly Time Scale. . 174

Figure 4.48. Comparison of the Performance of the Proposed Model vs. the abcd Model during the Half-Record Calibration Stage (Second Calibration Method) at the Annual Time Scale. ... 175

Figure 4.49. Comparison of the Performance of the Proposed Model vs. the Zhang Model during the Half-Record Calibration Stage (Second Calibration Method) at the Annual Time Scale. ... 176

Figure 4.50. Comparison of the Performance of the Proposed Model vs. the abcd Model during the Validation Stage (based on the Second Calibration Method) at the Daily Time Scale. 177

Figure 4.51. Comparison of the Performance of the Proposed Model vs. the Zhang Model during the Validation Stage (based on the Second Calibration Method) at the Daily Time Scale. 178

Figure 4.52. Comparison of the Performance of the Proposed Model vs. the abcd Model during the Validation Stage (based on the Second Calibration Method) at the Monthly Time Scale. .. 179

Figure 4.53. Comparison of the Performance of the Proposed Model vs. the Zhang Model during the Validation Stage (based on the Second Calibration Method) at the Monthly Time Scale. .. 180

Figure 4.54. Comparison of the Performance of the Proposed Model vs. the abcd Model during the Validation Stage (based on the Second Calibration Method) at the Annual Time Scale. 181

Figure 4.55. Comparison of the Performance of the Proposed Model vs. the Zhang Model during the Validation Stage (based on the Second Calibration Method) at the Annual Time Scale.	182
Figure 6.1. Catchment 07261000 (Arkansas).	195
Figure 6.2. Catchment 07346000 (East Texas).....	196
Figure 6.3. Catchments Overlapping 08171300 (Central Texas).	197
Figure 6.4. Catchment 08171300 (Red outline) (Central Texas).....	198
Figure 6.5. Topography between the Upstream Catchment and Catchment 08171300.	199
Figure 6.6. Catchment 02143040 (left) and catchment 02143500 (right).	200
Figure 6.7. Catchment 02349500 (South Atlanta, Georgia).	202
Figure 6.8. Saturated Hydraulic Conductivity for Catchment 02349500.	203

LIST OF TABLES

Table 3.1. Nash-Sutcliffe Coefficient of Efficiency Values for Model 13.	81
Table 3.2. Nash-Sutcliffe Coefficient of Efficiency Values for Model 14.	81
Table 3.3. Nash-Sutcliffe Coefficient of Efficiency Values for Model 15.	82
Table 4.1. Statistics for the Full-Record Calibration Stage.	148
Table 4.2. Statistics for the Half-Record Calibration Stage.	149
Table 4.3. Statistics for the Validation Stage.	150
Table 4.4. NSE Values at the Monthly Time Scale during the Validation Stage for Catchment 08085500.	165
Table 4.5. Statistics for the Half-Record Calibration Stage (Second Calibration Method).	169
Table 4.6. Statistics for the Validation Stage (based on the Second Calibration Method).	170
Table 4.7. NSE Values at the Monthly Time Scale during the Validation Stage (based on the Second Calibration Method) for Catchment 08085500.	179
Table 4.8. NSE Values at the Annual Time Scale during the Validation Stage (based on the Second Calibration Method) for Catchment 08085500.	181
Table 6.1. Full-Record Calibration Results at the Daily Time Scale.	207
Table 6.2. Full-Record Calibration Results at the Monthly Time Scale.	210
Table 6.3. Full-Record Calibration Results at the Annual Time Scale.	213
Table 6.4. Calibration and Validation Results at the Daily Time Scale.	216
Table 6.5. Calibration and Validation Results at the Monthly Time Scale.	219

Table 6.6. Calibration and Validation Results at the Annual Time Scale. 222

Table 6.7. Calibration and Validation Results at the Daily Time Scale (Second Analysis). 225

Table 6.8. Calibration and Validation Results at the Monthly Time Scale (Second Analysis).. 228

Table 6.9. Calibration and Validation Results at the Annual Time Scale (Second Analysis).... 231

CHAPTER 1: INTRODUCTION

Hydrologic models have a variety of applications. In water resources management, they have been implemented in the design and operation of reservoirs (Makhlouf & Michel, 1994). They have also been used, to a limited extent, for simulating snowmelt (Xu & Singh, 1998). They are employed for climate impact assessments (Makhlouf & Michel, 1994; Xu & Singh, 1998) and for predicting the hydrologic effects caused by climate and land use changes (Dunne & Leopold, 1978; Wang et al., 2009; Xu & Singh, 1998). They can be utilized to generate estimates of soil moisture and to fill gaps in streamflow records (Vandewiele et al., 1992), as well as to estimate lake water levels and groundwater levels (Dunne & Leopold, 1978). They have been used for the development of regional climate and hydrologic classifications and for providing hydrologic data for the validation of general circulation models (Xu & Singh, 1998). More commonly, they are implemented in streamflow prediction; though, in some cases, they have been applied in the quantification of groundwater recharge (Dripps & Bradbury, 2007). They have also been utilized for generating streamflow estimates in ungaged catchments (Alley, 1984; Vandewiele & Elias, 1995; Vandewiele et al., 1992; Xu & Singh, 1998) using interpolation techniques such as kriging or using parameter values from neighboring catchments (Vandewiele & Elias, 1995).

Though there are many different types of hydrologic models, most of these models can be divided into three main categories: (1) empirical models (i.e. black-box models), (2) physically-based models, and (3) models based on the water balance concept.

Empirical models, such as those based on the application of linear and nonlinear systems theory (Xu & Singh, 1998), make use of statistical and mathematical relationships to relate inputs to outputs. A major limitation of these models, however, is that they do not facilitate physical understanding of the hydrologic processes.

Physically-based equations, such as the Green-Ampt equation (Green & Ampt, 1911), are believed to govern water and energy processes in a vertical column of soil (Schaake et al., 1996). Models based on these equations are effective at representing the water budget at the point scale. Ideally, these models would form the basis of most hydrologic models. However, physically-based equations are most often used in models where accurate representation of surface runoff processes is not of great importance (Schaake et al., 1996). The reason is that at large spatial scales, application of the equations is difficult, due to the spatial heterogeneity of surface and subsurface characteristics.

Likewise, physically-based equations have been developed for applications at very short time scales, making them difficult for surface water budget estimations in applications at time scales greater than a day. Thus, either data at a very fine resolution is required to account for the spatial and temporal heterogeneity of surface runoff processes (which is currently infeasible) or, more commonly, a significant degree of spatial and temporal homogeneity must be assumed, which considerably limits the performance of physically-based models. Water balance models offer a simpler, and often, a more effective alternative method.

All water balance models are based on the water balance concept, a concept analogous to mass balance. Thornwaite (1944) defined it as the balance of precipitation and snowmelt (i.e. the

inflow of water) with evapotranspiration, groundwater recharge, and streamflow (i.e. the outflow of water) (Dunne & Leopold, 1978). A net change in the balance of water is usually accounted for and is most commonly expressed as a change in soil moisture.

The water balance concept can be used over various spatial scales ranging from a soil profile to a drainage basin (Dunne & Leopold, 1978) to a large geographic domain (Arnell, 1999). Additionally, models can be applied in a lumped (i.e. “aggregated”) or a distributed manner (usually as grid cells).

However, like the physically-based models, water balance models are difficult to apply at different temporal scales. The reason is that as time scales increase, the main controls of the physical processes on the water budget give way to climate controls. Thus, for daily and event time scales, physical controls, such as storm duration and intensity, topography, soil properties, and land cover tend to dominate while at mean annual time scales (i.e. multiple years per time period), climate controls, such as evapotranspiration, potential evapotranspiration, and precipitation tend to dominate.

Consequently, a great number of water balance models have been developed in the literature for application across various time scales. These models are usually developed for a particular time scale so that the controls with the greatest influence on rainfall partitioning are captured. For example, the curve number method, developed by the Soil Conservation Service, was developed to simulate direct runoff at the event scale (i.e. a single precipitation event) (USDA, 1972). The “abcd” model was developed by Thomas (1981) for application at the

monthly time scale. The Budyko model, and variations of it, was developed for long-term water balance (Budyko, 1974).

More recently, the proportionality hypothesis, which traces its origins from the SCS curve number method, has been identified as the commonality between these three hydrologic models. In the SCS curve number method, direct runoff is computed by a proportionality relationship. In the “abcd” model, evapotranspiration and storage at the end of each time period are computed by a proportionality relationship. However, evapotranspiration is computed based on an exponential relationship of storage and potential evapotranspiration while base flow is computed based on a linear reservoir model. In the Equity model (a variation of the Budyko model), runoff and evapotranspiration are computed by a proportionality relationship.

The objective of this thesis is to develop a conceptual hydrologic model structure for continuous simulations for multiple time scales. The model will be evaluated at various time scales, including the daily, monthly, and annual time scales. The primary difference of the proposed model in this thesis, as compared with the other three water balance models, is the application of the proportionality hypothesis to the partitioning of surface runoff and continuing abstraction as well as the partitioning of continuing evapotranspiration and subsurface flow.

In the remainder of Chapter 1, a general description of the hydrologic cycle and the processes involved will be provided and will be followed by a description of the generalized proportionality hypothesis. Chapter 2 will provide a brief introduction to water balance models and a literature review of several water balance models that have been applied at the daily, monthly, or at multiple time scales. In Chapter 3, the methodologies used in model evaluation

will be described, followed by a description of the initial model structure and the development of the model to its final stage. In Chapter 4, the proposed model will be evaluated and discussed. Finally, in Chapter 5, a summary of the results, findings, and future work will be provided.

1.1 The Proportionality Hypothesis

A significant difference in the proposed model structure, as opposed to more typical water balance models, is the incorporation of the proportionality hypothesis. The proportionality hypothesis is used as the basis for the relationships in the SCS curve number method and in Budyko models, such as the Equity model. The hypothesis states that the competition between two competing processes for the same supply is dictated by a proportional distribution of the supply based on the potential maximum deficits (or “needs”) of each of the two processes. This can also be expressed as follows:

$$\frac{X_a}{X_p} = \frac{Y_a}{Y_p} = \frac{\text{Actual}}{\text{Potential}} \quad (1.1)$$

where X_a and Y_a represent the actual amounts of supply “Z” distributed to each element X and Y, respectively. X_p and Y_p represent the deficits (or “needs”) of elements X and Y, respectively.

It is, of course, necessary to state how the sum of the two elements (X and Y) are related to the supply. Assuming that the supply (Z) is completely depleted after the competition:

$$X_a + Y_a = Z \quad (1.2)$$

In the SCS curve number method, this hypothesis is applied to the competition of continuing abstraction, F_a and direct runoff, Q_d :

$$\frac{F_a}{S} = \frac{Q_a}{P - I_a} \quad (1.3)$$

where S , I_a , and P represent the potential maximum retention, the initial abstraction, and the precipitation, respectively.

In the Equity model, the proportionality hypothesis is applied to the competition of runoff, Q , and continuing evapotranspiration, E_c :

$$\frac{E_c}{E_p - E_0} = \frac{Q}{P - E_0} \quad (1.4)$$

where E_p , E_0 , and P represent the potential evapotranspiration, the initial evapotranspiration, and the precipitation, respectively.

1.2 The Hydrologic Cycle and Hydrologic Processes

In the hydrologic cycle, precipitation falls on the land surface and is intercepted by surface vegetation and the top layer of soil. A portion of precipitation is contained by surface depressions and the vegetation, which is referred to as initial abstraction. This water is eventually removed by either infiltration into the soil or evaporation into the atmosphere. The portion of precipitation exceeding initial abstraction continues as surface runoff and as infiltration into the soil. The water that infiltrates the soil travels downward towards the saturated zone (groundwater table) while at the same time vegetation, via root systems, extracts water from this quantity (which is referred to as transpiration). Due to capillary action and molecular forces between water and soil particles (Linsley et al., 1992), a certain amount of water overcomes the influence

of gravity and remains suspended in the unsaturated zone (i.e. the field capacity, θ_{fc}); this water can be extracted by vegetation, but it cannot contribute to streamflow.

The remaining infiltrated water reaches the groundwater table and raises it. If groundwater levels are equal to or higher than the surrounding groundwater table before this water is added, then some groundwater will flow outward to the stream as baseflow.

Similar to baseflow, some unsaturated flow moves outward in response to the variability in soil moisture and reaches the stream before it reaches the groundwater table; this unsaturated flow, a component of the subsurface flow, is typically referred to as interflow. Streamflow, or total runoff, represents the sum of surface runoff, interflow, and baseflow.

Evapotranspiration includes both the processes of evaporation through the surface of the soil and transpiration from the roots of vegetation through the stems and leaves. While evaporation is limited to a small depth of the soil column, transpiration may continue down to significant depths.

A typical water budget describes the overall mass balance of the hydrologic processes. For example,

$$\Delta S = P - E - Q \tag{1.5}$$

where ΔS denotes the change of storage, P represents the precipitation, E represents evapotranspiration, and Q represents the total runoff (streamflow).

The processes of precipitation, infiltration, and runoff are driven by gravity, while evapotranspiration is driven by the net solar radiation (R_n) via the latent heat flux ($L_e E$).

Evapotranspiration (E) is the resulting impact of potential evapotranspiration (E_p) on the hydrologic cycle and is, like the other hydrologic processes, influenced by topography, land cover, and soil processes. However, in addition to these factors, the evapotranspiration rate (the transpiration rate, specifically) is influenced by the nonlinear water demand of vegetation. Vegetation water demand varies based on vegetation type (different types of vegetation have different demand rates and root depths) and distribution (density of vegetation and how various types of vegetation are spatially distributed in regards to each other).

Evapotranspiration is the second largest component in the water balance equation (Budyko, 1974). Thus, it is important that evapotranspiration be regarded and treated as a process specifically different from the other hydrologic processes. Otherwise, it may be difficult to diagnose structural weaknesses in proposed hydrologic models. In practice, it is usually calculated as a function of the soil moisture and the potential evapotranspiration (Xu & Singh, 1998).

CHAPTER 2: LITERATURE REVIEW

2.1 Introduction

Many water balance models have been developed for application at monthly time scales (Palmer, 1965; Thomas, 1981; Thornthwaite & Mather, 1955); though some of these models have also been applied successfully at the annual time scale (Alley, 1984). Other models have been developed for the mean annual time scale (Budyko, 1974; Fu, 1981). Some models have been developed for the daily time scale (Arnell, 1999; Dripps & Bradbury, 2007; Schaake et al., 1996) and are applicable at even smaller time scales (Schaake et al., 1996). Models have also been developed for the event time scale (i.e. a single precipitation event) (USDA, 1972). Some models, to a limited extent, are applicable at multiple time scales (Schaake et al., 1996; Zhang et al., 2008). Most models have been developed at the monthly time scale because smaller time scale models (daily, hourly, etc.) tend to be more complex and data-intensive (Xu & Singh, 1998) due to the fact that additional processes are necessary to simulate the greater degree of variability in hydrologic processes.

As mentioned by Xu and Singh (1998), water balance models have many attributes in common. For example, most models are calibrated by estimating their parameters using observed hydrologic data. Second, most water balance models have been developed for the purpose of streamflow prediction. Third, all water balance models are based on the water budget equation.

There are also some general differences between models. These are mainly the input data requirements, how groundwater and soil moisture storage are handled (e.g. the number of storages), and the number of hydrologic processes accounted for (Xu & Singh, 1998).

A major limitation in the development of hydrologic models is the limited available data that can be used to calibrate a model. Water balance models, however, typically require only hydroclimatic data, which is widely available in the United States. In general, water balance models have to be calibrated using available streamflow data, precipitation, and surface meteorological data (Schaake et al., 1996) from the catchments they model (or from multiple nearby catchments in the application of models to ungaged catchments). Basin characteristics are represented in the model parameters. These parameters must be calibrated (or in some cases, determined from available data, such as the model proposed by (Arnell, 1999)).

Models such as the Thornthwaite and Mather model, abcd model, and the Palmer model use precipitation and temperature as input for the models. On the other hand, some models have been developed that use only precipitation as input. In these models, such as the Tennessee Valley Authority (TVA) model developed by Snyder (1963), evapotranspiration is calculated as a fraction of precipitation. However, these models tend to be unreliable at longer than monthly time scales. Most models use monthly rainfall and potential evapotranspiration as input.

2.1.1 History of Water Balance Models

The first well-known monthly water balance model was developed by Thornwaite (1948) and formally introduced in Thornthwaite and Mather (1955, 1957). This model was later

modified by Alley (1984) who added a parameter to this model to partition a fraction of precipitation into direct runoff ($T\alpha$ model).

Palmer (1965) developed a water balance model to create an index on meteorological drought (Alley, 1984; Xu & Singh, 1998). A “root constant” is applied to this model in the form of an upper and lower soil moisture layer. Like the Thornthwaite and Mather model, the Palmer model relies on the threshold concept, where runoff and recharge are modeled so that they do not occur until the soil moisture layer is completely saturated (Alley, 1984).

Thomas (1981) developed the “abcd” model, which, like the Thornthwaite and Mather model, has two separate layers for soil moisture and groundwater. Its treatment of evapotranspiration is similar to the method used in the Thornthwaite and Mather model. The model was later applied by Thomas et al. (1983) across 40 catchments in New England (Alley, 1984). Many modifications have been made to the abcd model. For example, Martinez and Gupta (2010) modified the abcd model to handle snow dynamics and Sankarasubramanian and Vogel (2002) used the abcd model to derive expressions for the evaporation ratio.

The Soil Conservation Service (SCS) developed a water balance model for applications at the event scale (i.e. each rainfall event) (USDA, 1972). The model calculates “rainfall excess” using a proportionality relationship. The model has no parameters but requires the estimation of “curve numbers” that vary based on the land cover type.

Makhlouf and Michel (1994) developed a two parameter monthly water balance model for use with catchments in France (GR2M). They found that the performance of the abcd model and the GR2M model performed similarly, while the Thornthwaite and Mather model and the

Vandewiele model performed worse. Most notably, they showed that models that account for soil moisture perform considerably better than those that do not.

Schaake et al. (1996) developed the five-parameter “simple water balance” (SWB) model for use at small time scales (daily, hourly, etc.). It is designed to be coupled with an atmospheric model or for use on a stand-alone basis. Schaake et al. (1996) compared its performance against the complex Sacramento soil moisture accounting (SAC-SMA) model, the soil hydrology model developed at Oregon State University (OSU), and the Manabe Bucket model and found that the model compared favorably against the more sophisticated SAC-SMA and OSU models.

Zhang et al. (2008) proposed a four-parameter dynamic water balance (DWB) model for application at multiple time steps and tested it against 265 catchments in Australia. A particularly unique aspect of this model is the application of three Budyko-type equations to describe the partitioning of water between various processes. The model bears a strong similarity to the abcd model by Thomas (1981) in regards to the concepts of the definitions of “available water” and “evapotranspiration opportunity”. Also, like the abcd model, this model does not rely on the threshold concept, which improves the ability of the model to simulate streamflow in arid climates. However, unlike the abcd model, it allows both linear and nonlinear relationships to be modeled. The model is very robust, and was in fact used as a performance metric by Li and Sankarasubramanian (2012) against the abcd and VIC models in the testing of multi-model combination techniques. Wang et al. (2011) developed a variation of this model (i.e. the “Wapaba” model).

Dripps and Bradbury (2007) developed a physically-based daily water balance model that accepts GIS data in addition to hydroclimatic data. The model was developed for use as a groundwater recharge estimation tool that can be used to provide input data for groundwater models. The model was designed to be generally applicable for temperate humid climates, such as Wisconsin, though it has been applied to other climates, such as the semi-arid High Plains region (Stanton et al., 2011).

2.1.2 Water Balance Modeling Methods

Different methodologies have been presented for the application of water balance models. In most studies, models are applied on a stand-alone basis (i.e. the “traditional approach”). However, a few studies have focused on alternative methodologies.

For example, Alley (1985) showed that incorporating state variables from the Thomas abcd and Thornthwaite and Mather models into time series models with exogenous terms lead to improvements over using the models themselves. He attributed this improvement in performance to the seasonal biases implicit in the water balance model structures and confirmed this by correcting the seasonal biases using separate regression equations for each month, which significantly improved the results from the water balance models to the point that the results were similar to the time series approach.

Fernandez et al. (2000) introduce another methodology termed “regional calibration” where all sites in a region are calibrated simultaneously. However, when this methodology was applied using the abcd model at three different sites, they found that the strong regional

relationships obtained during the calibration stage were misleading, because the validation results lead to nearly the same streamflow estimations when compared with the traditional approach (Fernandez et al., 2000).

Another methodology that has been proposed involves combining hydrologic models with climate models. In the study by (Block et al., 2009), they coupled two hydrologic models, the abcd model and the Soil Moisture Accounting Procedure (SMAP) to multiple global climate models (GCMs) by generating precipitation from the GCMs, downscaling the results using regional climate models (RCMs) and feeding the results to the hydrologic models. Results showed that the coupled models performed better than the hydrologic models did alone.

A related study was performed by Li and Sankarasubramanian (2012). In their study, two hydrologic models, the VIC model and the “abcd” model (Thomas, 1981), were used to test two multiple model combination methods. They found that in the presence of high model structural and measurement uncertainty, the multi-model techniques tend to perform better than the individual models alone.

2.1.3 Number of Parameters

Models have been developed with only a single parameter, such as the Manabe bucket model or the Fu equation (Schaake et al., 1996; Zhang et al., 2008) to many parameters, such as the 12-parameter model developed by Pitman (1973, 1978) for African catchments. However, as stated by Schaake et al. (1996), “...a need exists for models with a small number of parameters and intermediate in complexity between a simple bucket, with only one parameter, and more

complex hydrologically oriented models with many parameters such as the Sacramento model.” In a reply to comments, Jakeman and Hornberger (1994) said, “...conceptual and physically based models developed and used for describing rainfall runoff processes tend to be overparameterized. They are no more useful for prediction than are simpler models whose parameters are identifiable from available data.” Conversely, “...the ability to produce identifiable models with about a half dozen parameters opens up opportunities to learn about how to generalize catchment response by studying a large number of catchments.” Furthermore, Xu and Singh (1998) state that models with fewer parameters contain more information and are more likely to represent specific catchment characteristics, which facilitates the application of water balance models to the estimation of streamflow at ungaged catchments. Furthermore, Xu and Singh (1998) suggest that three to five parameters may be sufficient at the monthly time scale for humid regions, though they suggest that a more complex model structure may be necessary for arid and semi-arid environments. Thus, a major challenge in the development of water balances models is seeking an appropriate balance in model complexity to meet the intended application of the model (Dripps & Bradbury, 2007; Zhang et al., 2008).

2.2 Summary of Models

In the Sections 2.3 to 2.11, several water balance models will be discussed in detail. Many of these models, particularly the abcd model, Vandewiele model, Thornthwaite and Mather model, Palmer model, and others discussed by Xu and Singh (1998) have been evaluated in numerous comparison studies, but none have been found that are clearly superior to the others

(Fernandez et al., 2000). Two of these, specifically the Dynamic Water Balance model by Zhang et al. (2008) and the abcd model by Thomas (1981), will be used to evaluate the performance of the model proposed in this thesis. They will be referred to in the results as the Zhang model and the abcd model, respectively. The abcd model was chosen because it is a popular model for comparison studies and the Zhang model was chosen because its intended use is for multiple time scales.

2.2.1 Climate and Model Performance

In a study by Sankarasubramanian and Vogel (2002), the abcd model was used to characterize the annual hydrology of the continental United States. In their study, they found that the model tends to produce the best results in the humid eastern and northwestern regions of the United States. Another study by Martinez and Gupta (2010) found that the abcd model's performance decreased in more arid climates and towards the Southeastern United States. This trend is not limited to the abcd model, but is common in many other water balance models. This is primarily due to the fact that (1) infiltration excess plays a significant role in surface runoff generation in arid climates and (2) there is a very high spatial and temporal variation in precipitation (Potter et al., 2005). As suggested by Xu and Singh (1998), models with more complex model structures may be more appropriate for arid climates. Additionally, it should be a priority to consider the impact that climate variability has on model performance because it could be an indicator of the weaknesses or strengths of a particular model structure.

To classify catchments from humid to arid climates, the mean annual aridity index is used. The mean annual aridity index is defined as the ratio of mean annual potential evapotranspiration to the difference between mean annual precipitation and soil water storage change:

$$\text{Aridity Index} = \frac{E_p}{(P - \Delta S)} \quad (2.1)$$

Aridity indices greater than 1 indicate dry climates while values below indicate humid climates. In Chapter 4, the aridity index is used to assess how climate affects model performance.

2.3 Thornthwaite and Mather Model

Most model structures (with the exclusion of those based on the Budyko framework) are essentially variations of the Thornthwaite and Mather model. The model, which was introduced by Thornthwaite and Mather (1955), assumes a single soil moisture layer and an infinite capacity groundwater storage reservoir.

The soil moisture layer has a capacity limit, Φ . S_{i-1} represents soil moisture storage at the beginning of month i while S_i represents the soil moisture storage at the end of month i . Storage changes based on the addition of water via precipitation, P_i , and the subtraction of water via potential evapotranspiration, $E_{p,i}$. If P_i exceeds $E_{p,i}$,

$$S_i = \min\{(P_i - E_{p,i}) + S_{i-1}, \Phi\} \quad P_i \geq E_{p,i} \quad (2.2)$$

On the other hand, if $E_{p,i}$ exceeds P_i ,

$$S_i = S_{i-1} \exp\left[-\frac{(E_{p,i} - P_i)}{\Phi}\right] \quad P_i < E_{p,i} \quad (2.3)$$

For water to leave the soil moisture layer and add to “water surplus” (i.e. for recharge to groundwater to occur), the soil moisture must be at its capacity. Consequently, precipitation must also exceed potential evapotranspiration,

$$\begin{cases} R_i = (P_{n,i} - E_{p,i}) + S_{i-1} - \Phi & S_i = \Phi \\ R_i = 0 & S_i \neq \Phi \end{cases} \quad (2.4)$$

where R_i is the addition to the linear reservoir (addition to water surplus). This water is added to the “water surplus” (i.e. a groundwater reservoir). Streamflow is derived from this quantity.

Since models such as the Thornthwaite-Mather model assume a lumped model form, there is a delay, especially in large catchments, in the time it takes precipitation to travel from the point where it infiltrates the soil (or travels across) to where it reaches the stream. Thus, to account for this effect on groundwater discharge, a fraction, λ , of recharge and groundwater storage at the beginning of the month, $(G_{i-1} + R_i)$, remains as groundwater storage at the end of the month, G_i , and the remaining fraction, $1 - \lambda$, leaves as groundwater discharge, Q . λ varies based on the depth of the soil and the soil type, the size and topography of the catchment, and the characteristics of the groundwater system (Alley, 1985).

$$Q = (1 - \lambda)(G_{i-1} + R_i) \quad (2.5)$$

$$G_i = \lambda(G_{i-1} + R_i) \quad (2.6)$$

where Q is runoff for month i . Even in the case where there is no addition to the linear reservoir (i.e. $R_i = 0$), there will be some outflow that becomes runoff.

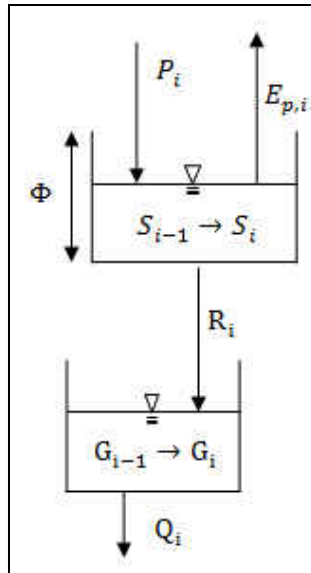


Figure 2.1. Thornthwaite and Mather Model

2.3.1 $T\alpha$ Variant of the Thornthwaite and Mather Model

The $T\alpha$ model is a slight modification of the Thornthwaite and Mather model proposed by Alley (1984, 1985). This model assumes that “some fraction, α , of the precipitation was direct runoff prior to performing the other water balance computations.” Though this is a minor change to the model structure itself, it takes into account the surface runoff component, which was neglected in the original model.

This model variant was also used by Makhoulf and Michel (1994), where it was referred to as the “Thornthwaite and Mather model” (X_1 is α). For clarification, see the equations and the diagram listed below.

$$P_{n,i} = (1 - \alpha)P_i \quad (2.7)$$

$$\begin{cases} S_i = \min\{(P_{n,i} - E_{p,i}) + S_{i-1}, \Phi\} & P_{n,i} \geq E_{p,i} \\ S_i = S_{i-1} \exp\left[-\frac{(E_{p,i} - P_{n,i})}{\Phi}\right] & P_{n,i} < E_{p,i} \end{cases} \quad (2.8)$$

$$\begin{cases} R_i = (P_{n,i} - E_{p,i}) + S_{i-1} - \Phi & S_i = \Phi \\ R_i = 0 & S_i \neq \Phi \end{cases} \quad (2.9)$$

$$Q = (1 - \lambda)(G_{i-1} + R_i) + \alpha P_i \quad (2.10)$$

$$G_i = \lambda(G_{i-1} + R_i) \quad (2.11)$$

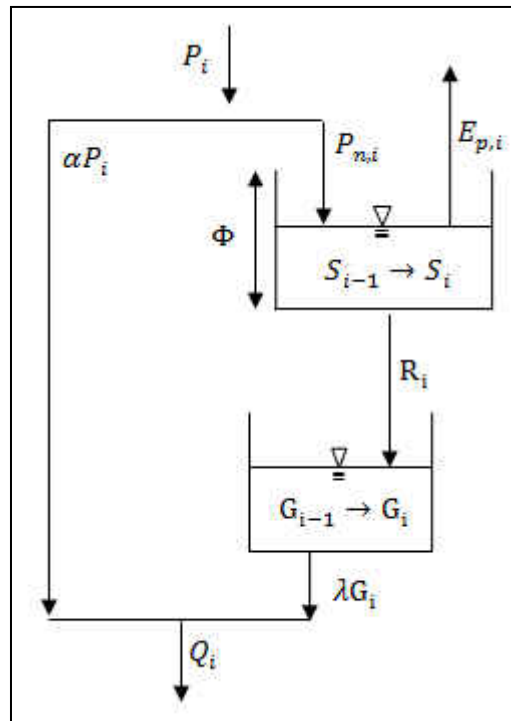


Figure 2.2. T α -variant of the Thornthwaite and Mather Model.

2.4 Palmer Model

The Palmer (1965) model is a two-soil moisture layer model with two parameters. The upper and lower soil moisture layers have capacities Φ_a and Φ_b , respectively. The total soil moisture capacity is defined as the sum of both quantities:

$$\Phi = \Phi_a + \Phi_b \quad (2.12)$$

Soil moisture is denoted as S_{i-1}^a and S_i^a for the upper layer and S_{i-1}^b and S_i^b , for the lower layer at the beginning and end of the time period, respectively.

Evapotranspiration in the upper layer, E_i^a , is assumed to occur at the potential rate (Alley, 1984), as described in the following equation:

$$E_i^a = \begin{cases} PE_i & PE_i \leq \Phi_a \\ \Phi_a & PE_i > \Phi_a \end{cases} \quad (2.13)$$

where PE_i is the potential evapotranspiration rate during time period i . The soil moisture in the upper layer is then updated using the following equation:

$$S_i^a = \begin{cases} S_{i-1}^a + P - E_i^a & S_i^a < \Phi_a \\ \Phi_a & S_i^a \geq \Phi_a \end{cases} \quad (2.14)$$

Evapotranspiration also occurs in the lower layer and is denoted as E_i^b . E_i^b does not occur unless all available soil moisture has been removed from the upper layer. Then, the evapotranspiration rate will occur in the lower layer at the rate described in Equation (2.15):

$$E_i^b = \frac{[(PE_i - P_i) - E_i^a]S_{i-1}^b}{\Phi} \quad \begin{matrix} E_i^b \leq S_{i-1}^b \\ (PE_i - P_i) - E_i^a > 0 \end{matrix} \quad (2.15)$$

Recharge to the lower layer (i.e. excess soil moisture from the upper layer) does not occur unless the upper layer soil moisture reaches its capacity (Alley, 1984).

$$S_i^b = \begin{cases} S_{i-1}^b - E_i^b & S_i^a = 0 \\ S_{i-1}^b + (S_{i-1}^a + P - E_i^a - \Phi_a) & S_i^a = \Phi_a \\ S_{i-1}^b & 0 < S_i^a < \Phi_a \end{cases} \quad (2.16)$$

Next, and similar to the Thornthwaite and Mather model (excluding the $T\alpha$ variant), the Palmer model relies on the threshold concept for recharge. That is, recharge, R_i , cannot occur until soil moisture in both layers equals their capacities:

$$R_i = P - (E_i^a + E_i^b) - (S_i^a + S_i^b) \quad S_i^b + S_i^a = \Phi_b + \Phi_a \quad (2.17)$$

A diagram of this model is displayed in Figure 2.3.

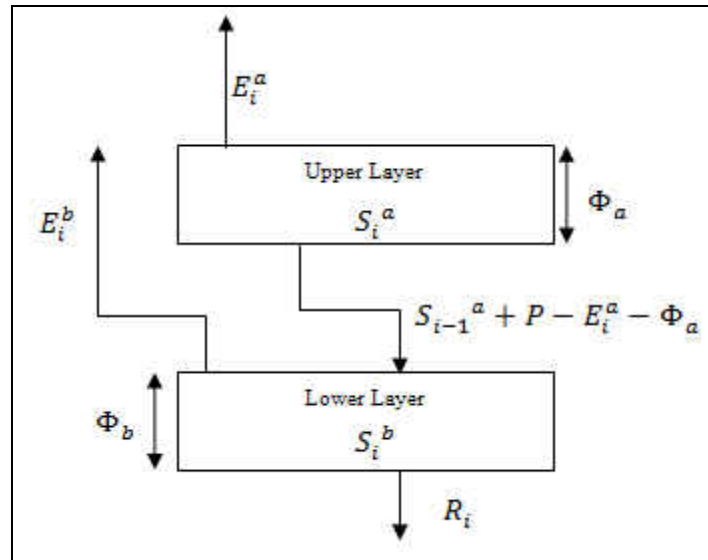


Figure 2.3. Palmer Model.

2.5 Thomas “abcd” Model

In the Thomas (1981) “abcd” model, there are two layers of storage: soil moisture (top layer) representing the unsaturated zone, and groundwater storage (bottom layer) representing the saturated zone.

Water from soil moisture at the end of the previous month (S_{i-1}) and precipitation (P_i) in the current month represent the available water (W_i) for evapotranspiration, groundwater recharge, and direct runoff (i.e. $W_i = P_i + S_{i-1}$).

After precipitation combines with the previous month’s soil moisture, some water remains in the soil moisture layer, known as the evapotranspiration opportunity (y_i) and represents the summation of evapotranspiration and soil moisture storage for the current month (i.e. $y_i = E_i + S_i$). The evapotranspiration opportunity represents the maximum potential water that evapotranspiration could potentially extract from the soil moisture layer; any fraction of this water that does not actually evaporate remains in the soil moisture layer for the next time period. The evapotranspiration opportunity can be alternatively viewed as the soil moisture opportunity (the case where evapotranspiration is negligible). The remaining water ($W_i - y_i$) leaves as groundwater recharge and direct runoff. An important assumption this model makes is that some recharge and direct runoff will occur before the soil moisture layer is fully saturated. Another important assumption this model makes is that evapotranspiration takes place only in the unsaturated zone.

In order to derive a relationship between available water and evapotranspiration opportunity, the following proportionality relationship is assumed:

$$\frac{y_i}{W_i} = \frac{(b - y_i)}{(b - ay_i)} \quad (2.18)$$

where “b” represents the maximum storage capacity of the soil moisture layer and has the same units as soil storage (S_i and S_{i-1}). As mentioned previously, evapotranspiration opportunity can be viewed as the soil moisture opportunity, hence, parameter b represents the upper limit of y_i . Parameter “a” represents the “propensity of runoff to occur before the soil [moisture layer] is fully saturated”. As “a” increases, this tendency decreases so that when $a = 1$, all available water (W_i) will be allocated to y_i (will evaporate or remain in the soil moisture layer) as long as W_i remains below the potential of y_i (b). Theoretically, a ranges between 0 to 1. However, Thomas et al. (1983) found that values tend to be at least 0.95. Similarly, values reported by Alley (1984) were always above 0.97. To calculate y_i , the equation above is represented with y_i as a function of W_i :

$$y_i(W_i) = \frac{W_i + b}{2a} - \sqrt{\left(\frac{W_i + b}{2a}\right)^2 - \frac{W_i b}{a}} \quad (2.19)$$

To calculate evapotranspiration from the evapotranspiration opportunity, Thomas (1981) hypothesized that the rate loss of soil moisture by evapotranspiration is proportional to the potential evapotranspiration $-\frac{dS}{dt} \propto E_{p,i}$. Thomas assumes that the constant of proportionality for this relationship is the ratio of soil moisture at the end of the month to the upper bound of soil moisture (i.e. the degree of soil saturation, or S_i/b). Thus, the relationship can be written as:

$$\frac{dS}{dt} = -\frac{E_{p,i}}{b} S \quad (2.20)$$

As mentioned previously, the opportunity for soil moisture storage is the same as the evapotranspiration opportunity (y_i). Thus, water at the beginning of the allocation between evapotranspiration and soil moisture storage is expressed as:

$$S_i = S_{i-1} \exp\left(-\frac{E_{p,i}}{b}\right) \quad (2.21)$$

Since $E_i = y_i - S_i$,

$$E_i = y_i \left[1 - \exp\left(-\frac{E_{p,i}}{b}\right)\right] \quad (2.22)$$

Next, the remaining water ($W_i - y_i$) is allocated between direct runoff and recharge, which is assumed to have a constant ratio “c”:

$$Q_{d,i} = (1 - c)(W_i - y_i) \quad (2.23)$$

$$R_i = c(W_i - y_i) \quad (2.24)$$

Finally, using the mass balance of groundwater, Thomas (1981) derived an expression for groundwater storage at the end of the month (G_i)

$$R_i + G_{i-1} = dG_i + G_i \quad (2.25)$$

where dG_i is the groundwater discharge (i.e. baseflow) and “d” represents the reciprocal of the groundwater residence time (Thomas, 1981). That is,

$$G_i = \frac{1}{1+d}(R_i + G_{i-1}) \quad (2.26)$$

Thus,

$$Q_{bi} = dG_i \quad (2.27)$$

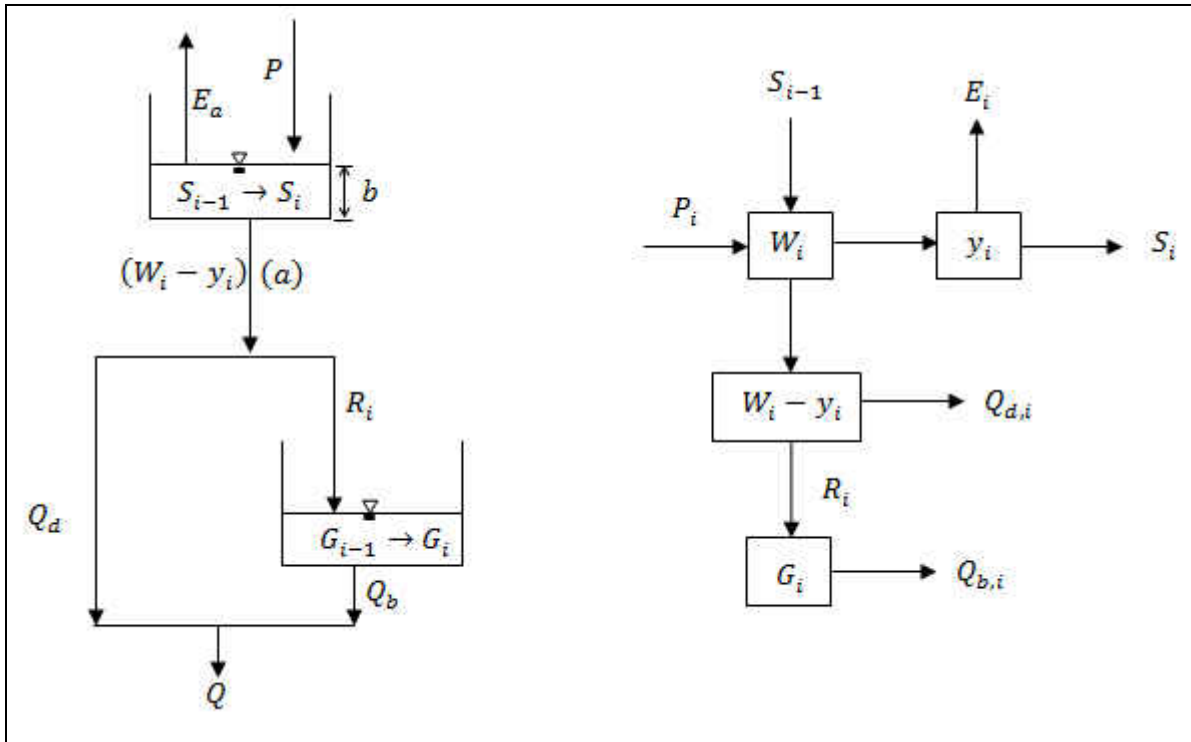


Figure 2.4. Thomas (1981) abcd Model.

2.5.1 Abcd-type Budyko model

In an effort to account for the effects of soil moisture in Budyko-type equations, Sankarasubramanian and Vogel (2002) derived the following equation for the evapotranspiration ratio based on the abcd model:

$$\bar{E}/\bar{P} = 0.5 \left[1 + \gamma(1 - R) - \sqrt{1 - 2\gamma(1 - R) + \gamma^2(1 - 2R + R^2)} \right] \quad (2.28)$$

where γ represents the soil moisture storage index (a parameter to be calibrated), \bar{E} is mean annual evaporation, \bar{P} is mean annual precipitation, and R is an exponential equation. These terms are defined below:

$$\bar{E} = \bar{P} - \bar{Q} \quad (2.29)$$

$$\gamma = b/\bar{P} \quad (2.30)$$

$$R = \exp\left(-\frac{1\bar{E}_p}{\gamma\bar{P}}\right) \quad (2.31)$$

where \bar{E}_p is the mean annual aridity index.

2.6 SCS Curve Number Method

The curve number method is an event-scale model that requires no parameters to calibrate (USDA, 1972). There are two primary differences between this model and the ones discussed previously: (1) the curve number method does not account for the accumulation of soil moisture from previous time periods and (2) it does not account for evapotranspiration and baseflow. In the model, losses are accounted for by “abstractions”. The model defines two types of abstractions: (1) initial and (2) continuing. Initial abstraction, I_a , subtracts from the available water (i.e. the precipitation, P) before direct runoff, Q_d , can occur. Continuing abstraction, on the other hand, occurs concurrently with direct runoff.

Assuming that initial abstraction is less than the precipitation, there will be some water that can become direct runoff. It was originally assumed that $I_a = 0.2S$, where S denotes the potential maximum retention (a measure of the maximum soil moisture capacity). S is approximated using the following equation:

$$S = \frac{1000}{CN} - 10 \quad (2.32)$$

In this equation, CN refers to the curve number and S is the potential maximum retention (inches). The curve number is not calibrated. Instead, it is estimated from tables provided by the Soil Conservation Service (USDA, 1972).

Assuming that precipitation exceeds the initial abstraction (i.e. $P - I_a > 0$), continuing abstraction, F_a , and direct runoff, Q_d will compete for the excess water via the following proportionality relationship:

$$\frac{F_a}{S} = \frac{Q_d}{P - I_a} \quad (2.33)$$

The equation of continuity is defined as

$$P = Q_d + I_a + F_a \quad (2.34)$$

Direct runoff can be calculated by solving Equation (2.34) for F_a and substituting it into (2.33), then solving the equation for Q_d :

$$Q_d = \frac{(P - I_a)^2}{P - I_a + S} \quad (2.35)$$

A representation of the model is provided in Figure 2.5.

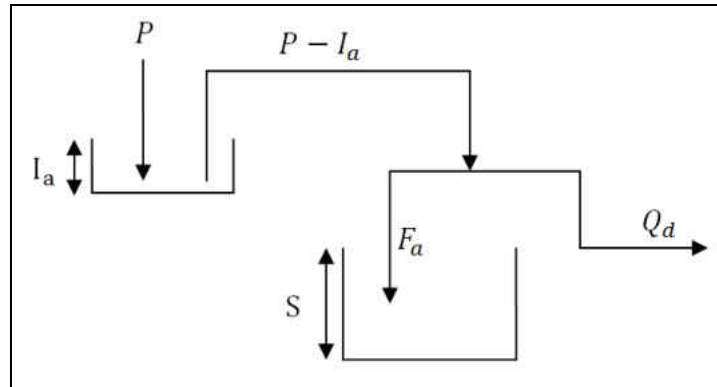


Figure 2.5. Model of the Curve Number Method.

2.7 SWB Model

The SWB model, developed by Schaake et al. (1996), is a 5-parameter water balance model designed to operate for any time step up to approximately 24 hours.

The model has two soil moisture layers. Both layers have capacity limits, which define two of its five parameters. As defined by the author, the state of soil moisture is represented as a deficit “only because moisture deficit may be useful in diagnosing model performance”. Thus, the soil layer capacity limits are defined as “maximum deficits” and are equivalent to maximum soil moisture capacity.

A thin upper layer comprises the soil surface and the vegetation canopy. It represents initial abstraction (i.e. water from interception and water stored in small depressions on the soil surface) as well as water from the top few millimeters of the soil surface. The water budget for the upper layer is expressed as:

$$\frac{dD_u}{dt} = D_u - D_{u,i} = E_u - P + P_x \quad (2.36)$$

where $D_{u,i}$ and D_u represents the moisture storage deficit in the upper layer at the beginning and at the end of the time period, respectively. The maximum deficit is represented by $D_{u,max}$ and also represents the maximum storage capacity of the upper layer. Precipitation is denoted as P . P_x represents excess inflow (i.e. precipitation or the sum of stemflow and throughfall), which supplies water to the lower soil moisture layer if D_u reaches zero (i.e. the soil moisture layer reaches its capacity).

In this model, evaporation is divided between the two layers. For the upper layer, the evaporation rate is represented by E_u and is defined as:

$$E_u = E_p \left(1 - \frac{D_{u,i}}{D_{u,max}} \right) \quad (2.37)$$

where E_p is the potential evapotranspiration rate. Note that there is a possibility that $E_u > D_{u,max} - D_{u,i} + P$, which will cause D_u to exceed the maximum capacity, $D_{u,max}$.

The water budget equation can be written analytically as two equations:

$$\frac{dD_u}{dt} = E_u - P \quad (2.38)$$

$$\begin{cases} D_u = 0 & P_x = - \left(\frac{dD_u}{dt} + D_{u,i} \right) & \frac{dD_u}{dt} + D_{u,i} < 0 \\ D_u = \frac{dD_u}{dt} + D_{u,i} & P_x = 0 & \text{otherwise} \end{cases} \quad (2.39)$$

The lower layer is the main soil moisture storage reservoir. It represents the vegetation root zone and the groundwater. The moisture deficit in this layer is denoted as D_b . Similar to the

upper layer, the maximum soil moisture capacity of the lower layer is denoted as $D_{b,max}$. The water budget for the lower layer is expressed as:

$$\frac{dD_b}{dt} = E_b + Q_s + Q_g - P_x \quad (2.40)$$

The water budget equation for the lower layer can be written analytically as:

$$D_b = E_b + Q_s + Q_g - P_x + D_{b,i} \quad (2.41)$$

where $D_{b,i}$ and D_b represents the moisture storage deficit in the lower layer at the beginning and at the end of the time period, respectively and where Q_s represents surface runoff, Q_g represents subsurface runoff, and E_b represents evapotranspiration in the lower layer¹. Surface runoff, Q_s is expressed as:

$$Q_s = \frac{P_x^2}{P_x + I_c} \quad (2.42)$$

which is nearly equivalent to the SCS curve number method equation (USDA, 1972). I_c is the spatially averaged infiltration capacity. P_x , which is partitioned into surface runoff and infiltration, is expressed as:

$$P_x = Q_s + I \quad (2.43)$$

¹ In the original equations of Schaake et al. (1996), particularly for E_b and Q_g , Schaake et al. refer to the soil moisture deficit, but they do not indicate if it is the soil moisture deficit at the beginning of the time period, the soil moisture deficit at the end of the time period (which would require a trial-and-error estimation), or the updated soil moisture deficit after a previous process has run (which would require the equations to be calculated in a certain order). In this thesis, it has been assumed that the equations refer to the initial soil moisture deficit ($D_{b,i}$). Also, in the equations for E_b and Q_g , though some of them refer to the maximum soil moisture deficit ($D_{b,max}$), they do not constrain E_b and Q_g so that D_b remains below the maximum deficit. A modification to this model was considered which adds a constraint to the equations to prevent this condition. However, doing so requires that each of the three state variables be executed sequentially. Since no indication was made in regards to what order these three variables (E_b , Q_s , and Q_g) should be calculated, this modification was rejected. Additionally, as far as the author is aware, Schaake et al. did not verify that the soil moisture deficit was not exceeded. It may be that $D_{b,max}$ only serves as a scaling factor on E_b .

or, written explicitly for Q_s ,

$$Q_s = P_x - I \quad (2.44)$$

I is the spatially averaged actual infiltration, expressed as:

$$I = \frac{P_x I_c}{P_x + I_c} \quad (2.45)$$

which is a combination of the equations for Q_s and P_x . The infiltration capacity is written as follows:

$$I_c = D_{b,i} [1 - \exp(-K_{at} * \Delta t)] \quad (2.46)$$

If the evapotranspiration rate from the upper soil layer is equal to the potential rate (i.e. $E_u = E_p$), then E_b is zero. E_b is expressed as:

$$E_b = (E_p - E_u) \left(1 - \frac{D_{b,i}}{D_{b,max}} \right) \quad (2.47)$$

As with the upper layer evapotranspiration, the lower layer evapotranspiration, E_b , could potentially be greater than the soil moisture capacity, $D_{b,max}$. Schaake et al. (1996) did not mention a constraint for this. Thus, a constraint is not applied.

Subsurface runoff Q_g , is modeled as the lower layer moisture content that exceeds S_{max} , the minimum threshold of D_b .

$$Q_g = \begin{cases} Q_{max} \left(1 - \frac{D_{b,i}}{S_{max}} \right), & D_{b,i} < S_{max} \\ 0 & \text{otherwise} \end{cases} \quad (2.48)$$

where Q_{max} represents the potential subsurface runoff that occurs when the lower layer is saturated ($D_b = 0$). According to Schaake et al. (1996), S_{max} is usually less than $D_{b,max}$. Note that the equation above doesn't prevent the possibility that $Q_g > D_{b,max} - D_{b,i}$.

The total streamflow is then calculated as $Q = Q_s + Q_g$. The parameters to be calibrated are $D_{u,max}$, $D_{b,max}$, Q_{max} , S_{max} , K_{dt} . A diagram of the model is provided in Figure 2.6.

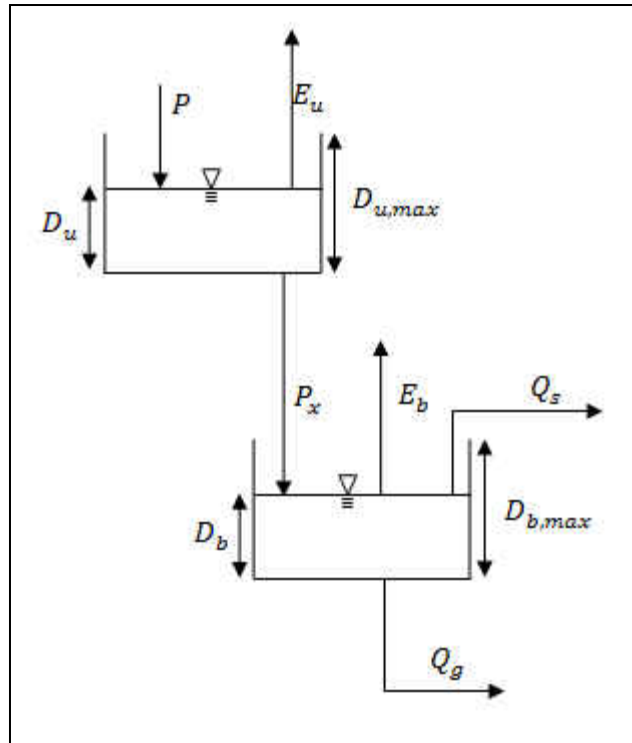


Figure 2.6. SWB Model.

2.8 Vandewiele Model

Vandewiele and Elias (1995) presented a single-reservoir model with three free parameters. In the model, a fraction of the runoff can be immediately calculated:

$$Q_b = a_2(S_{t-1})^{b_1} \quad (2.49)$$

where Q_b is the first component of runoff, S_{t-1} is the soil moisture storage at the beginning of the time period, a_2 is a free parameter to be calibrated, and b_1 is one of the two restricted parameters having values of 0.5, 1, or 2. The water quantity available for evapotranspiration is defined as:

$$W = P + S_{t-1} \quad (2.50)$$

In this equation, P represents the precipitation during the time period. In the model, evapotranspiration, E , is expressed in either of two equations:

$$E = \begin{cases} E_p \left[1 - a_1 \left(\frac{W}{E_p} \right) \right] & E < W \\ W & \text{otherwise} \end{cases} \quad (2.51)$$

$$E = \begin{cases} W \left[1 - \exp \left(-\frac{E_p}{a_1} \right) \right] & E < E_p \\ E_p & \text{otherwise} \end{cases} \quad (2.52)$$

where E_p represents the potential evapotranspiration and a_1 is a free parameter to be calibrated.

The fraction of precipitation reduced by the evapotranspiration is defined as:

$$P_n = P - E \left[1 - \exp \left(-\frac{P}{E} \right) \right] \quad (2.53)$$

The second component of runoff is defined as:

$$Q_r = a_3 (S_{t-1})^{b_2} \cdot P_n \quad (2.54)$$

where a_3 is the third free parameter to be calibrated and b_2 is a restricted parameter with possible values of 0, 0.5, 1, or 2. The total runoff is defined as:

$$Q = Q_b + Q_r \quad (2.55)$$

Then, the soil moisture storage is updated for the next time period based on the water balance equation:

$$S_t = S_{t-1} + P - E - Q \quad (2.56)$$

In the model above, there are two restricted parameters (b_1 and b_2), and two equations for evapotranspiration. Thus, there are a total number of $3 \times 4 \times 2 = 24$ model forms to test. In their study, Vandewiele and Elias (1995) found that the model form (model #24) with $b_1 = 2$, $b_2 = 2$, and the second evapotranspiration equation worked best.

The model is similar to Vandewiele et al. (1992) (as described by (Makhlouf & Michel, 1994)). The primary difference is the expression of P_n :

$$P_n = P - E_p [1 - \exp(P/E_p)] \quad (2.57)$$

Makhlouf and Michel (1994) tested the Vandewiele et al. (1992) model and assumed that b_1 was 2 and b_2 was 1 (second model form). In their study they used the first equation for evapotranspiration. A diagram of the model is provided in Figure 2.7.

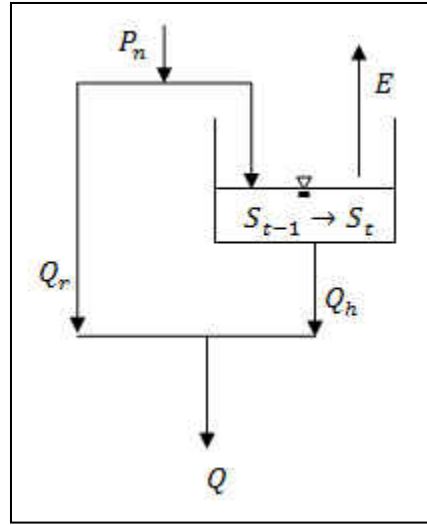


Figure 2.7. Vandewiele Model

2.9 GR2M Model

GR2M is a two-storage model with two free parameters and two assumed parameters (Makhlouf & Michel, 1994). In the model, evaporation and a modified value of precipitation are calculated as:

$$P_n = P - \left[\frac{P \cdot E_p}{(P^{0.5} + E_p^{0.5})^2} \right] \quad (2.58)$$

$$E_n = E_p - \left[\frac{P \cdot E_p}{(P^{0.5} + E_p^{0.5})^2} \right] \quad (2.59)$$

where E_p is potential evapotranspiration and P is precipitation. Next, these values are modified by the following equations:

$$P'_n = X_1 P_n \quad (2.60)$$

$$E'_n = X_1 E_n \quad (2.61)$$

In the first storage reservoir, H is the storage at the beginning of the time period. It is then updated to H_1 via the following equation:

$$H_1 = \frac{H + AV}{1 + \left(\frac{HV}{A}\right)} \quad (2.62)$$

where

$$V = \tanh(P'_n/A) \quad (2.63)$$

Makhlouf and Michel (1994) assumed in their study that $A = 200$ mm. Rainfall excess, P_e , is calculated as

$$P_e = P'_n + H - H_1 \quad (2.64)$$

The first storage reservoir is updated a second time to H_2 :

$$H_2 = \frac{H_1(1 - W)}{\left\{1 + W \left[1 - \left(\frac{H_1}{A}\right)\right]\right\}} \quad (2.65)$$

Similar to V , W is defined as

$$W = \tanh(E'_n/A) \quad (2.66)$$

In the second storage reservoir, S is the storage at the beginning of the time period. It is then updated to S_1 via the following equation:

$$S_1 = S + (1 - F)P_e \quad (2.67)$$

Makhlouf and Michel (1994) assumed F was 0.2 in their study. The second reservoir releases a certain amount of runoff, Q_s :

$$Q_s = X_2 S_1 \quad (2.68)$$

Then, storage in the second reservoir is updated to S_2 :

$$S_2 = S_1 - Q_s \quad (2.69)$$

The total runoff can then be calculated as follows:

$$Q = Q_s + F \cdot P_e \quad (2.70)$$

H_2 and S_2 then become H and S , respectively, for the next month. Makhoulf and Michel (1994) recommend that A and F not be allowed to vary, at least for catchments located in France, though “in other climatic and physiographic settings, these two constant parameters may take on differing values” (Makhoulf & Michel, 1994). A diagram of the model is displayed in Figure 2.8.

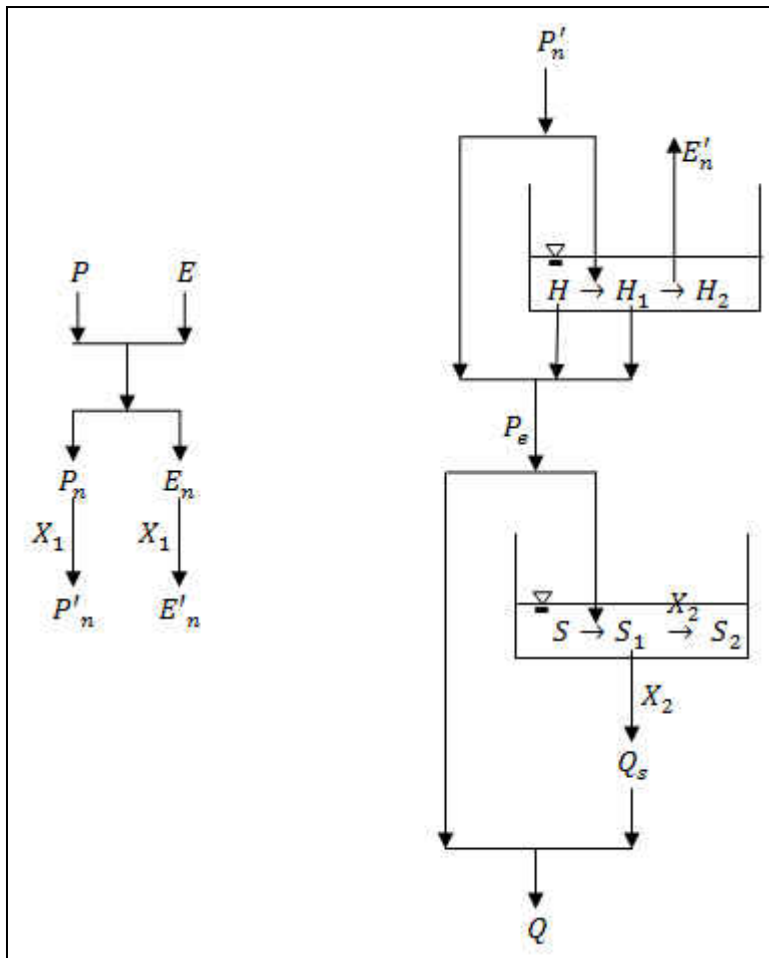


Figure 2.8. GR2M Model.

2.10 Dynamic Water Balance Model

The fundamental concept behind the Zhang et al. (2008) dynamic water balance model (DWB) is the application of the Fu equation (Fu, 1981) at multiple time scales.

The principle behind the Fu equation is the same as most other models based on the Budyko framework. In the Fu equation, it is assumed that the dominant control on the water

balance is the climate (water availability, P , and atmospheric demand, E and E_p), expressed by terms such as the evaporation ratio (E/P) and the aridity index (E_p/P). It is also assumed that storage change (ΔS) is negligible, so that the water budget can be approximated by $P = Q + E$. This assumption has been shown to be strong for applications at the annual time scale to the mean annual time scale (i.e. one year per time period to multiple years per time period). The equation itself is commonly expressed as

$$\left(\frac{E}{P}\right)_i = 1 + \frac{E_p}{P} - \left[1 + \left(\frac{E_p}{P}\right)^w\right]^{1-w} \quad (2.71)$$

where E is the evapotranspiration, E_p is the potential evapotranspiration, and w is a parameter to be calibrated. This equation can be rewritten with w replaced by α :

$$\left(\frac{E}{P}\right)_i = 1 + \frac{E_p}{P} - \left[1 + \left(\frac{E_p}{P}\right)^{\frac{1}{1-\alpha}}\right]^{1-\alpha} \quad (2.72)$$

where $\alpha = 1 - \frac{1}{w}$.

In applying the original Fu equation to time scales finer than the annual time scale, Zhang et al. saw a greater need to account for the increasing impact of storage change to simulate storage control and slow release processes. This required increasing model complexity and including additional processes. Thus, the Budyko framework is generalized to a demand and supply framework, i.e., the application of the “limits” concept, (Zhang et al., 2008) which is similar to the limits concept behind the abcd model.

The DWB model uses two storage reservoirs: (1) a root zone storage and (2) a groundwater storage. It is assumed that precipitation, P , is divided between catchment rainfall retention, X , and direct runoff, Q_d :

$$P(t) = Q_d(t) + X(t) \quad (2.73)$$

where $X(t)$ is the rainfall retained by the catchment for evapotranspiration, $E(t)$, soil moisture storage change, $S(t) - S(t-1)$, and recharge, $R(t)$. $X_p(t)$ represents the potential of $X(t)$ and is defined as the sum of available storage capacity (or soil moisture deficit), $S_{max} - S(t-1)$, and potential evapotranspiration:

$$X_p(t) = [S_{max} - S(t-1)] + E_p(t) \quad (2.74)$$

Thus, $X(t)$ can be calculated as a function of $X_p(t)/P(t)$ and α_1 using a Fu-type equation:

$$X(t) = P(t) \cdot F\left(\frac{X_p(t)}{P(t)}, \alpha_1\right) \quad (2.75)$$

where $F\left(\frac{X_p(t)}{P(t)}, \alpha_1\right)$ represents the Fu equation as a function of $X_p(t)/P(t)$ and α_1 . That is,

$$X(t) = P(t) \cdot \left[1 + \frac{X_p(t)}{P(t)} - \left[1 + \left(\frac{X_p(t)}{P(t)} \right)^{\frac{1}{1-\alpha_1}} \right]^{1-\alpha_1} \right] \quad (2.76)$$

where α_1 is the retention efficiency (a parameter to be calibrated). $X_p(t)/P(t)$ is analogous to the aridity index and is an expression of how supply and demand regulates the partitioning of precipitation. From the expression for precipitation, direct runoff can be calculated:

$$Q_d(t) = P(t) - X(t) \quad (2.77)$$

Water availability, $W(t)$, analogous to “available water” in the abcd model, is defined as:

$$W(t) = X(t) + S(t-1) \quad (2.78)$$

$W(t)$ is then partitioned between evapotranspiration opportunity, $Y(t)$, and recharge $R(t)$.

The definition of $Y(t)$ is identical to the definition in the abcd model, and is defined as the sum of evapotranspiration and storage, $Y(t) = E(t) + S(t)$. The partitioning of $Y(t)$ from $W(t)$ is defined as:

$$Y(t) = W(t)F\left(\frac{E_p(t) + S_{max}}{W(t)}, \alpha_2\right) \quad (2.79)$$

where α_2 is the evapotranspiration efficiency. That is,

$$Y(t) = W(t) \left[1 + \frac{E_p(t) + S_{max}}{W(t)} - \left[1 + \left(\frac{E_p(t) + S_{max}}{W(t)} \right)^{\frac{1}{1-\alpha_2}} \right]^{1-\alpha_2} \right] \quad (2.80)$$

so that:

$$R(t) = W(t) - Y(t) \quad (2.81)$$

Next, to partition the water from $Y(t)$ between $E(t)$ and $S(t)$, the following Fu-type equation is defined for $E(t)$:

$$E(t) = W(t)F\left(\frac{E_p(t)}{W(t)}, \alpha_2\right) \quad (2.82)$$

or,

$$E(t) = W(t) \left[1 + \frac{E_p(t)}{W(t)} - \left[1 + \left(\frac{E_p(t)}{W(t)} \right)^{\frac{1}{1-\alpha_2}} \right]^{1-\alpha_2} \right] \quad (2.83)$$

α_2 is used for both the definition of $Y(t)$ and $E(t)$ because Zhang et al. assumed that groundwater recharge is mainly determined by evapotranspiration efficiency. It is also identical to enforce the condition that $0 < S(t) < S_{max}$. Thus,

$$S(t) = Y(t) - E(t) \quad (2.84)$$

Groundwater storage from the previous time period is partitioned into groundwater discharge:

$$Q_b(t) = dG(t-1) \quad (2.85)$$

where the parameter d is the recession constant. Though this equation is similar to the abcd model (even the same parameter symbol is used), it is different in that the abcd model uses the groundwater storage from the current time step.

Thus, groundwater storage in the current time step is determined by:

$$G(t) = (1 - d) \cdot G(t-1) + R(t) \quad (2.86)$$

Also,

$$Q = Q_b + Q_d \quad (2.87)$$

where Q is the total runoff. Below is a diagram of the model.

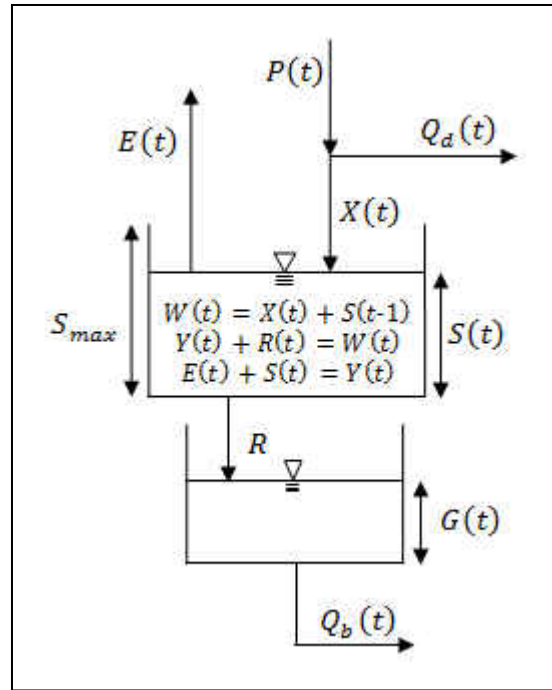


Figure 2.9. Dynamic Water Balance (DWB) Model.

2.11 Equity Model

The Fu Equation, as discussed in the Dynamic Water Balance model by Zhang et al. (2008) is one of several different types of Budyko models. One Budyko-type model, proposed by Wang and Tang (2014), is based on a proportionality relationship similar to the curve number method. In this model, there are two components of evapotranspiration: (1) initial evapotranspiration and (2) continuing evapotranspiration. The definitions of these two components are analogous to the two components of abstraction in the curve number method.

Before runoff, Q , can occur, initial evapotranspiration, E_0 , removes a component of precipitation. After this process occurs, runoff and continuing evapotranspiration, E_c , complete

for the remaining supply of water (i.e. $P - E_0$). This process is described by the following proportionality relationship:

$$\frac{E_c}{E_p - E_0} = \frac{Q}{P - E_0} \quad (2.88)$$

where E_p represents the potential evapotranspiration. The numerators in this expression represent the competing processes while the denominators represent their potentials. The continuity equation for this model is expressed as follows:

$$P = Q + E \quad (2.89)$$

where $E = E_c + E_0$. This model is intended for application at the mean annual scale (i.e. each time step is three or more years), so that soil moisture and groundwater storage change is usually negligible. Substituting this expression into the proportionality relationship of Equation (2.88) and solving the equation for E/P results in the following equation:

$$\frac{E}{P} = \frac{\left(1 + \frac{E_p}{P}\right) - \sqrt{\left(1 + \frac{E_p}{P}\right)^2 - 4\varepsilon\left(\frac{E_p}{P}\right)(2 - \varepsilon)}}{2\varepsilon(2 - \varepsilon)} \quad (2.90)$$

where $\varepsilon = E_0/E$. In practice, ε is treated as a parameter to be calibrated, since there is no other method to estimate this ratio. The continuity equation in Equation (2.89) can be solved for Q to estimate the runoff. An illustration of this model is provided in Figure 2.10.

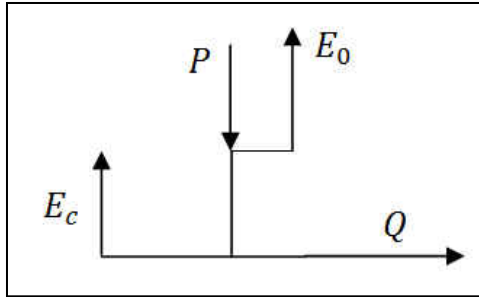


Figure 2.10. The Equity Model.

CHAPTER 3: METHODOLOGY

3.1 Data

In the simulation of daily, monthly, and annual streamflow, potential evapotranspiration and precipitation data are used as input data to the models, while streamflow data are outputs used to evaluate, calibrate, and validate the models.

3.1.1 MOPEX Data Set

All input data used in all models are mean areal values. Data used for evaluating, calibrating, and validating each model is primarily based on the Model Parameter Estimation Experiment (MOPEX) dataset (Duan et al., 2006). The MOPEX dataset provides daily data for potential evapotranspiration, precipitation, streamflow, and minimum and maximum temperatures, along with other data, for 438 catchments across the conterminous United States.

MOPEX Precipitation data is based on hourly and daily precipitation data sets from the National Climate Data Center (NCDC). MOPEX Potential evapotranspiration data are based on evaporation estimates obtained from the NOAA Freewater Evaporation Atlas (Farnsworth et al., 1982). MOPEX Daily streamflow measurements were collected by the US Geological Survey (USGS).

However, because the daily potential evapotranspiration data is hydro-climatological values and the MOPEX dataset lacks evapotranspiration data, the evapotranspiration and

potential evapotranspiration data were obtained from the Numerical Terradynamic Simulation Group at the University of Montana instead (Zhang, 2010).

In the study by Alley (1985), the abcd and Thornthwaite and Mather models were used to simulate streamflow for catchments in New Jersey. In his study, Alley (1985) concluded that the poor performance of the models during winter months could be due to a lack of accounting of the effects of snow and frozen ground. Dripps and Bradbury (2007) reached a similar conclusion in the application of a daily water balance model based on a modified Thornthwaite Mather model: he found that recharge estimates were highly overestimated during the months of February, citing the effects of frozen ground on infiltration. For this reason, and since the proposed model is not developed to incorporate the effects of frozen ground or snow accumulation, the selection of watersheds emphasized avoiding these types of areas. Thus, analysis was initially restricted to fifty-five catchments in the Southeastern United States (Figure 3.1).

However, seventeen additional watersheds in the West, Midwest, and Northeast were selected, with an emphasis placed on (1) avoiding mountainous areas, (2) choosing catchments with high mean annual aridity indices $\left(\frac{E_p}{P-\Delta S}\right)$ (except for the Northeast), (3) avoiding high percentage precipitation as snow (PPS) areas, and (4) by choosing low population density areas. In Figure 3.1, PPS contour lines are based on a map provided by Martinez and Gupta (2010) and were used as a guide in the selection process.

In regards to the first selection criterion, high sloping topography that could significantly impact hydrologic processes is not constrained to major mountain ranges; only a site-by-site investigation can reveal if a selected catchment is significantly impacted by high sloping

topography. Additionally, this criterion was not set for the selection of the first 55 catchments. Thus, a few of the catchments are located in mountainous areas.

For all 71 catchments, the areas range from 67 km² to 10,375 km² with an average of 3,655 km². A map of the storage-corrected mean annual aridity indices $\left(\frac{E_p}{P-\Delta S}\right)$ is provided in Figure 3.2. Climates in the South Central United States east of Texas tend to have very low aridity indices (humid climates) while climates in the West North Central and West South Central tend to have very high aridity indices (very dry climates).

In the model parameter calibrations that were performed, some watersheds that were selected persistently scored very low, regardless of the model or the time scale used. Six of these are the most significant and are discussed in the Section 6.1.

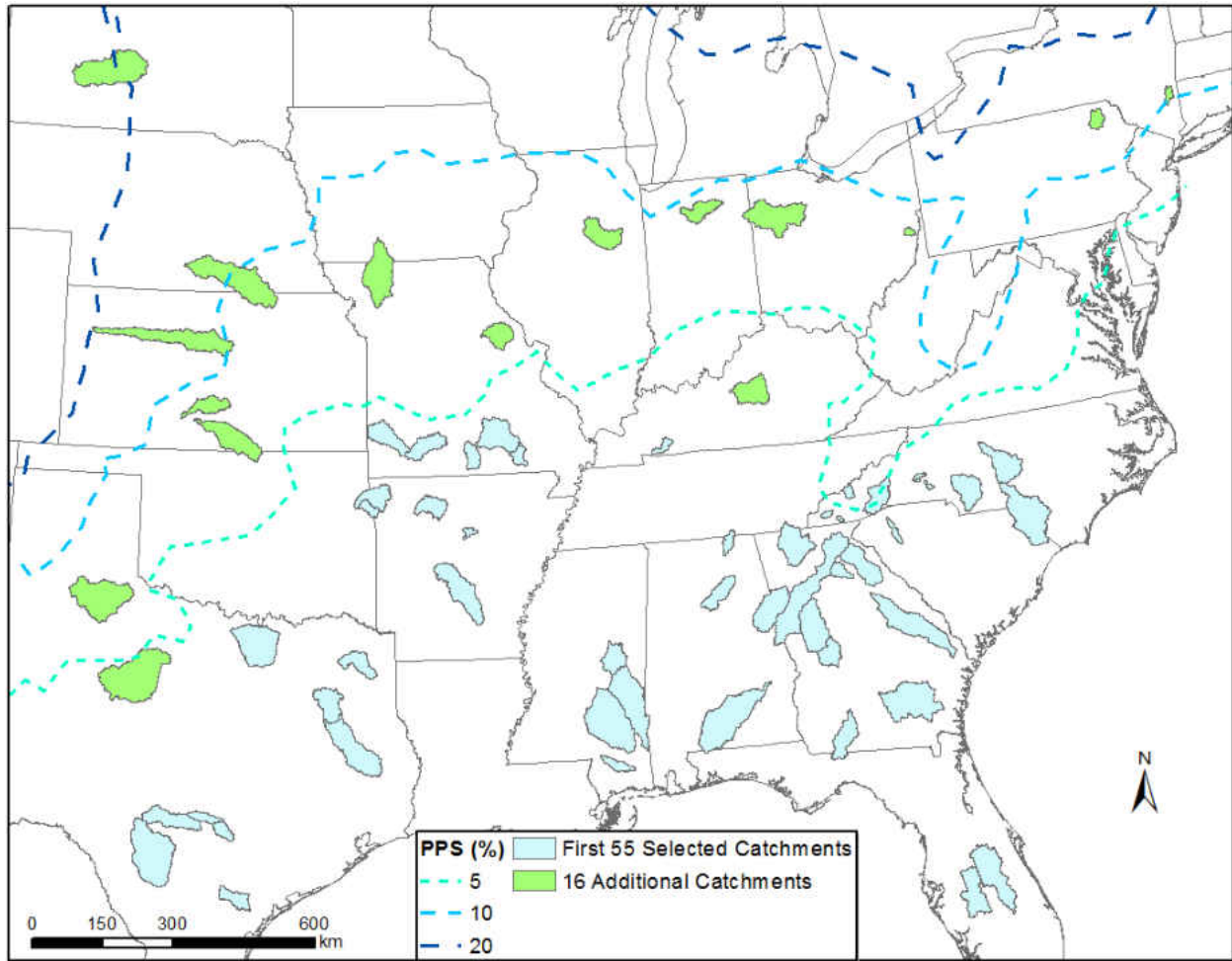


Figure 3.1. Selected Catchments for Analysis of the Proposed Model Structure. Blue catchments represent the initially selected 55 catchments. Green catchments represent the 16 additional catchments. Dash lines represent percentage precipitation as snow (PPS) as delineated by Martinez and Gupta (2010).

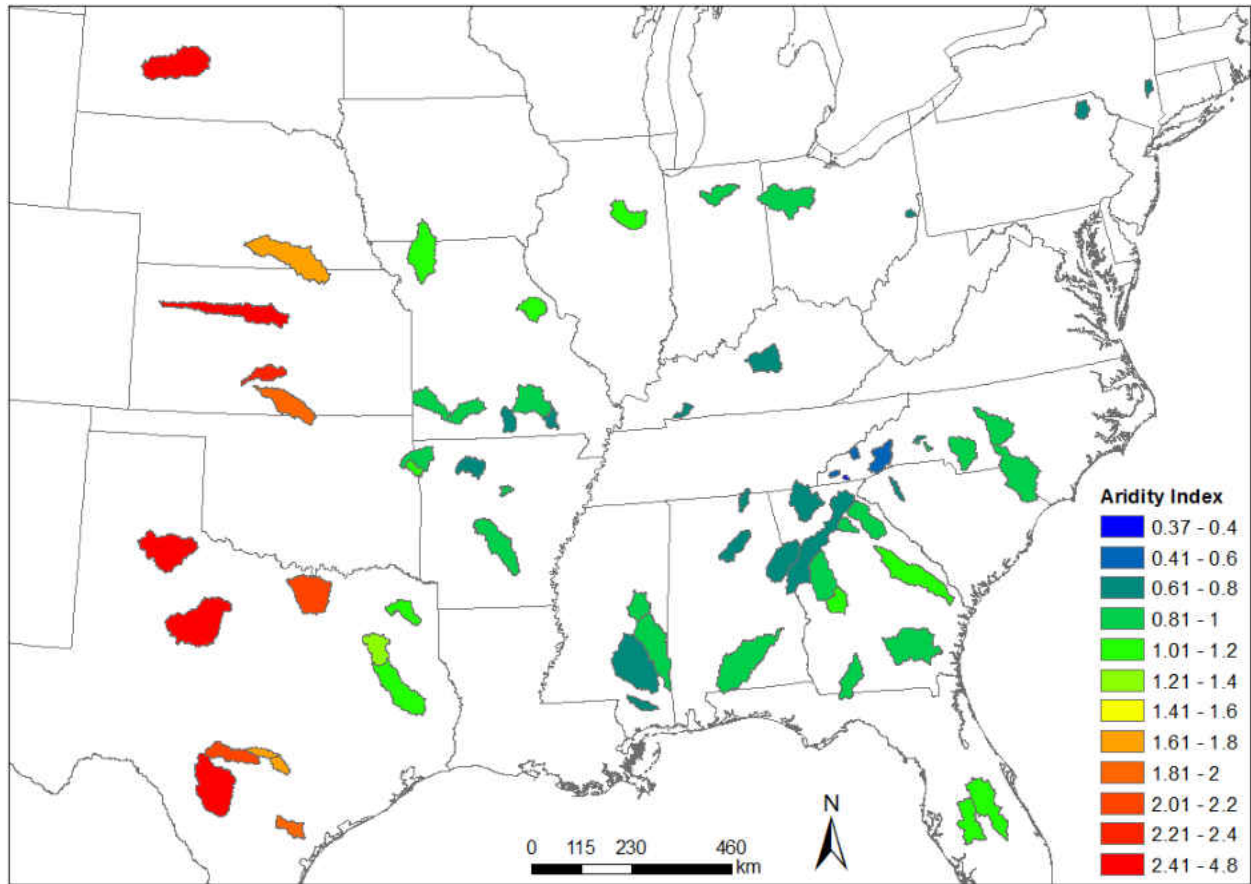


Figure 3.2. Aridity Index ($E_p/(P - \Delta S)$) for 71 MOPEX catchments.

3.1.2 Evapotranspiration and Potential Evapotranspiration Data Set

For the equations in this section, potential evapotranspiration (E_p) is referred to by the term *PET* for the sake of clarity. Daily evapotranspiration and monthly potential evapotranspiration data are provided at a spatial resolution of 8-km by the Numerical Terradynamic Simulation Group (NTSG) (Zhang, 2010). In the equations that follow, this data will be denoted by the subscript “NTSG”.

The MOPEX potential evapotranspiration data, accumulated to the monthly scale, is used to bias-correct the monthly NTSG PET data as follows

$$PET_j = \frac{\overline{PET_M^{MOPEX}}}{\overline{PET_M^{NTSG}}} \cdot PET_j^{NTSG} \quad (3.1)$$

where

$$\overline{PET_M^{NTSG}} = \frac{\sum_{j=1}^{n_m} (PET_j^{NTSG})}{n_m} \quad (3.2)$$

and

$$\overline{PET_M^{MOPEX}} = \frac{\sum_{j=1}^{n_m} (PET_j^{MOPEX})}{n_m} \quad (3.3)$$

where n_m is the number of matching months in both datasets. For the MOPEX and NTSG datasets, only the time period from 1/1983 to 12/2003 (21 years or 252 months) was used. PET_j represents the estimated PET data for month j , while PET_j^{NTSG} represents PET data for month j based on the NTSG dataset. $\overline{PET_M^{NTSG}}$ and $\overline{PET_M^{MOPEX}}$ represent the mean monthly NTSG PET and MOPEX PET, respectively.

Since NTSG PET data is only available at the monthly time-scale, this data was rescaled using the daily MOPEX PET data as follows:

$$PET_{i,j} = PET_{i,j}^{MOPEX} \times \frac{PET_j}{\left(\sum_{i=1}^{n_d} PET_{i,j}^{MOPEX}\right)} \quad (3.4)$$

where $PET_{i,j}^{MOPEX}$ represents the daily MOPEX PET data for day i of month j , $PET_{i,j}$ denotes the estimated PET data for day i of month j , and n_d represents the number of days in month j .

3.2 Test Statistics (Performance Metrics)

There are a large number of test statistics available in the literature, two of the most common being the mean square error (MSE), and the Nash-Sutcliffe coefficient of efficiency (Nash & Sutcliffe, 1970). The MSE is defined as follows:

$$MSE = \frac{\sum_{i=1}^n (Q_{est,i} - Q_{obs,i})^2}{n} \quad (3.5)$$

where $Q_{est,i}$ represents the estimated (modeled) discharge, $Q_{obs,i}$ is the discharge from observation data, and n are the number of records of observation data.

The Nash–Sutcliffe coefficient of efficiency (NSE) is expressed as follows:

$$NSE = 1 - \frac{\sum_{i=1}^n (Q_{est,i} - Q_{obs,i})^2}{\sum_{i=1}^n (Q_{obs,i} - \bar{Q}_{obs})^2} \quad (3.6)$$

where \bar{Q}_{obs} represents the average of observed records. Values range between $-\infty < NSE < 1$.

Values closer to one are better (i.e. a value of one represents a perfect prediction). The NSE can be defined alternatively as:

$$NSE = 1 - MSE/\sigma_{Q_{obs}}^2 \quad (3.7)$$

where $\sigma_{Q_{obs}}^2$ represents the variance of the observed flows.

Martinez and Gupta (2010) provide a detailed discussion of the Nash-Sutcliffe coefficient of efficiency. In particular, they mention that a major weakness of the NSE is its strong tendency to underestimate the variability of flows.

In the calibration of model parameters, the NSE is the sole criterion used, particularly because it is a commonly used criterion and it facilitates the comparison of model results with results found in the literature (Makhlouf & Michel, 1994; Martinez & Gupta, 2010).

3.3 Optimization Methodology

Most hydrological models have multiple parameters that need to be calibrated before they can be used. Calibration is usually done using an algorithm; one commonly used algorithm is the shuffled complex evolution (SCE-UA) algorithm Duan et al. (1992; 1994). It has been used for several models in numerous studies, including calibration of the SWB model (Schaake et al., 1996), the abcd model (Martinez & Gupta, 2010; Sankarasubramanian & Vogel, 2002), and the Wapaba model (Wang et al., 2011).

In this study, model parameters were calibrated using the “ga” (genetic algorithm) function in Matlab 7. For all models during parameter calibration, simulations were run 20 times for all 71 catchments at each time scale ($71 \times 20 \times 3 = 4,260$ simulations per model). The multiple simulations were necessary because, unlike optimization methods like the SCE-UA, genetic algorithms are susceptible to premature convergence, which can prevent them from reaching an optimal solution. Premature convergence is usually caused by a loss in “genetic diversity” within the “population” and is difficult to predict because the population generated by the algorithm is determined by a random number generator. However, setting the population count high enough tends to reduce the frequency of this phenomenon considerably to the point that its influence on the final result tends to be negligible. In the case of this study, a population of 500 was used.

Additionally, identical upper limits were set for soil moisture capacities for all models. For two-tank models, like the proposed model, this was done by writing $S_{1,max} = k_0 S_{max}$ and $S_{2,max} = (1 - k_0) S_{max}$. For the daily and monthly time scales, the limit was set to 1500 mm, while for the annual time scale, the limit was increased to 2600 mm to account for the increased need for routing. This modification was especially important for the abcd model and the proposed model.

3.4 Problems Encountered in Hydrologic Modeling

3.4.1 Effect of Temporal Lumping on Data Quality

Whenever hydrologic data is temporally aggregated (or “lumped”), valuable information is lost regarding the timing of precipitation and evapotranspiration. This is most pronounced between the daily and monthly time scales, but dramatically increases at the annual scale, where seasonality is no longer evident. For example, at the monthly time scale (using monthly data as input to a hydrologic model), prediction errors can occur when a significant fraction of the daily precipitation occurs late in the month (Thomas, 1981).

In order to account for the loss of this important variability at larger time scales, it is common to represent the partitioning of available water to evapotranspiration prior to or concurrently with surface runoff. At shorter time scales, however, it is more appropriate to divide the precipitation between the soil and surface runoff first. Then, soil water allocation can be split between evapotranspiration and baseflow demands. However, evapotranspiration, in a

sense, still competes with surface runoff by lowering the water level in the soil moisture for the next time period.

In a frequency analysis of streamflow, low frequency variability (i.e. low variation in streamflow or “slow flow”) is more likely to be associated with baseflow while high frequency variability (“fast flow”) is primarily the result of direct runoff (i.e. the sum of interflow and surface runoff) (Eckhardt, 2005). However, interflow, which is subsurface flow through the unsaturated zone, has a fast component and slow component, and consequently, fast interflow will be interpreted as direct runoff while slow interflow will be lumped with baseflow (Xu & Singh, 1998).

This presents a challenge in the modeling of runoff at larger-than-daily time scales because, as time scales increase, the variability in streamflow, precipitation, and evapotranspiration decreases, which tend to decrease the quantity of direct runoff simulated. A model developed at one time scale to simulate baseflow and direct runoff processes will need to be able to simulate a higher portion of baseflow occurring at larger time scales.

To deal with this problem, routing is usually performed. However, each routing process often requires an additional parameter. It should be noted that routing is also important for delaying the runoff response in large catchments, though routing processes typically account for this effect along with the effect of temporal lumping on input data simultaneously.

3.4.2 Regional Groundwater Flow

Groundwater, which is not restricted by topography in the same way that surface water is, has a much greater tendency to cross catchment boundaries. This can be a significant factor when catchments are located by large neighboring bodies of water. One particular example is Greers Ferry Lake, located next to catchment 07261000 (Figure 3.3). However, to simplify the analysis, most studies assume that the effects of regional groundwater flow are negligible so that the entire measured streamflow can be accounted for by the precipitation that falls within the catchment boundaries.

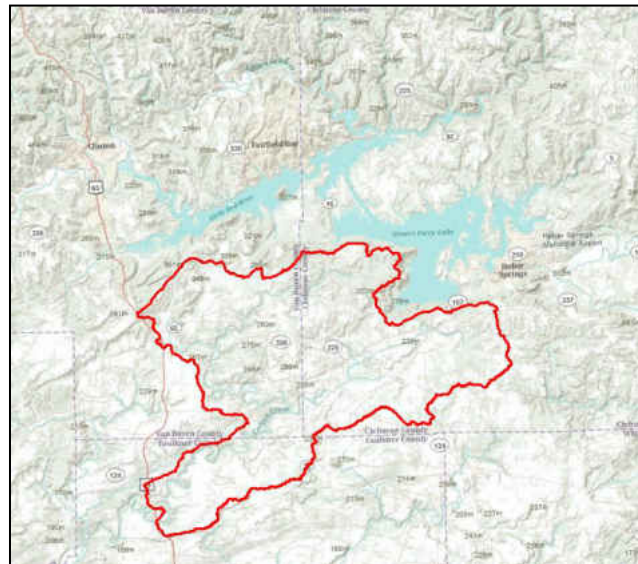


Figure 3.3. Catchment 07261000.

3.4.3 Saturation Excess vs. Infiltration Excess

Saturation excess occurs when the soil moisture layer reaches its capacity (is saturated) so that any additional precipitation produces surface runoff. Infiltration excess generated overland flow, also known as Hortonian flow, occurs when the rainfall intensity rates exceed the infiltration capacity of the soil (Walter, 2005a, 2005b).

“Bucket models” (i.e. models that use limited-capacity reservoirs to represent soil moisture storage) generally model saturation excess well. Infiltration excess is more difficult to simulate with these models; however, it can be modeled more accurately at smaller time steps, but each time step would need to be small enough for cumulative precipitation values to accurately represent rainfall intensity rates (i.e. a time step of hours or minutes).

Better predictions from a bucket model are typically during wet seasons where saturation excess is the primary driver of direct runoff generation.

3.4.4 Fluctuating Groundwater Table

Evapotranspiration rates, largely determined by the available energy provided by solar radiation, are also strongly dependent on the availability of water in the soil column. As discussed previously, vegetation provides the medium for evapotranspiration processes to occur far below the soil surface. Vegetation water extraction rates are higher in the saturated zone (below the groundwater table) compared with the unsaturated zone (above the groundwater table). This variation is caused by capillarity and the adhesive forces between water and soil particles (i.e. the matric potential). These mechanisms play a major role in the ability of the soil

in the unsaturated zone to transmit water through the soil column. It results in the varying water availability throughout the unsaturated zone and impedes the extraction of water by vegetation.

As groundwater levels decline, the proportion of water from the saturated and unsaturated zones changes. Thus, vegetation with shallow root systems may not be able to extract water from the saturated zone and will have to rely on water from the unsaturated zone, causing actual evapotranspiration rates to vary disproportionately with potential evapotranspiration rates.

Ideally, hydrologic models should incorporate a maximum root depth term to represent this aspect. However, doing so may be difficult to express, especially if a bucket model with multiple tanks is used.

3.5 Model Calibration and Validation

During the full-record calibration stage, models were calibrated to all 21 years of data to evaluate the ability of the models to match the observed streamflow records. In the half-record calibration stage, the models were calibrated to the first 10 years of data. In the validation stage, models were validated across the remaining 11 years of data using the parameters obtained from the half-record calibration stage to test the skill of the individual models as streamflow prediction tools. This methodology (excluding the full-record calibration) is based on the one used by Zhang et al. (2008) where it was referred to as the “split-sample test”. Parameter calibrations for the full-record and half-record calibration stages were done for the daily, monthly, and annual time scales.

The models required setting initial conditions for the soil moisture and groundwater reservoirs. For all models, the initial soil moisture condition was assumed to be at capacity ($S = S_{max}$ or $S = b$ for the abcd model). Also, all groundwater reservoirs are assumed to be initially empty.

It was assumed that the models could self-correct for the true storage values if they were given an initial warm-up period (i.e. a short time interval at the beginning when the model performance is not evaluated). At the monthly time scale, the warm-up period was set to 24 months. This value was determined subjectively and was believed to be sufficiently long enough to diminish the effects of the assumed initial conditions. At the daily time scale, 24 daily data records were used for warm-up because an analysis of various warm-up periods did not find an advantage in using a longer time period. For the annual time scale, 3 years of annual data were used because data records were much more limited. Shorter and longer warm-up periods were tested for the annual time scale, and in fact model performance improved when two years of data were used. However, this apparent advantage is likely due to the particular time period chosen for the warm-up rather than the actual length of the warm-up period. With such a short data record to calibrate, warm-up, and validate the models over, the influence that the variability of individual annual data records has on model performance is significant. Thus, the warm-up time period for the annual time scale was kept at three years.

3.5.1 Model Assumptions

Though the assumptions regarding the application of the models are usually made in other water balance model simulations, it is worth mentioning. First, it is assumed that all of the models can be applied in a lumped (“aggregated”) manner. Second, water that drains into lakes, wetlands, and swamps is not accounted for (land cover is assumed to be uniform across each catchment). Third, all infiltration is assumed to occur as one-dimensional vertical infiltration. Fourth, the effects of erosion caused by throughfall, vegetation, and infiltration on the soil profile are considered insignificant. Fifth, and most importantly, it is assumed, as was done by Martinez and Gupta (2010), that the distribution and timing of precipitation events, potential evapotranspiration, etc. at smaller time scales is negligible.

3.6 Development of the Proposed Model

Developing a model where all processes are included is not only impractical (if not impossible), but would also require a substantial quantity of data to calibrate the model that is not available. Thus, in the pursuit of a parsimonious model structure, and in recognition of the fact that various processes have varying degrees of influence at different time scales, only the most significant processes (for any time scale) will be included. As stated by Zhang et al. (2008), “the interaction and co-evolution of [individual hydrologic processes] may manifest themselves in such a way that the overall behavior of the catchment can be described by simple relationships.”

In the development of the model, different model structures and processes will be investigated. Model variations which lead to higher performance values (using the NSE) will be selected for further model development.

The model being developed is intended to be used as a lumped model (i.e. input data is spatially aggregated for the entire area of interest). The following sections will describe the model development until the selection of the proposed model.

3.6.1 Initial Model Stage

The initial model structure is based on a two-stage two-bucket and tank model. The data inputs to the model are precipitation (P) and potential evapotranspiration ($E_p(t)$), which produce outputs of baseflow ($Q_b(t)$), direct (surface) runoff ($Q_d(t)$), total runoff $Q(t)$, and evapotranspiration ($E(t)$). The internal processes include initial and continuing abstraction ($I_a(t)$ and $F_a(t)$), initial and continuing evapotranspiration ($E_0(t)$ and $E_c(t)$), recharge ($R(t)$), storages for both buckets ($S_1(t)$ and $S_2(t)$), groundwater discharge ($G(t)$), and river network routing $N(t)$. Parameters that need to be calibrated include the maximum storages in the first and second buckets ($S_{1,max}$ and $S_{2,max}$, respectively), and three other parameters (k_1 , k_2 , and k_3).

3.6.1.1 Model Processes in Stage 1

In Stage 1, precipitation first enters bucket 1. Bucket 1 represents the top layer of soil, which is primarily subjected to the effects of surface vegetation, subsurface vegetation (i.e. root

systems), and a portion of the unsaturated zone. Precipitation must exceed the deficit in bucket 1 before it can move any further into the soil.

In this model, the deficit is represented by the initial abstraction:

$$I_a(t) = S_{1max} - S_1(t-1) \quad (3.8)$$

where $S_1(t-1)$ represents the water levels in bucket 1 at the beginning of the time period.

If the available water exceeds the initial abstraction, the available water will be allocated between continuing abstraction and direct runoff. To handle this allocation, which is modeled as a competition between the demands of the two processes, the proportionality hypothesis is employed. See the Section 1.1 for an explanation of the proportionality hypothesis.

$$\frac{F_a(t)}{S_{2max} - S_2(t-1)} = \frac{Q_d(t)}{P(t) - I_a(t)} \quad (3.9)$$

where $S_2(t-1)$ represents the water levels in bucket 2 at the beginning of the time period. The denominator on the left hand is the deficit of bucket 2, which is the driving force for the demand of continuing abstraction ($F_a(t)$). Unlike the potential of $F_a(t)$, direct runoff has no upper limit. Thus, $Q_d(t)$ is limited by only the potential of $F_a(t)$ that is expressed through the proportionality hypothesis. No further processes will involve $Q_d(t)$ until baseflow is generated. $F_a(t)$ is related to $Q_d(t)$ by:

$$F_a(t) = P(t) - I_a(t) - Q_d(t) \quad (3.10)$$

Substituting this relationship into the proportionality relationship and solving for $Q_d(t)$ results in:

$$Q_a(t) = \frac{(P(t) - I_a(t))^2}{S_{2,max} - S_2(t-1) + P(t) - I_a(t)} \quad (3.11)$$

3.6.1.2 Model Processes in Stage 2

At this stage, evapotranspiration is calculated in two parts: initial evapotranspiration, $E_0(t)$, occurs in bucket 1, which is followed by continuing evapotranspiration, $E_c(t)$, in bucket 2 if the evapotranspiration demand ($E_p(t)$) is not met by the moisture storage of bucket 1 ($E_0(t) > S_1(t)$).

Continuing evapotranspiration, $E_c(t)$, competes with recharge, $R(t)$ using the following relationship, which is based on the proportionality hypothesis:

$$\frac{E_c(t)}{E_p(t) - E_0(t)} = \frac{R(t)}{E_c(t) + R(t)} \quad (3.12)$$

Since this relationship does not define the available water in bucket 2, $S_2(t)$, and because there are two unknown variables with only one relationship, a separate equation is derived to model recharge as the runoff response of a linear reservoir:

$$R(t) = k_1 S_2(t) \quad (3.13)$$

Solving this equation for $E_c(t)$ leads to:

$$E_c(t) = 0.5[-R(t) + \sqrt{R^2(t) + 4E_p(t)R(t) - 4E_0(t)R(t)}] \quad (3.14)$$

Next, recharge empties into a groundwater reservoir, or “tank”, with infinite storage potential. The groundwater reservoir is assumed to be initially empty. Baseflow is routed from the tank using a linear regression relationship. The following equations dictate this relationship:

$$Q_b(t) = k_2 \cdot [G(t-1) + R(t)] \quad (3.15)$$

$$G(t) = G(t-1) + R(t) - Q_b(t) \quad (3.16)$$

Next, Q_b and Q_d are routed through a second reservoir (i.e. network routing), $N(t)$, to account for the time for water to flow across the catchment to the outlet:

$$Q(t) = k_3 [N(t-1) + Q_d(t) + Q_b(t)] \quad (3.17)$$

$$N(t) = N(t-1) + Q_d(t) + Q_b(t) - Q(t) \quad (3.18)$$

The following figure is an illustration of this model.

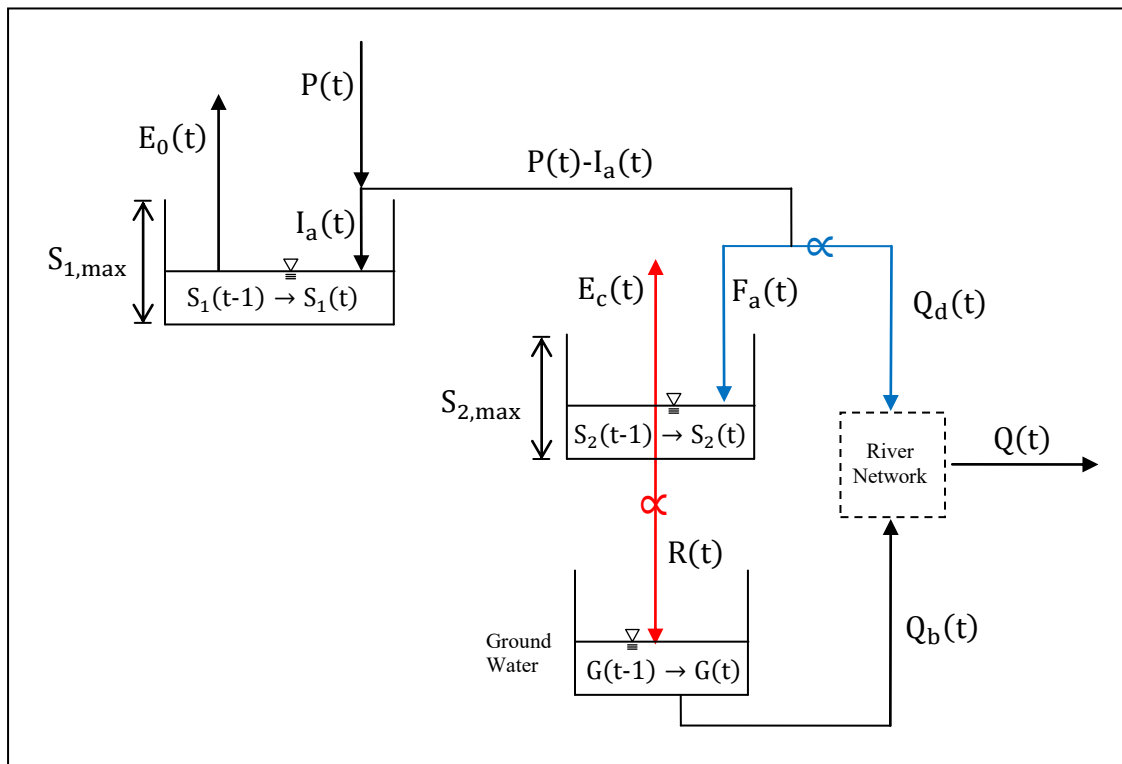


Figure 3.4. Initial Model Structure of the Proposed Model. The blue and red arrows with the proportionality symbols refer to the competition between hydrologic processes described by the proportionality hypothesis.

3.6.2 Correcting the Second Proportionality Relationship

A major problem with the original model (“Model 1”) relates to the E_c and R proportionality relationship, described in Equation (3.12). In this equation, the sum of both would often exceed S_2 . When this equation is used in conjunction with Equation (3.13), the sum of both E_c and R sometimes increases beyond S_2 , suggesting that there is no correlation between R and E_c . In the second model development stage, emphasis is placed on modifying the partitioning of subsurface flow (modeled by recharge in the initial model) to continuing evapotranspiration.

In the following sections that describe the development of the model, equations will omit the “(t)” term, which represents the current time period. This was done for the sake of clarity. Exceptions to this are the storage and routing terms (e.g. S_1 , S_2 , and G).

3.6.2.1 Models 2, 3, and 5

The first step to diagnose this problem was to use an interpolation factor ($S_2/(E_c + R)$) to rescale both E_c and R for (only) cases when this problem occurred. This modification is described as “Model 2”.

In the second modification, “Model 3”, river routing was disabled for the model (with the interpolation factor included).

The third modification, “Model 5”, replaced the $R = k_1 \cdot S_2$ equation with an abcd-type equation that describes the relationship between E_c and R:

$$E_c(t) = [S_2(t) - R] \cdot \left[1 - \exp\left(-\frac{E_p - E_0}{S_{2,max}}\right) \right] \quad (3.19)$$

However, there are problems with using these two equations together, even though there is no problem with the abcd-type equation. First, when $E_c = 0$, the proportionality relationship described by Equation (3.12) results in $R/R = 0$, or $1 = 0$, which is false. Another way to look at this equation is as follows:

$$R(t) = \frac{E_c^2}{(E_p - E_0 - E_c)} \quad (3.20)$$

Additionally, it was observed that recharge would decrease as E_c approached zero. Second, there is nothing in this equation to prevent the tank from being completely drained. Thus, it would seem that the problem is with the proportionality relationship itself. However, it was later determined that including continuing evapotranspiration, E_c , into the definition of Equation (3.13) solved this problem.

3.6.2.2 Model 7

The development of the fourth model (Model-7a) was an attempt to find a relationship to replace the E_c and R proportionality relationship presented in Equation (3.12). Model-7a redefines the proportionality relationship by combining recharge (R) with a portion of baseflow (Q_{b1}) and having it compete against continuing evapotranspiration. This was done because E_c is a factor of vegetation while R and Q_{b1} are vertical and horizontal processes of gravity. The potential of R (R_p) is based on the original linear reservoir equation ($R_p = k_1 S_2$) while the

potential of Q_{b1} ($Q_{b1,p}$) is based on a power relationship ($Q_{b1,p} = \alpha S_2(t)^\beta$). The proportionality hypothesis for E_c and R then becomes:

$$\frac{E_c}{E_p - E_0} = \frac{Q_{b1} + R}{\alpha S_2(t)^\beta + k_1 S_2(t)} \quad (3.21)$$

In this equation, the total supply of water for the competition between E_c and $Q_{b1} + R$ is represented by the denominator on the right side of the equation. The equation of continuity, solved for E_c , is

$$E_c = \alpha S_2(t)^\beta + k_1 S_2(t) - (Q_{b1} + R) \quad (3.22)$$

Substituting Equation (3.22) into (3.21) results in the following:

$$\frac{\alpha S_2(t)^\beta + k_1 S_2(t) - (Q_{b1} + R)}{E_p - E_0} = \frac{Q_{b1} + R}{\alpha S_2(t)^\beta + k_1 S_2(t)} \quad (3.23)$$

This equation is then solved for $Q_{b1} + R$.

$$Q_{b1} + R = \frac{(\alpha S_2(t)^\beta + k_1 S_2(t))^2}{[(E_p - E_0) + (\alpha S_2(t)^\beta + k_1 S_2(t))]} \quad (3.24)$$

However, to allocate water between Q_{b1} and R , an additional parameter, λ , is included:

$$R = \lambda(Q_{b1} + R) \quad (3.25)$$

$$Q_{b1} = (1 - \lambda)(Q_{b1} + R) \quad (3.26)$$

E_c is calculated using Equation (3.22). As mentioned previously, river routing is disabled for this model. Q_{b2} and $G(t)$ are calculated via the following equations:

$$Q_{b2} = k_2 \cdot [G(t-1) + R] \quad (3.27)$$

$$G(t) = G(t-1) + R - Q_{b2} \quad (3.28)$$

Total streamflow is

$$Q = Q_d + Q_{b1} + Q_{b2} \quad (3.29)$$

Theoretically, the potential of $Q_{b1} + R$ could exceed the actual water supply in the second reservoir, $S_2(t)$, particularly when $\beta \geq 1$ and $\alpha + k_1 > 1$. Thus, application of this model required careful monitoring of the storage values generated during model simulations.

A second problem with the model is that it has too many parameters (7). To address this, the parameter, λ , is redefined in Model-7b, reducing the number of parameters to six:

$$\lambda = \frac{k_1 S_2(t)}{k_1 S_2(t) + \alpha S_2(t)^\beta} \quad (3.30)$$

This equation assumes that the partitioning between R and Q_{b1} is determined by the magnitude of their potentials. However, it was determined that six parameters were too many for a water balance model. Thus, an alternative model with fewer parameters was investigated.

3.6.2.3 Model 8

Model 8-a has only four parameters. In this model, the E_c and R proportionality relationship is expressed as:

$$\frac{E_c}{E_p - E_0} = \frac{R}{S_2(t)} \quad (3.31)$$

To solve this equation, E_c is defined as:

$$E_c = k_1 S_2(t) - R \quad (3.32)$$

So that:

$$R = \frac{k_1 S_2(t)^2}{E_p - E_0 + S_2(t)} \quad (3.33)$$

In this case, the $k_1 S_2$ component prevents recharge and E_c from extracting the full depth of tank 2. This is to prevent the unrealistic possibility that tank 2 is always empty. Of course, a weakness of this modeling approach is that the tank should be empty at times of severe drought.

In the second variation of Model 8 (i.e. Model 8-b), the k_1 parameter is removed from the model (3 parameters total), allowing the S_2 tank to be empty at times (and consequently, always at the *end* of every time period):

$$E_c = S_2(t) - R \quad (3.34)$$

Redefining the relationship between R and E_c as:

$$R = \frac{S_2(t)^2}{E_p - E_0 + S_2(t)} \quad (3.35)$$

Ideally, the tank should be allowed to be partially full, completely full, and completely empty at different times. Models 8-a and 8-b cannot model both conditions simultaneously, however. It may be possible to use both versions of Model 8 under different conditions; however, this possibility was not investigated.

3.6.2.4 Model 9

In Model 9, another approach was made to fix the E_c and R proportionality relationship. This model redefines the groundwater storage tank so that it has a maximum limit (G_{max}).

$$\frac{E_c}{E_p - E_0} = \frac{R}{G_{max} - G(t-1)} \quad (3.36)$$

Solving this equation for R:

$$R = \frac{k_1 S_2(t) [G_{max} - G(t-1)]}{[E_p - E_0] + [G_{max} - G(t-1)]} \quad (3.37)$$

The equation for E_c is defined the same as Equation (3.32) in Model 8-a (assumed to never be empty). An alternative relationship, based on the F_a/Q_d proportionality could alternatively be used:

$$E_c = G_{max} - G(t-1) - R \quad (3.38)$$

however, this definition was not tested in Model 9.

3.6.2.5 Summary of Models 2, 3, 5, 7, 8, and 9

The models were tested at the monthly time scale and produced similar results. The models produced NSE between 0.67 to and 0.69 for one MOPEX catchment in Pennsylvania (please see Figure 3.5 below). Of these models, Model 9 performed marginally better.



Figure 3.5. MOPEX catchment in Pennsylvania (01574000) used for testing the initial model structures.

In additional testing of the model structure, it was found that modifying the potential evapotranspiration rate had a large impact of the performance on the model. In some cases, the model performance improved significantly. The next model development stage discusses these modifications.

3.6.3 Modifications to the Expression of Evapotranspiration

Model 9 was selected as a candidate for testing various modifications to the expressions of evapotranspiration because it had previously performed very well for the Pennsylvania catchment and because its inclusion of a capacity limit for the groundwater storage (G_{max}) was deemed to be more realistic. For this model, several different methods were used to modify the relationship of E_c and E_0 with E_p . These modifications were evaluated using the same MOPEX catchment in Pennsylvania (01574000) along with three other catchments. These include a large

catchment in Florida (02273000), a small catchment in North Carolina (03550000), and a large catchment in Texas (08033500). The catchments were chosen on the basis of their representation of different climates. A map of these catchments is provided in Figure 3.6.

The next series of models were tested at the monthly time scale. The monthly time scale, it was later determined, is the least sensitive to modifications in model structure. Thus, differences between modifications could be difficult to determine from the performance results. Additionally, most models tend to do better at the monthly time scale. That is, even the simple Thornthwaite and Mather model performs well at this time scale (though not as well at other time scales).

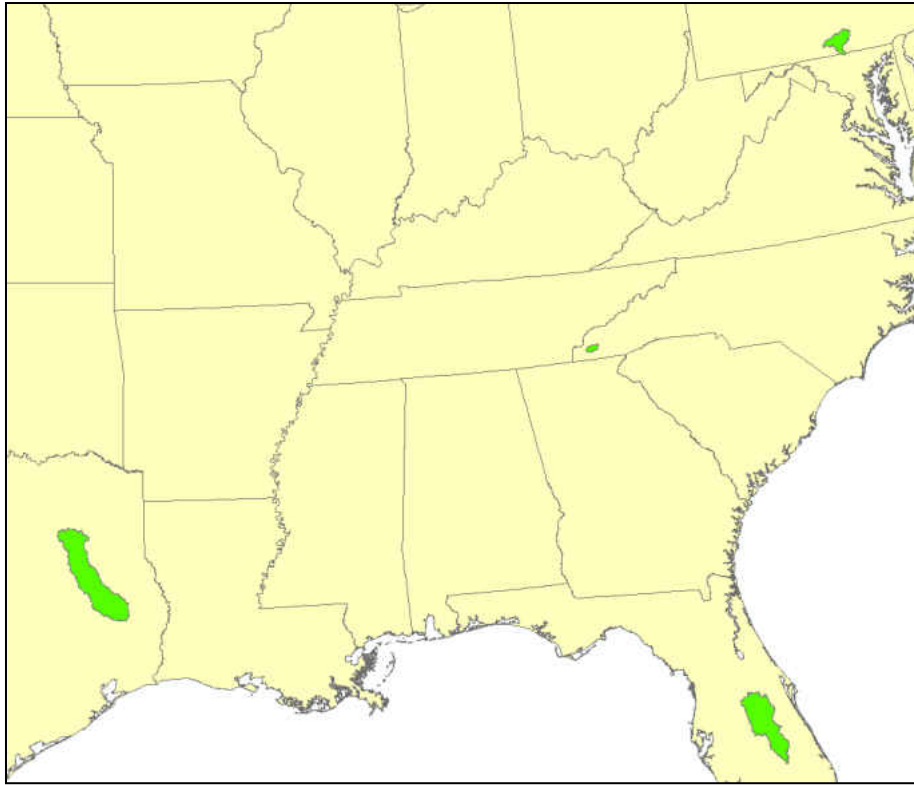


Figure 3.6. Four MOPEX watersheds chosen for initial model evaluation.

3.6.3.1 Modifications of Model 9 Evapotranspiration Expressions

In Model 9-E1, a parameter, λ , was multiplied by potential evapotranspiration for the first tank to set an upper limit for initial evapotranspiration; i.e. the maximum initial evapotranspiration is restricted to either the available water in the first tank ($S_{1,max}$) or a fraction of the potential evapotranspiration (λE_p). Similarly, the maximum rate of continuing

evapotranspiration, represented in the denominator of the left-hand side of Equation (3.39), is

$$\frac{E_c}{(E_p - E_0) \cdot \lambda} = \frac{R}{G_{max} - G(t-1)} \quad (3.39)$$

This can be written as:

$$R = \frac{k_1 S_2(t) [G_{max} - G(t-1)]}{(E_p - E_0) \cdot \lambda + [G_{max} - G(t-1)]} \quad (3.40)$$

A second modification to the evapotranspiration rate was tested in Model 9-E2. For this model, λ is replaced by a scaling factor. The scaling factor is based on the deficit of each bucket so that when the deficit is small (i.e. the bucket is nearly full), the potentials of E_0 and E_c are the same as their theoretical potentials (i.e. $E_0 = E_p$ when $S_1(t) \geq E_p$ or $E_0 = S_1(t)$ when $S_1(t) < E_p$, and $E_c = E_p - E_0$). The purpose of this modification is to model the increased difficulty for evapotranspiration to reach its potential when soil deficits are higher. To summarize:

$$\begin{cases} E_0 = S_1(t) \left[1 - \frac{S_{1max} - S_1(t)}{S_{1max}} \right] & S_1(t) < E_p \\ E_0 = E_p \left[1 - \frac{S_{1max} - S_1(t)}{S_{1max}} \right] & S_1(t) \geq E_p \end{cases} \quad (3.41)$$

For continuing evapotranspiration,

$$\frac{E_c}{(E_p - E_0) \cdot \left(1 - \frac{S_{2max} - S_2(t)}{S_{2max}} \right)} = \frac{R}{G_{max} - G(t-1)} \quad (3.42)$$

which can be written as

² The potential is not $(E_p \lambda - E_0)$. This is because E_p is not an actual quantity, but a potential quantity, so the only demand that would be reduced is the demand that is met. There is still some demand left over $(E_p(1 - \lambda))$, which will drive the continuing evapotranspiration rate.

$$R = \frac{k_1 S_2(t) [G_{max} - G(t-1)]}{\left[(E_p - E_0) * \left(1 - \frac{S_{2max} - S_2(t)}{S_{2max}} \right) \right] + [G_{max} - G(t-1)]} \quad (3.43)$$

Model results, however, were very poor, particularly for the Florida catchment.

The next model, Model 9-E3, is based on the first variant (Model 9-E1). The difference is that λ is applied to only the potential of E_0 (i.e. the potential of $E_c = E_p - E_0$ while the potential of $E_0 = \lambda E_p$). Model performance was generally the same as the first model variation (Model 9-E1). This is to be expected since most of the evapotranspiration occurs in the first tank.

It was reasoned that since modifications of the second evapotranspiration term were negligible, then E_c itself must be negligible, and so removing the E_c term altogether would not impact the model significantly. This assumption was partially correct, since model performance did decline slightly. However, using only four catchments is not enough to conclude that the evapotranspiration/subsurface flow process is negligible.

3.6.3.2 Conclusions

The results from Model 9 indicate that modification to the evapotranspiration term, E_0 has the most significant impact on the model. However, the improvements tend to be small. The modification to E_0 was similarly applied to Model 8 and, likewise, resulted in minor improvements. More importantly, their impact at other time scales must be assessed to determine whether these “improvements” actually improve the model performance.

3.6.4 Modifications of Subsurface Runoff and Evapotranspiration Processes

The lack of responsiveness from the model to modifications suggests that the hydrologic processes themselves are not the cause, but rather the model structure itself. Additionally, it may be necessary to increase model complexity if the current model structure is to be used, or certain components of the model structure need to be redesigned. The following questions must then be asked: Do all processes occur in the correct order? Are there some processes that are missing? Are some processes that are in competition with each other supposed to occur sequentially (one after the other)?

The models discussed in the following sections have been developed to answer these questions. This includes Models 13 through 15, and in the next section, Models 16, 17, and 19.

3.6.4.1 Models 13 Through 15

The focus of the previous models has primarily been on resolving the weaknesses of the proportionality relationship between the subsurface flow and evapotranspiration. However, no effort was made to see if the competition between these two processes should be modeled differently. That is, all prior models consider the competition to be between recharge (R) and continuing evapotranspiration (E_c).

In Models 13 and 14, competition between subsurface flow and evapotranspiration is described as a competition between Q_{b1} (the first component of baseflow) and E_c .

$$\frac{E_c}{E_p - E_0} = \frac{Q_{b1}}{E_c + Q_{b1}} \quad (3.44)$$

After this competition, a fraction of the water remaining in the second tank becomes recharge (i.e. $R = k_1 S_2$). This recharge adds to the groundwater reservoir (as it was in the initial model structure) and the second component of baseflow (i.e. Q_{b2}) is combined with Q_{b1} and Q_d to produce the total streamflow. The equations for Q_{b2} are identical to those in the initial model structure.

In Model 13, the additional equation required to solve the proportionality relationship described in Equation (3.44) is defined as follows:

$$E_c = (S_2(t) - Q_{b1})\alpha \quad (3.45)$$

In this equation, E_c is defined similarly to the definition of evapotranspiration in the abcd model. α is defined as:

$$\alpha = \left[1 - \exp\left(\frac{E_0 - E_p}{S_{2,max}}\right) \right] \quad (3.46)$$

The following quadratic equation is derived when these two equations are substituted into the proportionality relationship:

$$E_c = \frac{-b - \sqrt{b^2 - 4ac}}{2a} \quad \begin{aligned} a &= (1 - \alpha) \\ b &= (E_0 - \alpha \cdot S_2(t) - E_p) \\ c &= \alpha \cdot S_2(t)(E_p - E_0) \end{aligned} \quad (3.47)$$

In Model 14, Equation (3.45) is redefined in terms of Q_{b1} so that the coefficient applies to Q_{b1} instead of E_c . Also, the α term is replaced by a constant parameter, to be determined from calibration:

$$Q_{b1} = k_3(S_2(t) - E_c) \quad (3.48)$$

Thus, a second quadratic equation is defined as follows:

$$E_c = \frac{-b + \sqrt{b^2 - 4ac}}{2a} \quad \begin{aligned} a &= (1 - k_3) \\ b &= k_3 (E_p - E_0 + S_2(t)) \\ c &= k_3 S_2(t) (E_0 - E_p) \end{aligned} \quad (3.49)$$

Note that $k_3 \neq 1$, otherwise, the equation will result in division by zero.

With the introduction of Models 13 and 14, it was recognized that several other possible models were possible which would not need the proportionality statement defined in Equation (3.44).

Testing these models would provide evidence of the strength (or weakness) of the proportionality relationship described in Equation (3.44). Thus, in Model 15, three possible combinations were tested:

1. E_c and Q_{b1} occur simultaneously, as before, by combining Equations (3.45) and (3.48)
2. E_c occurs first via Equation (3.45), which requires removing Q_{b1} from the equation (i.e. $E_c = \alpha S_2(t)$). It is then followed by Q_{b1} via Equation (3.48)
3. The same as the second approach, except the factor k_3 in Equation (3.48) is applied to only E_c (i.e. $Q_{b1} = (S_2(t) - k_3 E_c)$)

3.6.4.2 Three Routing Methods

Since Q_{b1} represents subsurface flow, it is likely that it will need to be routed similarly to Q_{b2} . Thus, three routing methods were considered. The first routing method adds Q_{b1} directly to the total runoff (no routing through a linear reservoir). The second method routes Q_{b1} through the groundwater reservoir (i.e. Q_{b1} is added to R when it is routed through the groundwater reservoir). The third method adds Q_{b1} back to the soil moisture so that recharge will only take a fraction of Q_{b1} and $S_2(t)$. Thus, in a sense, the third method routes Q_{b1} through R and the groundwater reservoir.

3.6.4.3 Results of the Three Routing Methods and Models 13, 14, and 15

The three models (and their three variations) were applied to the same four catchments tested previously. The results are displayed in Tables 3.1, 3.2, and 3.3. In the following tables, (a), (b), and (c) refer to the three routing methods. Types 1, 2, and 3 for Model 15 refer to the three variations of Model 15.

From the results, it is clear that the second and third routing methods (b and c) were always inferior to the first method (a). Additionally, Model 13 performed poorly overall (this model used the abcd-type expression for E_c). Model 15 Type 3 also performed very poorly. Models 14 (a), 15 (a) Type 1, and 15 (a) Type 2 did moderately well.

Comparing these results with the previous models (see Figure 3.7) indicates that Models 14(a) and Models 15(a) Type 1 performed the best. Models 7-b and 15(a) Type 2 both performed well. Model 8 (with the modifications of evapotranspiration), and Model 9-E3 performed less well, but their performance was comparatively better than the other models. Model 9-E3 performed better than the variations of Model 8, except for the Florida catchment.

It is recognized that all of the proposed models have difficulty simulating streamflow at the Florida catchment (02273000). An analysis of the USGS GAP land cover data for the catchment reveals that a large portion of the catchment is covered by a combination of wetlands and large water bodies, especially in the northern half of the catchment. Additionally, the catchment overlies the Floridan Aquifer, a highly efficient aquifer covering the entire state of Florida and parts of Georgia, South Carolina, and Alabama. The aquifer is likely responsible for significant deep groundwater recharge, which is typically not captured by water balance models.

Table 3.1. Nash-Sutcliffe Coefficient of Efficiency Values for Model 13.

Location	Station	Model 13 (a)	Model 13 (b)	Model 13 (c)
Florida	02273000	-0.04	-0.04	-0.04
North Carolina	03550000	0.28	0.21	0.21
Texas	08033500	0.48	0.48	0.48
Pennsylvania	01574000	0.69	0.69	0.69
Average		0.35	0.33	0.33

Table 3.2. Nash-Sutcliffe Coefficient of Efficiency Values for Model 14.

Location	Station	Model 14 (a)	Model 14 (b)	Model 14 (c)
Florida	02273000	0.10	-0.06	-0.01
North Carolina	03550000	0.77	0.28	0.21
Texas	08033500	0.53	0.52	0.54
Pennsylvania	01574000	0.69	0.69	0.69
Average		0.52	0.36	0.36

Table 3.3. Nash-Sutcliffe Coefficient of Efficiency Values for Model 15.

Location	Station	Model 15 (Type1) (a)	Model 15 (Type1) (b)	Model 15 (Type1) (c)
Florida	02273000	0.11	-0.06	-0.04
North Carolina	03550000	0.76	0.23	0.21
Texas	08033500	0.48	0.46	0.47
Pennsylvania	01574000	0.69	0.69	0.69
Average		0.51	0.33	0.33

Location	Station	Model 15 (Type2) (a)	Model 15 (Type2) (b)	Model 15 (Type2) (c)
Florida	02273000	0.08	-0.06	-0.04
North Carolina	03550000	0.65	0.28	0.21
Texas	08033500	0.48	0.48	0.48
Pennsylvania	01574000	0.69	0.69	0.69
Average		0.47	0.35	0.33

Location	Station	Model 15 (Type3) (a)	Model 15 (Type3) (b)	Model 15 (Type3) (c)
Florida	02273000	-1.50	-0.06	-0.04
North Carolina	03550000	-0.56	0.20	0.21
Texas	08033500	-0.09	0.44	0.48
Pennsylvania	01574000	0.59	0.69	0.69
Average		-0.39	0.32	0.33

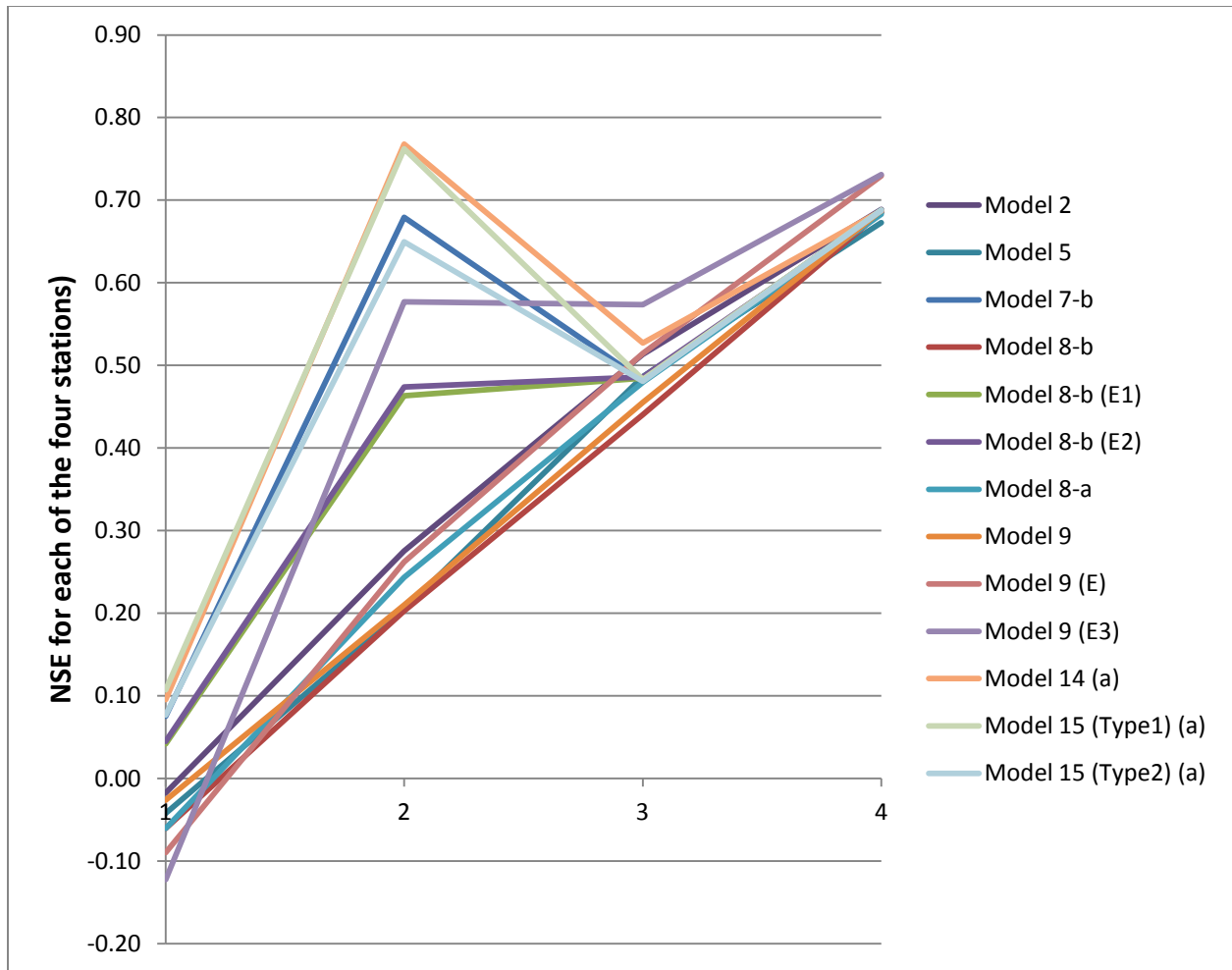


Figure 3.7. NSE for Models 2 through 15. From left to right: Florida, North Carolina, Texas, Pennsylvania.

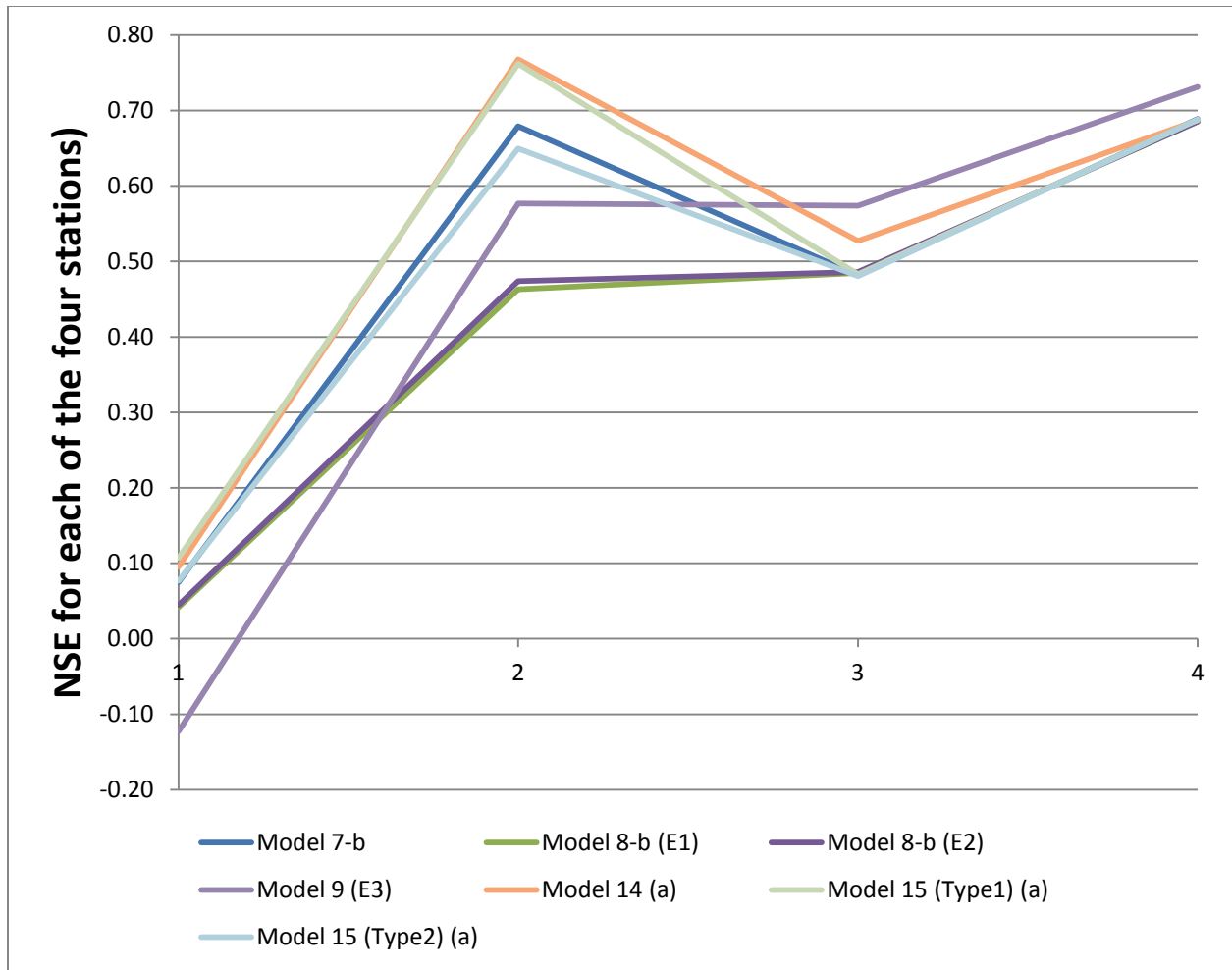


Figure 3.8. NSE Values from the Best Models Illustrated in Figure 3.7.

3.6.5 Additional Model Structure Changes

3.6.5.1 Model 16

In the previous models, various modifications of the relationship between subsurface flow (via expressions of R or both R and Q_{b1}) and evapotranspiration E_c were formulated.

However, all models assumed that R would supply water to a linear groundwater reservoir (G). To test the necessity of routing the subsurface flow through G , and hence, routing of streamflow in general, the proportionality relationship for subsurface flow and evapotranspiration is redefined such that the groundwater reservoir is excluded from the model:

$$\frac{E_c}{E_p - E_0} = \frac{Q_b}{E_c + Q_b} \quad (3.50)$$

which is identical to Equations (3.12) and (3.44) with the exception that the subsurface flow is represented by Q_b . A representation of this modification to the model structure is illustrated in Figure 3.9.

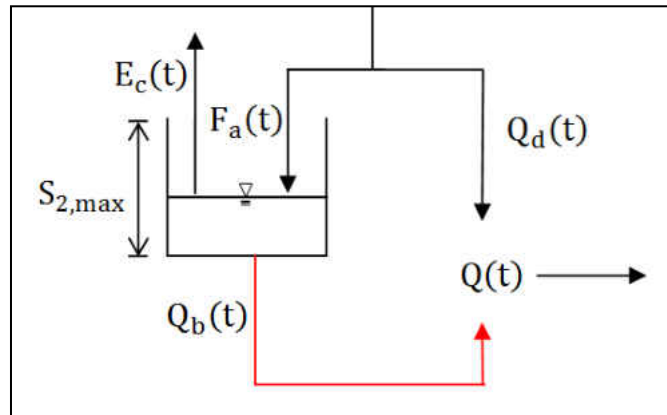


Figure 3.9. Model 16. The red arrow denotes the modification to the model structure.

After competition, Q_b is immediately added to Q_d to produce total streamflow. Equation (3.48) is used to relate Q_b and E_c to the storage capacity, $S_2(t)$:

$$Q_b = k_3(S_{2,1}(t) - E_c) \quad (3.51)$$

Thus,

$$S_{2,2}(t) = S_{2,1}(t) - E_c - Q_b \quad (3.52)$$

where $S_{2,1}(t)$ and $S_{2,2}(t)$ refer to the soil moisture storage, $S_2(t)$, before and after Q_b , respectively. What is particularly interesting regarding Equations (3.51) and (3.52) is that they are similar to the equations used for routing recharge through the groundwater reservoir.

These equations may explain why in a later analysis the storage term for the second tank was observed to vary considerably between time scales; routing processes tend to vary with different time scales, especially for large time scales. It appears that the model structure treats the second storage tank as a routing mechanism and not just a mechanism for partitioning hydrologic processes.

3.6.5.2 Models 17 and 19

The evaluation results from model 16 were promising. However, model 16 did not perform as well when compared with model 14 for 55 catchments across the daily and monthly time scales, as illustrated by the normal distribution curves of Figure 3.11. To improve the performance of model 16, model 17 includes a second initial evapotranspiration term, ϕ .

$$\phi = \lambda(E_p - E_0) \quad (3.53)$$

This term is similar to E_0 in that it is a function of only the evapotranspiration demand (E_p). In this model, ϕ occurs before any subsurface flow can be partitioned to baseflow. Equation (3.50) is then expressed as:

$$\frac{E_c}{E_p - E_0 - \phi} = \frac{Q_b}{E_c + Q_b} \quad (3.54)$$

This proportionality relationship is solved for E_c using Equation (3.13) with R replaced by Q_b .

As illustrated in Figure 3.10, results indicated an increase in performance during the monthly time scale, but a loss of performance during the daily time scale. In both time scales, Model 17 did not perform as well as Model 14.

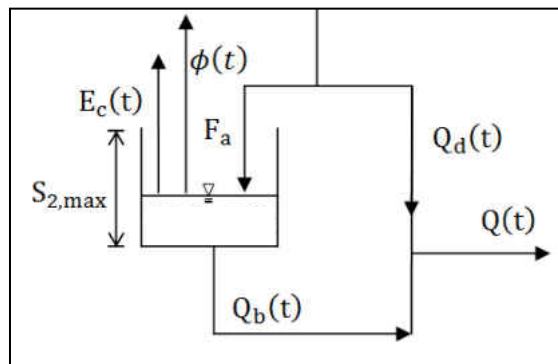


Figure 3.10. Model 17

To further improve this model structure, Model 19 allocates a fraction of the water in the second soil moisture reservoir (X) for the partition of water between baseflow and evapotranspiration. This fraction is defined by a constant parameter (k_1) and by the ratio of available water to maximum soil moisture capacity, which is a measure of the ability of the soil to retain water against the processes of gravity and evapotranspiration.

$$X = k_1 S_{2,1}(t) \cdot \left(\frac{S_{2,1}(t)}{S_{2,max}} \right) \quad (3.55)$$

The soil moisture is then updated to $S_{2,2}(t)$:

$$S_{2,2}(t) = S_{2,1}(t) - X \quad (3.56)$$

A fraction of X is first partitioned to ϕ before it is competed for by continuing evapotranspiration and baseflow.

$$\phi = X \cdot \left(1 - \exp \left[- \frac{\lambda \cdot S_{2,1}(t) \cdot \{E_p - E_0\}}{(S_{2,max})^2} \right] \right) \quad (3.57)$$

where λ is a parameter to be calibrated.

Two variations of the model that were evaluated considered the case when continuing evapotranspiration competed with baseflow (Model 19-T6) and when continuing evapotranspiration was considered negligible (Model 19-T7).

In Model 19-T6 (E_c competes with Q_b), the competition is again expressed using the proportionality hypothesis of Equation (3.54). However, the potential of Q_b is modified from $(E_c + Q_b)$ to $(X - \phi)$ in Equation (3.58).

$$\frac{E_c}{E_p - E_0 - \phi} = \frac{Q_b}{X - \phi} \quad (3.58)$$

This equation can be solved for Q_b with Equation (3.59):

$$E_c = X - \phi - Q_b \quad (3.59)$$

The total evapotranspiration is expressed as:

$$E = E_0 + E_c + \phi \quad (3.60)$$

In Model 19-T7, E_c is considered negligible so that all of the water left over from the partitioning of X to ϕ becomes baseflow:

$$Q_b = X - \phi \quad (3.61)$$

Finally, an expression was included for both model variations to allow the maximum capacity of the second soil moisture reservoir ($S_{2,max}$) to vary:

$$S_{2,max} = S_{2,max} - [S_{2,2}(t) - S_{2,1}(t)] \quad (3.62)$$

Results showed an improvement in model performance for both model variations.

At the daily time scale, both variations of Model 19 perform better than Models 14, 16, and 17 (Figure 3.11). Performance results at the monthly time scale indicate that Model 19 shows less variability in performance, but also has a lower average NSE value. Also, Model 19-T7 performs better at both time scales than T6, suggesting that only one term for evapotranspiration is sufficient for the second soil moisture reservoir.

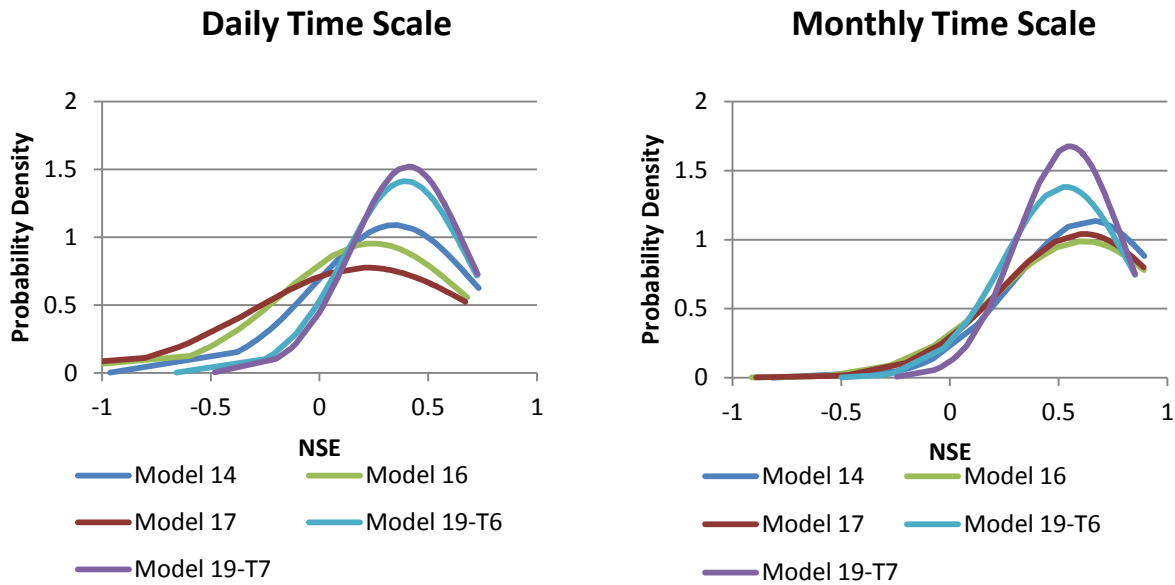


Figure 3.11. Performance of Models 14, 16, 17, and 19. The horizontal axis represents NSE values and the vertical axis represents the probability density. The horizontal position of the peaks represents the mean NSE values of 55 catchments.

3.6.6 Modifications to Model 14

Various modifications to Model 14 were evaluated, such as the variable capacity used in Model 19 and modifications to the initial evapotranspiration expression. However, only two modifications resulted in improvements in the model structure. A third modification was also made and is discussed below.

In Equation (3.48), Q_{b1} is represented as a fraction of the difference between the soil water storage in the second reservoir and the continuing evapotranspiration:

$$Q_{b1} = k_3(S_2(t) - E_c) \tag{3.48}$$

However, Q_{b1} and E_c are assumed to occur simultaneously in the proportionality relationship of Equation (3.44). To resolve this logically inconsistent relationship, the following equation is used in place of (3.48):

$$Q_{b1} = k_3 S_2(t) - E_c \quad (3.63)$$

This modification does not improve model performance, however.

3.6.6.1 Modification of Infiltration Processes prior to Surface Runoff Generation

In the first modification, continuing abstraction, F_a , is split into an initial component, F_{a1} , and a continuing component, F_{a2} , which competes against surface runoff, Q_s .

F_{a1} is similar to initial abstraction in that its demand must be met before surface runoff can occur. Physically, it represents the infiltration rate that occurs at the beginning of a precipitation event. More precisely, it represents the water that infiltrates the soil while the infiltration rate exceeds the precipitation rate. F_{a1} is partitioned to the second soil moisture layer after initial abstraction.

$$F_{a1} = \begin{cases} F_{a1,p} & P - I_a > F_{a1,p} \\ P - I_a & P - I_a \leq F_{a1,p} \end{cases} \quad (3.64)$$

where $F_{a1,p}$ represents the potential of F_{a1} .

Two variations of $F_{a1,p}$ were evaluated. In the first variation (V1), $F_{a1,p}$ is defined as a fraction of the deficit in the second soil moisture reservoir:

$$F_{a1,p} = k_5 [S_{2,max} - S_{2,0}(t)] \quad (3.65)$$

where $S_{2,0}(t)$ is the soil moisture at the beginning of the time period in the second soil moisture reservoir.

In the second variation (V2), $F_{a1,p}$ is defined as a fixed fraction of the soil moisture reservoir. If the deficit in the tank is smaller than this fraction, then F_{a1} cannot occur.

$$F_{a1,p} = \begin{cases} 0 & k_5 S_{2max} > (S_{2max} - S_{2,0}(t)) \\ k_5 S_{2max} & k_5 S_{2max} \leq (S_{2max} - S_{2,0}(t)) \end{cases} \quad (3.66)$$

Since water partitioned by F_{a1} enters the same reservoir as F_{a2} , the potential of F_{a2} in the competition of Q_s and F_{a2} should be reduced. This modified proportionality relationship is expressed as:

$$\frac{F_{a2}}{S_{2max} - S_{2,0}(t) - F_{a1}} = \frac{Q_s}{P - I_a - F_{a1}} \quad (3.67)$$

From continuity, F_{a2} is defined as:

$$F_{a2} = P - I_a - F_{a1} - Q_s \quad (3.68)$$

Equation (3.68) can then be substituted into (3.67) to solve for Q_s .

A third variation (V3), which does not use F_{a1} , but instead uses a third proportionality relationship, was evaluated. In all previous model variations, I_a is assumed to equal the deficit of the first soil moisture reservoir. In this model variation, I_a competes against the water that leaves the first soil moisture reservoir:

$$\frac{I_a}{S_{1,max} - S_{1,0}(t)} = \frac{P - I_a}{P} \quad (3.69)$$

where $S_{1,0}(t)$ is the soil moisture at the beginning of the time period. This equation can be solved for I_a without any substitutions:

$$I_a = \frac{P(S_{1,max} - S_{1,0}(t))}{P + (S_{1,max} - S_{1,0}(t))} \quad (3.70)$$

The three variations of Model 14 (V1, V2, and V3) were evaluated at the daily and monthly time scales (Figure 3.12). Models 14 (V1) and 14 (V2) perform approximately the same at the monthly time scale, though Model 14 (V2) performs much better at the daily time scale.

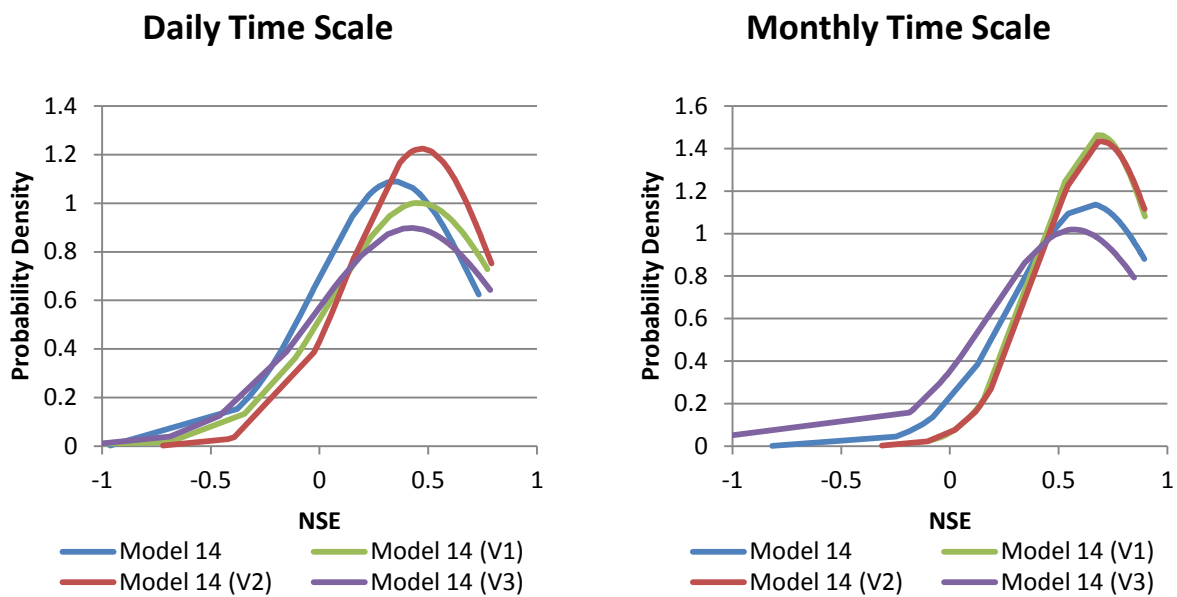


Figure 3.12. Performance of Model 14 Variations for 55 Catchments.

3.6.6.2 Modification of Expressions for Subsurface Flow

A second modification to Model 14's structure improved model performance. In this modification, recharge, R , was combined with Q_{b1} in the proportionality relationship of Equation (3.44). Thus, Q_{b1} represents the total subsurface flow, Q_{SS} and Equation (3.44) is rewritten as:

$$\frac{E_c}{E_p - E_0} = \frac{Q_{SS}}{E_c + Q_{SS}} \quad (3.71)$$

To separate recharge from Q_{b1} , the following equation is used:

$$R = k_1 Q_{SS} \quad (3.72)$$

where k_1 is a parameter to be calibrated. Q_{b1} is then calculated as:

$$Q_{b1} = Q_{SS} - R \quad (3.73)$$

It is recognized that Q_{b1} primarily represents interflow and is hereafter denoted as Q_i .

3.6.7 Model Selection

The first set of modifications evaluated for Model 14 (V1, V2, and V3) was also evaluated on Model 19 (T9, T8, and T10, respectively). As illustrated in Figure 3.13, Model 19-T9 has the highest probability density. However, the mean of Model 14 (V2) is the highest and is able to achieve slightly higher performance values than the other models. Thus, Model 14 (V2) was selected from these models. Additionally, the two other modifications discussed earlier (Equation (3.63) and the combination of recharge with Q_{b1}) are applied to Model 14's model structure. Finally, a fourth modification to Model 14's model structure, which improves model

performance, was made by including a second surface runoff and continuing abstraction competition.

Model development has continued until this stage because the objective was to improve the performance of the model structure (during parameter calibration) until it exceeded the performance of the abcd model and the Zhang model at the daily, monthly, and annual time scales. As discussed in Chapter 4, the modified version of Model 14 meets this requirement and is selected as the proposed model structure for this thesis. This model is discussed in detail in Section 3.6.9. A variation of the Model 14 (V2) model, which does not include the three other modifications mentioned previously, is discussed in the next section. Although this model variation does not perform as well as the proposed model or even the Model 14 (V2) model, it provides an example of a significantly different type of proportionality relationship.

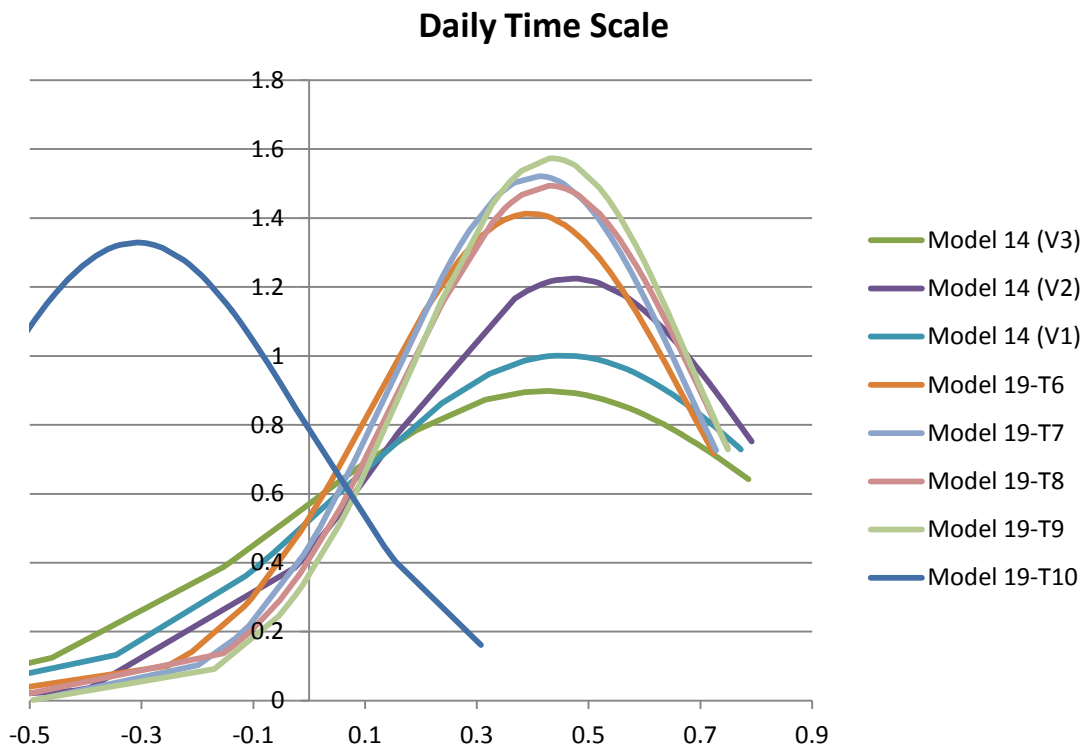


Figure 3.13. Performance of Model 14 and 19 Variations.

3.6.8 Model 21

Model 21 is based on the (V2) modification of Model 14. The model does not include the other three modifications discussed in the previous section. In this model, the competition between continuing evapotranspiration and Q_{b1} is replaced with the competition between continuing evapotranspiration and soil moisture storage and the competition between Q_{b1} and soil moisture storage. Thus,

$$\frac{E_c}{E_p - E_0} = \frac{S_{2,2}(t)}{S_{2,1}(t)} \quad (3.74)$$

Where $S_{2,1}(t)$ and $S_{2,2}(t)$ refer to the soil moisture in the second reservoir before and after the competition, respectively. The continuity equation at this stage is expressed as:

$$S_{2,1}(t) = S_{2,2}(t) + E_c \quad (3.75)$$

This expression is then solved for E_c and substituted into Equation (3.78) to solve for $S_{2,2}(t)$.

The second competition is expressed as:

$$\frac{Q_{b1}}{S_{2,2}(t) \cdot \left[k_2 \frac{S_{2,2}(t)}{S_{2,max}} \right]} = \frac{S_{2,3}(t)}{S_{2,2}(t)} \quad (3.76)$$

Where $S_{2,2}(t)$ and $S_{2,3}(t)$ refer to the soil moisture in the second reservoir before and after the competition, respectively. The continuity equation at this stage is expressed as:

$$S_{2,2}(t) = S_{2,3}(t) + Q_{b1} \quad (3.77)$$

This expression is then solved for Q_{b1} and substituted into Equation (3.76) to solve for $S_{2,3}(t)$.

In Equation (3.76), the potential of Q_{b1} is based on a fraction of the total available water $S_{2,2}(t)$ determined by a fixed constant k_2 and the ratio $S_{2,2}(t)/S_{2,max}$. The reason the potential maximum value of Q_{b1} is restricted to a fraction of the available water, $S_{2,2}(t)$, is because the soil can never be completely drained by gravity. This concept is referred to in the literature as the field capacity of the soil. Model 21 was evaluated at the daily time scale, but was found to have a lower performance than Model 14 (V2).

3.6.9 Final Model (Proposed Model)

In the final model structure, the first tank represents the water from interception and the soil moisture that is held in place by the matric potential. The second tank primarily represents the water that exceeds the field capacity. It will flow laterally and downward, though possibly at a very slow rate.

Most monthly water balance models, such as the Palmer model and Thornthwaite and Mather models, assume that evapotranspiration is equal to potential evapotranspiration when rainfall is greater than potential evapotranspiration (Alley 1984; Zhang et al. 2008). A notable difference in the proposed model structure is that evapotranspiration is dependent on the soil moisture condition, which occurs after rainfall has been partitioned to runoff and storage. This method is different because it is assumed that evapotranspiration doesn't occur before streamflow partitioning, but rather after infiltration/direct runoff partitioning and alongside baseflow partitioning.

In the equations and illustrations that follow, the second number in the subscript represents the updated value of a process. For example, $S_{1,0}$ represents the value of S_1 at the beginning of the time period. $S_{1,1}$ represents the first updated value of S_1 and $S_{1,2}$ represents the second updated value of S_1 . This numbering scheme is also applied to the second soil moisture reservoir, S_2 , to the groundwater reservoir, G , and surface runoff, Q_s .

3.6.9.1 First Stage

In the first stage, precipitation, P , enters the first soil moisture layer and combines with the initial soil moisture content, $S_{1,0}$. This soil moisture layer has a capacity defined by $S_{1,max}$.

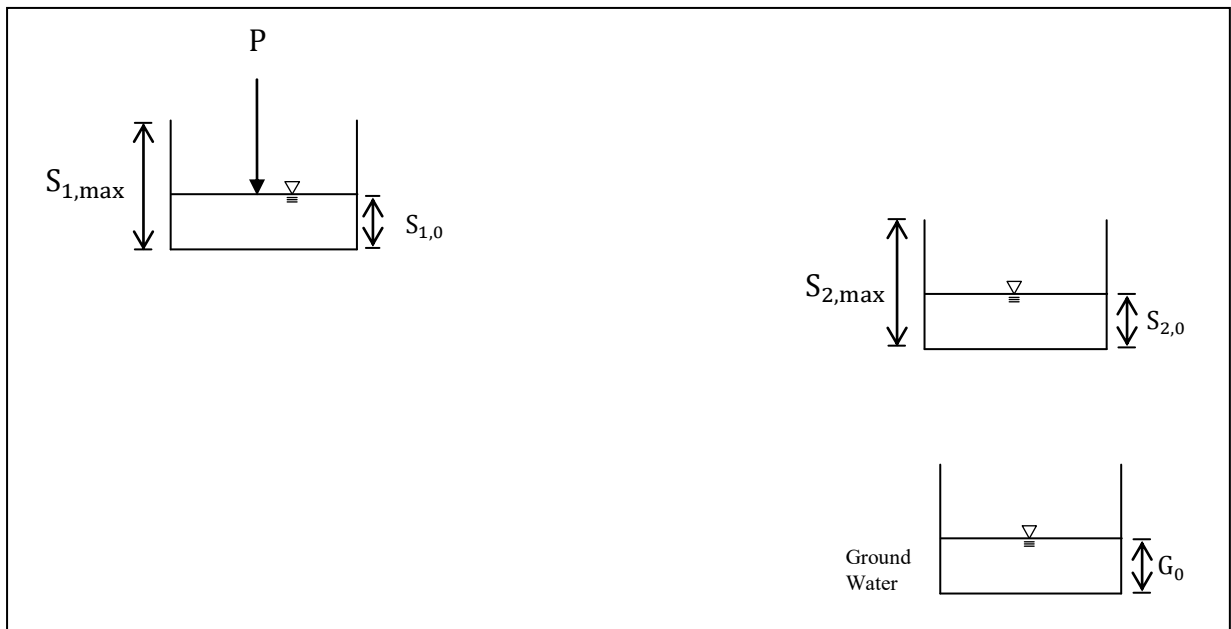


Figure 3.14. Stage 1 of the Final Model Structure.

3.6.9.2 Second Stage

In the second stage, if precipitation exceeds the capacity of the first tank, it will continue as $P - I_a$, where I_a primarily represents the initial abstraction. The standard definition of initial abstraction includes water that is abstracted by interception and surface depressions (i.e. water that cannot become surface runoff). In this model, initial abstraction includes the standard

definition as well as the water that infiltrates into the soil but does not exceed the matric potential (i.e. the water that does not flow downward but is held in place by the molecular forces of soil particles).

If the deficit in the first tank is not exceeded, then precipitation will be completely partitioned to the first tank:

$$\begin{cases} I_a = S_{1,max} - S_{1,0} & P > S_{1,max} - S_{1,0} \\ I_a = P & P \leq S_{1,max} - S_{1,0} \end{cases} \quad (3.78)$$

So that the soil moisture state in the first tank is updated to $S_{1,1}$.

$$S_{1,1} = S_{1,0} + I_a \quad (3.79)$$

Assuming that precipitation exceeds the deficit of the first tank, a fraction of the remaining water, $P - I_a$, directly enters the second tank as F_{a1} . The term F_{a1} is defined as the fraction of the water that exceeds the matric potential but which must be satisfied before surface runoff can occur. According to Brutsaert (2005), precipitation rates rarely exceed the soil infiltration capacity. Most often, precipitation that isn't intercepted will infiltrate into the soil. F_{a1} is not the infiltration capacity, though it is similar to the infiltration rate that occurs at the beginning of a precipitation event. Except for exceptionally large precipitation events (which are more likely to generate surface runoff via infiltration excess), the soil must be saturated by a certain extent in order for surface runoff to occur. F_{a1} captures this aspect. In the case that the deficit in the second tank is smaller than F_{a1} , (i.e. the soil moisture levels are close enough to capacity), F_{a1} is neglected. This is to simulate the inability of the soil moisture layer to infiltrate water quickly enough when it is nearly saturated.

In the equations below, $F_{a1,p}$ represents the potential maximum value of F_{a1} .

$$F_{a1,p} = \begin{cases} 0 & k_5 S_{2max} > (S_{2max} - S_{2,0}) \\ k_5 S_{2max} & k_5 S_{2max} \leq (S_{2max} - S_{2,0}) \end{cases} \quad (3.80)$$

Thus, F_{a1} is defined as:

$$F_{a1} = \begin{cases} F_{a1,p} & P - I_a > F_{a1,p} \\ P - I_a & P - I_a \leq F_{a1,p} \end{cases} \quad (3.81)$$

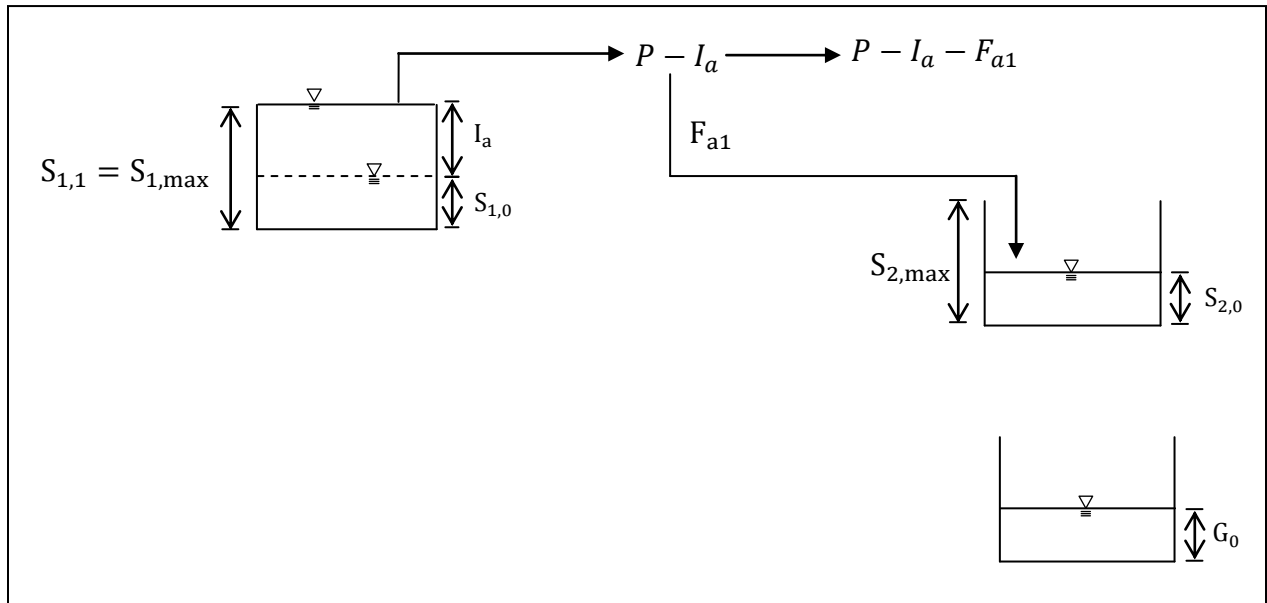


Figure 3.15. Stage 2 of the Final Model Structure.

3.6.9.3 Third Stage

In the third stage, water that cannot be infiltrated quickly enough is then subject to competition between surface runoff, $Q_{s,1}$, and the soil moisture layer, F_{a2} . F_{a2} can be considered

as the infiltration rate, which occurs at a rate proportional to the supply of water. This competition is expressed through an application of the proportionality hypothesis:

$$\frac{F_{a2}}{S_{2max} - S_{2,0} - F_{a1}} = \frac{Q_{s,1}}{P - I_a - F_{a1}} \quad (3.82)$$

where $S_{2,0}$ represents the initial soil moisture in the second soil moisture reservoir.

In Equation (3.82), the driving force of F_{a2} is assumed to be its potential maximum value, expressed as the deficit of the tank minus the water that was added to it by F_{a1} . Likewise, the potential maximum value of $Q_{s,1}$ is the available water for competition. The continuity equation at this stage is expressed as:

$$P - I_a - F_{a1} = F_{a2} + Q_{s,1} \quad (3.83)$$

Solving for F_{a2} and substituting into the proportionality statement:

$$\frac{P - I_a - F_{a1} - Q_{s,1}}{(S_{2max} - S_{2,0} - F_{a1})} = \frac{Q_{s,1}}{(P - I_a - F_{a1})} \quad (3.84)$$

This equation can be solved for $Q_{s,1}$

$$Q_{s,1} = \frac{(P - I_a - F_{a1})^2}{(S_{2max} - S_{2,0} - F_{a1}) + (P - I_a - F_{a1})} \quad (3.85)$$

F_{a2} can be calculated from Equation (3.83). Thus, the value of S_2 is updated as follows:

$$S_{2,1} = S_{2,0} + F_{a1} + F_{a2} \quad (3.86)$$

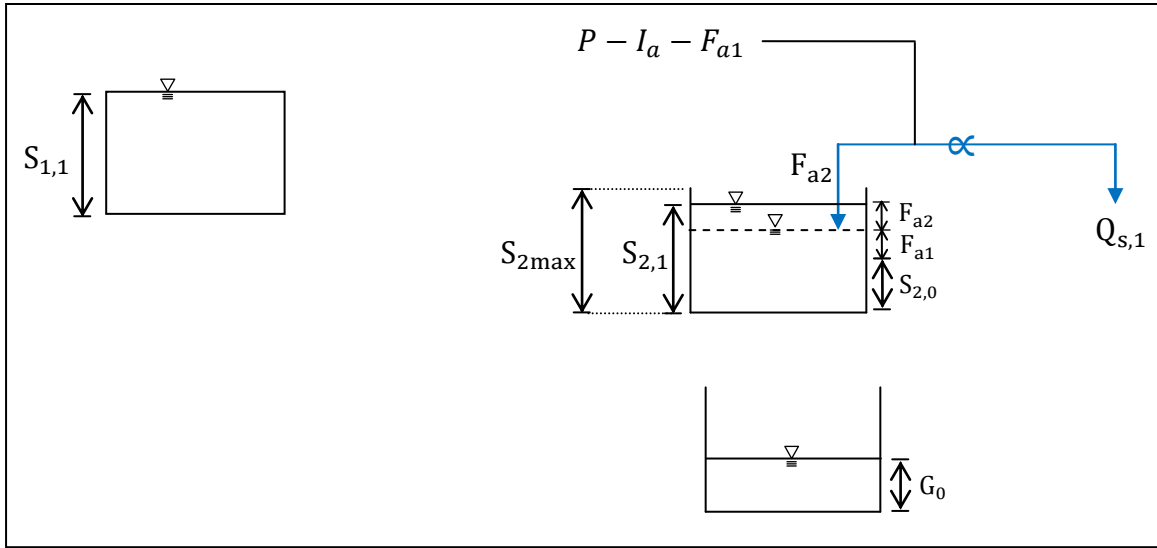


Figure 3.16. Stage 3 of the Final Model Structure. The blue arrow and proportionality symbol represent the competition between F_{a2} and $Q_{s,1}$.

3.6.9.4 Fourth Stage

Evapotranspiration takes place in the fourth stage. Evapotranspiration is driven by the potential evapotranspiration, E_p . This occurs first in the first tank as initial evapotranspiration, E_0 .

$$E_0 = \begin{cases} S_{1,1} & S_{1,1} < E_p \\ E_p & S_{1,1} \geq E_p \end{cases} \quad (3.87)$$

$$S_{1,2} = S_{1,1} - E_0 \quad (3.88)$$

Any remaining evapotranspiration demand (i.e. $E_p - E_0$) takes place in the second tank as continuing evapotranspiration, E_c . Often times, evapotranspiration demand is not large enough to compete against subsurface flow, so in typical cases, E_c will be close to zero. The

evapotranspiration in the second tank, E_c , competes against the subsurface flow (Q_{ss}) using the following proportionality hypothesis statement:

$$\frac{E_c}{E_p - E_0} = \frac{Q_{ss}}{E_c + Q_{ss}} \quad (3.89)$$

where $E_c + Q_{ss}$ represents the available water for partitioning between E_c and Q_{ss} and $E_p - E_0$ represents the remaining evapotranspiration demand. Q_{ss} and E_c are related to the storage by:

$$Q_{ss} + E_c = k_3 S_{2,1} \quad (3.90)$$

This expression can be solved for Q_{ss} and substituted into the proportionality statement to yield the following expression for E_c :

$$E_c = \frac{k_3 S_{2,1} (E_p - E_0)}{k_3 S_{2,1} + (E_p - E_0)} \quad (3.91)$$

Then, the subsurface flow can be calculated from the equation introduced previously:

$$Q_{ss} = k_3 S_{2,1} - E_c \quad (3.92)$$

The updated soil moisture in the second layer is the difference of E_c and Q_{ss} :

$$S_{2,2} = S_{2,1} - E_c - Q_{ss} \quad (3.93)$$

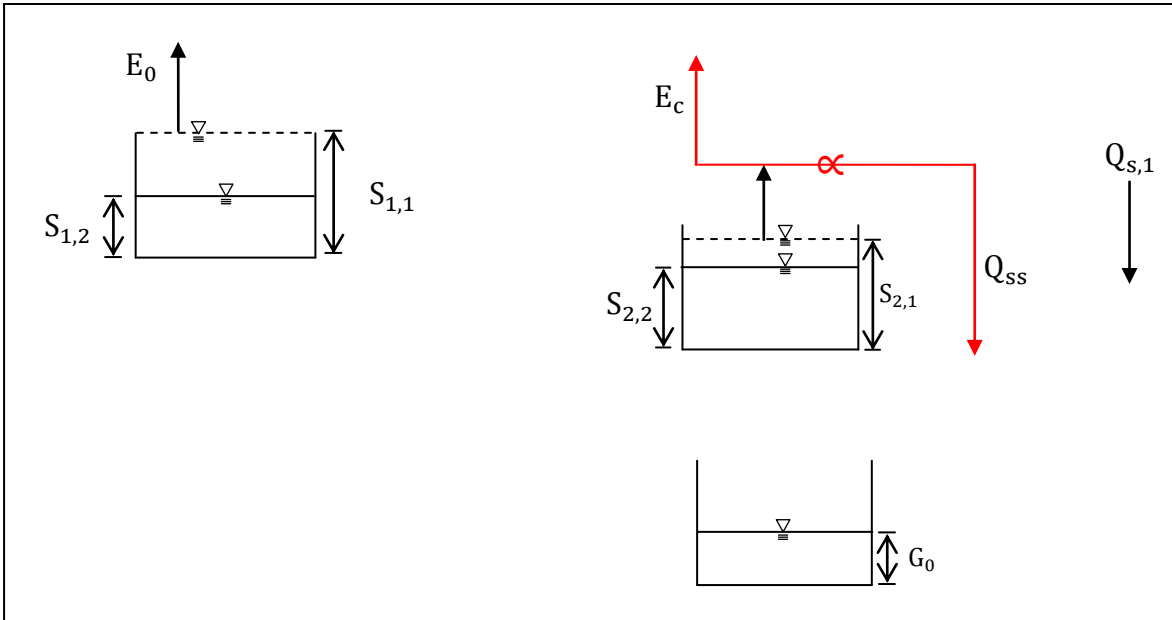


Figure 3.17. Stage 4 of the Final Model Structure. The red arrow and proportionality symbol represent the competition between E_c and Q_{ss} .

3.6.9.5 Fifth Stage

In the fifth stage, a fraction of the subsurface flow (Q_{ss}) is sent to the groundwater storage reservoir as recharge (R). The remaining subsurface flow travels to the catchment outlet as interflow (Q_i) (i.e. unsaturated flow).

$$R = k_1 Q_{ss} \quad (3.94)$$

$$Q_i = Q_{ss} - R \quad (3.95)$$

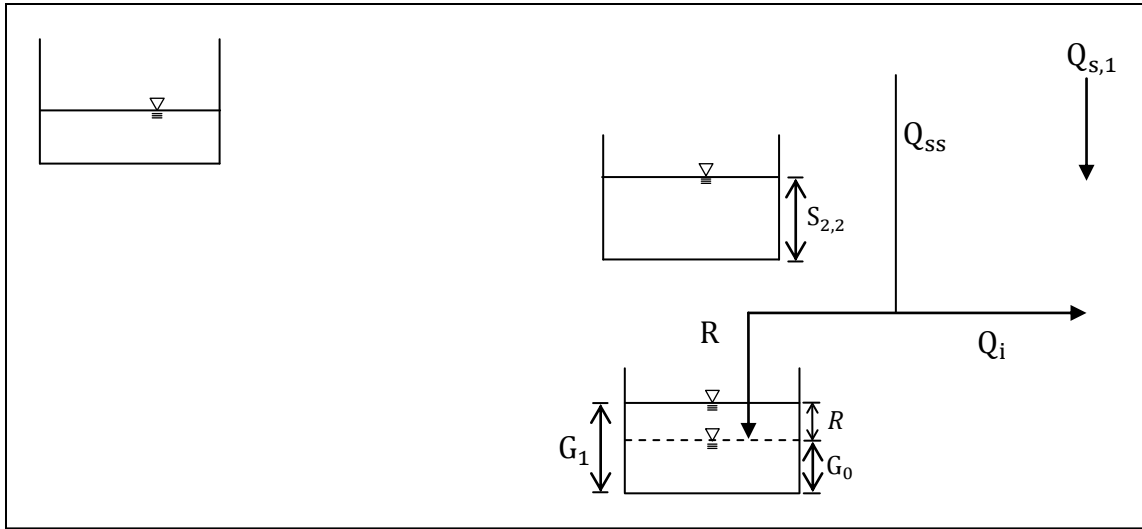


Figure 3.18. Stage 5 of the Final Model Structure.

3.6.9.6 Sixth Stage

In the sixth stage, a fraction of the recharge and the initial groundwater levels becomes baseflow, Q_b .

$$Q_b = k_2 \cdot (G_0 + R) \quad (3.96)$$

Groundwater levels are updated for the current time period:

$$G_1 = G_0 + R - Q_b \quad (3.97)$$

In this model, the groundwater reservoir does not have a maximum capacity limit.

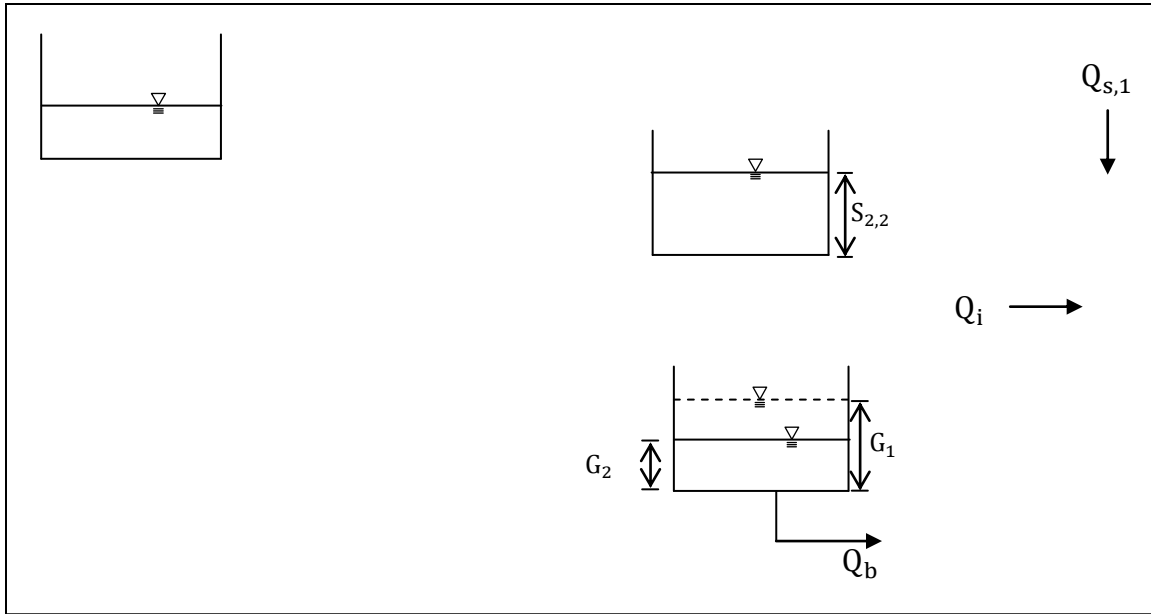


Figure 3.19. Stage 6 of the Final Model Structure.

3.6.9.7 Seventh Stage

Surface runoff is generated at every point of the catchment and must travel across regions of the land surface that may not be fully saturated before it reaches the outlet. This principle is sometimes used in distributed modeling and is incorporated into this model structure because results have shown improved model performance.

Thus, in the seventh stage, surface runoff, $Q_{s,1}$, has a second opportunity to enter the soil, via a second competition with the continuing abstraction, F_{a3} . Any surface runoff that does not infiltrate becomes the final surface runoff, $Q_{s,2}$.

$$\frac{F_{a3}}{S_{2,max} - S_{2,2}} = \frac{Q_{s,2}}{Q_{s,1}} \quad (3.98)$$

From continuity:

$$F_{a3} = Q_{s,1} - Q_{s,2} \quad (3.99)$$

Substituting Equation (3.99) into Equation (3.98) and solving for $Q_{s,2}$:

$$Q_{s,2} = \frac{Q_{s,1}^2}{S_{2,max} - S_{2,2} + Q_{s,1}} \quad (3.100)$$

Thus, the total streamflow is

$$Q = Q_d + Q_b + Q_i \quad (3.101)$$

Finally, the second soil moisture reservoir is updated to:

$$S_{2,3} = S_{2,2} + Q_{s,2} \quad (3.102)$$

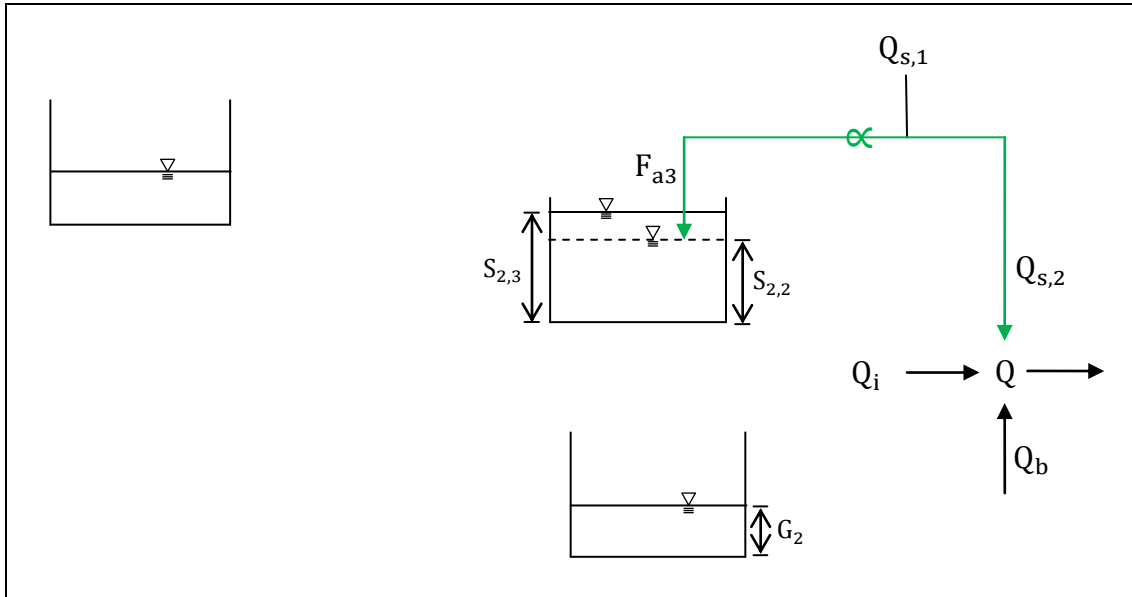


Figure 3.20. Stage 7 of the Final Model Structure. The green arrow and proportionality symbol represent the competition between F_{a3} and $Q_{s,2}$.

3.6.9.8 Model Structure Summary

Figure 3.21 below illustrates all stages of the proposed model structure.

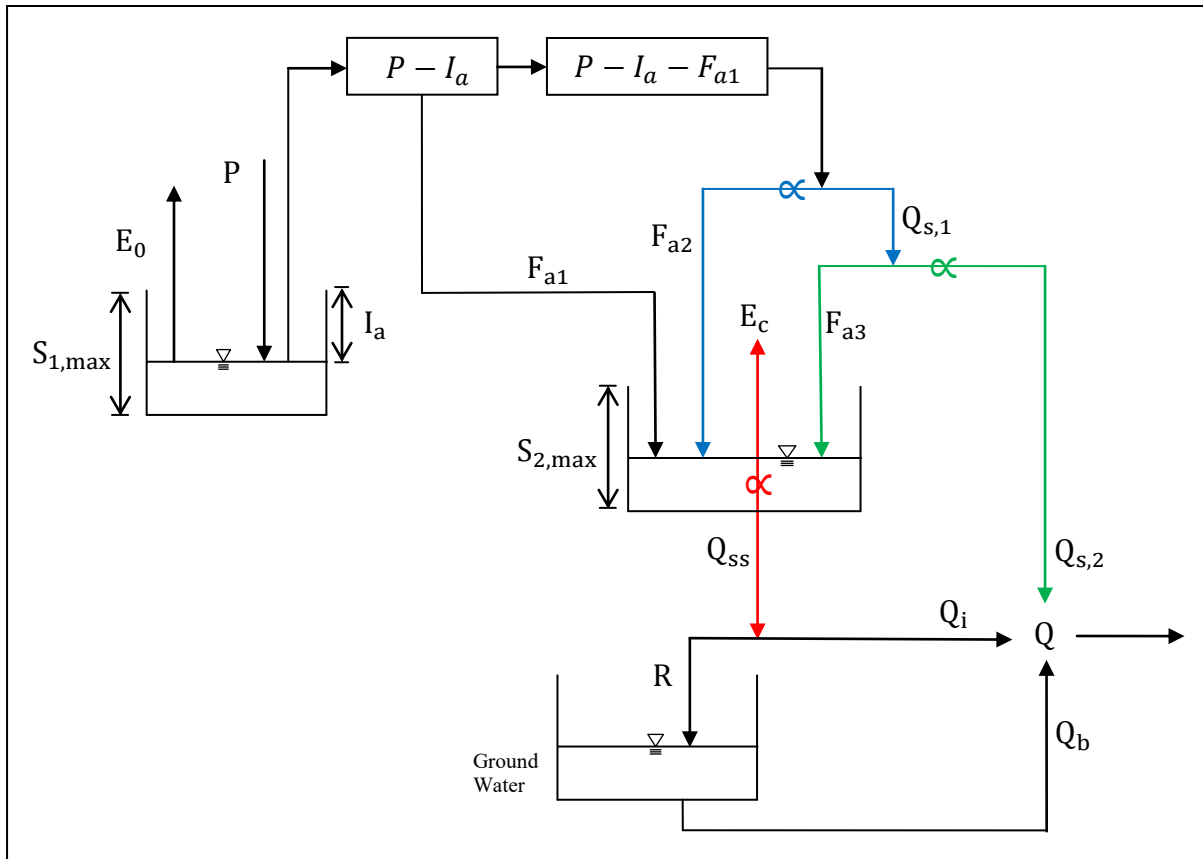


Figure 3.21. Final Model Structure. Blue, red, and green arrows with proportionality symbols refer to the competition between hydrologic processes described by the proportionality hypothesis.

CHAPTER 4: RESULTS AND DISCUSSION

The proposed model discussed previously was evaluated against the “abcd” model (Thomas, 1981) and the Dynamic Water Balance (DWB) model (Zhang et al., 2008) using data from 71 MOPEX catchments.

The evaluation of the model is broken down into three stages: (1) full-record calibration (2) half-record calibration, and (3) validation. The “full-record calibration” stage refers to the calibration of the models to streamflow data using all 21 years of available data for all time scales; that is, 21 records for the annual time scale, 252 records for the monthly time scale, and 7,670 records for the daily time scale. The “half-record calibration” stage refers to calibrations performed on the first 10 years of data (10 year for the annual records, 120 months for monthly records, and 3,653 days for the daily records). The validation stage uses the parameter sets obtained from the half-record calibration stage to simulate streamflow values across the remaining 11 years of data.

For parameters to be calibrated during both calibration stages, initial conditions must be set for the storage and routing terms (i.e. groundwater storage and soil moisture storage). For all models that have groundwater routing terms, the initial groundwater was assumed to be zero. Conversely, initial soil moisture storage values were set at their capacity. The assumptions were initially believed to not be particularly important unless a catchment was in a dry climate and was strongly influenced by streamflow regulation. Nonetheless, models were given a short “warm-up” period where their performance was not evaluated. This measure facilitates models in

self-correcting for the assumed initial conditions. For the daily, monthly, and annual time scales, this was set to 24 days, 24 months, and 3 years, respectively.

As discussed in Section 3.3, a genetic algorithm with a population of 500 was used 20 times for each catchment at all time scales and for all models to ensure that the optimal parameter set was obtained.

As mentioned previously, catchments were validated using the parameter sets obtained from the half-record calibration stage. In addition to this, the soil moisture and groundwater storage values at the end of the calibration period were used as the initial conditions for the validation stage. In the following sections, the results from the full-record calibration stage will be presented first, followed by results from the half-record calibration stage and the validation stage, respectively.

Before the results of the comparison are presented, however, an analysis of the parameters for the proposed model across the three time scales will be discussed for the full-record calibration stage and will be followed by a discussion of the hydrologic processes occurring in one catchment in Florida and an analysis of the model performance for the full-record calibration stage.

4.1 Analysis of the Proposed Model Parameters

The following analysis is based on the parameters obtained for the proposed model during the full-record calibration stage at the three time scales.

Soil moisture reservoirs can serve two purposes: (1) they can act as filtering mechanisms, allowing the slow release of water to additional hydrologic processes and (2) they can act as mechanisms which limit the amount of water that can pass through to additional processes (i.e. when the reservoir has more water, less water can pass through the reservoir and must be routed through a different process). In the case of the first soil moisture reservoir, there is a strong correlation between the optimal storage capacities at the daily time scale and the monthly time scale (Figure 4.1). This suggests that, at least between these two time scales, the model utilizes the first soil moisture mainly as a limiting mechanism (limiting water that is available for evapotranspiration or water that can pass to the second soil moisture reservoir). Between the monthly and annual time scale, the first soil moisture reservoir begins to function more as a filtering mechanism, as the soil moisture reservoir sizes increase significantly.

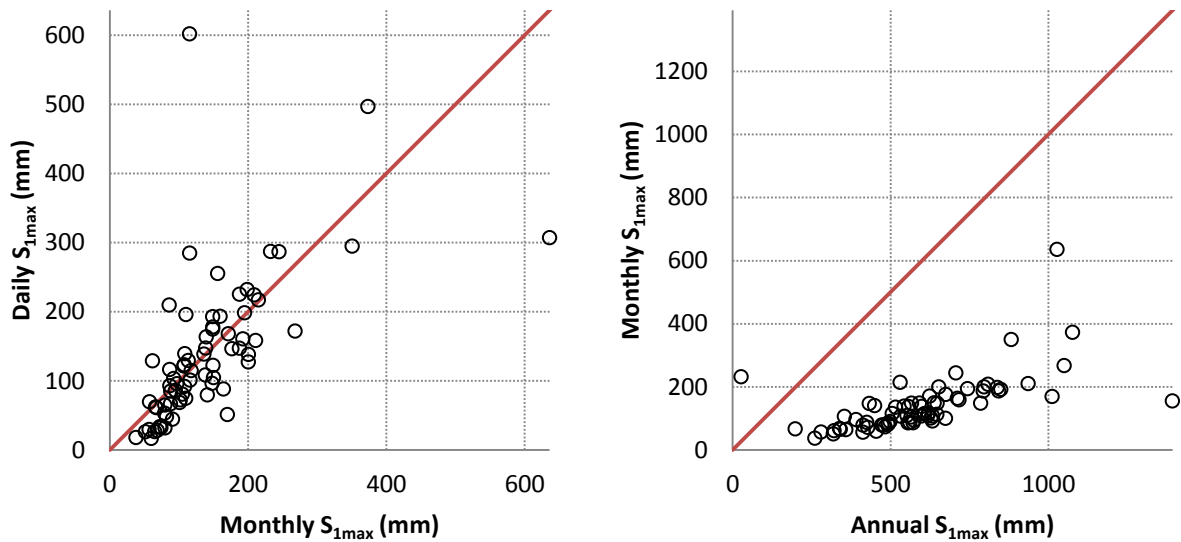


Figure 4.1. Relationships between the Maximum Capacity of the First Soil Moisture Reservoir, S_{1max} , of the Proposed Model at Different Time Scales for the Full-Record Calibration Stage.

The behavior in the second soil moisture reservoir is much different (Figure 4.2). Even between the daily and monthly time scales, there is very little similarity between the soil moisture capacities. This can be attributed to the increased impact that the filtering mechanism of the second reservoir plays on the model's performance. One important difference is that soil moisture storage tends to *decrease* slightly at the monthly time scale; this may be a consequence of the incorporation of the effects of seasonality into the model. Nonetheless, with the effects of seasonality negligible at the annual time scale and the greater effect that filtering has at larger time scales, the filtering mechanism becomes much more significant, causing the storage capacity to increase significantly between the annual and monthly time scales.

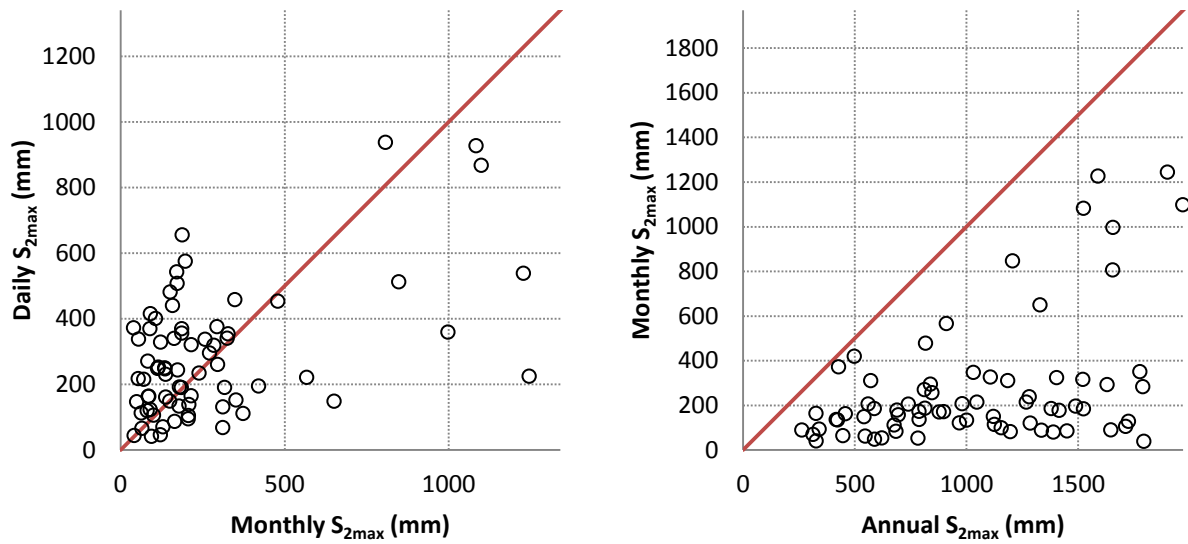


Figure 4.2. Relationships between the Maximum Capacity of the Second Soil Moisture Reservoir, S_{2max} , of the Proposed Model at Different Time Scales for the Full-Record Calibration Stage.

In the proposed model, k_1 represents the constant that regulates the partitioning of subsurface flow, Q_{SS} , into interflow, Q_i , and recharge, R . For example, when $k_1 = 1$, all subsurface flow becomes recharge, which is passed through the groundwater reservoir before being routed as streamflow.

Comparing how values of k_1 change between the daily and monthly time scales reveals only a weak relationship (Figure 4.3). However, it is interesting to note that at both the monthly and daily time scales there are no catchments where $k_1 = 0$, but many catchments have values of $k_1 = 1$. This emphasizes the importance of incorporating a routing mechanism into the model. At the annual time scale, the relationship of k_1 between time scales diminishes even further.

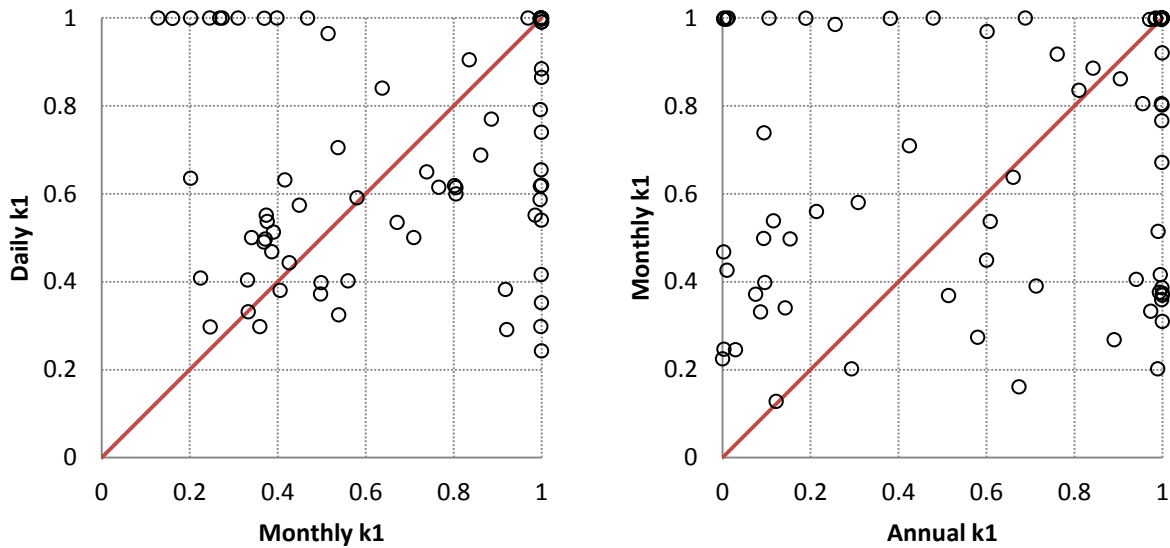


Figure 4.3. Relationships between Parameter k_1 of the Proposed Model at Different Time Scales for the Full-Record Calibration Stage.

The constant k_2 corresponds to the abcd model's d parameter, which is related to the groundwater residence time. It can be expected to increase at larger time scales as the effects of streamflow frequency filtering become more important; this is indeed the case at all three time scales illustrated in Figure 4.4.

In Figure 4.4, the value of k_2 at the daily time scale is often at zero. This finding reveals a mechanism implicit in the model structure that wasn't considered previously. In the model structure, the groundwater reservoir was assumed to have infinite capacity. It was assumed that the greater the amount of water that is stored in the reservoir, the greater the outflow rate. However, the results at the daily time scale suggest that k_1 was often 1 while k_2 was often 0.

This condition equates to a seepage loss function, because the groundwater reservoir will continually partition water away from the subsurface flow but will never contribute to the main streamflow. This is a realistic possibility, because, unlike surface water, groundwater is not restricted by topography and can cross catchment boundaries, potentially contributing to the outflow of other catchments. However, a closer examination of the results reveals that this condition does not occur often. Nonetheless, this effect should be considered in future development of this model, as was done in Kuczera (1983).

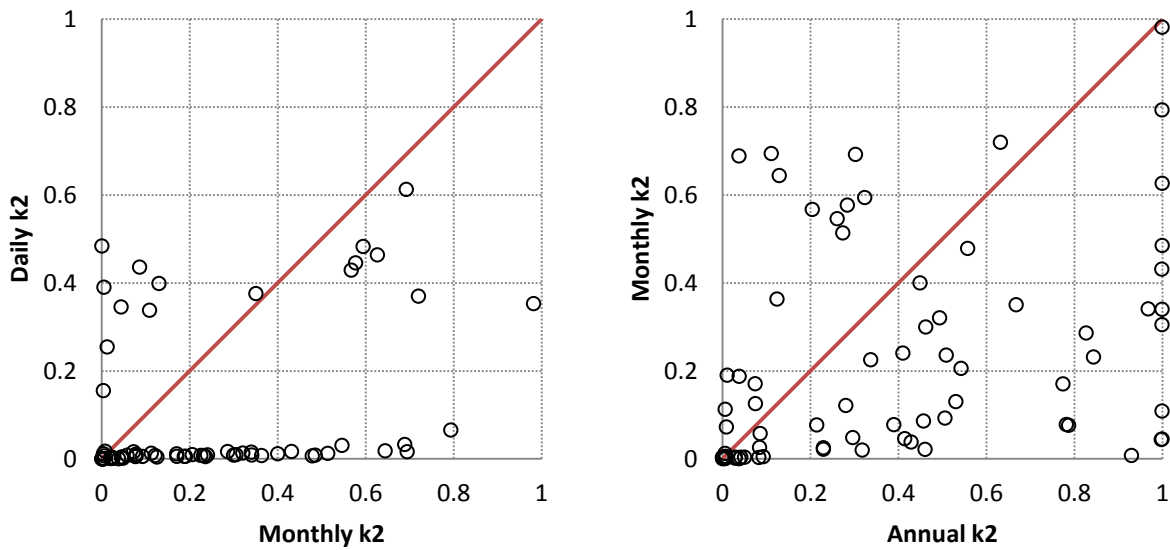


Figure 4.4. Relationships between Parameter k_2 of the Proposed Model at Different Time Scales for the Full-Record Calibration Stage.

The parameter k_3 represents the fraction of water in the second tank that is allocated between continuing evapotranspiration, E_c , and subsurface flow, Q_{SS} . When $k_3 = 1$, all of the

soil moisture is partitioned between evapotranspiration and subsurface runoff (i.e. the soil moisture at the end of the time period is empty). At the daily time scale, this parameter tends to be low relative to the monthly time scale. This is primarily due to the greater number of precipitation-free time periods and, correspondingly, the higher variability in precipitation. To counteract this higher level of variability (which would produce more streamflow and evapotranspiration), the parameter must be reduced.

From the monthly to the annual time scale, reservoir capacities increase significantly while variability in precipitation decreases slightly; the former will decrease the value of k_3 while the latter increases it. Since these two factors are not proportional to each other, it is reasonable that no relationship exists between the values of k_3 between the monthly and annual time scales.

In the figure on the right of Figure 4.5, a large number of catchments have values of $k_3 = 1$, especially at the annual time scale, which indicates that soils will be completely drained by subsurface flow or evapotranspiration by the end of the time period. This can be expected for shallow soils or soils with high hydraulic conductivities.

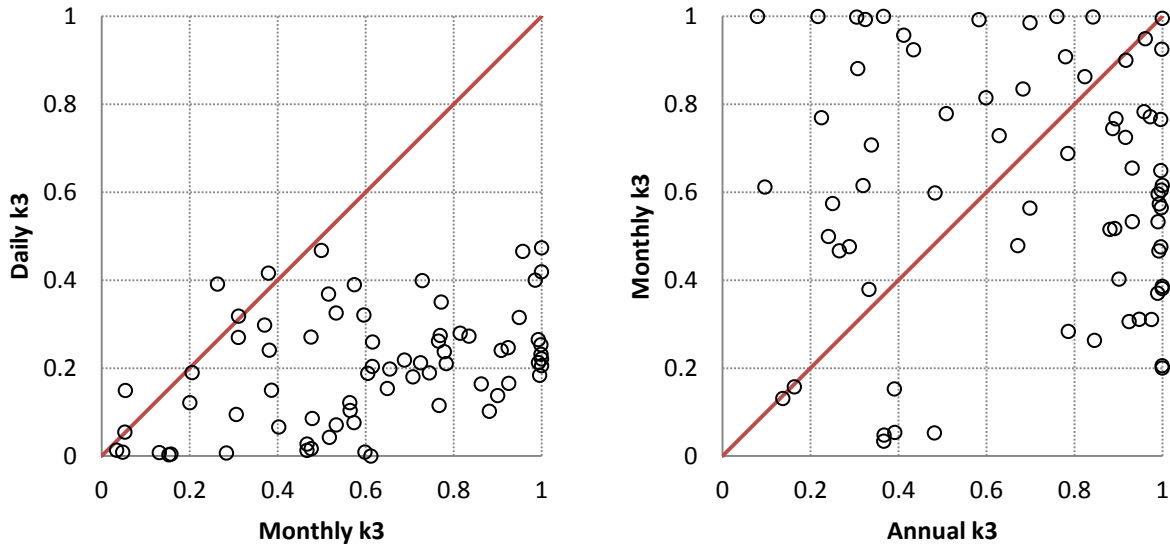


Figure 4.5. Relationships between Parameter k_3 of the Proposed Model at Different Time Scales for the Full-Record Calibration Stage.

The parameter k_5 indirectly regulates the level of influence that surface runoff, Q_s , has on the competition between infiltration, F_{a2} , for the water that leaves the first reservoir (i.e. $P - I_a$). Higher values decrease the influence of Q_s in the competition (and the frequency of occurrence of this competition). At the daily time scale, there are a large number of catchments with $k_5 = 0$, indicating that surface runoff is a considerable factor (Figure 4.6). This impact declines at the monthly time scale, as indicated by the larger values of k_5 . At the annual time scale, values of k_5 decline slightly. This may be due to the significantly larger reservoir sizes, which increase the competitiveness of infiltration against surface runoff. That is, surface runoff still decreases at larger time scales, except with a different mechanism.

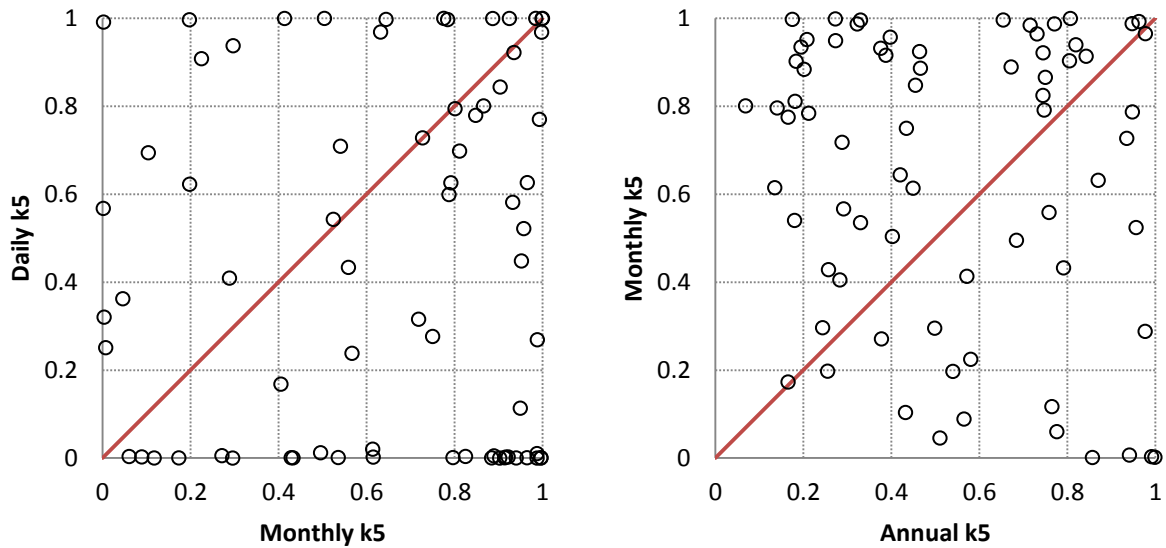


Figure 4.6. Relationships between Parameter k_5 of the Proposed Model at Different Time Scales for the Full-Record Calibration Stage.

4.2 Analysis of the Proposed Model at One Catchment in Florida

In this section, the results from the full-record calibration stage will be analyzed in detail from one catchment in Florida (02296750). The catchment is located 47 km southwest of Orlando and has a large number of lakes in the northern section of the catchment (Figure 4.7). The saturated hydraulic conductivity, as estimated from the STATSGO database, was found to be the highest of the 71 catchments (Soil Survey Staff, 2013). This is primarily because the catchment overlies the highly-efficient Floridan Aquifer, which suggests that the catchment may be subject to high leakage rates to this aquifer. The model as described, however, does not simulate groundwater storage that does not exit the catchment as streamflow (i.e. only shallow groundwater storage is modeled). Nonetheless, this catchment was selected because the mean

annual aridity index is close to one (1.06) and the number of dry and wet months, as defined by the mean monthly aridity index, is equal (6). Thus, this catchment represents a balance between humid and arid climates and its results are assumed to be a fair representation of the 71 catchments.

Different aspects of the proposed model will be analyzed across the three time scales, including, (1) how modeled evapotranspiration compares with actual evapotranspiration, (2) how initial and continuing evapotranspiration compare with each other, (3) how the different processes of surface runoff, interflow, and baseflow compare with each other, (4) how well simulated runoff models observed runoff, and (5) how model reservoir water levels fluctuate with time.

All years of data (excluding 3 years for model warm-up) will be used during the analysis of the annual simulation results. At the monthly time scale, the time period analyzed will be restricted to January 1994 through December 1995 (2 years) for the sake of clarity. Similarly, the number of results analyzed in the daily time scale will be restricted to a single year (1994); the reason that the daily time scale considers more records (365 vs. 24) is because seasonality has a strong impact on the results and analyzing only a month or two of daily records is insufficient to appropriately assess the model performance.



Figure 4.7. Topographic Map of Florida MOPEX Catchment (02296750).

4.2.1 Modeled vs. Actual Evapotranspiration

Total evapotranspiration is the sum of both the initial component in the first reservoir, E_0 , and the continuing component in the second reservoir, E_c . At the daily time scale, Figure 4.8 indicates that the modeled evapotranspiration tends to be higher than observation records. This is due to an overestimation of evapotranspiration in the first tank, which is very often at the potential rate (Figure 4.11). In the equations for initial evapotranspiration, the rate is set equal to the potential rate, provided there is enough water in the soil moisture layer to meet the demand. Otherwise, the initial evapotranspiration rate will equal the soil moisture in the reservoir. Modifications to this approach, limiting the initial evapotranspiration rate, were considered; however, all modifications (based on an abcd and Thornthwaite and Mather model approach) did not yield improved results.

In many cases, evapotranspiration is simulated as zero when it is observed between 1 and 4 millimeters. This is a second consequence of the initial evapotranspiration modeling approach. When the first soil moisture layer is completely drained (due to the evapotranspiration demand exceeding the capacity of the first reservoir) during the previous time period and there is no precipitation in the current time period, then initial evapotranspiration cannot occur.

At the monthly and annual time scales, the overestimation in modeled evapotranspiration is still evident and is especially significant at the annual time scale, though there are no occurrences of zero-modeled evapotranspiration (Figures 4.9 and 4.10).

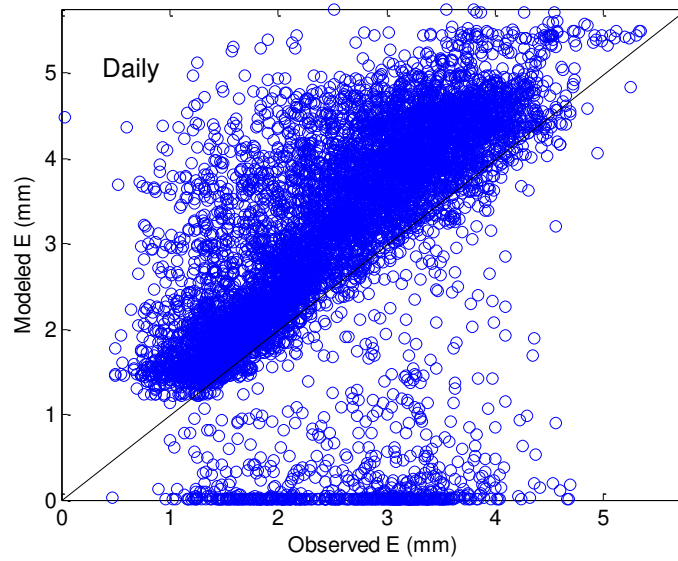


Figure 4.8. Modeled Daily Evapotranspiration vs. Observed Daily Evapotranspiration from 1/25/1983 to 12/31/2003 at the Florida Catchment. The plot excludes records during warm-up of the model.

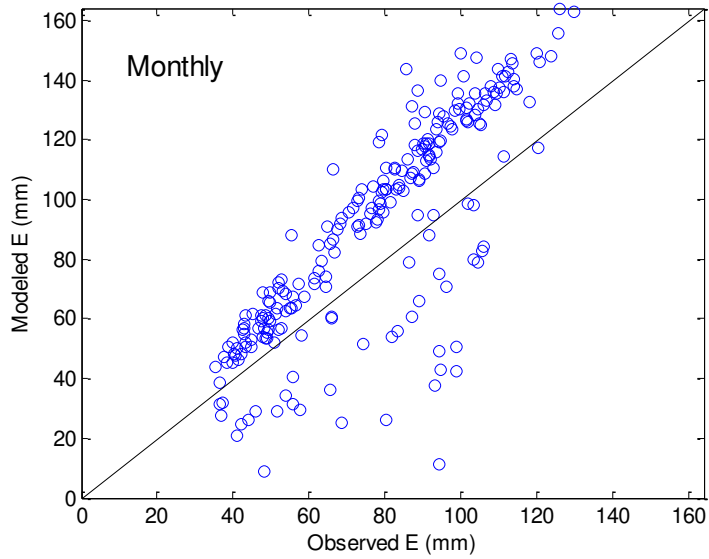


Figure 4.9. Modeled Monthly Evapotranspiration vs. Observed Monthly Evapotranspiration from 1/1985 to 12/2003 at the Florida Catchment. The plot excludes records during warm-up of the model.

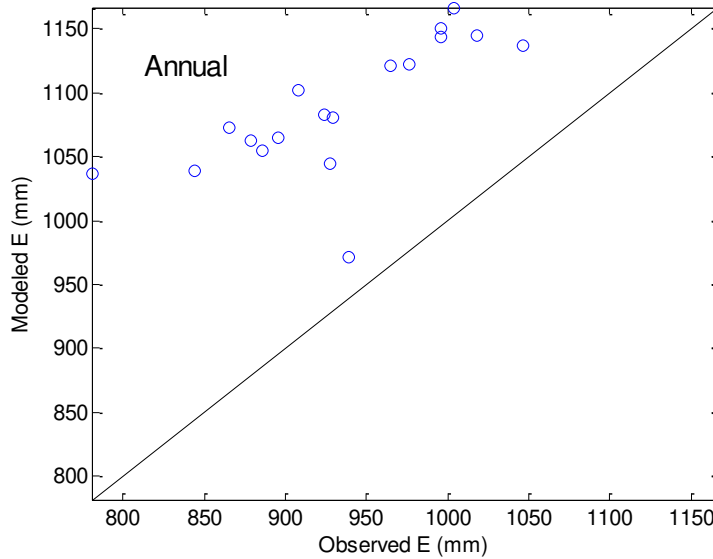


Figure 4.10. Modeled Annual Evapotranspiration vs. Observed Annual Evapotranspiration from 1/1/1983 to 12/31/2003 at the Florida Catchment.

4.2.2 Initial and Continuing Evapotranspiration

As was discussed previously, initial evapotranspiration during the daily time scale was most often at the potential rate (Figure 4.11). The only times continuing evapotranspiration is nonzero is when the demand cannot be met in the first soil moisture reservoir. In fact, the maximum continuing evapotranspiration rate was only 0.5 mm and was on average only 0.001 mm. Thus, the continuing evapotranspiration is a negligible process at the daily time scale.

At the monthly time scale, the continuing evapotranspiration is still a minor process, but is more significant (Figure 4.12). On average, it is approximately 0.9 mm per month and is at most 26 mm. In contrast, the dynamics at the annual time scale between the different hydrologic processes within the model change to the point that the initial evapotranspiration is a constant

935.78 mm (excluding 2000, which was 915.51 mm). This is due to the fact that the evapotranspiration demand is almost always greater than the capacity of the first storage reservoir.

The significance of the continuing evapotranspiration can be quantified by calculating the average of continuing evapotranspiration and dividing it by the average initial evapotranspiration; in the case of this catchment, the ratio was 0.17. Thus, continuing evapotranspiration becomes much more significant and should not be excluded from the annual time scale (Figure 4.13).

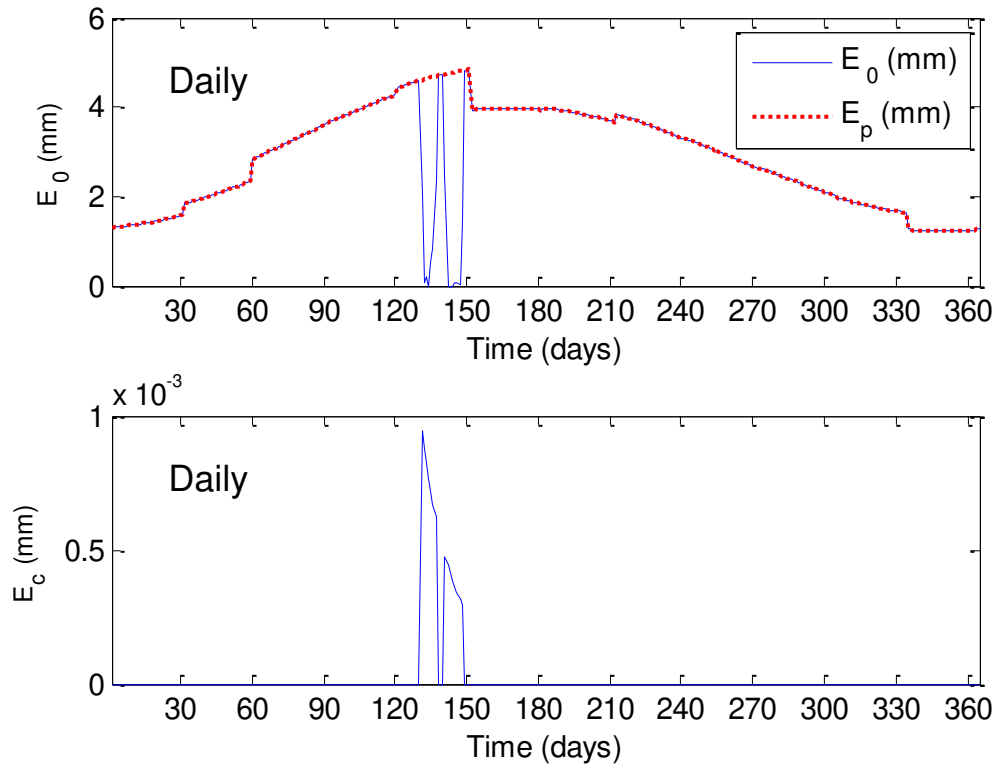


Figure 4.11. Modeled Daily Initial Evapotranspiration and Continuing Evapotranspiration for 1994 at the Florida Catchment. The top figure shows the initial evapotranspiration along with the potential evapotranspiration.

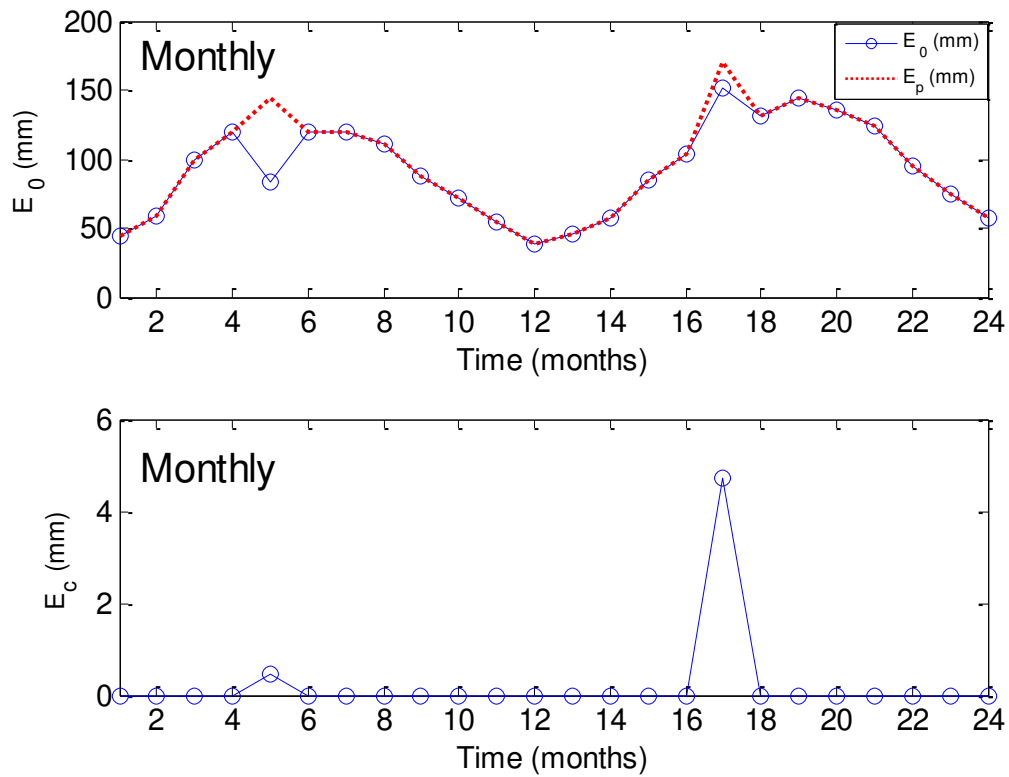


Figure 4.12. Modeled Monthly Initial Evapotranspiration and Continuing Evapotranspiration for 1994 through 1995 at the Florida Catchment. The top figure shows the time series of initial evapotranspiration and potential evapotranspiration. The bottom figure shows the time series of continuing evapotranspiration.

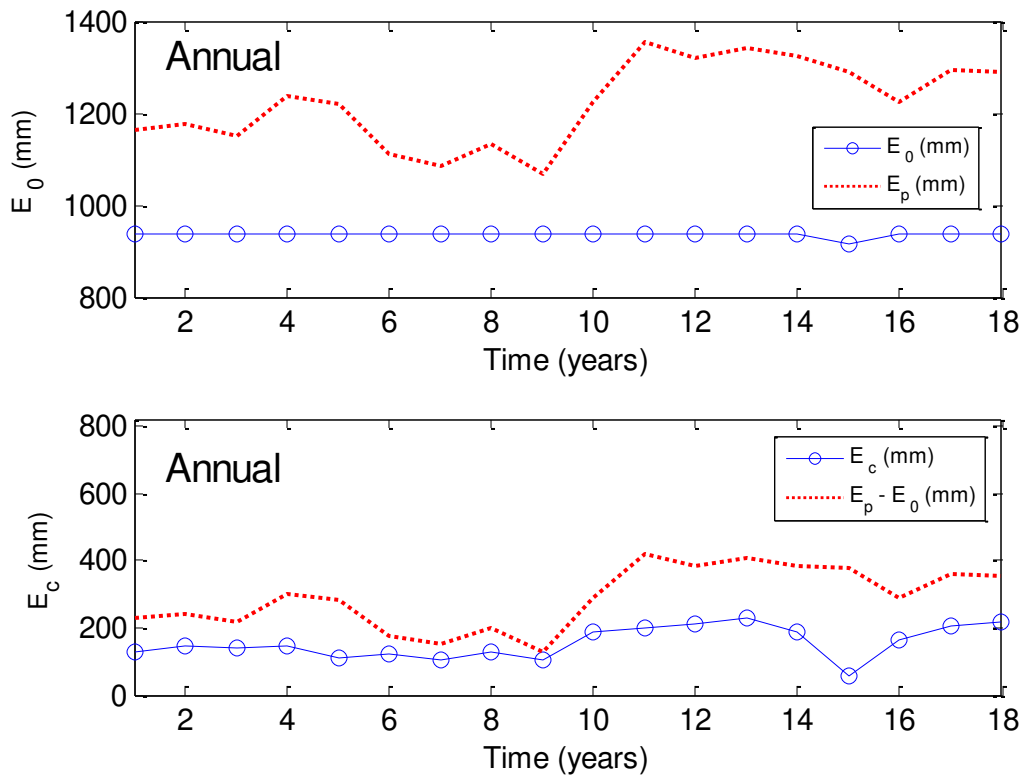


Figure 4.13. Modeled Annual Initial Evapotranspiration and Continuing Evapotranspiration for 1986 through 2003 at the Florida Catchment. The plot excludes records during warm-up of the model. The top figure shows the time series of initial evapotranspiration and potential evapotranspiration. The bottom figure shows the time series of continuing evapotranspiration and the remaining evapotranspiration demand after initial evapotranspiration.

4.2.3 Runoff Processes

At the daily time scale, surface runoff, Q_s , is negligible throughout the year. This result is not necessarily unrealistic, as most surface runoff will become interflow before it reaches the outlet of large catchments such as the one studied. Though there was no known reliable method

to assess the true surface runoff, it appears that the model underestimates the impact of surface runoff.

Interflow, as expected, is significantly larger than surface runoff and, in fact, makes up a majority of the total streamflow. The overall *behavior* of interflow in comparison with baseflow is reasonable. However, its magnitude in relation to baseflow is significantly larger than expected.

As discussed earlier in model 16, when the process of interflow is neglected (i.e. so that all subsurface flow becomes baseflow), the second soil moisture reservoir acts as a routing mechanism, similar to the groundwater reservoir. That is, even though the water that leaves the subsurface flow as interflow is not routed through another reservoir like groundwater, it is still being routed as a result of being passed through the second soil moisture reservoir. It may be that the separation of subsurface flow into interflow and recharge is too simplified; in the case of the proposed model, this separation is handled by $R = k_1 Q_{SS}$ and $Q_i = (1 - k_1) Q_{SS}$. A more realistic relationship would be based on the current water levels within the groundwater reservoir. This idea was attempted earlier by using a proportionality relationship:

$$\frac{R}{G_{max} - G(t-1)} = \frac{Q_i}{Q_{SS}} \quad (4.1)$$

However, this alternative method did not produce improved results. It may also be necessary to modify the definition of the groundwater reservoir as well. Future model development will focus on this aspect.

In Figure 4.14, the analysis at the daily time scale is restricted to 1994 only. In Figure 4.15, the monthly time scale analysis includes both 1994 and 1995. Thus, looking at the first half

of the data in Figure 4.15 shows that the behavior of the runoff processes at both time scales is similar. A notable difference is that a small component of runoff is simulated as surface runoff at the monthly time scale during the months of July through September (months 7-9 in Figure 4.15 or days 182 through 273 in Figure 4.16).

At the annual time scale, baseflow decreases substantially (Figure 4.16). In fact, the average baseflow is only a third of its corresponding average value at the daily time scale. The model allocates more runoff to surface runoff because routing (delay of streamflow response) is less significant and filtering (reduction of streamflow variability) is more important at longer time scales. In Stage 7 of the model, surface runoff enters the soil moisture layer a second time. This process is similar to how baseflow is filtered by the groundwater reservoir. This filtering causes a shorter delay in runoff response than the groundwater reservoir, which is why it is more significant at larger time scales.

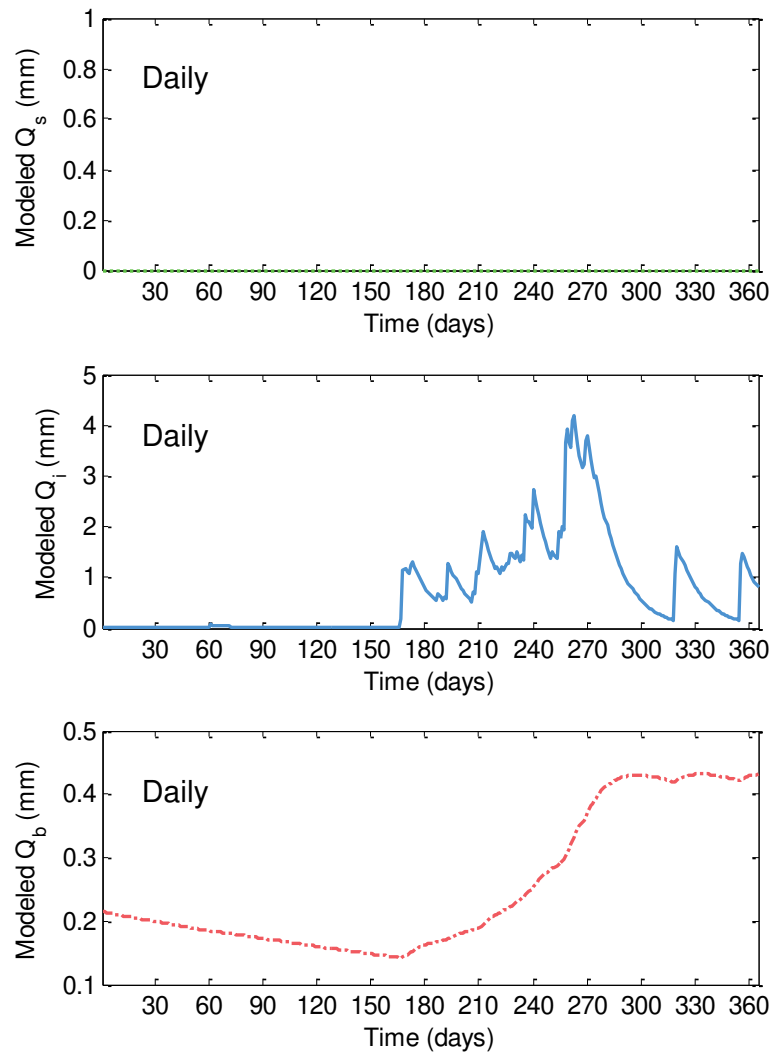


Figure 4.14. Time Series of Daily Surface Runoff, Interflow, and Baseflow during 1994 for the Florida Catchment.

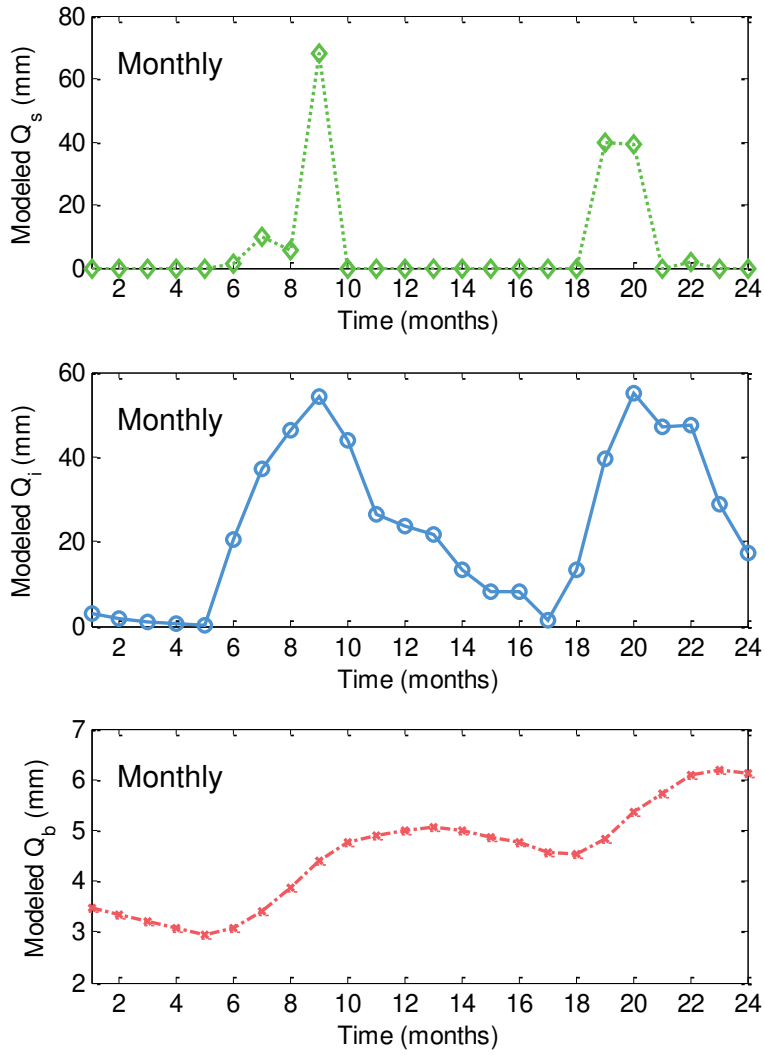


Figure 4.15. Time Series of Monthly Surface Runoff, Interflow, and Baseflow from 1994 to 1995 for the Florida Catchment.

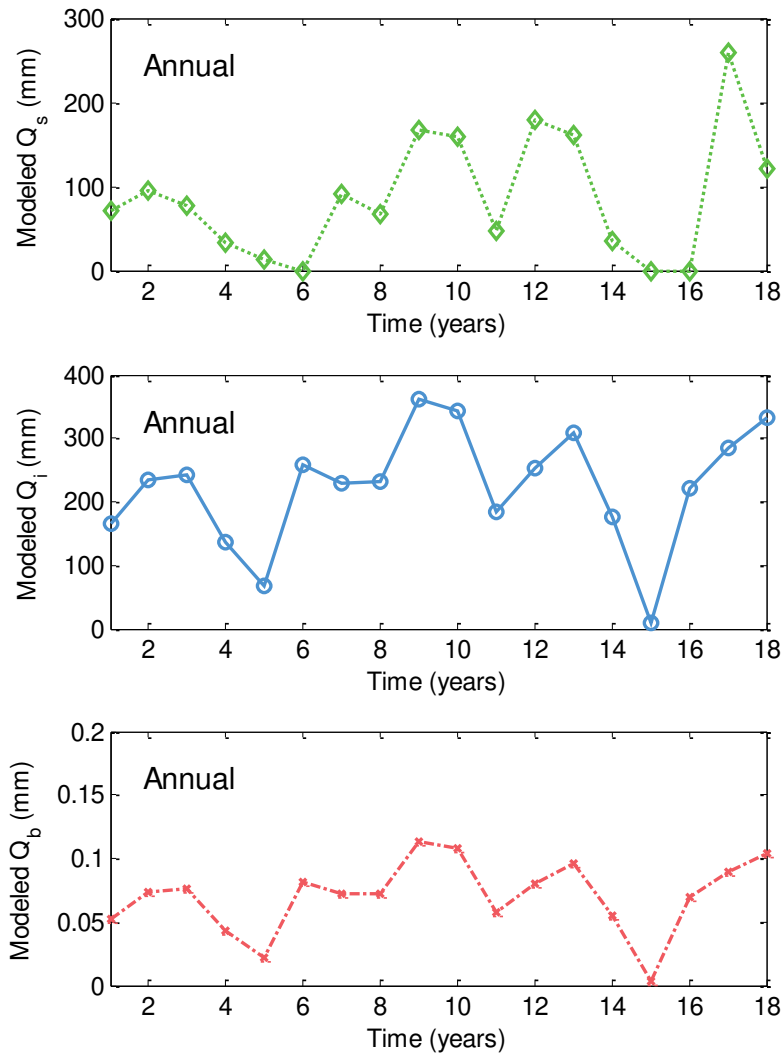


Figure 4.16. Time Series of Annual Surface Runoff, Interflow, and Baseflow from 1986 to 2003 for the Florida Catchment.

4.2.4 Simulated vs. Observed Runoff

Analysis of the daily streamflow simulations (Figure 4.17) suggests that the model is unable to handle large variations in streamflow between consecutive time records. This may be

due to an over-reliance of the model on interflow to handle direct runoff processes. Resolving this problem may help to improve model performance. Likewise, at the monthly time scale (Figure 4.18), it is evident that the model does not handle large variations well, but is otherwise able to simulate the observed streamflow closely. At the annual time scale (Figure 4.19), the inability of the model to handle large streamflow simulations is again evident, particularly for years 13 and 18 (1998 and 2003).

A comparison against baseflow separation techniques was considered. However, most of these techniques (if not all) separate streamflow into baseflow and direct runoff. By definition, direct runoff includes both interflow and surface runoff. In reality, however, interflow can be more appropriately described by dividing it into a fast component (which is typically assigned to direct runoff), and a slow component (which is typically attributed to baseflow). It would be difficult, then, to compare the proposed model against baseflow separation techniques. Consequently, evaluation of the simulated streamflow discharge was done against the total streamflow only.

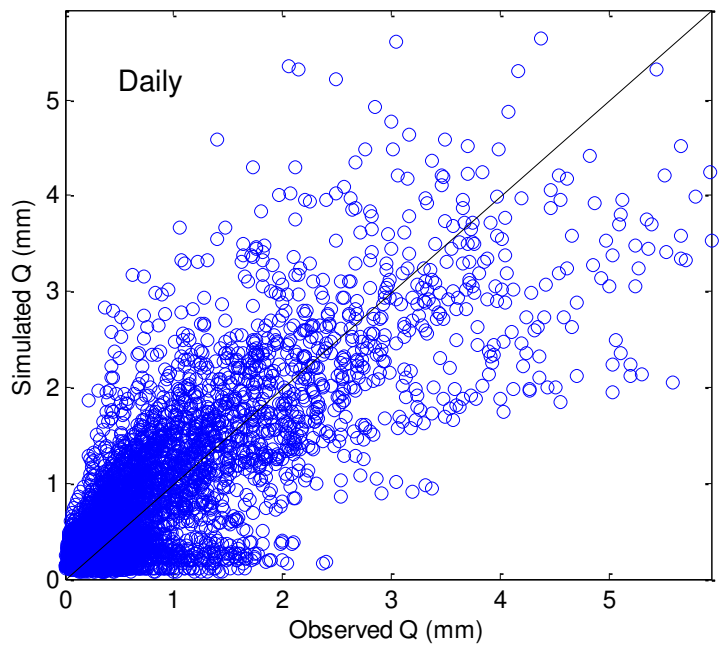
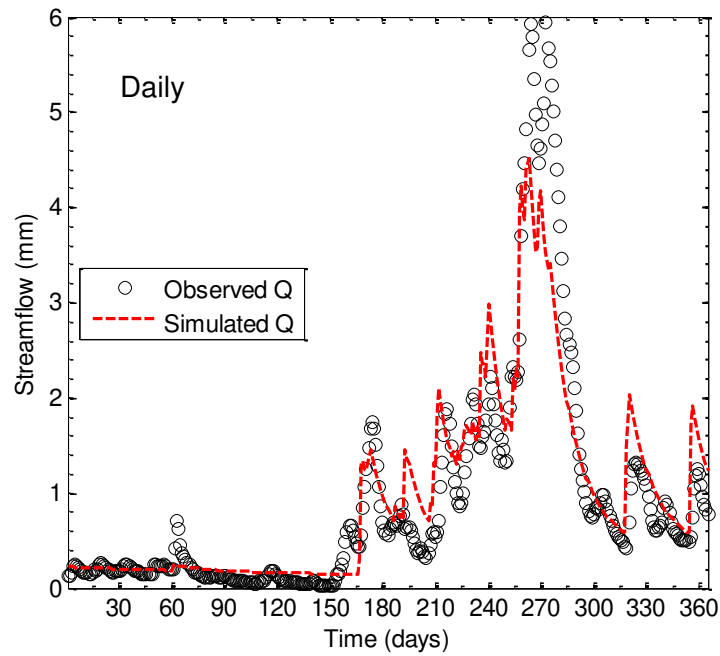


Figure 4.17. Daily Observed Runoff and Modeled Runoff for the Proposed Model at the Florida Catchment. The top figure shows the time series of observed runoff (streamflow) and modeled runoff for 1994. The bottom figure shows modeled runoff vs. observed runoff for all records excluding the warm-up time period.

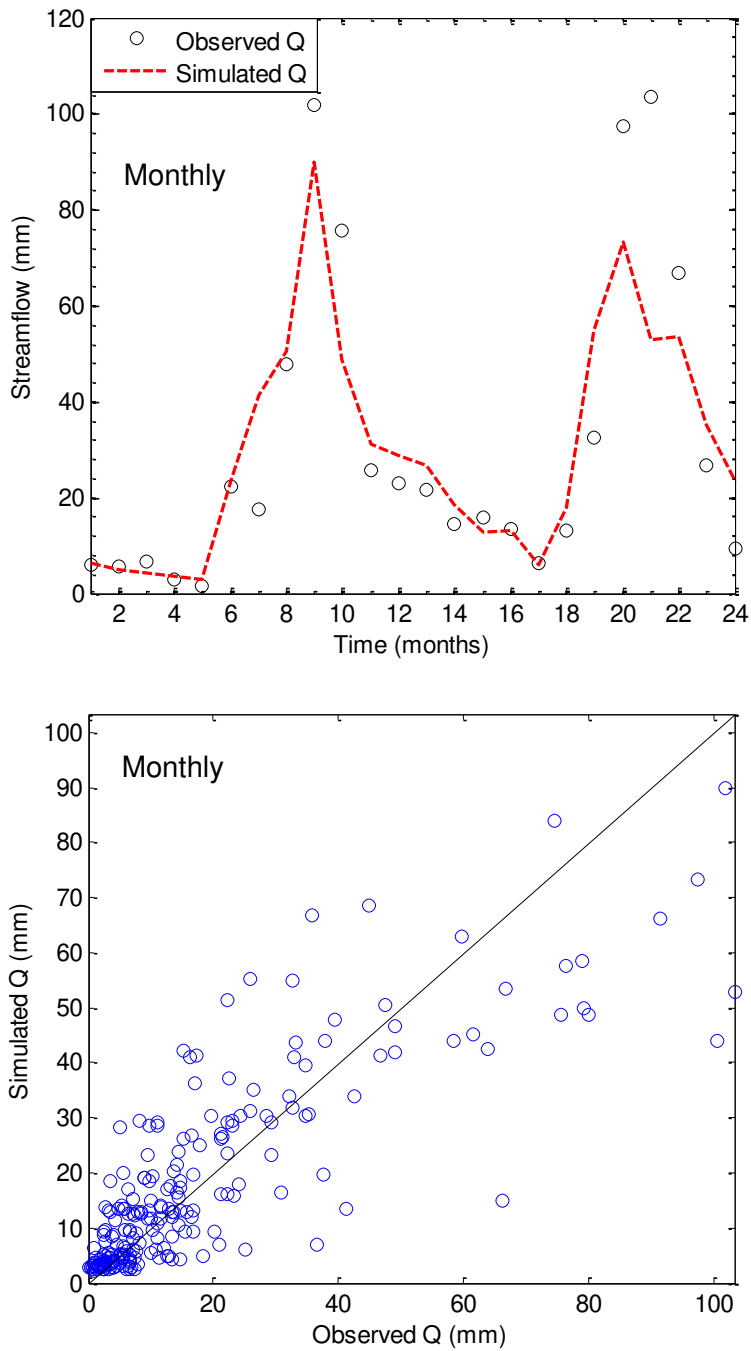


Figure 4.18. Monthly Observed Runoff and Modeled Runoff for the Proposed Model at the Florida Catchment. The top figure shows the time series of observed runoff (streamflow) and modeled runoff for 1994. The bottom figure shows modeled runoff vs. observed runoff for all records excluding the warm-up time period.

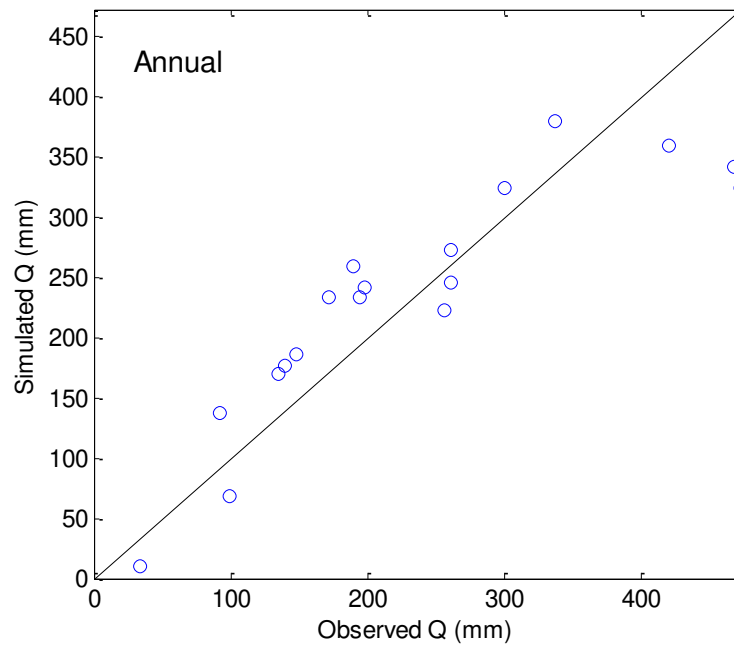
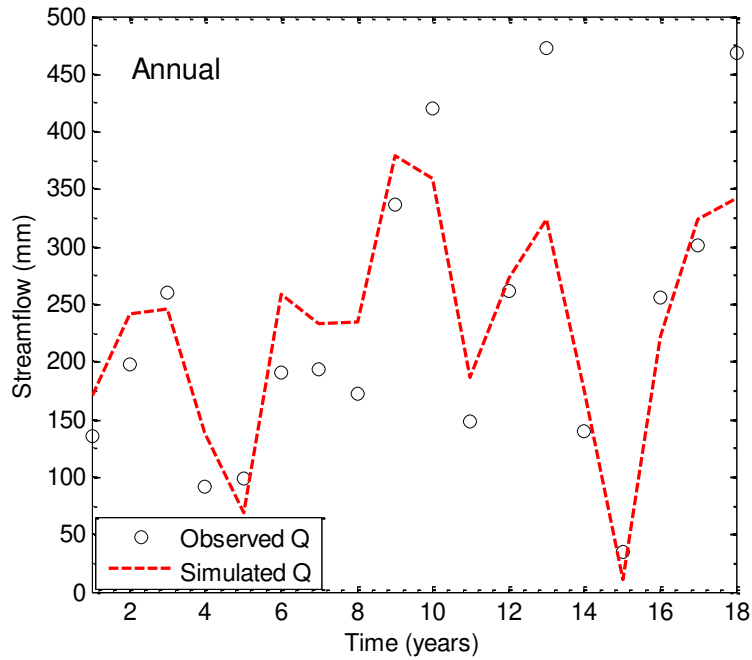


Figure 4.19. Annual Observed Runoff and Modeled Runoff for the Proposed Model at the Florida Catchment. The top figure shows the time series of observed runoff (streamflow) and modeled runoff for 1986 to 2003 (excludes the warm-up time period). The bottom figure shows modeled runoff vs. observed runoff for the same time period.

4.2.5 Soil Moisture Levels

In Figure 4.20, soil moisture for both soil moisture layers is displayed for the daily time scale. The soil moisture represented in the figure does not represent the maximum water levels that can occur in the reservoir, but what is left over from the hydrologic processes acting on the reservoirs.

Soil moisture levels in the first soil moisture reservoir, for the most part, remain fairly high through the year. However, beginning around the middle of March (day 75), groundwater levels decline drastically and, especially during May (days 120 to 150), groundwater levels are about their lowest. This time also corresponds to when potential evapotranspiration is at its highest (Figure 4.11). Water levels in the second reservoir are nearly empty at the end of each day until the middle of June. From June to September (days 150 to 180) the high frequency of precipitation events cause water levels in the second tank to rise and maintain water levels above zero for the rest of the year.

At the monthly time scale, reservoir water levels follow a similar pattern compared with the daily time scale (Figure 4.21). Moreover, the additional year in the monthly data shows that the zero soil moisture in the second reservoir for the first half of 1994 is not indicative of a problem with the soil moisture layer representation, as water levels during the same time period in 1995 remain above zero, even for the month of May (month 17).

The results for the annual time are quite different (Figure 4.22). The first soil moisture layer is consistently zero, primarily because the initial evapotranspiration rates are always equal to the soil moisture capacity (see E_0 in Figure 4.13), draining the first soil moisture layer during

each time period. Soil moisture levels at the end of each time step in the second layer are significantly lower than the maximum capacity, illustrating the magnitude of water that is transferred in the reservoir during the time period.

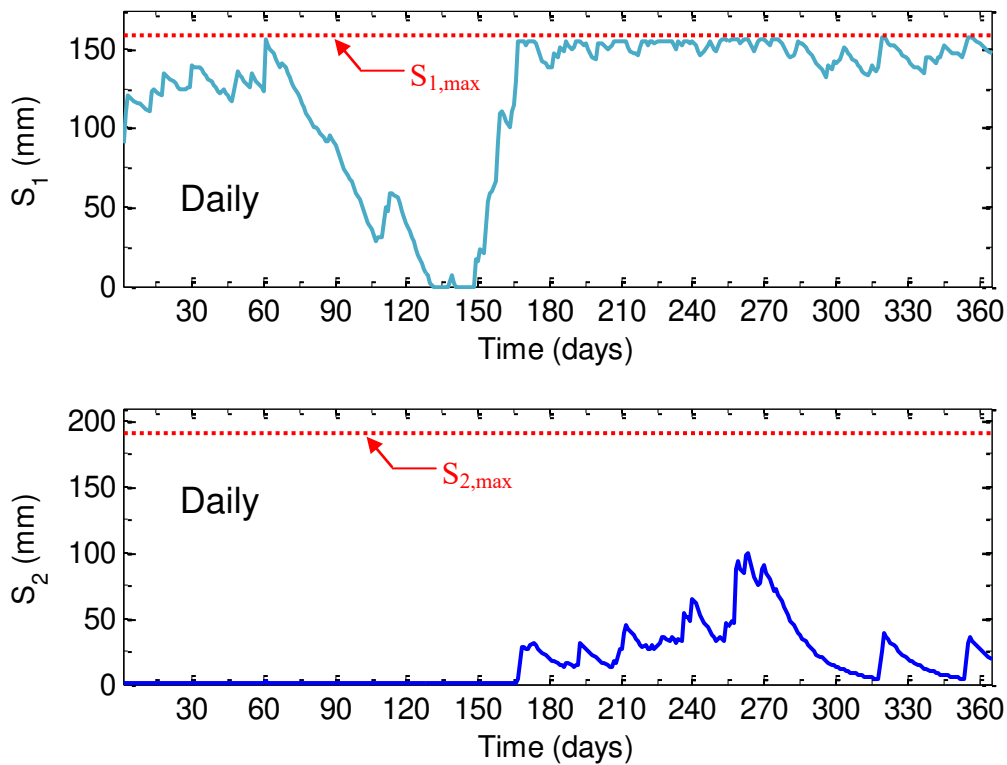


Figure 4.20. Daily Simulations during 1994 of Soil Moisture Storage at the End of the Day for the Upper and Lower Soil Moisture Layers. The red dashed line represents the capacity limits for each soil moisture layer.

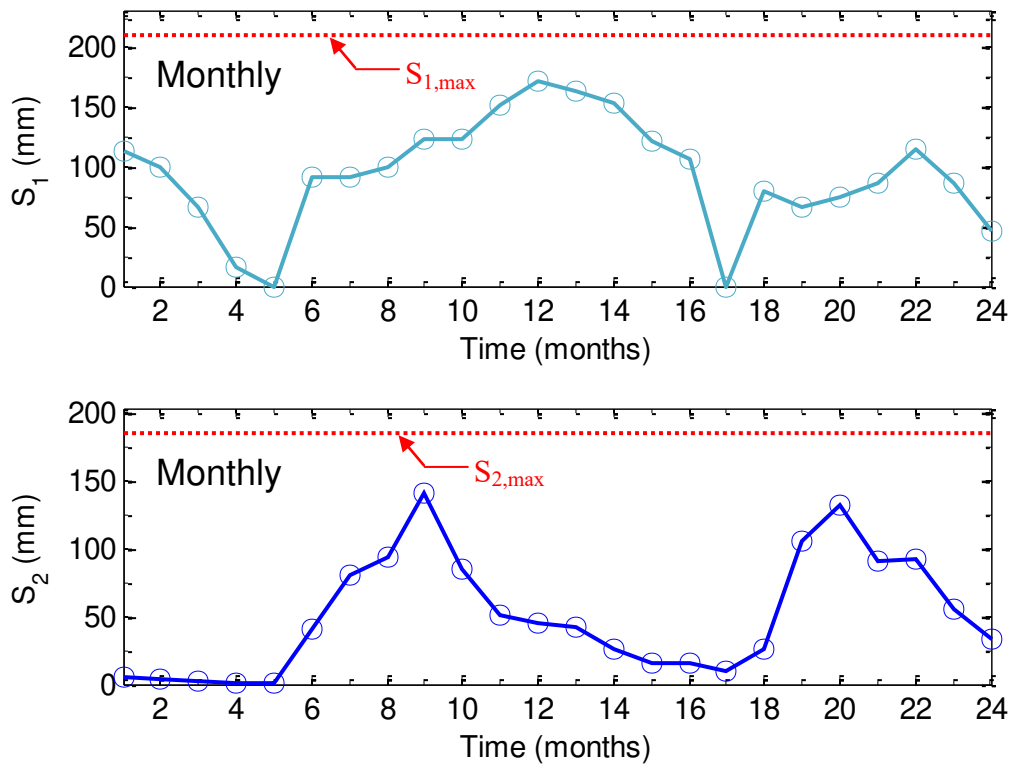


Figure 4.21. Monthly Simulations from January 1994 to December 1995 of the Soil Moisture Storage at the End of the Month for the Upper and Lower Soil Moisture Layers. The middle and bottom figures show the soil moisture for the lower soil moisture layer with and without the soil moisture capacity ($S_{2,max}$). The red dashed line represents the capacity limits for each soil moisture layer.

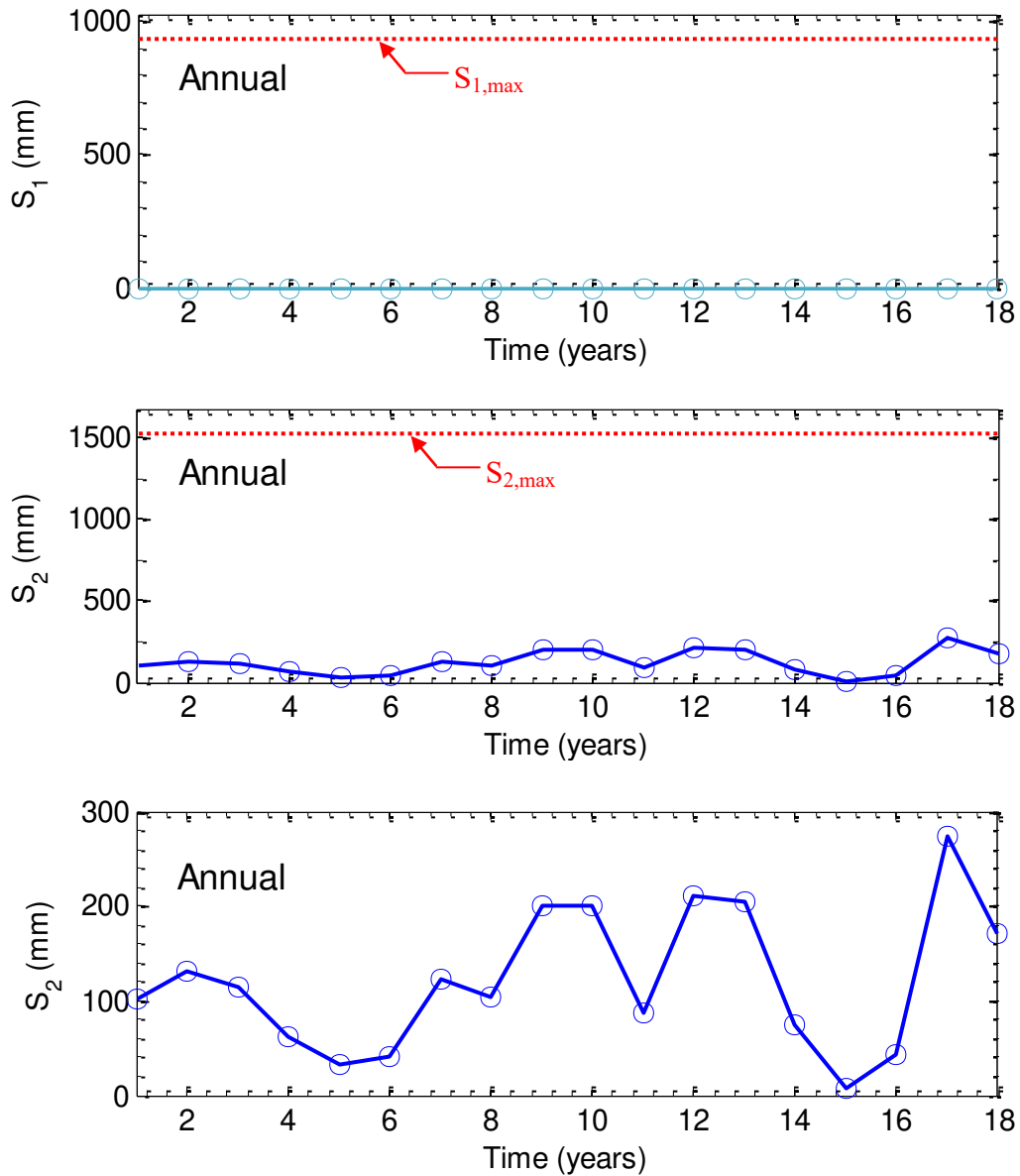


Figure 4.22. Annual Simulations from 1986 to 2003 of the Soil Moisture Storage at the End of the Year for the Upper and Lower Soil Moisture Layers. The red dashed line represents the capacity limits for each soil moisture layer. 1983 to 1985 were excluded since they were warm-up years.

4.3 Summary of Model Performance for the Proposed Model

The full-record calibration stage results for the proposed model across all 71 catchments are displayed graphically for the daily, monthly, and annual time scales in Figures 4.23, 4.24, and 4.25, respectively. The classification system used in the figures is based on the one used by Martinez and Gupta (2010). In their system, they classify catchments as bad if $NSE < 0.59$ (red), poor if $0.59 \leq NSE < 0.67$ (orange), acceptable if $0.67 \leq NSE < 0.75$ (yellow), and good if $0.75 \leq NSE < 1$ (green).

At the daily time scale, good and acceptable performance is restricted mainly to the Southeast, though there are a few catchments with good/acceptable performance in states like Arkansas and Kentucky (Figure 4.23). The effects of urbanization are a possible explanation for the poor performance of catchments in Northern Georgia, especially for catchment 02339500, which passes through the Atlanta metropolitan region (denoted by the dashed ellipse in Figure 4.23). As discussed in Section 6.1, the poor performance of catchment 02349500 is likely due to discharge of groundwater to the aquifer.

Except for areas in the Southwest, Northeast, and East North Central United States, performance of catchments is very good at the monthly time scale (Figure 4.24).

At the annual time scale, catchment performance declines in some of the Southern states while it increases in the Northern states (Figure 4.25). As mentioned earlier, evapotranspiration estimates are sharply overestimated at the annual time scale (Figure 4.10). Considering the larger role that evapotranspiration has in the Southern United States, additional refinement of evapotranspiration processes will likely improve streamflow estimates in this region.

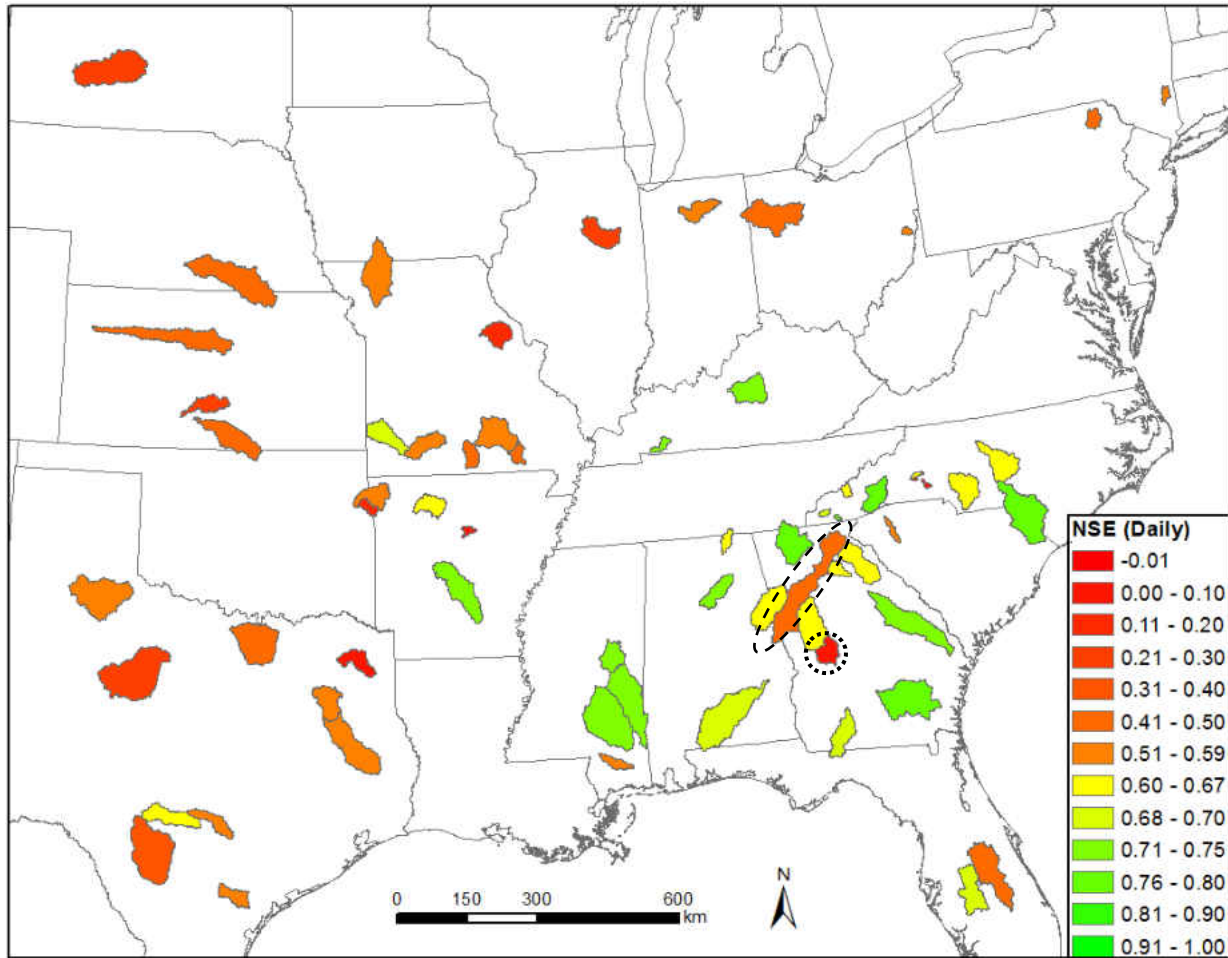


Figure 4.23. NSE Values for the Proposed Model at the Daily Time Scale during the Full-Record Calibration Stage. The dashed ellipse indicates the location of catchment 02339500 (dark orange). The dotted circle denotes the location of catchment 02349500 (dark red).

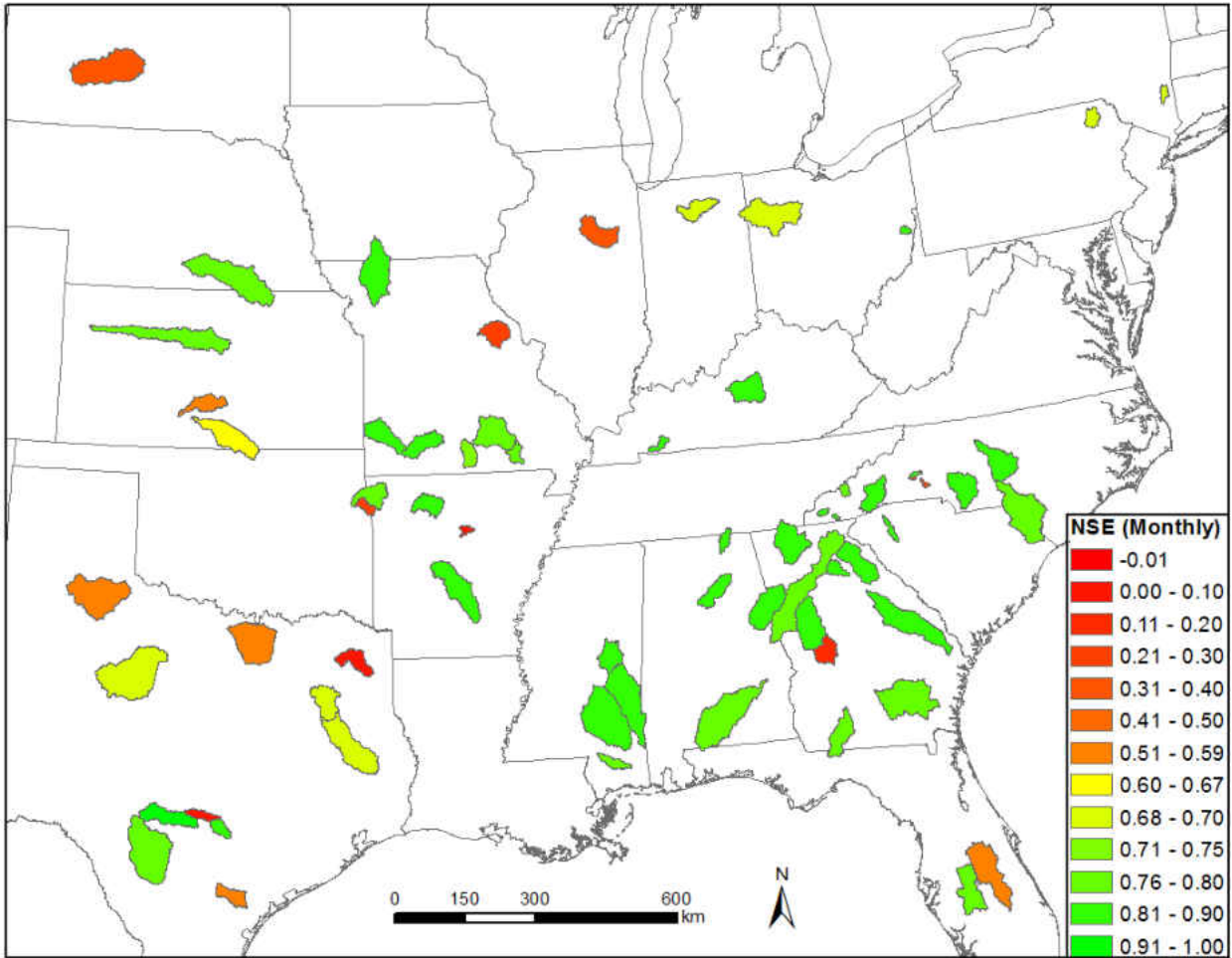


Figure 4.24. NSE Values for the Proposed Model at the Monthly Time Scale during the Full-Record Calibration Stage.

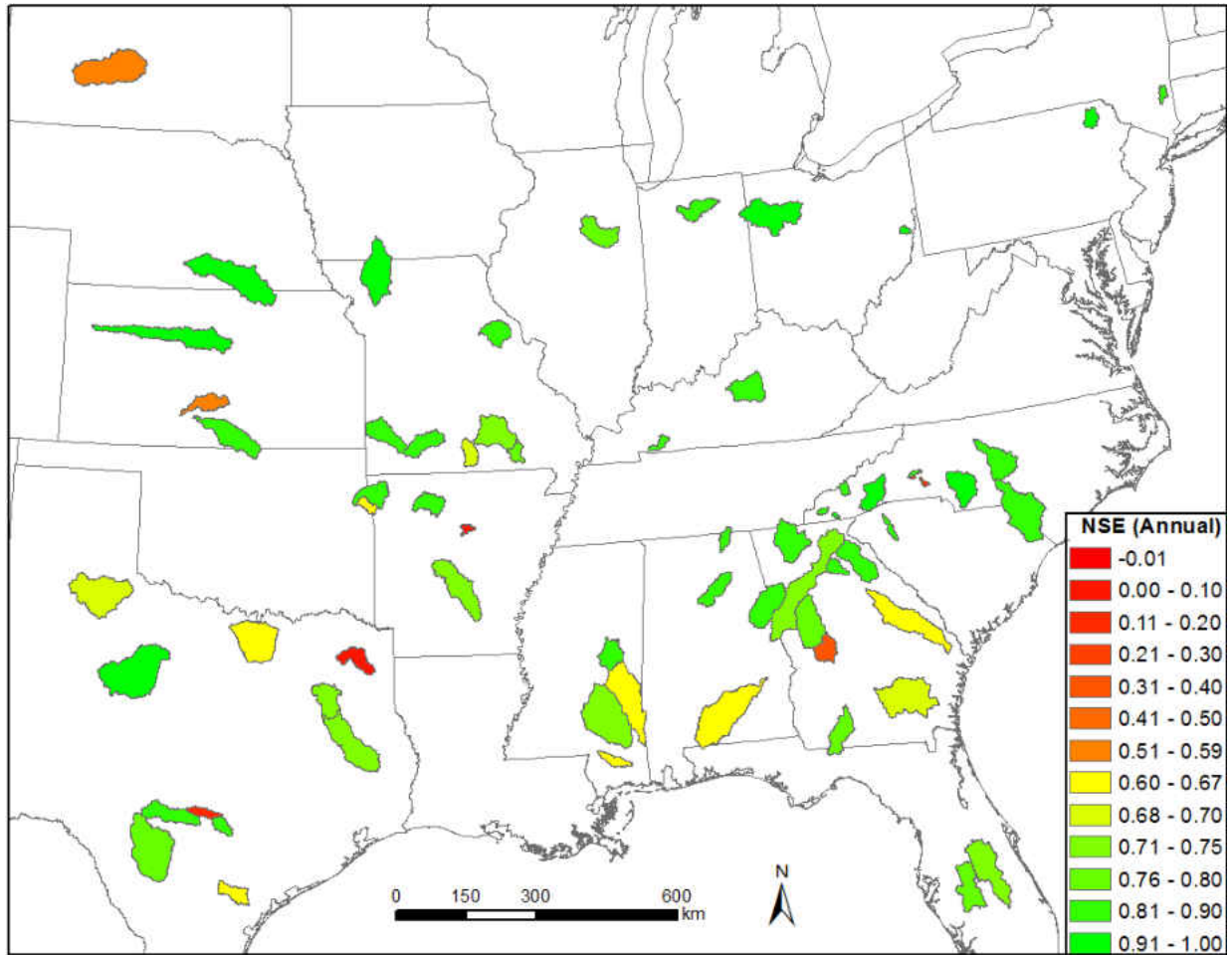


Figure 4.25. NSE Values for the Proposed Model at the Annual Time Scale during the Full-Record Calibration Stage.

4.4 Comparison between Models

In Sections 4.1 through 4.3, results from the full-record calibration stage for the proposed model were presented. In this section, the results of the model during the half-record calibration stage and validation stage are introduced, along with a comparison between two other water balance models.

A summary of the statistics during the full-record calibration stage, half-record calibration stage, and the validation stage are provided in Tables 4.1, 4.2, and 4.3, respectively. In these tables, μ represents the mean NSE of 71 catchments, C_v represents the coefficient of variation (standard deviation divided by the mean), and min and max represents the minimum and maximum NSE values.

Table 4.1. Statistics for the Full-Record Calibration Stage.

Time Scale	Statistics	Proposed Model	abcd Model	Zhang Model
Daily	μ	0.53	0.51	0.50
	C_v	0.41	0.43	0.51
	min	-0.01	-0.09	-0.05
	max	0.80	0.82	0.83
Monthly	μ	0.70	0.70	0.66
	C_v	0.33	0.34	0.35
	min	0.00	-0.05	0.01
	max	0.90	0.90	0.87
Annual	μ	0.75	0.68	0.68
	C_v	0.27	0.35	0.37
	min	0.09	-0.10	-0.30
	max	0.97	0.95	0.96

Table 4.2. Statistics for the Half-Record Calibration Stage.

Time Scale	Statistics	Proposed Model	abcd Model	Zhang Model
Daily	μ	0.54	0.52	0.49
	C_V	0.41	0.42	0.53
	min	-0.03	-0.07	-0.07
	max	0.81	0.81	0.83
Monthly	μ	0.70	0.68	0.65
	C_V	0.36	0.39	0.40
	min	-0.02	-0.14	-0.08
	max	0.93	0.92	0.88
Annual	μ	0.80	0.63	0.66
	C_V	0.32	0.78	0.76
	min	-0.41	-1.54	-2.89
	max	0.99	0.99	0.98

Table 4.3. Statistics for the Validation Stage.

Time Scale	Statistics	Proposed Model	abcd Model	Zhang Model
Daily	μ	0.43	0.47	0.33
	C_V	0.75	0.50	1.66
	min	-1.12	-0.21	-3.14
	max	0.76	0.83	0.81
Monthly	μ	0.59	0.62	0.59
	C_V	0.68	0.64	0.53
	min	-1.94	-1.84	-0.74
	max	0.90	0.90	0.92
Annual	μ	0.40	0.33	0.00
	C_V	1.80	2.59	489.54
	min	-4.32	-5.63	-5.72
	max	0.93	0.93	0.94

4.4.1 Full-Record Calibration Results

4.4.1.1 Daily Time Scale (Full-Record Calibration Stage)

From Figure 4.26, it is not apparent which model performs better. An analysis of the better performing catchments indicates a trend of higher performance with the proposed model. Some of the worse performing catchments favor the abcd model, but a majority of these, too, favor the proposed model.

From Figure 4.27, worse performing catchments, particularly those with a high aridity index, tend to perform better with the proposed model, as opposed to the Zhang model. Better performing catchments tend to favor the Zhang model. Overall performance is, however, better

with the proposed model because catchments that perform better with the proposed model tend to be significantly better than the Zhang model while catchments that perform better with the Zhang model tend to be only slightly better than the proposed model.

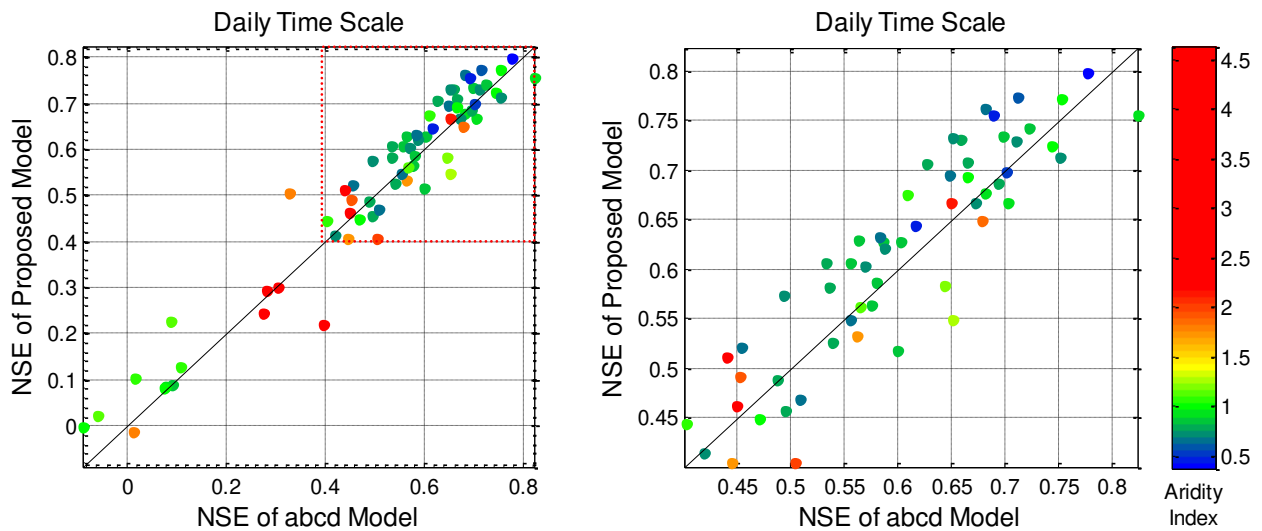


Figure 4.26. Comparison of the Performance of the Proposed Model vs. the abcd Model during the Full-Record Calibration Stage at the Daily Time Scale. Points above the diagonal line represent better performance using the proposed model. The red-dashed square in the figure on the left represents the extents of the figure on the right.

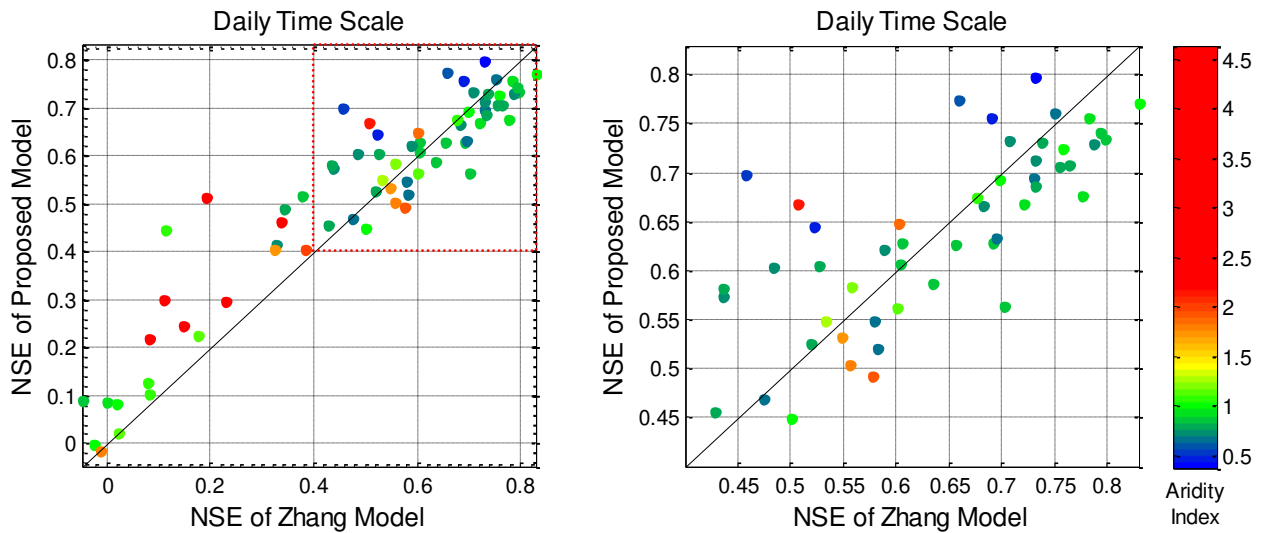


Figure 4.27. Comparison of the Performance of the Proposed Model vs. the Zhang Model during the Full-Record Calibration Stage at the Daily Time Scale. Points above the diagonal line represent better performance using the proposed model. The red-dashed square in the figure on the left represents the extents of the figure on the right.

4.4.1.2 Monthly Time Scale (Full-Record Calibration Stage)

At the monthly time scale, the advantage of the proposed model decreases so that performance of the model with respect to the abcd model is about the same (Figure 4.28). While some very arid catchments perform better with the abcd model, the ability to simulate highly arid or humid catchments is not advantaged by either model. On the other hand, catchments are clearly modeled better with the proposed model compared with the Zhang model (Figure 4.29).

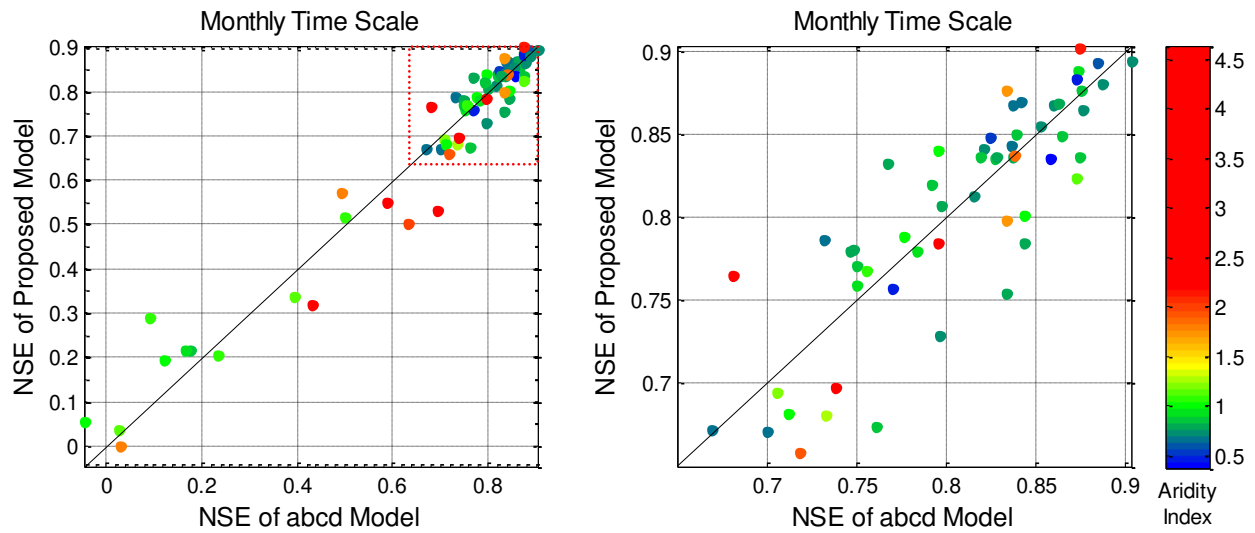


Figure 4.28. Comparison of the Performance of the Proposed Model vs. the abcd Model during the Full-Record Calibration Stage at the Monthly Time Scale. Points above the diagonal line represent better performance using the proposed model. The red-dashed square in the figure on the left represents the extents of the figure on the right.

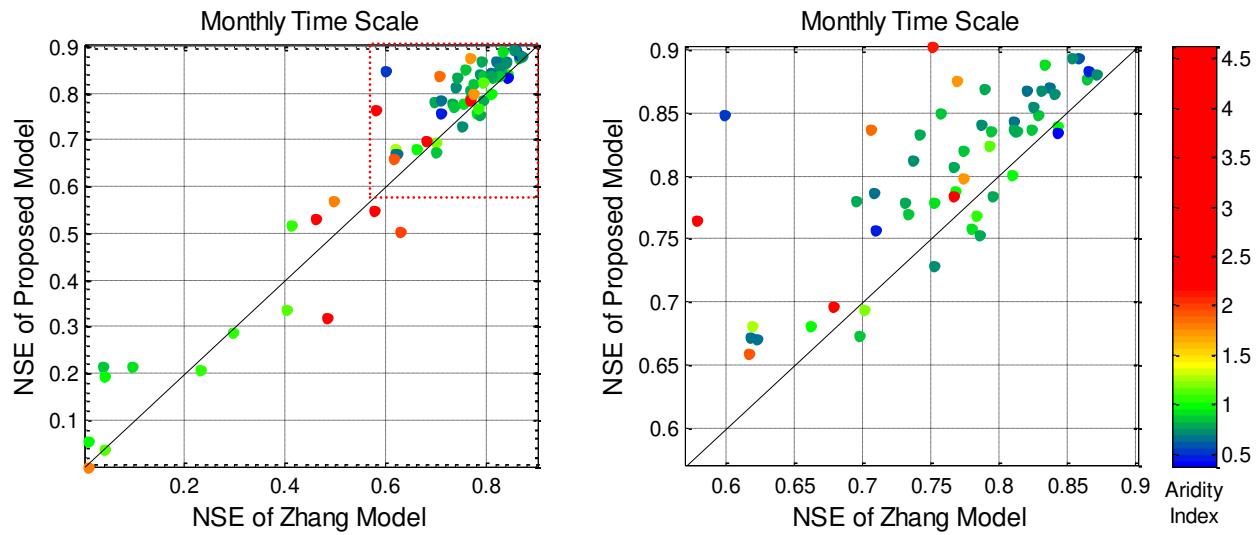


Figure 4.29. Comparison of the Performance of the Proposed Model vs. the Zhang Model during the Full-Record Calibration Stage at the Monthly Time Scale. Points above the diagonal line represent better performance using the proposed model. The red-dashed square in the figure on the left represents the extents of the figure on the right.

4.4.1.3 Annual Time Scale (Full-Record Calibration Stage)

At the annual time scale, the advantage of the proposed model is more pronounced. In fact, there are only two catchments that perform better with the abcd model (Figure 4.30). The proposed model performs better than the Zhang model as well, though more humid catchments tend to perform slightly better with the Zhang model.

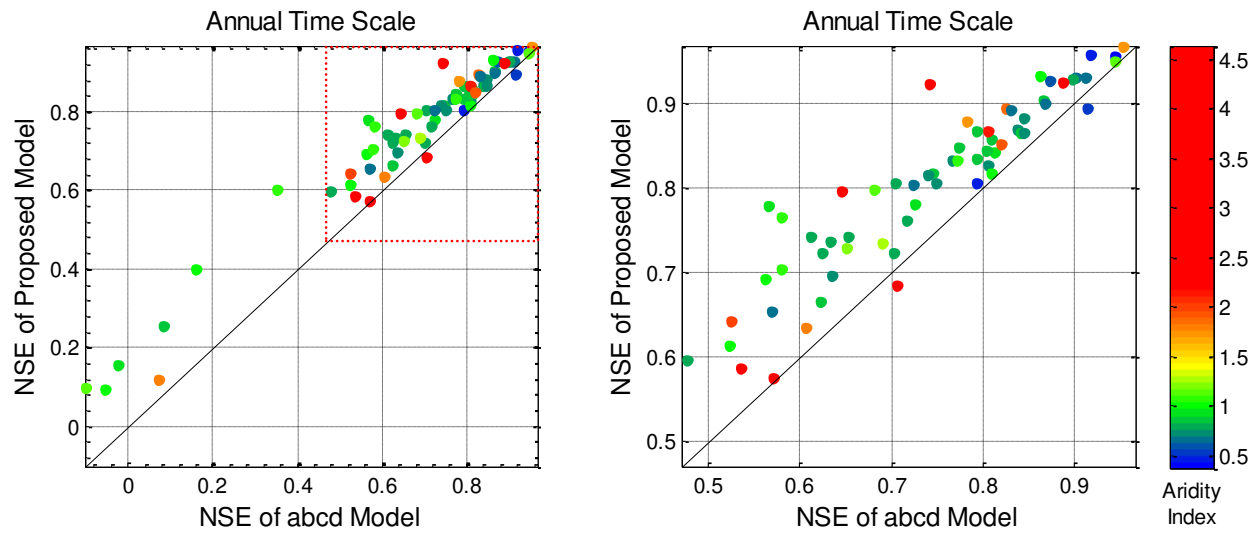


Figure 4.30. Comparison of the Performance of the Proposed Model vs. the abcd Model during the Full-Record Calibration Stage at the Annual Time Scale. Points above the diagonal line represent better performance using the proposed model. The red-dashed square in the figure on the left represents the extents of the figure on the right.

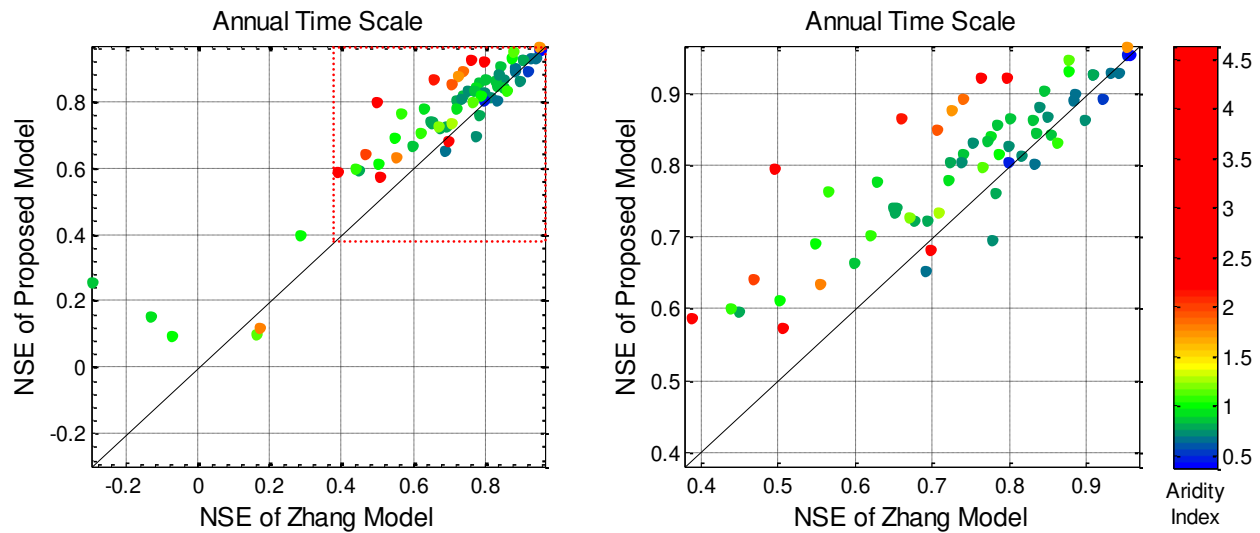


Figure 4.31. Comparison of the Performance of the Proposed Model vs. the Zhang Model during the Full-Record Calibration Stage at the Annual Time Scale. Points above the diagonal line represent better performance using the proposed model. The red-dashed square in the figure on the left represents the extents of the figure on the right.

4.4.2 Half-Record Calibration Results

Half-Record Calibration uses 10 of the 21 years of the available hydroclimatic records to calibrate model parameters. The procedure is otherwise identical to the full-record calibration stage. Model performance was expected to decrease during this time period because utilization of fewer records for calibration would increase the significance of irregularities in streamflow variation on the behavior of the model. However, in some cases, performance improved slightly during the half-record calibration stage (Tables 4.1 and 4.2). In these cases, this cause is likely due to the variability of the long-term climate in each catchment, which is not captured in the shorter-term records of the half-record calibration stage data.

4.4.2.1 Daily Time Scale (Half-Record Calibration Stage)

At the daily time scale, the performance of the individual catchments is slightly different for the proposed model, Zhang, and abcd models with respect to the corresponding analysis of the full-record calibration stage. However, taking into account the behavior of all 71 catchments indicates that their performance as a whole is nearly the same as the full-record calibration stage.

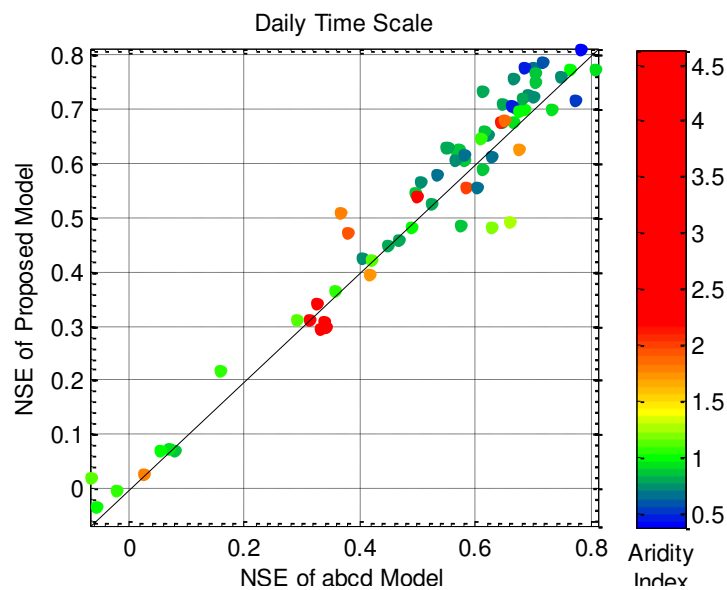


Figure 4.32. Comparison of the Performance of the Proposed Model vs. the abcd Model during the Half-Record Calibration Stage at the Daily Time Scale. Points above the diagonal line represent better performance using the proposed model.

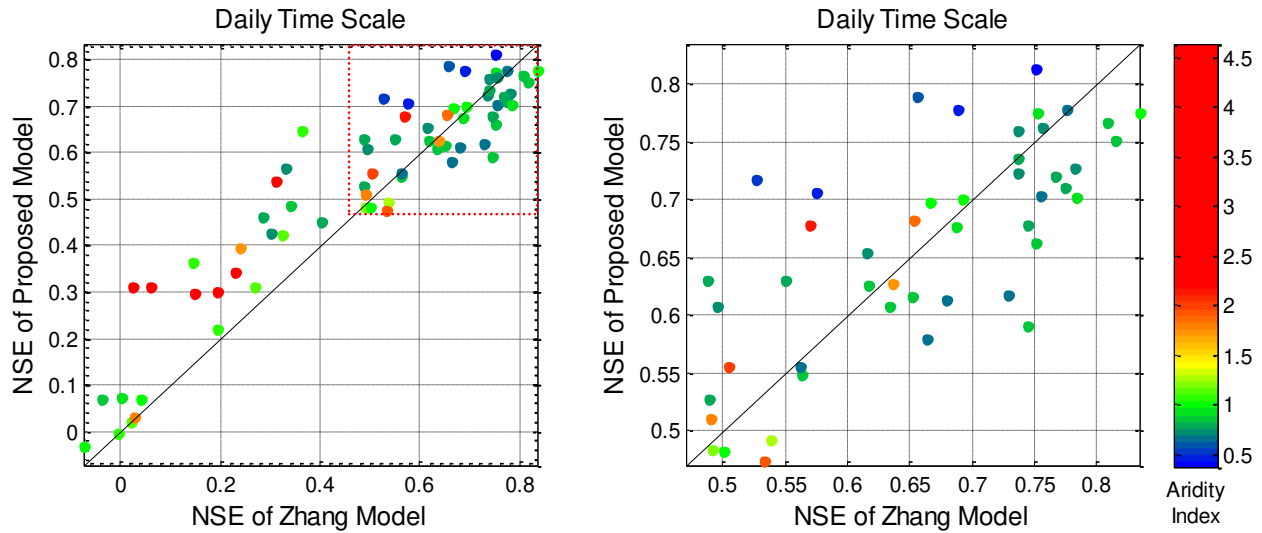


Figure 4.33. Comparison of the Performance of the Proposed Model vs. the Zhang Model during the Half-Record Calibration Stage at the Daily Time Scale. Points above the diagonal line represent better performance using the proposed model. The red-dashed square in the figure on the left represents the extents of the figure on the right.

4.4.2.2 Monthly Time Scale (Half-Record Calibration Stage)

There is a small improvement over the full-record calibration stage in the number of catchments that are modeled well ($NSE > 0.6$) by both the abcd model and the proposed model (60 vs. 56 in Figures 4.34 and 4.28, respectively). A similar observation is made for the Zhang model vs. the proposed model (Figures 4.35 and 4.29, respectively). However, the overall performance of the abcd model declines and the proposed model remains nearly the same. Similarly, the performance for the Zhang model is slightly reduced between the full-record and half-record calibration stages (Figures 4.29 and 4.35, respectively); this is observed by a small leftward shift of points with $NSE > 0.6$.

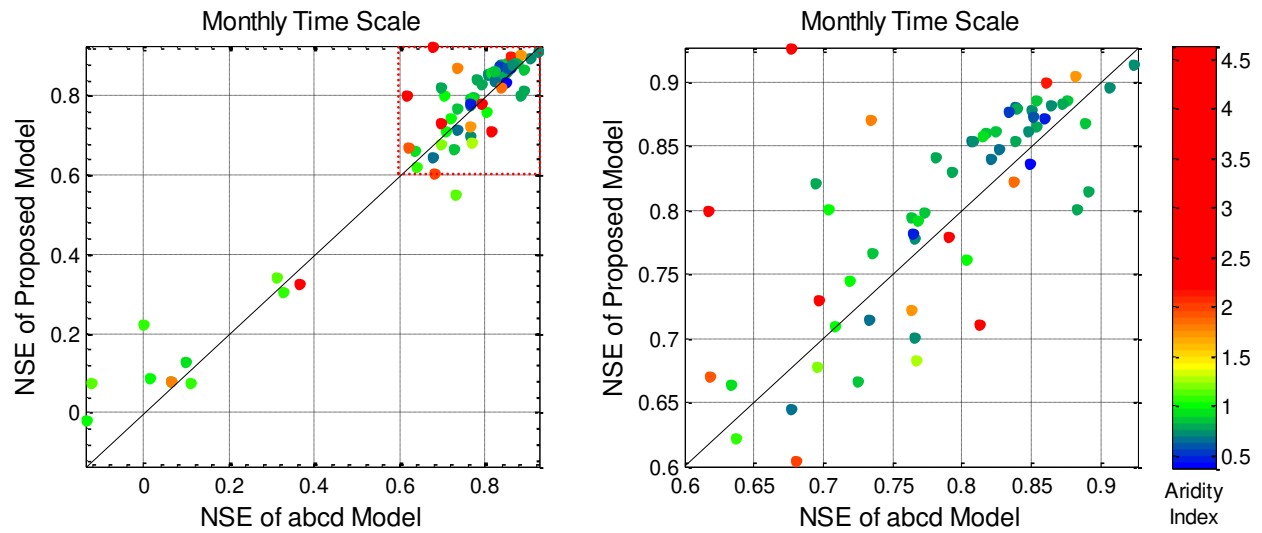


Figure 4.34. Comparison of the Performance of the Proposed Model vs. the abcd Model during the Half-Record Calibration Stage at the Monthly Time Scale. Points above the diagonal line represent better performance using the proposed model. The red-dashed square in the figure on the left represents the extents of the figure on the right.

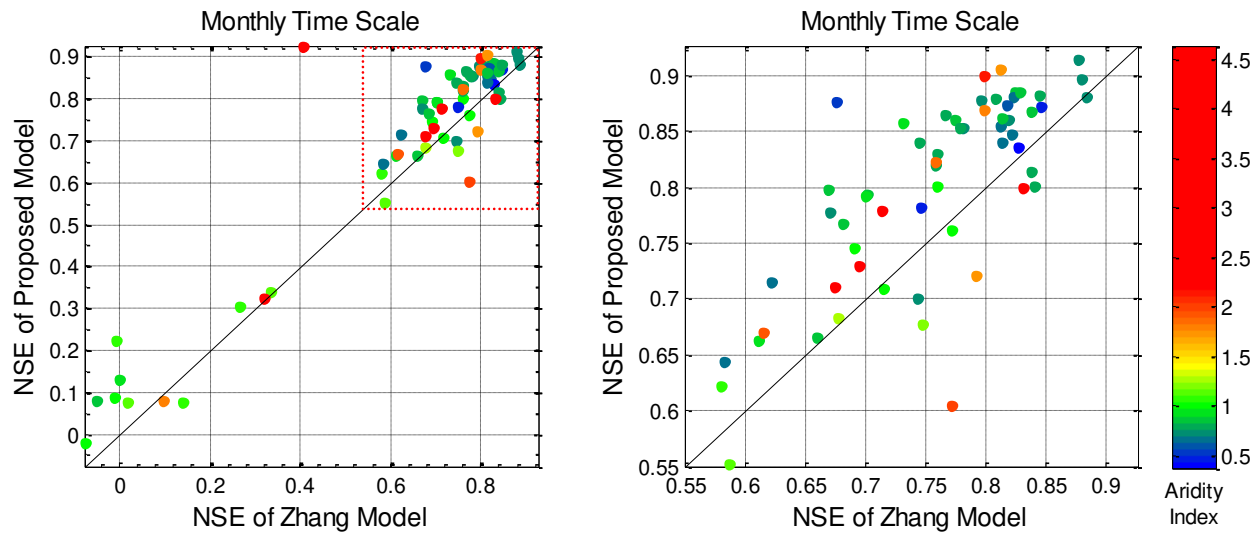


Figure 4.35. Comparison of the Performance of the Proposed Model vs. the Zhang Model during the Half-Record Calibration Stage at the Monthly Time Scale. Points above the diagonal line represent better performance using the proposed model. The red-dashed square in the figure on the left represents the extents of the figure on the right.

4.4.2.3 Annual Time Scale (Half-Record Calibration Stage)

For the half-record calibration stage at the annual time scale, the performance of the proposed model increases, whereas the abcd model decreases, as illustrated by the leftward and upward shift of points in the right figure of Figure 4.36 compared with the left figure of Figure 4.30. Similarly, for the proposed model and the Zhang model, an upward shift is observed in Figure 4.37 compared with Figure 4.31. However, a rightward shift is also observed. The reason the average performance of the Zhang model is lower during the half-record calibration stage is because one catchment has a very low performance (-2.9). Even with this catchment removed from the analysis, the proposed model performs better than the Zhang model.

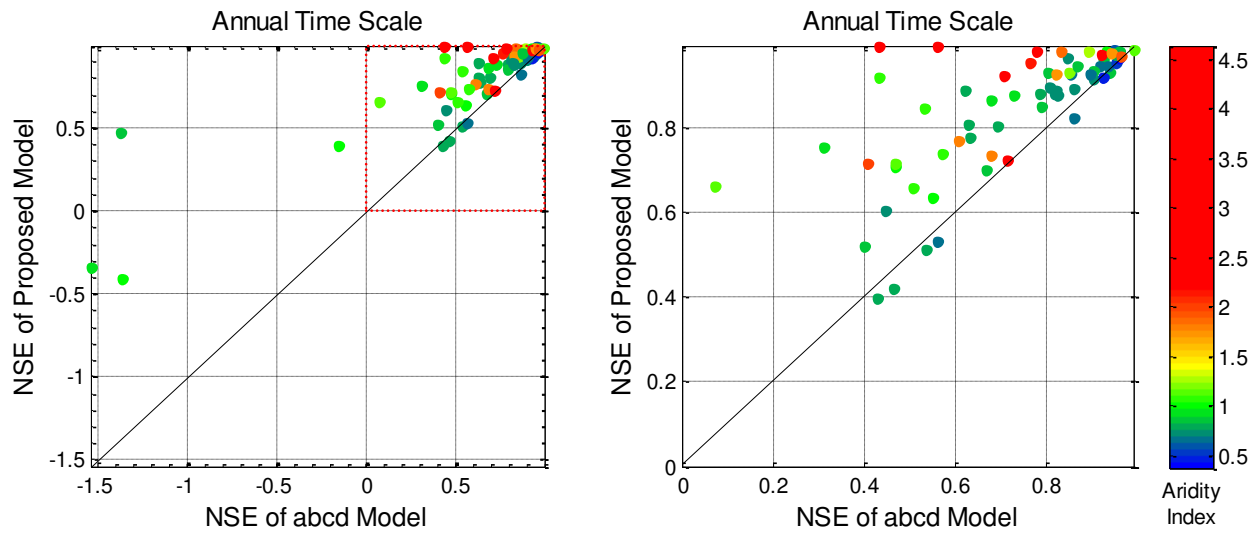


Figure 4.36. Comparison of the Performance of the Proposed Model vs. the abcd Model during the Half-Record Calibration Stage at the Annual Time Scale. Points above the diagonal line represent better performance using the proposed model. The red-dashed square in the figure on the left represents the extents of the figure on the right.

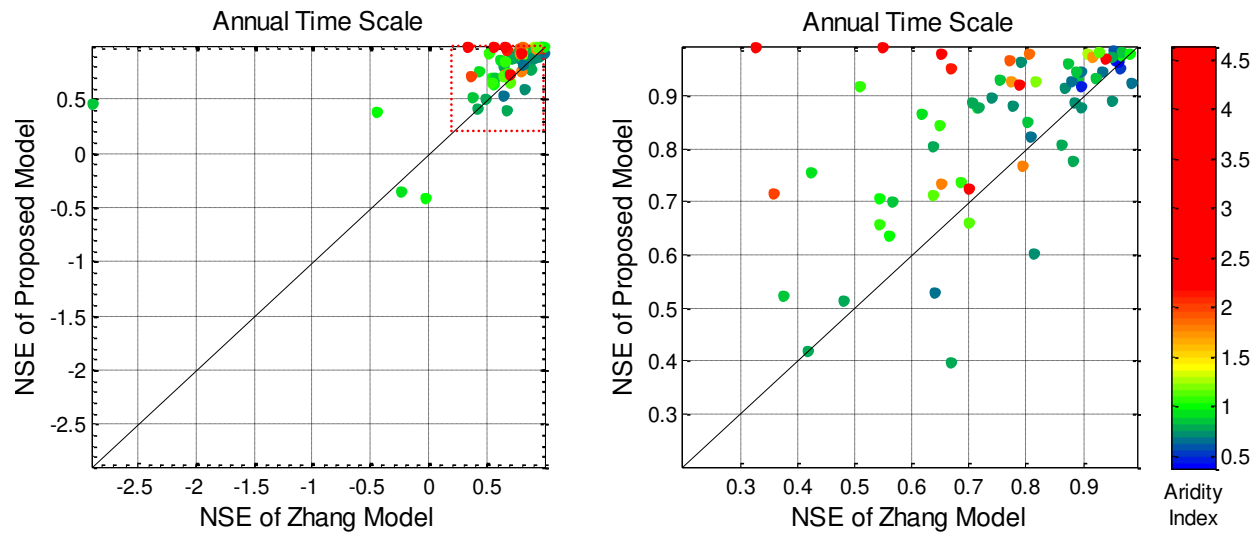


Figure 4.37. Comparison of the Performance of the Proposed Model vs. the Zhang Model during the Half-Record Calibration Stage at the Annual Time Scale. Points above the diagonal line represent better performance using the proposed model. The red-dashed square in the figure on the left represents the extents of the figure on the right.

4.4.3 Validation Results

4.4.3.1 Daily Time Scale (Validation Results)

Model performance at the daily time scale is generally worse with the proposed model with respect to the abcd model (Figure 4.38). However, this difference is not very significant except for six catchments. Also, except for four catchments, model performance below an NSE of 0.4 is higher for the abcd model.

The proposed model generally performs better than the Zhang model, particularly in the cases when $NSE > 0.2$ (Figure 4.39).

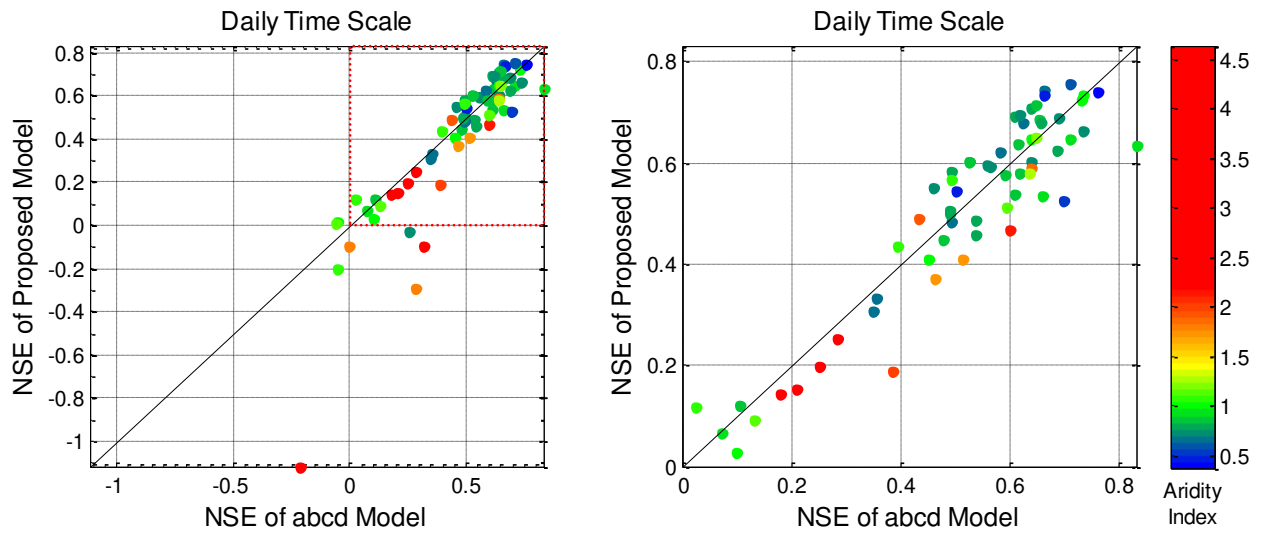


Figure 4.38. Comparison of the Performance of the Proposed Model vs. the abcd Model during the Validation Stage at the Daily Time Scale. Points above the diagonal line represent better performance using the proposed model. The red-dashed square in the figure on the left represents the extents of the figure on the right.

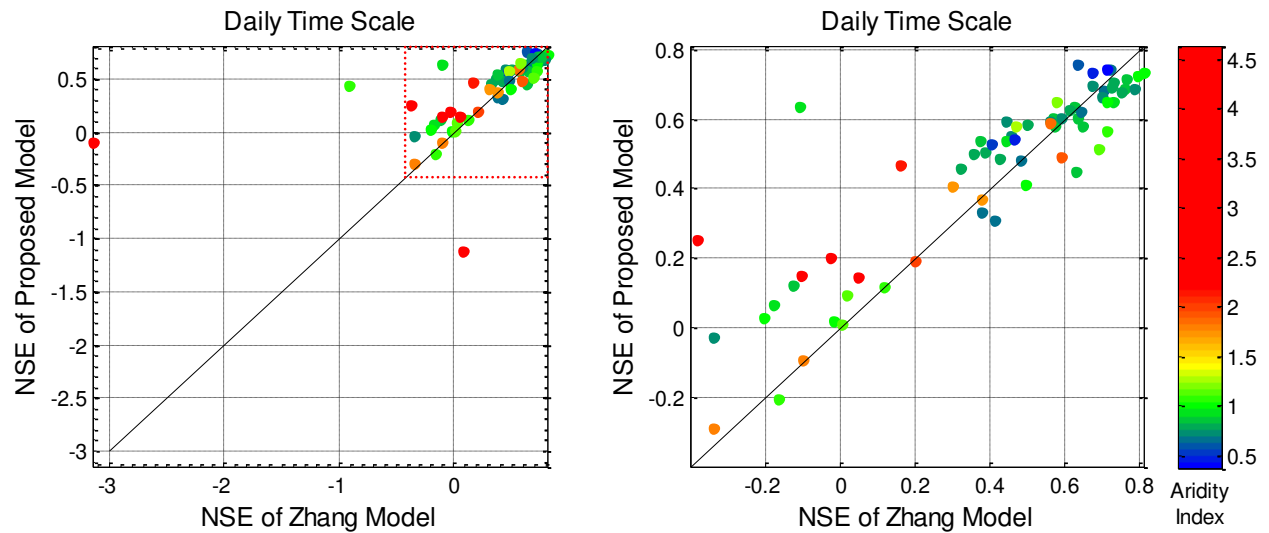


Figure 4.39. Comparison of the Performance of the Proposed Model vs. the Zhang Model during the Validation Stage at the Daily Time Scale. Points above the diagonal line represent better performance using the proposed model. The red-dashed square in the figure on the left represents the extents of the figure on the right.

4.4.3.2 Monthly Time Scale (Validation Results)

Model performance at the monthly time scale is generally higher for the abcd model in comparison with the proposed model (Figure 4.40). Additionally, the differences in catchment performance tend to be higher when the abcd model performs better than the proposed model.

Performance for the Zhang model is approximately the same as the proposed model, though the more arid catchments tend to perform better with the Zhang model (Figure 4.41).

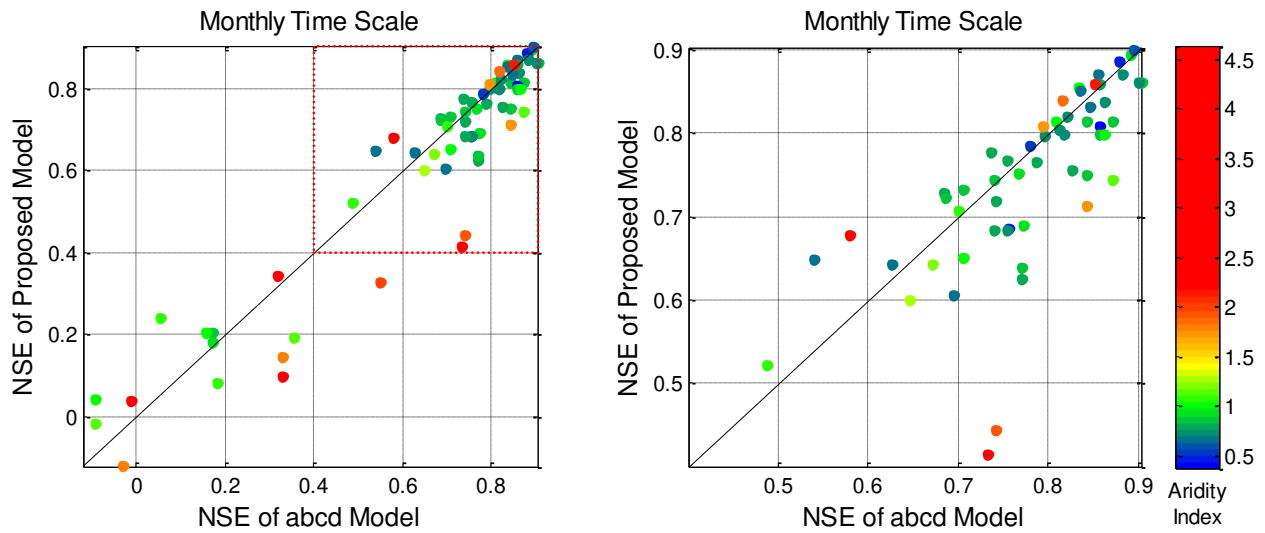


Figure 4.40. Comparison of the Performance of the Proposed Model vs. the abcd Model during the Validation Stage at the Monthly Time Scale. Points above the diagonal line represent better performance using the proposed model. The red-dashed square in the figure on the left represents the extents of the figure on the right. Catchment 08085500 is not illustrated in the figures but is listed in Table 4.5 instead for the sake of clarity.

Table 4.4. NSE Values at the Monthly Time Scale during the Validation Stage for Catchment 08085500.

Catchment	Proposed Model	abcd Model	Aridity Index
08085500	-1.94	-1.84	4.11

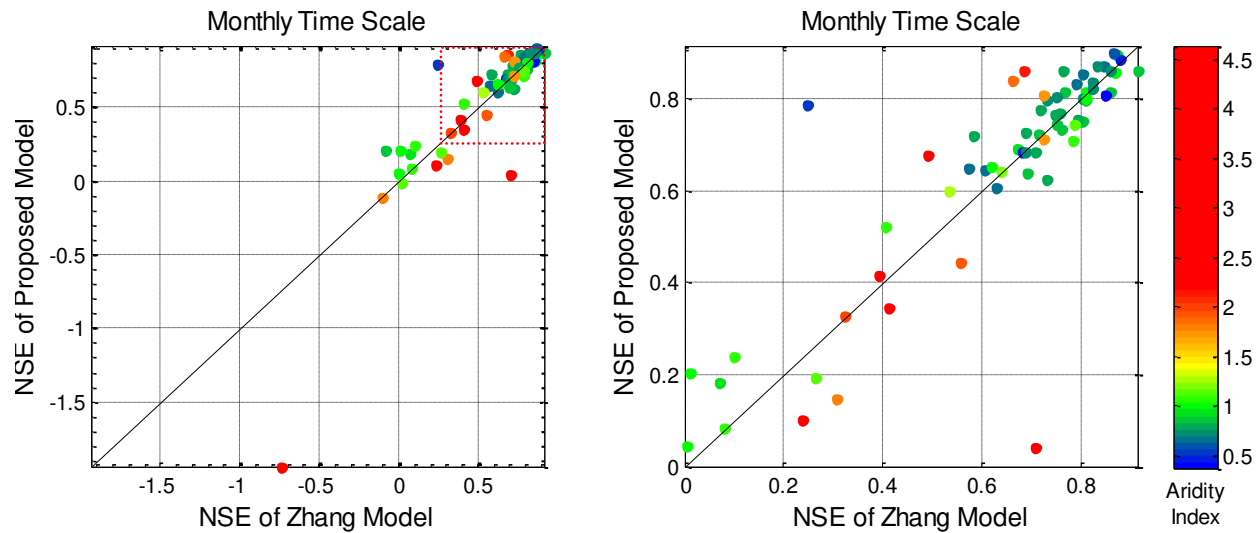


Figure 4.41. Comparison of the Performance of the Proposed Model vs. the Zhang Model during the Validation Stage at the Monthly Time Scale. Points above the diagonal line represent better performance using the proposed model. The red-dashed square in the figure on the left represents the extents of the figure on the right.

4.4.3.3 Annual Time Scale (Validation Results)

Performance of both the abcd model and the proposed model improve at the annual time scale. In Figure 4.42, the degree at which points are spread out is greater than at the daily or monthly time scales, illustrating a greater degree of difference in how the two models simulate streamflow. The same condition is observed in Figure 4.43. Overall, the proposed model shows a better performance compared with both the abcd and the Zhang models.

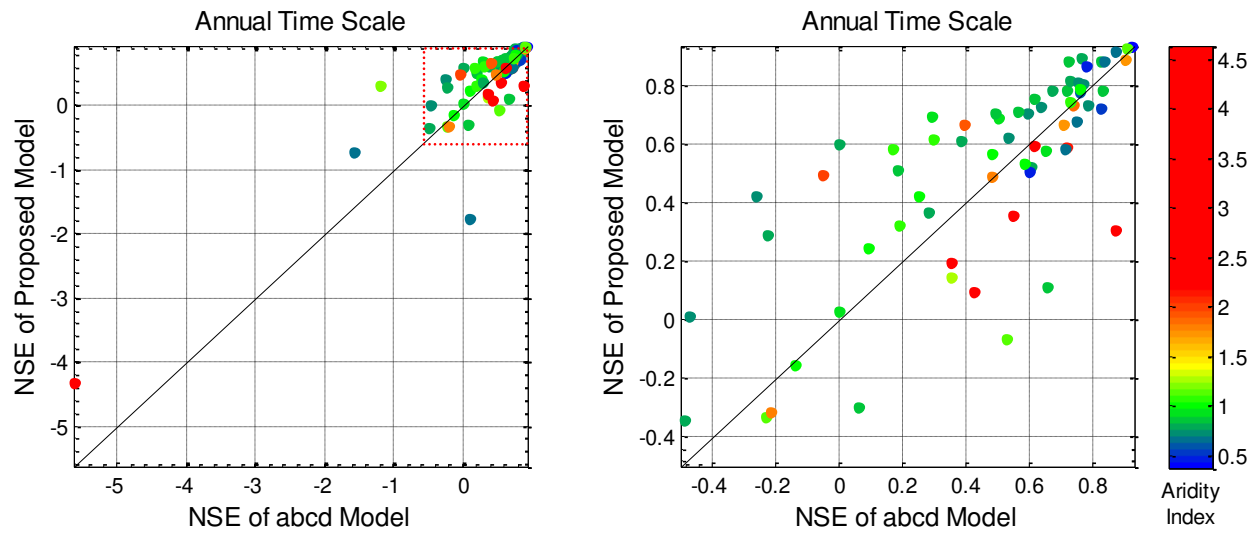


Figure 4.42. Comparison of the Performance of the Proposed Model vs. the abcd Model during the Validation Stage at the Annual Time Scale. Points above the diagonal line represent better performance using the proposed model. The red-dashed square in the figure on the left represents the extents of the figure on the right.

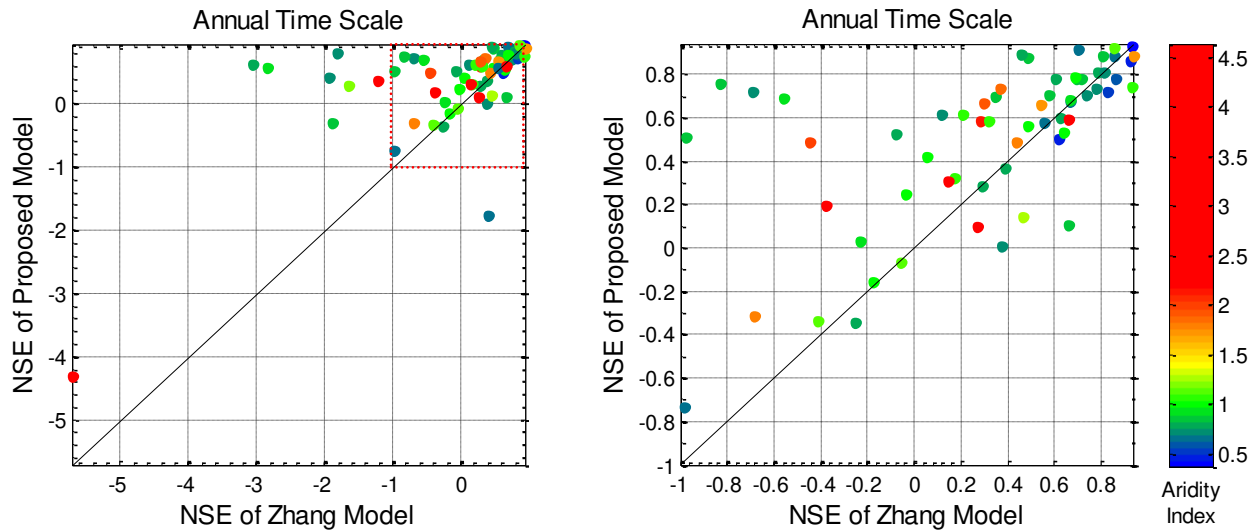


Figure 4.43. Comparison of the Performance of the Proposed Model vs. the Zhang Model during the Validation Stage at the Annual Time Scale. Points above the diagonal line represent better performance using the proposed model. The red-dashed square in the figure on the left represents the extents of the figure on the right.

4.5 Second Model Calibration and Validation Method

As mentioned previously, the initial soil moisture condition assumed plays a major role in the performance of a model. For example, during the development of the proposed model structure, it was mistakenly assumed that soil moisture was zero in the abcd model while the initial soil moisture was assumed to be at capacity for the other models. This resulted in a very poor performance by the abcd model at the daily time scale until the soil moisture condition was made consistent with the other models.

Taking this finding into consideration, the next step was to see if the proposed model is more sensitive to the assumed initial conditions during validation. This was done by setting the initial soil moisture and routing terms as parameters to be calibrated in the half-record calibration

stage. For the abcd and Zhang models, these terms include $S(t-1)$ and $G(t-1)$. For the proposed model, these terms include $S_{1,0}$, $S_{2,0}$, and G_0 .

A summary of the statistics during the second calibration/validation stages is provided in Tables 4.5 and 4.6. In these tables, μ represents the mean NSE of 71 catchments, C_V represents the coefficient of variation (standard deviation divided by the mean), and min and max represents the minimum and maximum NSE values.

Table 4.5. Statistics for the Half-Record Calibration Stage (Second Calibration Method).

Time Scale	Statistics	Proposed Model	abcd Model	Zhang Model
Daily	μ	0.54	0.51	0.51
	C_V	0.40	0.45	0.50
	min	0.01	-0.19	-0.08
	max	0.81	0.81	0.84
Monthly	μ	0.70	0.68	0.65
	C_V	0.36	0.39	0.38
	min	-0.02	-0.14	-0.08
	max	0.92	0.92	0.88
Annual	μ	0.80	0.64	0.67
	C_V	0.33	0.76	0.75
	min	-0.42	-1.45	-2.87
	max	0.99	0.99	0.98

Table 4.6. Statistics for the Validation Stage (based on the Second Calibration Method).

Time Scale	Statistics	Proposed Model	abcd Model	Zhang Model
Daily	μ	0.46	0.47	0.43
	C_V	0.56	0.53	0.70
	min	-0.32	-0.35	-0.34
	max	0.76	0.83	0.82
Monthly	μ	0.59	0.62	0.60
	C_V	0.65	0.73	0.50
	min	-1.71	-2.38	-0.60
	max	0.89	0.90	0.92
Annual	μ	0.43	0.26	0.21
	C_V	1.56	5.00	4.69
	min	-4.38	-9.86	-6.30
	max	0.94	0.93	0.94

4.5.1 Half-Record Calibration Results (Second Calibration Method)

Applying the second calibration method to the half-record calibration stage shows that performance was generally the same in comparison with the first calibration method. Plots of their performance are listed in Figures 4.44 and 4.45 for the daily time scale, Figures 4.46 and 4.47 for the monthly time scale, and Figures 4.48 and 4.49 for the annual time scale. The statistics for the second calibration method are displayed in Table 4.5.

4.5.1.1 Daily Time Scale (Half-Record Calibration Stage, Second Calibration Method)

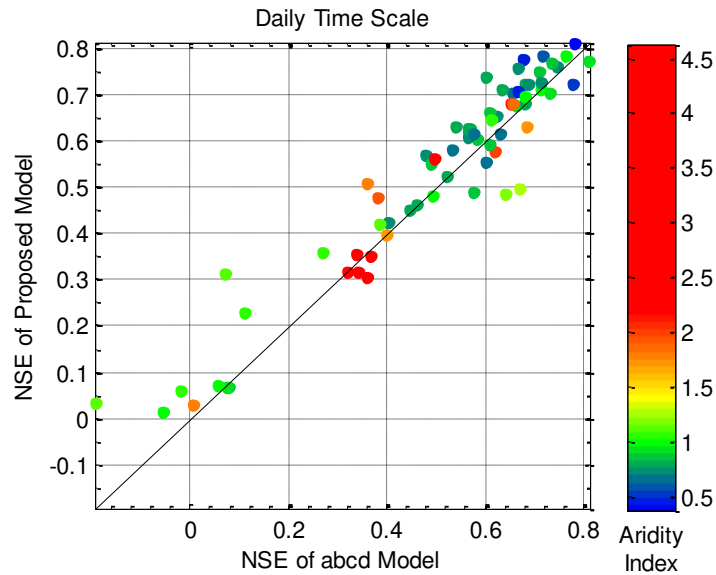


Figure 4.44. Comparison of the Performance of the Proposed Model vs. the abcd Model during the Half-Record Calibration Stage (Second Calibration Method) at the Daily Time Scale. Points above the diagonal line represent better performance using the proposed model.

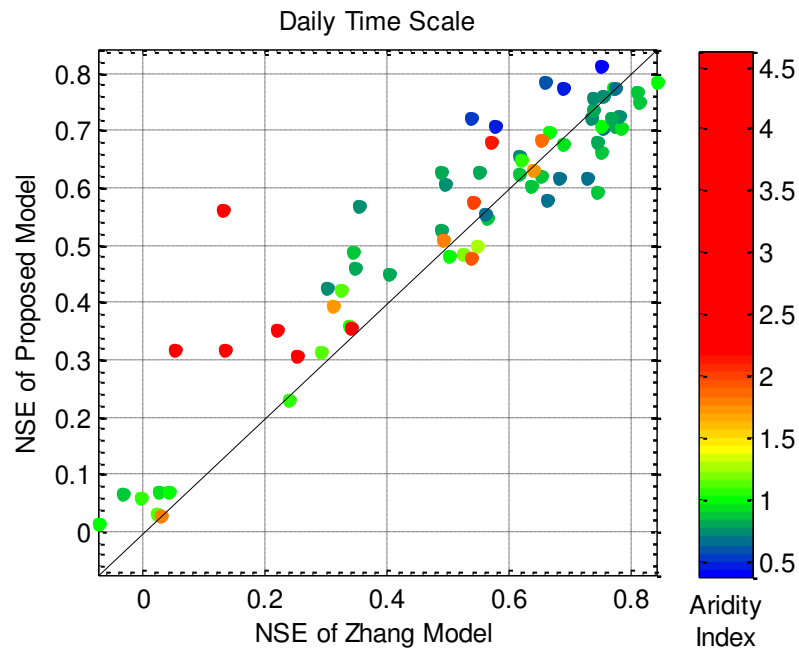


Figure 4.45. Comparison of the Performance of the Proposed Model vs. the Zhang Model during the Half-Record Calibration Stage (Second Calibration Method) at the Daily Time Scale. Points above the diagonal line represent better performance using the proposed model.

4.5.1.2 Monthly Time Scale (Half-Record Calibration Stage, Second Calibration Method)

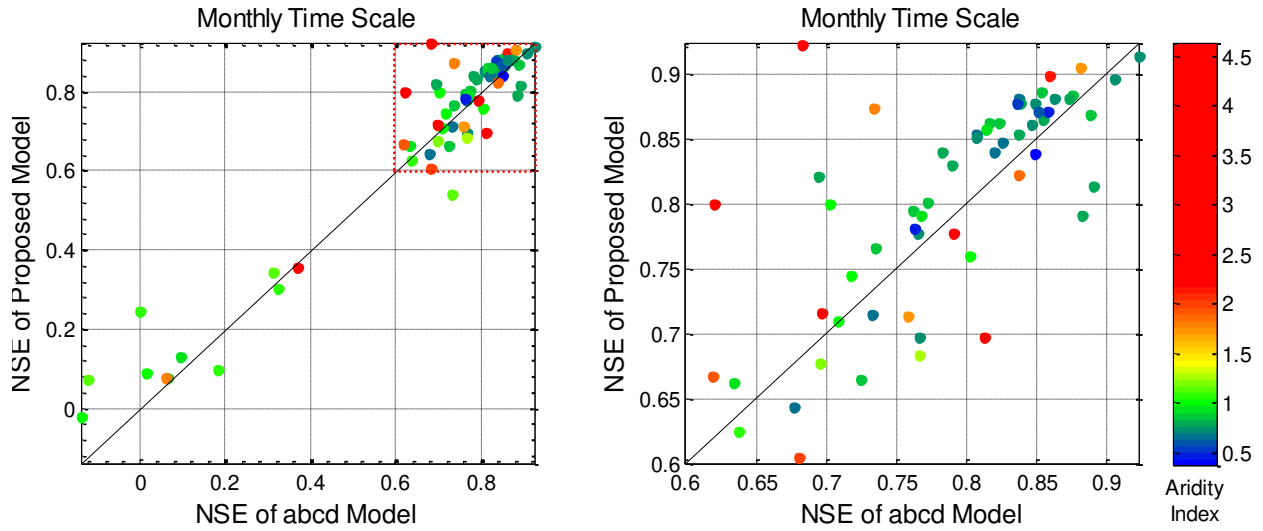


Figure 4.46. Comparison of the Performance of the Proposed Model vs. the abcd Model during the Half-Record Calibration Stage (Second Calibration Method) at the Monthly Time Scale. Points above the diagonal line represent better performance using the proposed model. The red-dashed square in the figure on the left represents the extents of the figure on the right.

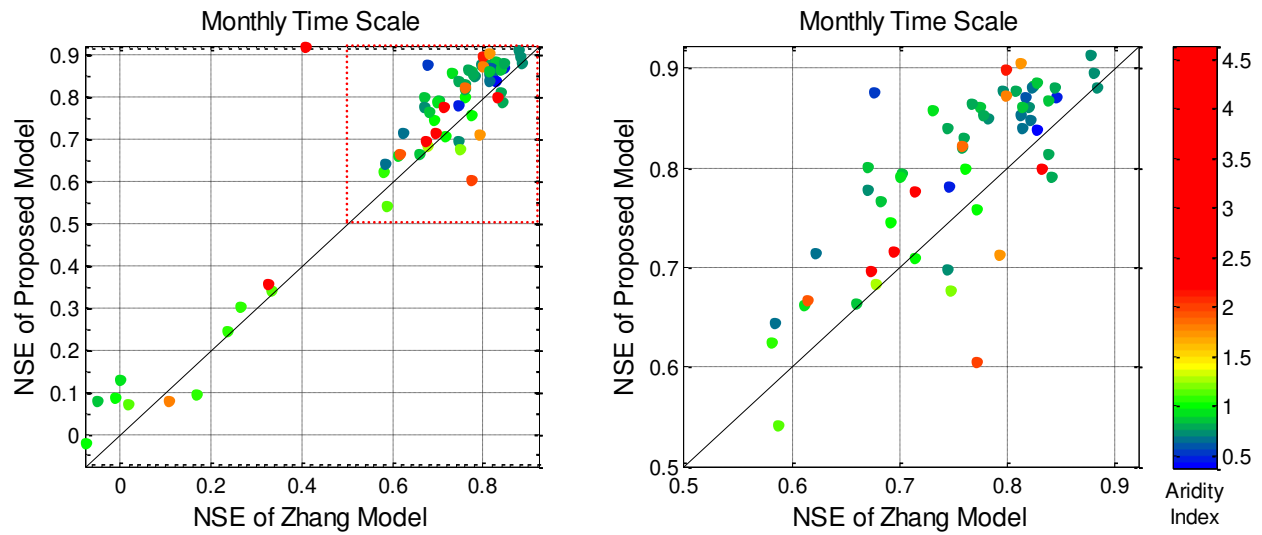


Figure 4.47. Comparison of the Performance of the Proposed Model vs. the Zhang Model during the Half-Record Calibration Stage (Second Calibration Method) at the Monthly Time Scale. Points above the diagonal line represent better performance using the proposed model. The red-dashed square in the figure on the left represents the extents of the figure on the right.

4.5.1.3 Annual Time Scale (Half-Record Calibration Stage, Second Calibration Method)

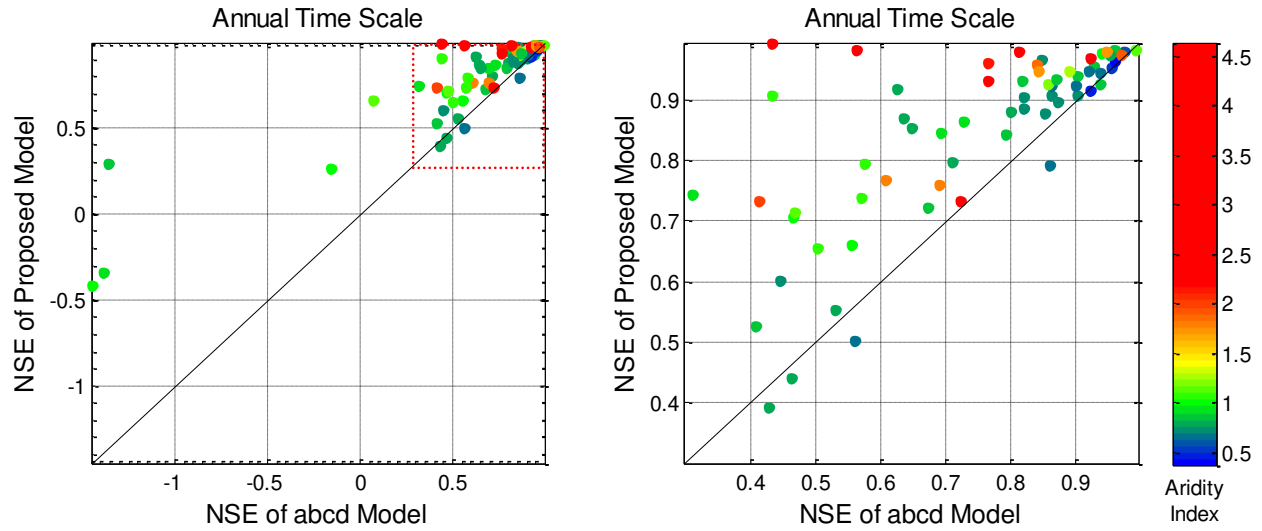


Figure 4.48. Comparison of the Performance of the Proposed Model vs. the abcd Model during the Half-Record Calibration Stage (Second Calibration Method) at the Annual Time Scale. Points above the diagonal line represent better performance using the proposed model. The red-dashed square in the figure on the left represents the extents of the figure on the right.

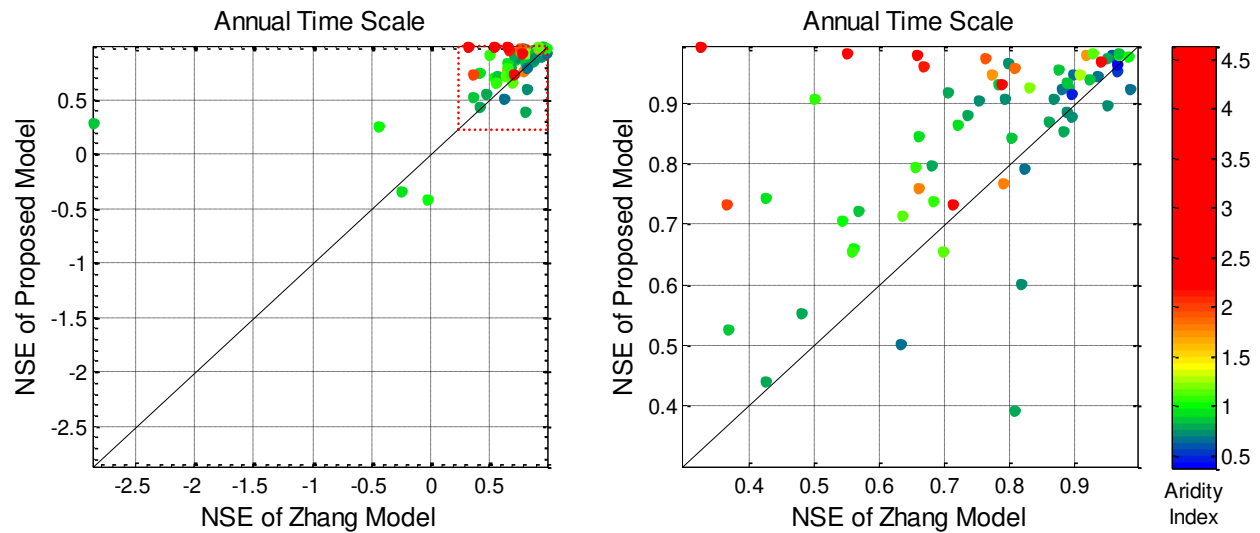


Figure 4.49. Comparison of the Performance of the Proposed Model vs. the Zhang Model during the Half-Record Calibration Stage (Second Calibration Method) at the Annual Time Scale. Points above the diagonal line represent better performance using the proposed model. The red-dashed square in the figure on the left represents the extents of the figure on the right.

4.5.2 Validation Results (Second Calibration Method)

The validation results based on the second calibration method showed that the performance of the proposed model increased slightly or remained the same. Additionally, the abcd model's performance decreased while the Zhang model's performance increased, particularly at the annual time scale.

4.5.2.1 Daily Time Scale (Validation based on the Second Calibration Method)

The difference of the results from the first and second calibration methods on the validation results is small at this time scale. However, a small leftward shift of points and an

even smaller upward shift of some points occurs, indicating a small improvement in the performance of the proposed model and a small loss of performance with the abcd model (Figures 4.50 and 4.38). In Figures 4.51 and 4.39, there is a slight rightward shift, particularly with the five most arid catchments, illustrating an improved performance by the Zhang model.

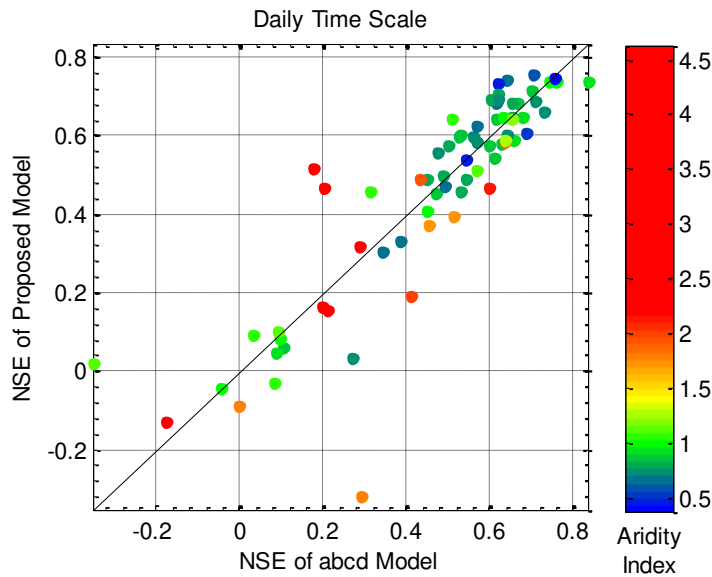


Figure 4.50. Comparison of the Performance of the Proposed Model vs. the abcd Model during the Validation Stage (based on the Second Calibration Method) at the Daily Time Scale. Points above the diagonal line represent better performance using the proposed model.

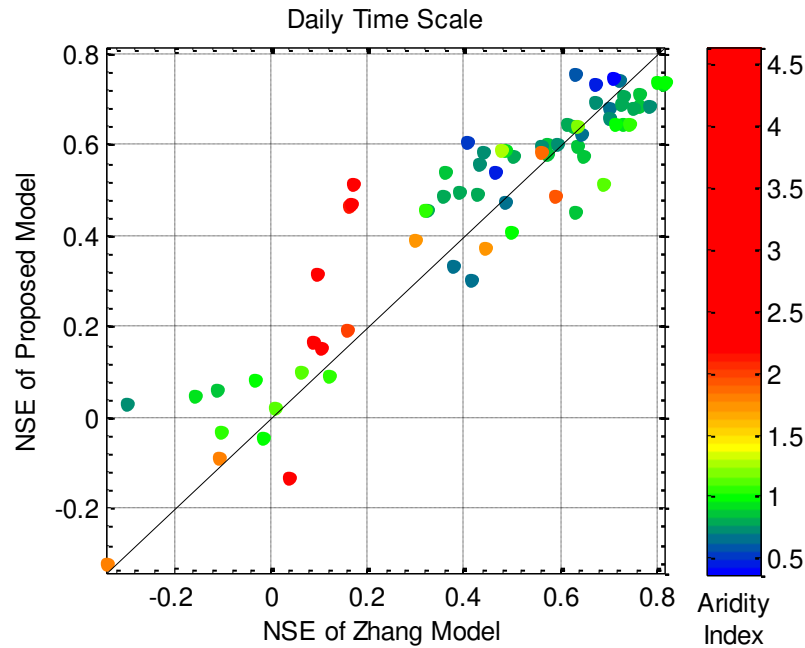


Figure 4.51. Comparison of the Performance of the Proposed Model vs. the Zhang Model during the Validation Stage (based on the Second Calibration Method) at the Daily Time Scale. Points above the diagonal line represent better performance using the proposed model.

4.5.2.2 Monthly Time Scale (Validation based on the Second Calibration Method)

Compared with the first validation results, there is no general improvement or decline in the performance of catchments with the second validation results in regards to the abcd model and the proposed model (Figures 4.52 and 4.40). Additionally, no trend was observed that explains the increasing or decreasing performance of some catchments; that is performance increases for some catchments are just as likely to be decreases with others. The same trend is observed for the Zhang model and the proposed model in Figures 4.53 and 4.41.

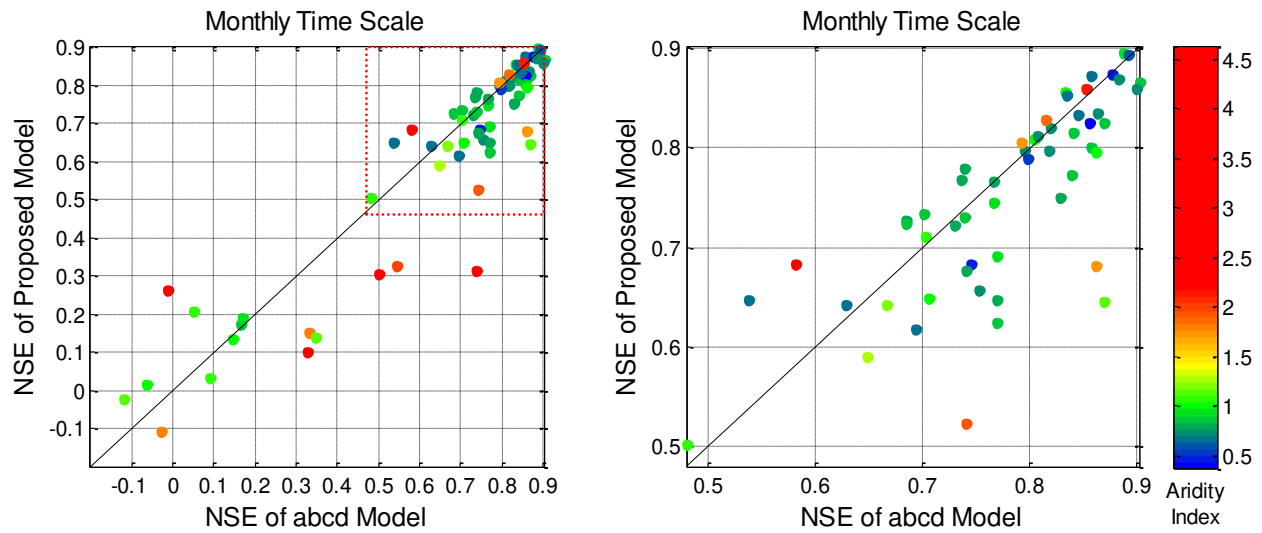


Figure 4.52. Comparison of the Performance of the Proposed Model vs. the abcd Model during the Validation Stage (based on the Second Calibration Method) at the Monthly Time Scale. Points above the diagonal line represent better performance using the proposed model. The red-dashed square in the figure on the left represents the extents of the figure on the right. Catchment 08085500 is not illustrated in the figures but is listed in Table 4.7 instead for the sake of clarity.

Table 4.7. NSE Values at the Monthly Time Scale during the Validation Stage (based on the Second Calibration Method) for Catchment 08085500.

Catchment	Proposed Model	abcd Model	Zhang Model	Aridity Index
08085500	-1.71	-2.38	-0.60	4.11

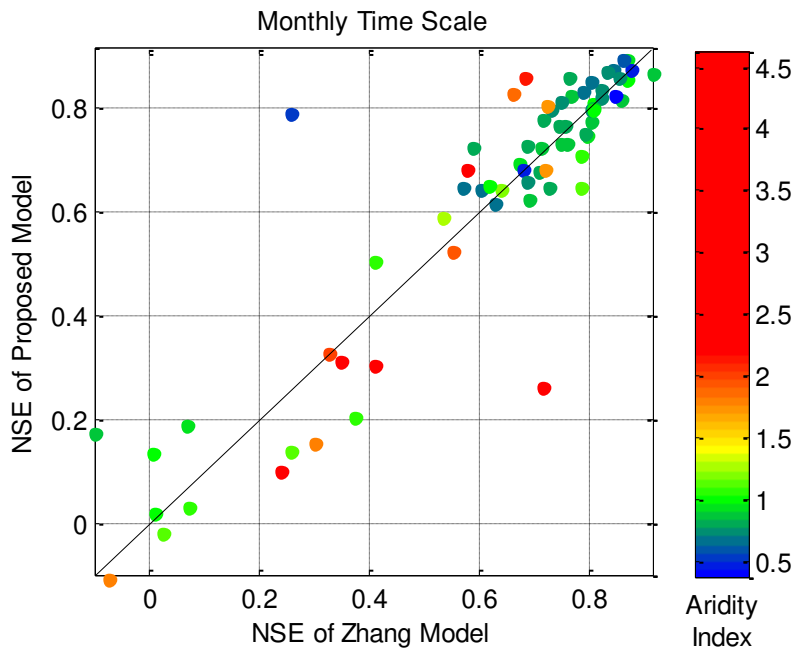


Figure 4.53. Comparison of the Performance of the Proposed Model vs. the Zhang Model during the Validation Stage (based on the Second Calibration Method) at the Monthly Time Scale. Points above the diagonal line represent better performance using the proposed model. The red-dashed square in the figure on the left represents the extents of the figure on the right. Catchment 08085500 is not illustrated in the figures but is listed in Table 4.7 instead for the sake of clarity.

4.5.2.3 Annual Time Scale (Validation based on the Second Calibration Method)

In Figures Figure 4.54, a small upward shift is observed in relation to Figure 4.42, indicating a minor improvement for the proposed model. The more arid catchments, however, show a small decline in performance. Additionally, a small leftward shift is observed, indicating a small decline in performance in the abcd model. The statistics suggest a larger decline in performance, however this is mainly due to a very poorly performing catchment (NSE is -9.86).

Finally, a rightward shift is observed in Figure 4.55 compared with Figure 4.43. This illustrates a major improvement at the annual time scale of the performance of the Zhang model. However, despite this significant improvement, the Zhang model does not perform as well as either the proposed model or the abcd model.

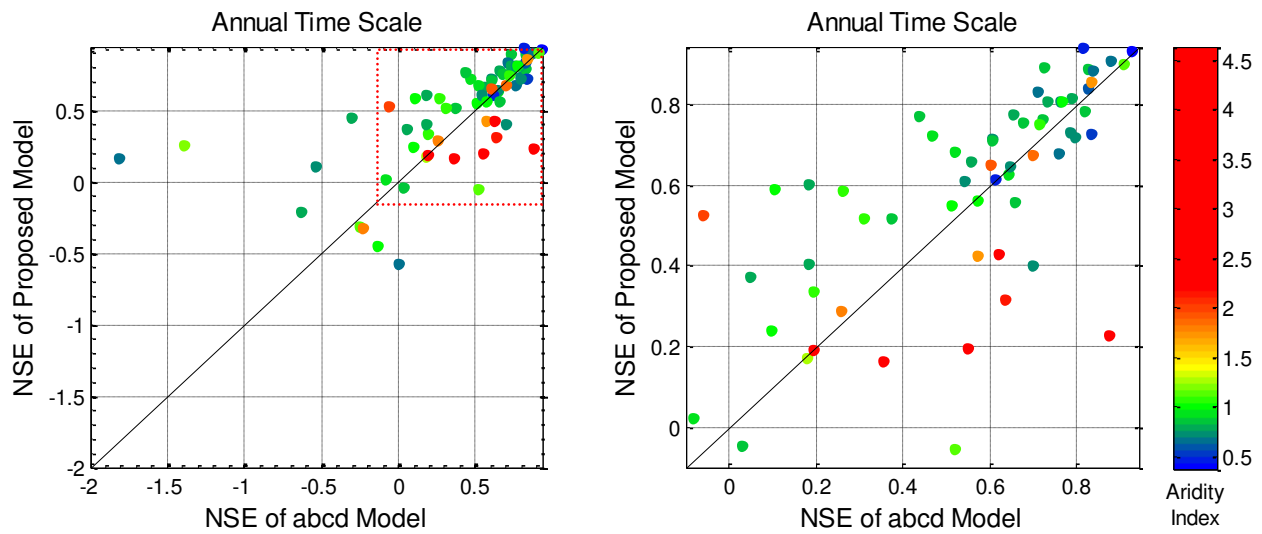


Figure 4.54. Comparison of the Performance of the Proposed Model vs. the abcd Model during the Validation Stage (based on the Second Calibration Method) at the Annual Time Scale. Points above the diagonal line represent better performance using the proposed model. The red-dashed square in the figure on the left represents the extents of the figure on the right. Catchment 08085500 is not illustrated in the figures but is listed in Table 4.8 instead for the sake of clarity.

Table 4.8. NSE Values at the Annual Time Scale during the Validation Stage (based on the Second Calibration Method) for Catchment 08085500.

Catchment	Proposed Model	abcd Model	Zhang Model	Aridity Index
8085500	-4.38	-9.86	-6.30	4.11

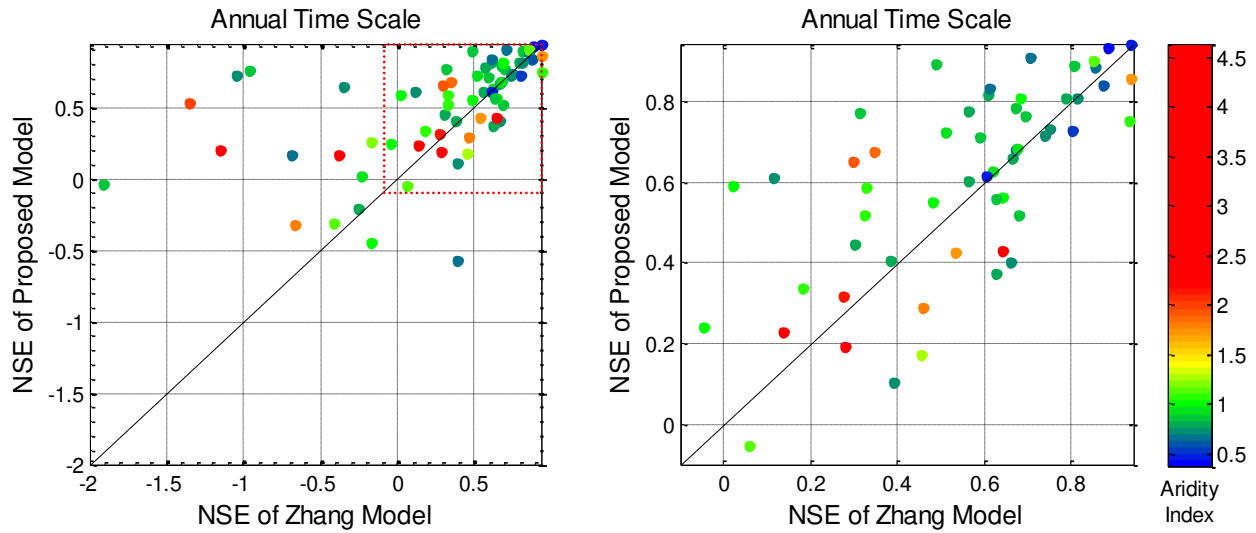


Figure 4.55. Comparison of the Performance of the Proposed Model vs. the Zhang Model during the Validation Stage (based on the Second Calibration Method) at the Annual Time Scale. Points above the diagonal line represent better performance using the proposed model. The red-dashed square in the figure on the left represents the extents of the figure on the right. Catchment 08085500 is not illustrated in the figures but is listed in Table 4.8 instead for the sake of clarity.

4.6 Additional Discussion

An important assumption made previously in the development of the model structure is that all precipitation that falls within the catchment will become a combination of streamflow and evapotranspiration. This assumption is shared by the abcd and Zhang models. However, other models, such as the one developed by Kuczera (1983), use a seepage loss function because annual water balance and stream chemistry studies have suggested that only a fraction of runoff produced within a catchment is accounted for in streamflow observations (Xu & Singh, 1998). It may be that the incorporation of such a process would improve the model performance.

CHAPTER 5: SUMMARY AND CONCLUSIONS

Water balance models are advantageous to physically-based models due to their applicability to different spatial and temporal scales. However, a particular limitation of water balance models is that their applicability is typically restricted to certain time scales. The reason is that climate and physical controls have varying influences on each time scale. At the daily and event time scale, physical controls dominate, while at the long-term time scale (i.e. many years), climate controls dominate.

In the comparison of several water balance models, a commonality was discovered between them, which is termed the “proportionality hypothesis”. The proportionality hypothesis states that the competition between two processes competing for the same supply will be governed by a proportional distribution of the supply based on the potential maximum deficits (or “needs”) of each of the two processes.

The objective of this thesis was to develop a hydrologic model structure for continuous simulations for multiple time scales. To accomplish this, a model structure was developed with an emphasis on applying the proportionality hypothesis to as many hydrologic processes as possible, while at the same time reducing the number of model parameters. While models which use the proportionality hypothesis such as the SCS curve number method and the Equity model typically restrict its application to a single competition of processes, the proposed model applies the proportionality hypothesis to two separate competitions of processes.

Development of the proposed model structure continued until performance during parameter calibration was found to exceed the performance of two other water balance models—the Zhang model (Zhang et al., 2008) and the “abcd” model (Thomas, 1981). The proposed model structure includes six parameters which were calibrated in Matlab using a genetic algorithm.

The proposed model was evaluated against the abcd model and the Zhang model at the daily, monthly, and annual time scales using data from 71 MOPEX catchments. Model evaluation was performed at three different stages, including calibration of the models to all 21 years of data (“full-record calibration”), calibration of the models to the first ten years of data (“half-record calibration”), and validation of the models across the next eleven years of data using parameters obtained from the half-record calibration.

Results from the full-record calibration stage and the half-record calibration stage show that the proposed model performs better or approximately as well as the two other models at the daily and monthly time scales. For the validation stage, however, the proposed model does not perform as well as the abcd model at the daily and monthly time scales, though results are comparable. The proposed model does perform better than the Zhang model at the daily time scale and approximately as well at the monthly time scale.

In contrast, the proposed model does significantly better at the annual time scale than both models for the full and half-record calibration stages and the validation stage.

In both calibration stages, model initial conditions, including the soil moisture and groundwater levels at the beginning of the first time period, were based on assumed values. It is

possible that some models may be relatively unaffected by the assumed values for initial conditions while others may be very sensitive. Thus, the half-record calibration and validation stages were performed a second time to determine if the proposed model was more sensitive than the other models to the assumed initial conditions. In this approach, initial conditions were obtained by treating them as parameters to be calibrated by the model. However, the method did not change the conclusions made earlier for the models.

The results obtained from the full-record calibration stage were used to investigate how the parameters of the proposed model change with each of the three time scales. Between the daily and monthly time scales, storage capacities tended to decrease slightly, possibly due to the incorporation of the effects of seasonality into the model. On the other hand, capacities tended to increase significantly in both soil moisture layers from the monthly to the annual time scales, demonstrating the increasing role that the soil moisture layers play in streamflow filtering.

For the first soil moisture layer, soil moisture capacities showed a strong linear relationship between all three time scales, suggesting that the model utilizes the first soil moisture reservoir primarily to limit the rainfall being transferred to other processes. In the second soil moisture layer, the soil moisture capacity displays very little correlation between time scales, indicating that the main function of the soil moisture layer is to filter runoff.

This analysis also revealed a mechanism implicit in the model structure that wasn't considered previously—in a small number of catchments, parameters k_1 and k_2 were 1 and 0, which caused the groundwater reservoir to act as a seepage loss function without the ability to produce baseflow.

The results of the proposed model were also analyzed for the full-record calibration stage at the three time scales. At the daily time scale, good and acceptable performance was observed to be mainly restricted to the Southeast United States. Performance improved substantially at the monthly time scale, and most catchments in the Southeast and some catchments north of Texas were found to have good performance. At the annual time scale, performance declined for some catchments in the South but improved even further for catchments in the North; the poorer performance of the southern catchments may be due to the evapotranspiration estimates, which are highly overestimated at the annual time scale and play a larger role in the partitioning of catchment water in the southern states.

The analysis of one of these southern catchments, particularly a catchment in Florida (02296750), showed that evapotranspiration was generally overestimated by the model at all three time scales. This is a consequence of the equations used to describe initial evapotranspiration in the model. Actual evaporation is not only a function of the demand (E_p) but also of available water. Thus, models which only account for the capacity of soil water storage are insufficient. The equations for initial evapotranspiration take this fact into consideration.

In the equations for initial evapotranspiration, the initial evapotranspiration rate is set equal to the potential rate, provided there is enough water in the soil moisture layer to meet the demand. Otherwise, the initial evapotranspiration rate will equal the soil moisture in the reservoir. Thus, in the case of the Florida catchment at the daily and monthly time scales, initial evapotranspiration was typically equal to the potential evapotranspiration while continuing

evapotranspiration was almost always negligible. This behavior changed substantially at the annual time scale, where initial evapotranspiration was limited by the capacity of the first reservoir, causing continuing evapotranspiration to become a significant process.

Another issue that was observed was that there were many cases when evapotranspiration would be simulated as zero when observation records estimated it to be between 1 and 4 millimeters. Transpiration, which E_c primarily represents, particularly in catchments with high vegetation, should be a major component of evapotranspiration. However, the model, as applied to the catchment in Florida, suggests that transpiration, which is what E_c primarily represents, is nearly negligible at the daily and monthly time scales, which is unrealistic. Modifications to the expressions of the initial evapotranspiration rate were considered; however, all modifications, including those based on the abcd and Thornthwaite and Mather model approach, did not yield improved results. It may be that the implementation of E_0 as the sole mechanism of drainage from the first reservoir is the cause of poor model performance. A variation of the model was evaluated that allowed a fraction of the storage in the first reservoir to enter the second, but this did not improve the model performance.

Modifications to the model structure after the competition between continuing abstraction, F_a , and surface runoff, Q_s , did not usually yield substantial gains in model performance. On the other hand, modifications to the model structure before and during this competition have often led to substantial gains or losses in model performance. Consequently, weaknesses in the model structure may be found in components of the model taking place during the infiltration of water into the second reservoir or before that (during the accumulation of water

in the first reservoir). That is, further model development should consider removing or re-ordering the processes of initial evapotranspiration, initial abstraction, or continuing abstraction. For instance, the process of initial evapotranspiration could be re-ordered to compete against the surface runoff or continuing abstraction. Furthermore, additional processes should be considered. For example, a second continuing abstraction process, F_{a1} , was added to the proposed model structure. It should be emphasized, however, that the most significant improvements to the model were not due to different process formulations, but to modifications of the model structure.

Lack of a surface routing mechanism has been suggested as a possible cause of reduced model performance (Dripps & Bradbury, 2007; Zhang et al., 2008). In the development of the proposed model, the incorporation of the seventh model stage (i.e. a second competition between continuing abstraction and surface runoff) was shown to improve model performance.

Model results during the calibration stages performed very well and performed better than the other models at all three time scales; however, performance declined significantly during model prediction. These results suggest that future model development should be focused not only on the evaluation of model forms during the parameter calibration stage, but also during prediction (validation). Otherwise, processes which facilitate the ability of the model to match the observed data but which are in reality a poor representation of the true physical processes may be incorrectly validated as superior to more accurate relationships.

While the results indicate that the current form of the proposed model does not offer an advantage over the abcd model and offers only a small improvement over the Zhang model,

additional development of the model structure should lead to better model predictive ability.

More importantly, model results suggest the potential for a series of better models.

Application of the proportionality hypothesis demonstrates that it can be used to model hydrologic processes at multiple time scales. This hypothesis facilitates the development of more parsimonious model structures due to its simplicity, which makes it relatively easy to formulate relationships for various hydrologic processes. Additionally, relationships based on the proportionality hypothesis typically do not require more than one parameter

In regards to the proportionality hypothesis in general, model formulations based on the proportionality hypothesis are limited in their applicability to two-way competitions. Modeling processes as a two-way competition is sufficient if the competition between processes is weighted mainly between two processes. However, if the competition is weighted fairly similarly between three or more processes, this approach can lead to significant modeling errors. An example of a three-way competition is when evapotranspiration (via root systems), the soil adhesive forces of soil particles (matric potential), and the subsurface flow compete for water in the soil.

In order to use the proportionality hypothesis in cases such as this, one competition must be neglected or the processes must be modeled sequentially. An example of the first case is the competition between the subsurface flow, Q_{SS} , and continuing evapotranspiration, E_C , in the proposed model. In this model, the competition of the soil against E_C and Q_{SS} is replaced with an expression representing a fraction of the total soil moisture in the second reservoir (i.e. $Q_{SS} + E_C = k_3 S_2$, where $k_3 S_2$ is a fraction of the soil moisture). An example of the second case is

Model 21. In this model, the competition between the evapotranspiration and the soil occurs first and is followed by a competition between the soil and a fraction of the baseflow, Q_{b1} .

Though the proportionality hypothesis is limited to two-way competitions, this limitation does not disadvantage the hypothesis from processes used in other hydrologic models, such as the abcd and Zhang models, since these models do not describe a competition between more than two processes. Furthermore, the general objective in model development is to develop parsimonious water balance models, an objective that may become compromised by including complex relationships described by the competition of more than two simultaneously competing processes.

Though the model structure demonstrates that it can be applied at multiple time scales, there are many areas of the model that can be improved upon. For example, some of the existing proportionality relationships may need to be modified. In particular, the expression of continuing evapotranspiration and how it relates to the subsurface flow processes is not strong. Typically, values of E_c are nearly negligible, causing the model to assign evapotranspiration processes primarily to E_0 .

In the model structure, the mechanism preventing surface runoff is the first soil moisture layer. However, this mechanism may be responsible for the over-estimation of E_0 which causes evapotranspiration to often occur at the potential rate. An alternative methodology for preventing direct runoff from occurring may need to be considered in future model development.

Likewise, alternative processes for modeling groundwater storage and release should be considered. For instance, the groundwater reservoir is modeled as a linear reservoir, a practice

common among many other water balance models. However, a different mechanism could be described, such as one based on a proportionality relationship.

Treatment of the separation between interflow and recharge may be too simplified. In the case of the proposed model, this separation is handled by $R = k_1 Q_{SS}$ and $Q_i = (1 - k_1) Q_{SS}$. For example, a more physically-based relationship would be based on the current water levels within the groundwater reservoir.

More importantly, the model does not simulate groundwater storage that does not exit the catchment as streamflow (only shallow groundwater storage is modeled). Addressing this limitation is especially important for applications to catchments where deep groundwater recharge is a significant factor, such as catchments in Florida. To address this, a seepage loss function could be implemented into the model.

Another factor that is not modeled is the variability of water table depths. While the groundwater and soil moisture storages are allowed to vary, they do not influence the depth of the unsaturated zone. This has important implications because as groundwater levels increase, the ability of the soil moisture layer to retain water decreases, potentially increasing the magnitude and frequency of surface runoff. Also, as groundwater levels decrease, vegetation with shallow root systems may be unable to extract water from the saturated zone, limiting transpiration to the unsaturated zone, where vegetation must contend with the forces of adhesion between soil and water particles. Inclusion of a process representing average vegetation root depths may improve estimates of evapotranspiration. Alternatively, a different model structure could be pursued with a different number of tanks.

In addition to further modifications of the model structure, some areas of the model development process need to be adjusted. For instance, the model development strategy pursued in this thesis was found not to be efficient and led to slow model progress. Application of a more methodical model development strategy, such as the “Top Down” approach suggested by Sivapalan et al. (2003) will likely expedite the modeling process and may lead to even better model forms.

The methodology for calibration and validation used in this thesis employed the split-sample test used by Zhang et al. (2008). This methodology assumes that the climate does not change and is largely cyclical. However, short-term changes in the climate, such as the El Nino effect, can have a substantial impact on local climates, causing periods of drought and flooding to occur. If a series of extreme events occurs primarily in one half of the streamflow records, these events will create a strong bias.

An alternative method of calibration/validation should be considered in future analysis of the proposed model. For example, Alley (1984) calibrated his model by sequentially calibrating the model to ten (non-overlapping) years of data at a time, starting with the first ten years, then the second ten years, etc. and using the data not used in calibration to validate the model. For example, using a dataset of 50 years, there were five calibration periods, with the first calibration using years 1-10 and the validation using years 11-50, the second calibration using years 11-20 and the validation using years 1-10 and 21-50, etc.

The selection of a large number of catchments improved the reliability of model results and simplified the analysis because statistical measures, such as the mean NSE value of all

catchments, became more representative of the overall performance of the models. Future model development should include even more catchments to increase this benefit.

As model development at the daily time scale led to the most significant increases in model performance, future development of the model should focus on evaluating the model at even shorter time scales (i.e. hourly).

CHAPTER 6: ADDITIONAL DISCUSSION

6.1 Six Poorly Performing Catchments

Six catchments, particularly catchments 07261000, 08171300, and 07346000, were found to perform very poorly throughout all time scales and throughout all models.

Catchment 07261000 has an area of about 446 km² and is located in a relatively hilly area. However, what may be the main cause for the poor performance is that it neighbors a large 119 km² lake (Greers Ferry Lake in Arkansas), which likely contributes a significant amount of groundwater to the catchment.

The catchment is illustrated below along with a land cover map provided by the National Gap Analysis Program (GAP) (US Geological Survey, 2011).

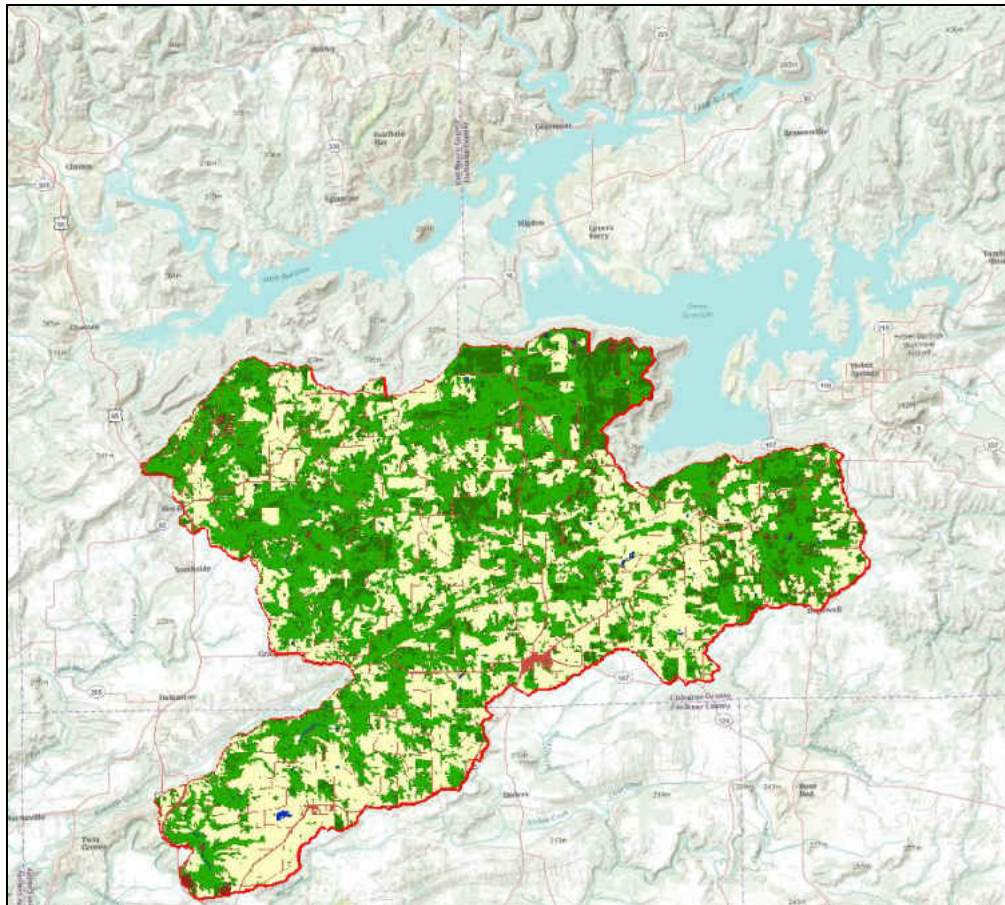


Figure 6.1. Catchment 07261000 (Arkansas). Blue represents open water bodies. Teal represents wetland areas. Red represents urban areas. Light yellow represents pasture (open areas). Different shades of green (including dark yellow) represent various types of forested areas.

Catchment 07346000, located in East Texas, has a very large lake/coastal plain spanning the length of the catchment. Additionally, there are multiple dams and urban areas located in the region, suggesting a high level of streamflow regulation in the area.

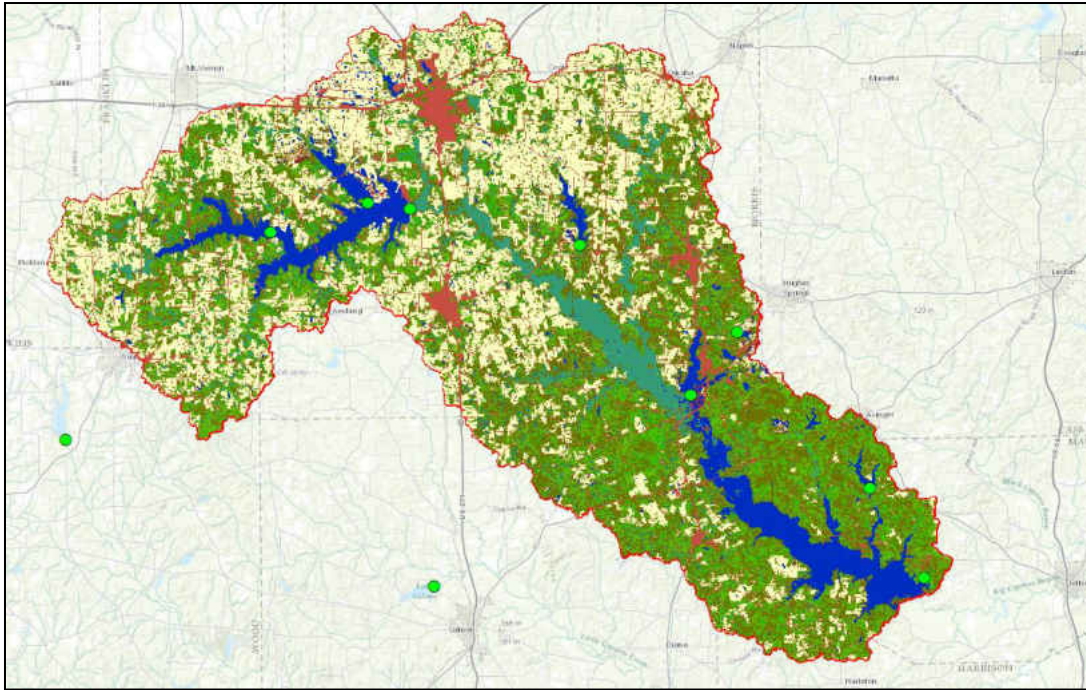


Figure 6.2. Catchment 07346000 (East Texas). Blue represents open water bodies. Teal represents wetland areas. Red represents urban areas. Light yellow represents pasture (open areas). Different shades of green (including dark yellow) represent various types of forested areas. Green circles denote dam locations.

What is surprising is that one of the worst performing catchments (08171300, located north of San Antonio, Texas) is based on streamflow measurements taken upstream and downstream of streamflow gages for two other very good performing catchments. No dams were observed in this catchment either. Additionally, there is very little urban area in the catchment. Additionally, the USGS Annual Water-Data Report for this catchment’s streamflow gage station rates the records for all three stations as “Fair”.

An analysis of the topography, however, indicated that the area between this catchment and the upstream catchment is characterized by very high relief (Figure 6.5). Specifically, this

area is known as the Balcones Fault Zone, which crosses the Blanco River before station 08171300. The USGS report mentions that most of the low flow enters the limestone soil layers in this zone (US Geological Survey, 2014b). Thus, water balance models will tend to overestimate streamflow during periods of low flow.

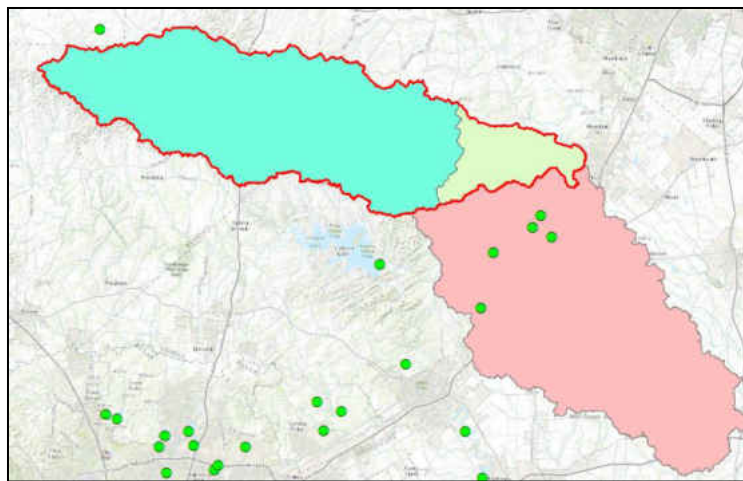


Figure 6.3. Catchments Overlapping 08171300 (Central Texas). Light yellow (with red outline) represents catchment 08171300. Catchment 08171000 (light blue) is upstream of catchment 08171300. Catchment 08172000 (light red) is downstream and overlapped by the other two catchments. The stream gages upstream and downstream of catchment 08171300 both perform very well and very similarly, unlike 08171300, which performs very poorly.

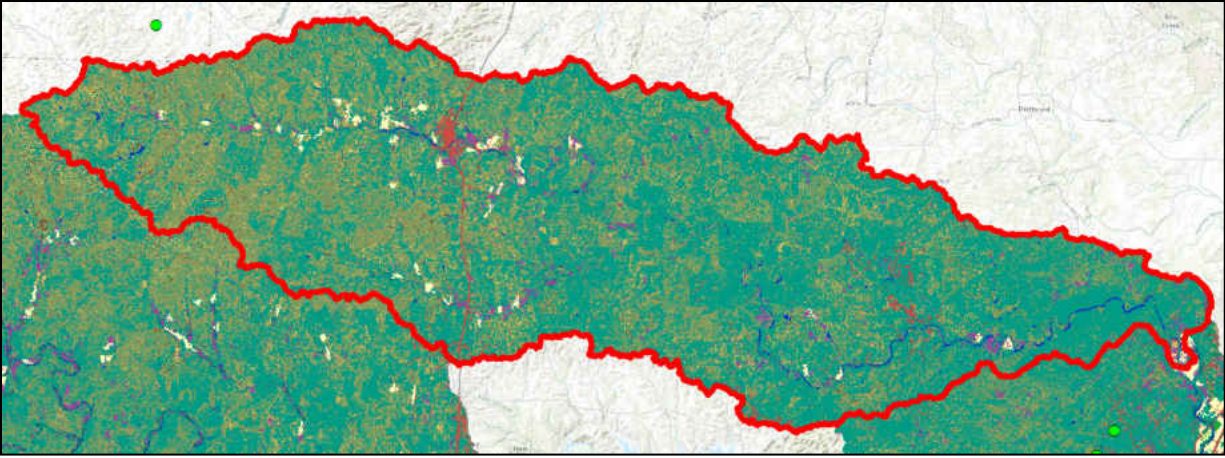


Figure 6.4. Catchment 08171300 (Red outline) (Central Texas). Blue represents open water bodies. Teal represents wetland areas. Red represents urban areas. Light yellow represents pasture (open areas). Different shades of green (including dark yellow) represent various types of forested areas. Green circles denote dam locations.

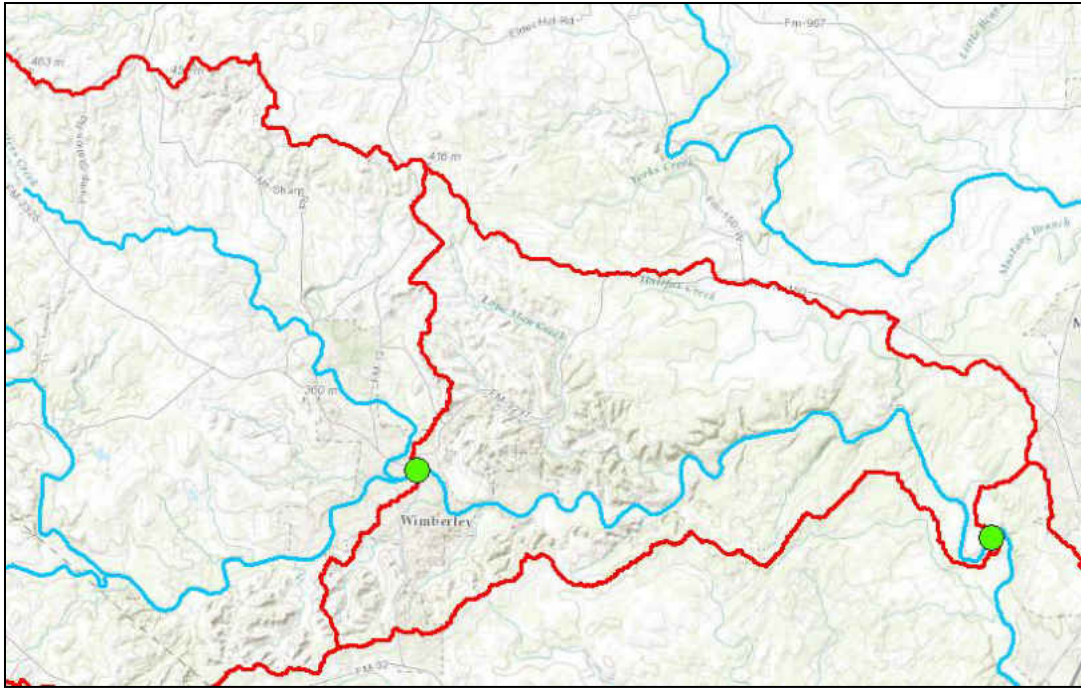


Figure 6.5. Topography between the Upstream Catchment and Catchment 08171300. Blue lines represent streamlines. Red lines represent catchment boundaries. The green point on the left refers to the upstream catchment gage station. The point on the right refers to the gage station for catchment 08171300.

Three additional catchments also, though to a lesser degree, performed poorly throughout all time scales and all models. Two of them, catchments 02143040 and 02143500, are located in North Carolina and are in close proximity to each other. Catchment 02143040 is located entirely within the South Mountains, which may account for the poor performance. However, catchment 02143500 is not significantly urbanized, has an aridity index below one, and is not located near any mountains. Additionally, the USGS Annual Water-Data Report for this catchment's streamflow gage station rates the records as "Good" (US Geological Survey, 2014a). However,

the report also mentions that streamflow regulation has affected minimum discharges since 1963, which may be a significant factor in the decreased performance for this catchment.

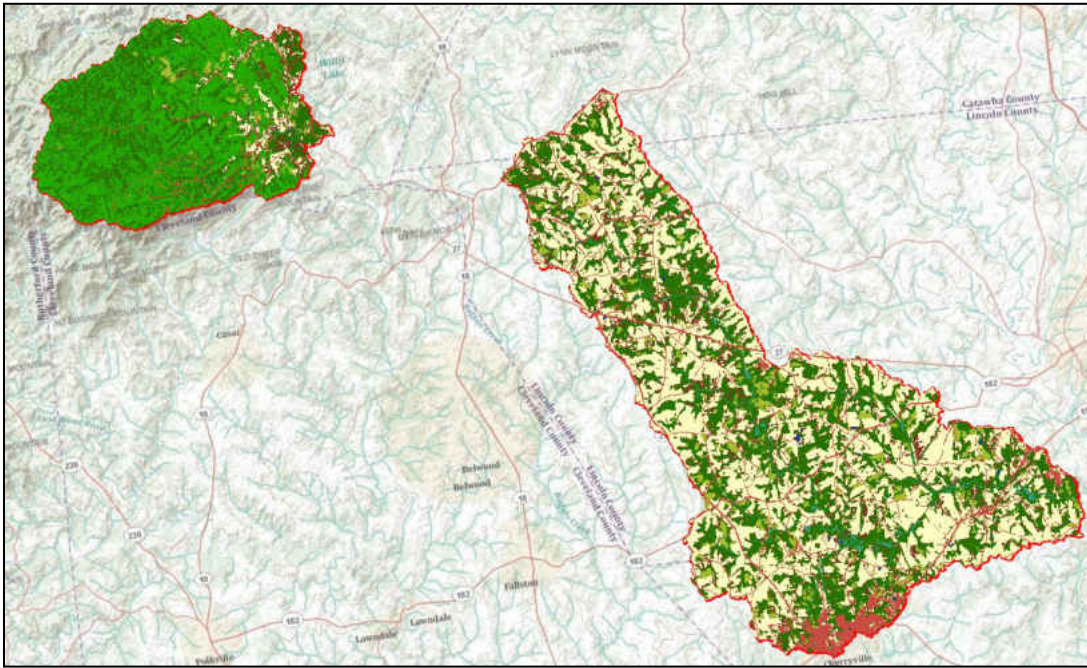


Figure 6.6. Catchment 02143040 (left) and catchment 02143500 (right). Both are located in North Carolina. Blue represents open water bodies. Teal represents wetland areas. Red represents urban areas. Light yellow represents pasture (open areas). Different shades of green (including dark yellow) represent various types of forested areas.

The headwaters of the sixth catchment (02349500) are within the Atlanta Metropolitan area, six miles from the city center. Analysis of the land cover map revealed that this area is highly urbanized, suggesting a high level of streamflow regulation. However, the catchment upstream to this one typically has much higher performance values.

Another possible explanation may be the large floodplain in the southern part of the catchment, which could be a significant source of surface-water storage (Figure 6.7).

A third possible explanation is the loss of water to deep groundwater storage (aquifers). This explanation is plausible for two reasons. First, none of the three models evaluated can simulate this condition well. Second, the catchment outlet is located 10 miles from the Floridan Aquifer (Figure 6.8) and an analysis of the soil shows a much higher hydraulic conductivity in the region downstream of the upstream catchment (the region affecting streamflow measurements for catchment 02349500).

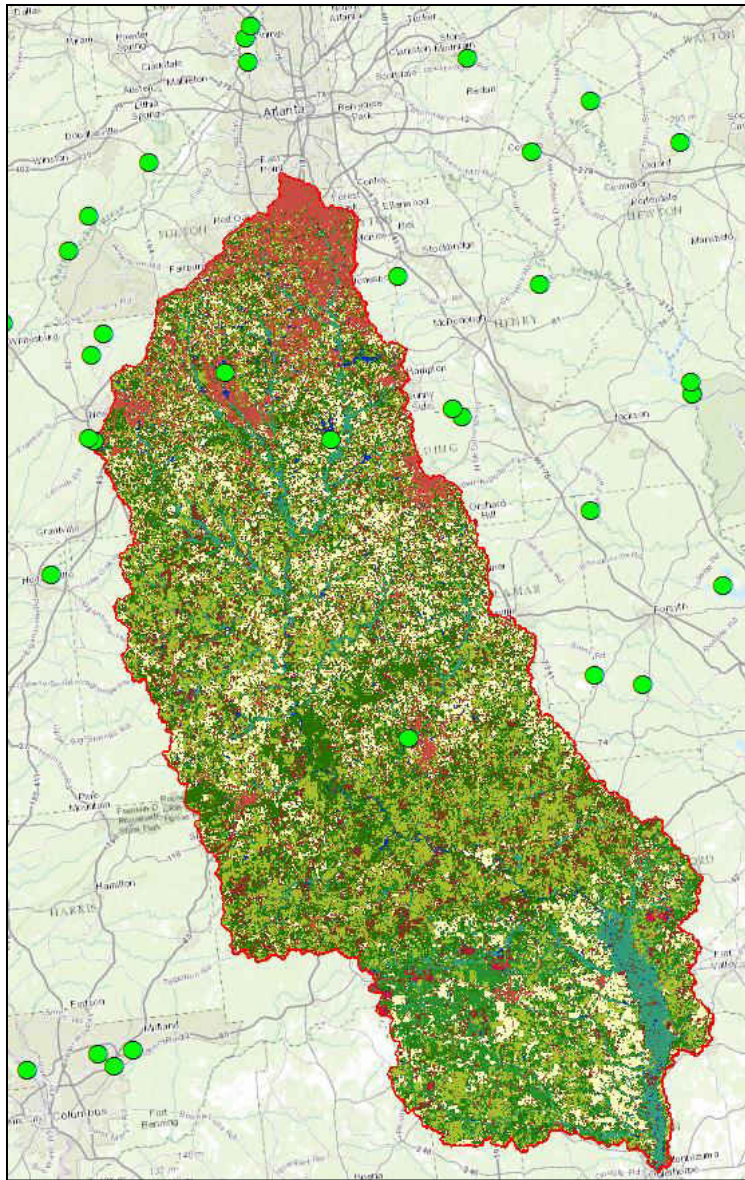


Figure 6.7. Catchment 02349500 (South Atlanta, Georgia). Blue represents open water bodies. Teal represents wetland areas. Red represents urban areas. Light yellow and dark red represents grasses (open areas). Different shades of green (including dark yellow) represent various types of forested areas. Green circles denote dam locations.

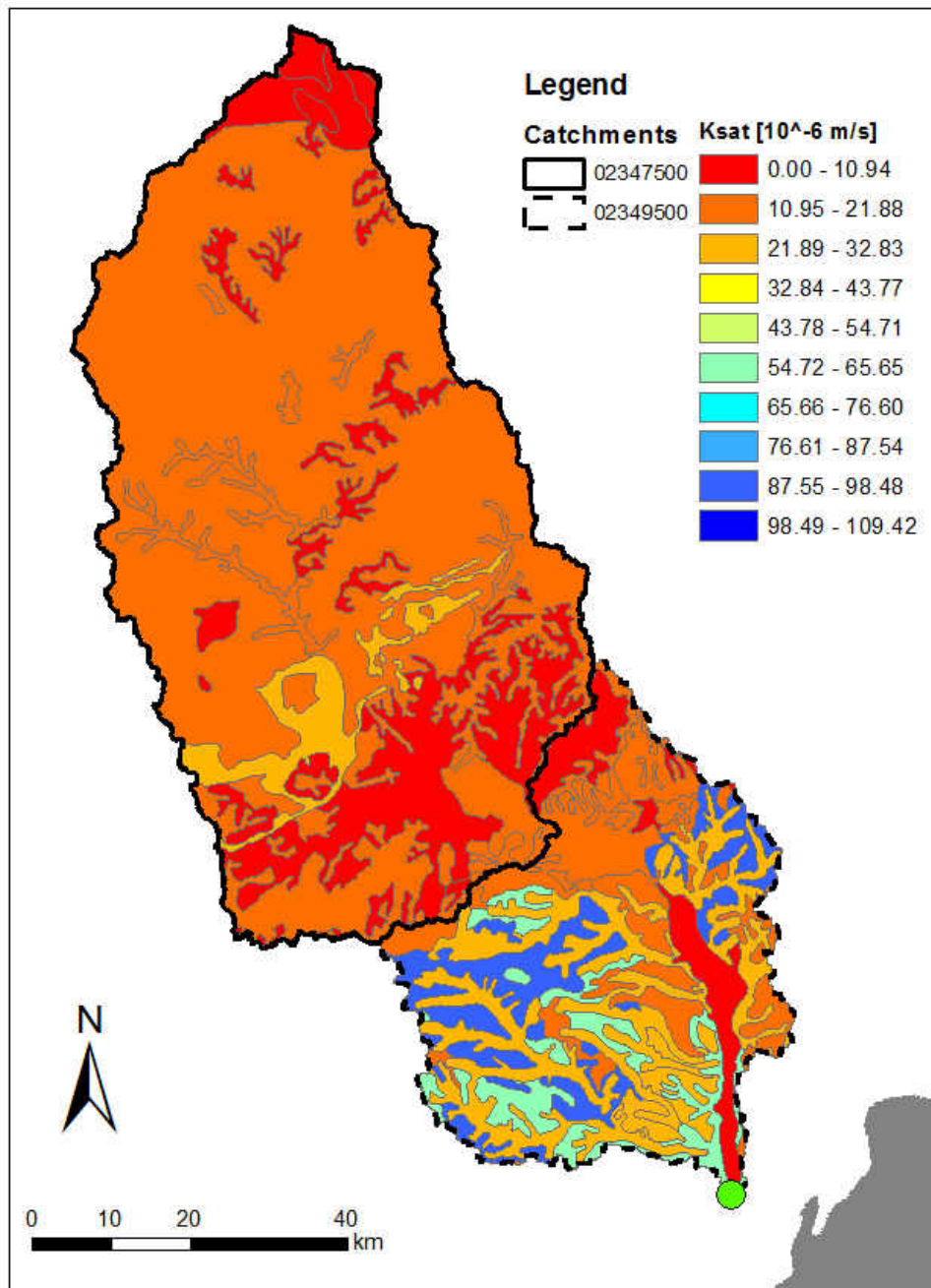


Figure 6.8. Saturated Hydraulic Conductivity for Catchment 02349500. The corresponding USGS station for the catchment is denoted by a green circle. The gray region in the bottom-right corner denotes the Floridan Aquifer System. Catchment 02349500 includes the area outlined by the solid and dashed black lines. The upstream catchment (02347500) is denoted by the solid black line.

6.2 The Equity Equation vs. the “abcd” Model

The expression for E/P used by the Equity model, described earlier in Section 2.11, bears a striking resemblance to the abcd model’s equation for evapotranspiration opportunity.

This equation is reintroduced below:

$$\frac{E}{P} = \frac{\left(1 + \frac{E_p}{P}\right) - \sqrt{\left(1 + \frac{E_p}{P}\right)^2 - 4\varepsilon\left(\frac{E_p}{P}\right)(2 - \varepsilon)}}{2\varepsilon(2 - \varepsilon)} \quad (2.90)$$

Consider the abcd equation proposed by Thomas (1981):

$$y_i(W_i) = \frac{W_i + b}{2a} - \sqrt{\left(\frac{W_i + b}{2a}\right)^2 - \frac{W_i b}{a}} \quad (2.19)$$

Dividing this equation by b:

$$\frac{y_i}{b} = \frac{1 + \frac{W_i}{b} - \sqrt{\left(1 + \frac{W_i}{b}\right)^2 - 4a\frac{W_i}{b}}}{2a} \quad (6.1)$$

Then substituting $a = \varepsilon(2 - \varepsilon)$ into the equation:

$$\frac{y_i}{b} = \frac{1 + \frac{W_i}{b} - \sqrt{\left(1 + \frac{W_i}{b}\right)^2 - 4\varepsilon(2 - \varepsilon)\frac{W_i}{b}}}{2\varepsilon(2 - \varepsilon)} \quad (6.2)$$

Now define two relationships:

$$\begin{cases} \frac{W_i}{b} = \frac{E_p}{P} \\ \frac{y_i}{b} = \frac{E}{P} \end{cases} \quad (6.3)$$

These two relationships assume that $W_i = E_p$, $y_i = E$, and $b = P$. Note that $a = \varepsilon(2 - \varepsilon)$ can also be expressed as $\varepsilon = 1 - \sqrt{1 - a}$. If these relationships are substituted into Equation (6.2), the equation becomes identical to Equation (2.90).

An analysis of the relationship between ε and a revealed that when a approaches 1, especially when $a > 0.9$, E_0 increases considerably. From the literature, it was found that a is typically high (0.95~0.99). This suggests that E_0 , based on its definition and its relationship to the other parameters in Equation (2.90), should be a dominant component of evapotranspiration, and that, in contrast with initial abstraction and continuing abstraction, the continuing component should be the minimal component and the initial component should be the dominant component. If this is true, then it further suggests that E_c is a minor component in the competition between E_c and subsurface flow.

Though these equations appear similar, they are not directly related to each other. While the relationship between E/P and E_p/P in the Equity model is concerned with how the climate affects the evapotranspiration (and total runoff), y_i and W_i in the abcd model are concerned with how water availability affects soil moisture storage and evapotranspiration—a different relationship which exhibits a similar equation structure.

**APPENDIX A:
PERFORMANCE RESULTS FOR EACH CATCHMENT**

A.1 Full-Record Calibration Results for Each Catchment

A.1.1 Daily Time Scale

Table 6.1. Full-Record Calibration Results at the Daily Time Scale.

Catchment	Proposed Model	abcd Model	Zhang Model
2102000	0.63	0.59	0.66
2143040	0.09	0.09	-0.05
2143500	0.08	0.08	0.00
2126000	0.63	0.60	0.61
2135000	0.76	0.82	0.78
2192000	0.61	0.56	0.60
2387000	0.69	0.65	0.73
2228000	0.77	0.75	0.83
2202500	0.72	0.74	0.76
2143000	0.60	0.57	0.48
2349500	0.08	0.07	0.02
2217500	0.61	0.53	0.53
2414500	0.62	0.59	0.59
2165000	0.57	0.49	0.44
2475500	0.63	0.56	0.69
2387500	0.76	0.68	0.75
2339500	0.49	0.49	0.34
2472000	0.71	0.63	0.75
2329000	0.68	0.68	0.78
2482000	0.73	0.70	0.80
2347500	0.67	0.70	0.72
2456500	0.73	0.71	0.79
2479300	0.52	0.45	0.58
2475000	0.71	0.67	0.76
2375500	0.69	0.69	0.73
3438000	0.71	0.75	0.73
3443000	0.76	0.69	0.69
3512000	0.64	0.62	0.52

Catchment	Proposed Model	abcd Model	Zhang Model
3550000	0.70	0.70	0.46
3451500	0.77	0.71	0.66
3504000	0.80	0.78	0.73
3574500	0.63	0.58	0.69
7057500	0.41	0.42	0.33
7052500	0.59	0.58	0.63
7068000	0.46	0.50	0.43
7067000	0.53	0.54	0.52
7056000	0.67	0.67	0.68
7197000	0.10	0.02	0.08
8055500	0.40	0.50	0.38
7186000	0.69	0.67	0.70
7261000	0.00	-0.09	-0.03
7196500	0.56	0.58	0.70
7363500	0.73	0.66	0.74
8167500	0.67	0.65	0.51
7346000	0.02	-0.06	0.02
8171000	0.65	0.68	0.60
8205500	0.30	0.30	0.11
8033500	0.58	0.64	0.56
8189500	0.50	0.33	0.56
8032000	0.55	0.65	0.53
8172000	0.53	0.56	0.55
8171300	-0.01	0.01	-0.01
2478500	0.74	0.72	0.79
2296750	0.67	0.61	0.68
2273000	0.44	0.40	0.11
1372500	0.55	0.55	0.58
1534000	0.47	0.51	0.47
3111500	0.58	0.54	0.44
3331500	0.52	0.60	0.38
3301500	0.73	0.65	0.71
4191500	0.45	0.47	0.50
5555300	0.23	0.09	0.18
5514500	0.13	0.11	0.08
6441500	0.25	0.27	0.15

Catchment	Proposed Model	abcd Model	Zhang Model
6869500	0.46	0.45	0.34
6884400	0.40	0.44	0.32
6897500	0.56	0.57	0.60
7144780	0.22	0.39	0.08
7152000	0.49	0.45	0.58
8085500	0.29	0.28	0.23
7307800	0.51	0.44	0.19

A.1.2 Monthly Time Scale

Table 6.2. Full-Record Calibration Results at the Monthly Time Scale.

Catchment	Proposed Model	abcd Model	Zhang Model
2102000	0.83	0.83	0.81
2143040	0.22	0.18	0.04
2143500	0.22	0.17	0.10
2126000	0.88	0.88	0.86
2135000	0.76	0.75	0.78
2192000	0.85	0.84	0.76
2387000	0.87	0.84	0.84
2228000	0.79	0.78	0.77
2202500	0.84	0.80	0.84
2143000	0.87	0.86	0.83
2349500	0.19	0.12	0.04
2217500	0.87	0.86	0.79
2414500	0.84	0.82	0.79
2165000	0.81	0.82	0.74
2475500	0.85	0.86	0.83
2387500	0.87	0.84	0.82
2339500	0.78	0.75	0.69
2472000	0.84	0.84	0.81
2329000	0.78	0.78	0.75
2482000	0.84	0.82	0.79
2347500	0.89	0.87	0.83
2456500	0.85	0.85	0.83
2479300	0.79	0.73	0.71
2475000	0.81	0.80	0.77
2375500	0.78	0.75	0.73
3438000	0.86	0.88	0.84
3443000	0.88	0.87	0.87
3512000	0.76	0.77	0.71
3550000	0.85	0.82	0.60
3451500	0.89	0.88	0.86
3504000	0.83	0.86	0.84

Catchment	Proposed Model	abcd Model	Zhang Model
3574500	0.84	0.84	0.81
7057500	0.73	0.80	0.75
7052500	0.84	0.87	0.82
7068000	0.75	0.83	0.79
7067000	0.78	0.84	0.79
7056000	0.89	0.90	0.85
7197000	0.29	0.09	0.29
8055500	0.50	0.63	0.63
7186000	0.80	0.84	0.81
7261000	0.05	-0.05	0.01
7196500	0.77	0.75	0.73
7363500	0.83	0.77	0.74
8167500	0.90	0.87	0.75
7346000	0.04	0.03	0.04
8171000	0.84	0.84	0.71
8205500	0.76	0.68	0.58
8033500	0.69	0.71	0.70
8189500	0.57	0.49	0.50
8032000	0.68	0.73	0.62
8172000	0.88	0.83	0.77
8171300	0.00	0.03	0.01
2478500	0.82	0.79	0.77
2296750	0.77	0.76	0.78
2273000	0.52	0.50	0.41
1372500	0.67	0.67	0.62
1534000	0.67	0.70	0.62
3111500	0.84	0.83	0.81
3331500	0.67	0.76	0.70
3301500	0.88	0.89	0.87
4191500	0.68	0.71	0.66
5555300	0.34	0.40	0.40
5514500	0.21	0.23	0.23
6441500	0.32	0.43	0.48
6869500	0.78	0.80	0.77
6884400	0.80	0.83	0.77
6897500	0.82	0.87	0.79

Catchment	Proposed Model	abcd Model	Zhang Model
7144780	0.53	0.70	0.46
7152000	0.66	0.72	0.62
8085500	0.70	0.74	0.68
7307800	0.55	0.59	0.58

A.1.3 Annual Time Scale

Table 6.3. Full-Record Calibration Results at the Annual Time Scale.

Catchment	Proposed Model	abcd Model	Zhang Model
2102000	0.86	0.81	0.78
2143040	0.25	0.08	-0.30
2143500	0.16	-0.03	-0.13
2126000	0.90	0.87	0.84
2135000	0.84	0.81	0.77
2192000	0.82	0.75	0.74
2387000	0.93	0.90	0.93
2228000	0.69	0.56	0.55
2202500	0.61	0.52	0.50
2143000	0.83	0.81	0.80
2349500	0.40	0.16	0.29
2217500	0.80	0.70	0.72
2414500	0.83	0.77	0.75
2165000	0.81	0.75	0.74
2475500	0.83	0.79	0.77
2387500	0.90	0.87	0.88
2339500	0.74	0.63	0.65
2472000	0.74	0.65	0.65
2329000	0.78	0.57	0.63
2482000	0.87	0.79	0.80
2347500	0.78	0.73	0.72
2456500	0.87	0.84	0.85
2479300	0.65	0.57	0.69
2475000	0.72	0.70	0.68
2375500	0.60	0.48	0.45
3438000	0.82	0.74	0.81
3443000	0.96	0.92	0.95
3512000	0.80	0.79	0.80
3550000	0.89	0.91	0.92
3451500	0.93	0.87	0.91
3504000	0.95	0.95	0.96

Catchment	Proposed Model	abcd Model	Zhang Model
3574500	0.80	0.72	0.83
7057500	0.70	0.63	0.78
7052500	0.86	0.84	0.83
7068000	0.76	0.72	0.78
7067000	0.72	0.62	0.69
7056000	0.88	0.85	0.84
7197000	0.60	0.35	0.44
8055500	0.64	0.53	0.47
7186000	0.82	0.81	0.79
7261000	0.09	-0.05	-0.07
7196500	0.84	0.80	0.85
7363500	0.74	0.61	0.65
8167500	0.87	0.81	0.66
7346000	0.10	-0.10	0.16
8171000	0.89	0.83	0.74
8205500	0.80	0.64	0.50
8033500	0.73	0.65	0.67
8189500	0.63	0.61	0.55
8032000	0.73	0.69	0.71
8172000	0.88	0.78	0.72
8171300	0.12	0.07	0.17
2478500	0.67	0.62	0.60
2296750	0.76	0.58	0.56
2273000	0.70	0.58	0.62
1372500	0.89	0.83	0.88
1534000	0.93	0.91	0.94
3111500	0.93	0.90	0.91
3331500	0.85	0.77	0.83
3301500	0.86	0.85	0.90
4191500	0.93	0.86	0.88
5555300	0.80	0.68	0.77
5514500	0.83	0.77	0.86
6441500	0.59	0.54	0.39
6869500	0.92	0.89	0.76
6884400	0.97	0.95	0.95
6897500	0.95	0.95	0.88

Catchment	Proposed Model	abcd Model	Zhang Model
7144780	0.57	0.57	0.51
7152000	0.85	0.82	0.71
8085500	0.92	0.74	0.80
7307800	0.68	0.71	0.70

A.2 Calibration and Validation Results for Each Catchment

A.2.1 Daily Time Scale

Table 6.4. Calibration and Validation Results at the Daily Time Scale.

Catchment	Half-Record Calibration			Validation		
	Proposed Model	abcd Model	Zhang Model	Proposed Model	abcd Model	Zhang Model
2102000	0.62	0.57	0.65	0.64	0.62	0.63
2143040	0.07	0.08	-0.04	0.12	0.11	-0.12
2143500	0.07	0.07	0.00	0.06	0.07	-0.18
2126000	0.63	0.57	0.62	0.58	0.62	0.57
2135000	0.77	0.81	0.75	0.64	0.83	-0.11
2192000	0.61	0.58	0.63	0.60	0.53	0.57
2387000	0.70	0.67	0.76	0.68	0.63	0.70
2228000	0.78	0.76	0.83	0.73	0.73	0.81
2202500	0.70	0.68	0.69	0.72	0.73	0.80
2143000	0.61	0.56	0.49	0.59	0.56	0.44
2349500	0.07	0.05	0.04	0.03	0.10	-0.20
2217500	0.63	0.55	0.55	0.58	0.49	0.50
2414500	0.65	0.62	0.62	0.60	0.56	0.56
2165000	0.57	0.51	0.33	0.55	0.46	0.46
2475500	0.66	0.62	0.75	0.60	0.53	0.64
2387500	0.78	0.70	0.78	0.74	0.66	0.72
2339500	0.46	0.47	0.29	0.51	0.49	0.39
2472000	0.71	0.65	0.77	0.69	0.61	0.73
2329000	0.70	0.73	0.78	0.54	0.66	0.44
2482000	0.75	0.70	0.82	0.69	0.65	0.76
2347500	0.68	0.67	0.69	0.65	0.71	0.73
2456500	0.73	0.69	0.78	0.69	0.69	0.79
2479300	0.58	0.53	0.66	0.31	0.35	0.41
2475000	0.72	0.68	0.77	0.68	0.66	0.75
2375500	0.68	0.65	0.74	0.62	0.69	0.61
3438000	0.76	0.75	0.76	0.66	0.73	0.70
3443000	0.78	0.69	0.69	0.73	0.66	0.67

Catchment	Half-Record Calibration			Validation		
	Proposed Model	abcd Model	Zhang Model	Proposed Model	abcd Model	Zhang Model
3512000	0.71	0.66	0.57	0.54	0.50	0.46
3550000	0.72	0.77	0.53	0.53	0.70	0.41
3451500	0.79	0.72	0.66	0.76	0.71	0.64
3504000	0.81	0.78	0.75	0.74	0.76	0.71
3574500	0.62	0.58	0.73	0.62	0.58	0.64
7057500	0.43	0.40	0.30	-0.03	0.26	-0.34
7052500	0.55	0.49	0.56	0.58	0.59	0.65
7068000	0.45	0.45	0.40	0.46	0.54	0.32
7067000	0.53	0.52	0.49	0.49	0.54	0.43
7056000	0.72	0.70	0.74	0.60	0.64	0.59
7197000	0.00	-0.02	0.00	0.12	0.03	0.12
8055500	0.56	0.58	0.50	0.19	0.39	0.20
7186000	0.70	0.68	0.67	0.65	0.64	0.71
7261000	-0.03	-0.06	-0.07	0.02	-0.05	-0.01
7196500	0.59	0.61	0.74	0.45	0.48	0.63
7363500	0.73	0.61	0.74	0.71	0.64	0.73
8167500	0.68	0.64	0.57	0.47	0.60	0.16
7346000	0.02	-0.07	0.02	0.01	-0.06	0.01
8171000	0.68	0.65	0.65	0.59	0.64	0.56
8205500	0.31	0.31	0.03	0.25	0.29	-0.38
8033500	0.48	0.63	0.49	0.65	0.65	0.58
8189500	0.51	0.36	0.49	-0.29	0.28	-0.34
8032000	0.49	0.66	0.54	0.58	0.64	0.47
8172000	0.63	0.68	0.64	0.41	0.51	0.30
8171300	0.03	0.03	0.03	-0.09	-0.01	-0.10
2478500	0.77	0.70	0.81	0.72	0.65	0.77
2296750	0.65	0.61	0.36	0.57	0.49	0.72
2273000	0.36	0.36	0.15	0.44	0.40	-0.91
1372500	0.61	0.63	0.68	0.48	0.49	0.48
1534000	0.55	0.60	0.56	0.33	0.36	0.38
3111500	0.63	0.55	0.49	0.50	0.49	0.36
3331500	0.49	0.57	0.34	0.54	0.61	0.37
3301500	0.76	0.66	0.74	0.70	0.62	0.67
4191500	0.48	0.49	0.50	0.41	0.45	0.50

Catchment	Half-Record Calibration			Validation		
	Proposed Model	abcd Model	Zhang Model	Proposed Model	abcd Model	Zhang Model
5555300	0.31	0.29	0.27	0.09	0.13	0.02
5514500	0.22	0.16	0.20	-0.21	-0.05	-0.16
6441500	0.30	0.33	0.15	0.14	0.18	0.05
6869500	0.30	0.34	0.20	-0.10	0.32	-3.14
6884400	0.40	0.41	0.24	0.37	0.46	0.38
6897500	0.42	0.42	0.33	0.51	0.60	0.69
7144780	0.31	0.34	0.06	0.15	0.21	-0.10
7152000	0.47	0.38	0.53	0.49	0.43	0.59
8085500	0.34	0.33	0.23	-1.12	-0.21	0.07
7307800	0.54	0.50	0.31	0.20	0.25	-0.03

A.2.2 Monthly Time Scale

Table 6.5. Calibration and Validation Results at the Monthly Time Scale.

Catchment	Half-Record Calibration			Validation		
	Proposed Model	abcd Model	Zhang Model	Proposed Model	abcd Model	Zhang Model
2102000	0.79	0.76	0.70	0.81	0.84	0.86
2143040	0.08	0.07	-0.05	0.20	0.17	-0.09
2143500	0.13	0.10	0.00	0.18	0.17	0.07
2126000	0.86	0.82	0.78	0.86	0.90	0.92
2135000	0.66	0.63	0.61	0.75	0.77	0.80
2192000	0.80	0.77	0.67	0.81	0.87	0.76
2387000	0.85	0.81	0.81	0.87	0.86	0.84
2228000	0.75	0.72	0.69	0.81	0.81	0.81
2202500	0.80	0.70	0.76	0.86	0.83	0.87
2143000	0.85	0.81	0.78	0.84	0.86	0.82
2349500	0.09	0.01	-0.01	0.20	0.16	0.01
2217500	0.86	0.85	0.77	0.86	0.86	0.76
2414500	0.88	0.85	0.80	0.80	0.79	0.73
2165000	0.78	0.77	0.67	0.80	0.81	0.75
2475500	0.89	0.88	0.82	0.75	0.84	0.80
2387500	0.88	0.84	0.82	0.85	0.84	0.80
2339500	0.82	0.69	0.76	0.72	0.74	0.58
2472000	0.88	0.84	0.81	0.75	0.83	0.79
2329000	0.79	0.77	0.70	0.69	0.77	0.67
2482000	0.89	0.85	0.83	0.74	0.74	0.75
2347500	0.86	0.82	0.73	0.89	0.89	0.87
2456500	0.86	0.85	0.82	0.82	0.82	0.82
2479300	0.85	0.83	0.82	0.65	0.54	0.57
2475000	0.83	0.79	0.76	0.76	0.79	0.75
2375500	0.85	0.84	0.78	0.73	0.68	0.69
3438000	0.90	0.91	0.88	0.80	0.82	0.80
3443000	0.87	0.86	0.85	0.89	0.88	0.88
3512000	0.78	0.76	0.75	0.69	0.76	0.68
3550000	0.88	0.83	0.68	0.79	0.78	0.25

Catchment	Half-Record Calibration			Validation		
	Proposed Model	abcd Model	Zhang Model	Proposed Model	abcd Model	Zhang Model
3451500	0.87	0.85	0.82	0.90	0.89	0.87
3504000	0.84	0.85	0.83	0.81	0.86	0.85
3574500	0.84	0.82	0.81	0.83	0.85	0.79
7057500	0.70	0.77	0.74	0.68	0.75	0.69
7052500	0.87	0.89	0.84	0.80	0.86	0.81
7068000	0.80	0.88	0.84	0.62	0.77	0.73
7067000	0.81	0.89	0.84	0.68	0.74	0.71
7056000	0.91	0.92	0.88	0.87	0.88	0.83
7197000	0.22	0.00	-0.01	0.24	0.06	0.10
8055500	0.60	0.68	0.77	0.33	0.55	0.32
7186000	0.76	0.80	0.77	0.80	0.86	0.81
7261000	-0.02	-0.14	-0.08	0.04	-0.09	0.00
7196500	0.77	0.74	0.68	0.73	0.71	0.76
7363500	0.84	0.78	0.74	0.78	0.74	0.72
8167500	0.90	0.86	0.80	0.86	0.85	0.68
7346000	0.07	-0.12	0.02	-0.01	-0.09	0.02
8171000	0.82	0.84	0.76	0.84	0.82	0.66
8205500	0.93	0.68	0.41	0.04	-0.01	0.71
8033500	0.68	0.70	0.75	0.64	0.67	0.64
8189500	0.87	0.73	0.80	0.15	0.33	0.31
8032000	0.68	0.77	0.68	0.60	0.65	0.53
8172000	0.90	0.88	0.81	0.81	0.79	0.72
8171300	0.08	0.06	0.10	-0.12	-0.03	-0.10
2478500	0.86	0.82	0.81	0.72	0.69	0.71
2296750	0.62	0.64	0.58	0.71	0.70	0.78
2273000	0.31	0.33	0.26	0.52	0.49	0.40
1372500	0.71	0.73	0.62	0.64	0.63	0.60
1534000	0.64	0.68	0.58	0.61	0.69	0.63
3111500	0.88	0.87	0.84	0.77	0.75	0.76
3331500	0.67	0.73	0.66	0.64	0.77	0.69
3301500	0.88	0.86	0.88	0.86	0.90	0.86
4191500	0.71	0.71	0.71	0.65	0.71	0.62
5555300	0.34	0.31	0.33	0.19	0.35	0.27
5514500	0.08	0.11	0.14	0.08	0.18	0.08

Catchment	Half-Record Calibration			Validation		
	Proposed Model	abcd Model	Zhang Model	Proposed Model	abcd Model	Zhang Model
6441500	0.80	0.62	0.83	0.10	0.33	0.24
6869500	0.71	0.81	0.68	0.68	0.58	0.49
6884400	0.72	0.76	0.79	0.71	0.84	0.72
6897500	0.55	0.73	0.59	0.74	0.87	0.79
7144780	0.32	0.37	0.32	0.41	0.73	0.39
7152000	0.67	0.62	0.61	0.44	0.74	0.56
8085500	0.78	0.79	0.71	-1.94	-1.84	-0.74
7307800	0.73	0.70	0.69	0.35	0.32	0.41

A.2.3 Annual Time Scale

Table 6.6. Calibration and Validation Results at the Annual Time Scale.

Catchment	Half-Record Calibration			Validation		
	Proposed Model	abcd Model	Zhang Model	Proposed Model	abcd Model	Zhang Model
2102000	0.96	0.93	0.87	0.78	0.72	0.69
2143040	0.47	-1.37	-2.89	-0.30	0.06	-1.88
2143500	-0.34	-1.54	-0.24	0.03	0.00	-0.23
2126000	0.93	0.94	0.89	0.88	0.83	0.81
2135000	0.88	0.73	0.71	0.57	0.65	-2.83
2192000	0.93	0.80	0.75	0.51	0.18	-0.97
2387000	0.95	0.93	0.93	0.88	0.84	0.85
2228000	0.71	0.47	0.54	0.56	0.48	0.48
2202500	0.64	0.55	0.56	0.42	0.25	0.05
2143000	0.96	0.85	0.79	0.73	0.79	0.78
2349500	-0.41	-1.36	-0.03	0.25	0.09	-0.03
2217500	0.88	0.79	0.72	0.52	0.61	-0.08
2414500	0.90	0.81	0.74	0.72	0.64	-0.69
2165000	0.88	0.82	0.78	0.42	-0.26	-1.94
2475500	0.70	0.67	0.57	0.78	0.83	0.71
2387500	0.95	0.92	0.90	0.68	0.75	0.67
2339500	0.81	0.69	0.64	0.61	0.38	-3.05
2472000	0.51	0.53	0.48	0.78	0.68	0.60
2329000	0.76	0.31	0.42	0.69	0.50	0.67
2482000	0.85	0.79	0.80	0.88	0.73	0.49
2347500	0.87	0.68	0.62	0.69	0.30	-0.56
2456500	0.91	0.90	0.87	0.71	0.60	0.74
2479300	0.53	0.56	0.64	-0.74	-1.58	-0.98
2475000	0.42	0.46	0.42	0.89	0.77	0.46
2375500	0.40	0.43	0.67	-0.34	-0.49	-0.25
3438000	0.89	0.86	0.95	0.62	0.53	0.12
3443000	0.97	0.96	0.95	0.87	0.78	0.93
3512000	0.92	0.92	0.89	0.50	0.60	0.62
3550000	0.95	0.95	0.96	0.72	0.83	0.83

Catchment	Half-Record Calibration			Validation		
	Proposed Model	abcd Model	Zhang Model	Proposed Model	abcd Model	Zhang Model
3451500	0.99	0.95	0.95	0.78	0.76	0.87
3504000	0.96	0.96	0.96	0.93	0.93	0.93
3574500	0.93	0.85	0.88	-1.76	0.11	0.40
7057500	0.60	0.45	0.81	0.01	-0.47	0.38
7052500	0.93	0.90	0.92	0.70	0.50	0.35
7068000	0.81	0.63	0.86	0.60	0.00	0.63
7067000	0.78	0.63	0.88	0.29	-0.22	0.29
7056000	0.88	0.83	0.90	0.80	0.77	-1.83
7197000	0.92	0.43	0.51	0.32	0.19	0.17
8055500	0.72	0.41	0.36	0.49	-0.05	-0.44
7186000	0.98	0.95	0.97	0.53	0.59	0.64
7261000	0.39	-0.16	-0.44	-0.15	-0.14	-0.18
7196500	0.98	0.96	0.97	0.71	0.57	0.58
7363500	0.89	0.62	0.70	0.37	0.28	0.39
8167500	0.95	0.76	0.67	0.59	0.72	0.29
7346000	0.66	0.07	0.70	-0.33	-0.23	-0.41
8171000	0.98	0.83	0.81	0.73	0.74	0.37
8205500	0.99	0.56	0.55	0.36	0.55	-1.21
8033500	0.93	0.85	0.82	0.30	-1.20	-1.64
8189500	0.74	0.68	0.65	0.49	0.48	0.44
8032000	0.98	0.89	0.91	0.15	0.36	0.46
8172000	0.93	0.82	0.77	0.66	0.71	0.54
8171300	0.77	0.61	0.79	-0.31	-0.22	-0.68
2478500	0.52	0.40	0.37	0.76	0.61	-0.83
2296750	0.85	0.53	0.65	0.58	0.17	0.32
2273000	0.66	0.51	0.54	0.62	0.30	0.21
1372500	0.82	0.86	0.81	0.58	0.71	0.56
1534000	0.93	0.90	0.98	0.91	0.88	0.70
3111500	0.97	0.95	0.95	0.81	0.73	0.79
3331500	0.95	0.87	0.89	0.11	0.66	0.66
3301500	0.89	0.82	0.88	0.81	0.76	0.82
4191500	0.98	0.93	0.98	0.79	0.76	0.69
5555300	0.71	0.47	0.64	-0.07	0.53	-0.05
5514500	0.74	0.57	0.68	0.74	0.73	0.93

Catchment	Half-Record Calibration			Validation		
	Proposed Model	abcd Model	Zhang Model	Proposed Model	abcd Model	Zhang Model
6441500	0.97	0.92	0.94	0.20	0.35	-0.38
6869500	0.99	0.43	0.33	0.31	0.87	0.14
6884400	0.97	0.94	0.92	0.89	0.91	0.94
6897500	0.98	0.99	0.93	0.92	0.91	0.85
7144780	0.98	0.78	0.65	0.10	0.43	0.27
7152000	0.97	0.96	0.77	0.67	0.40	0.30
8085500	0.92	0.71	0.79	-4.32	-5.63	-5.72
7307800	0.72	0.72	0.70	0.59	0.62	0.66

A.3 Second Calibration and Validation Results for Each Catchment

A.3.1 Daily Time Scale

Table 6.7. Calibration and Validation Results at the Daily Time Scale (Second Analysis).

Catchment	Half-Record Calibration (Second Calibration Method)			Second Validation		
	Proposed Model	abcd Model	Zhang Model	Proposed Model	abcd Model	Zhang Model
2102000	0.62	0.57	0.65	0.64	0.61	0.63
2143040	0.07	0.08	-0.04	0.06	0.11	-0.11
2143500	0.07	0.07	0.03	0.05	0.09	-0.16
2126000	0.63	0.57	0.62	0.58	0.63	0.57
2135000	0.77	0.81	0.77	0.74	0.83	0.81
2192000	0.60	0.58	0.64	0.60	0.53	0.57
2387000	0.70	0.65	0.76	0.68	0.61	0.70
2228000	0.78	0.76	0.84	0.74	0.74	0.82
2202500	0.71	0.71	0.75	0.74	0.76	0.80
2143000	0.61	0.56	0.50	0.59	0.57	0.44
2349500	0.07	0.06	0.04	0.08	0.10	-0.03
2217500	0.63	0.56	0.55	0.58	0.50	0.50
2414500	0.65	0.62	0.62	0.60	0.56	0.56
2165000	0.57	0.48	0.35	0.56	0.48	0.43
2475500	0.66	0.61	0.75	0.60	0.52	0.64
2387500	0.78	0.68	0.78	0.74	0.64	0.72
2339500	0.46	0.46	0.35	0.50	0.49	0.39
2472000	0.71	0.63	0.77	0.69	0.60	0.73
2329000	0.70	0.73	0.79	0.59	0.66	0.49
2482000	0.75	0.71	0.82	0.68	0.67	0.76
2347500	0.68	0.66	0.69	0.65	0.68	0.73
2456500	0.73	0.71	0.78	0.69	0.71	0.79
2479300	0.58	0.53	0.66	0.30	0.34	0.41
2475000	0.72	0.68	0.77	0.68	0.65	0.75
2375500	0.68	0.68	0.75	0.65	0.66	0.61
3438000	0.76	0.75	0.76	0.66	0.73	0.70

Catchment	Half-Record Calibration (Second Calibration Method)			Second Validation		
	Proposed Model	abcd Model	Zhang Model	Proposed Model	abcd Model	Zhang Model
3443000	0.77	0.68	0.69	0.73	0.62	0.67
3512000	0.71	0.67	0.58	0.54	0.54	0.47
3550000	0.72	0.78	0.54	0.61	0.69	0.41
3451500	0.79	0.72	0.66	0.76	0.71	0.63
3504000	0.81	0.78	0.75	0.75	0.76	0.71
3574500	0.62	0.57	0.73	0.62	0.57	0.64
7057500	0.42	0.40	0.30	0.03	0.27	-0.30
7052500	0.55	0.49	0.56	0.58	0.60	0.65
7068000	0.45	0.45	0.40	0.46	0.53	0.32
7067000	0.53	0.52	0.49	0.49	0.54	0.43
7056000	0.72	0.69	0.74	0.60	0.64	0.59
7197000	0.06	-0.02	0.00	0.09	0.03	0.12
8055500	0.58	0.62	0.54	0.19	0.41	0.16
7186000	0.70	0.68	0.67	0.65	0.63	0.71
7261000	0.01	-0.06	-0.08	-0.04	-0.05	-0.02
7196500	0.59	0.61	0.75	0.45	0.47	0.63
7363500	0.74	0.60	0.74	0.71	0.62	0.73
8167500	0.68	0.65	0.57	0.47	0.60	0.16
7346000	0.03	-0.19	0.02	0.02	-0.35	0.01
8171000	0.68	0.66	0.65	0.59	0.64	0.56
8205500	0.32	0.32	0.05	0.32	0.29	0.09
8033500	0.48	0.64	0.53	0.64	0.65	0.63
8189500	0.51	0.36	0.49	-0.32	0.29	-0.34
8032000	0.50	0.67	0.55	0.59	0.64	0.48
8172000	0.63	0.69	0.64	0.39	0.51	0.30
8171300	0.03	0.01	0.03	-0.09	0.00	-0.10
2478500	0.77	0.74	0.81	0.71	0.70	0.76
2296750	0.65	0.61	0.62	0.64	0.51	0.74
2273000	0.36	0.27	0.34	0.46	0.31	0.32
1372500	0.62	0.63	0.68	0.47	0.49	0.48
1534000	0.56	0.60	0.56	0.33	0.39	0.38
3111500	0.63	0.54	0.49	0.49	0.45	0.36
3331500	0.49	0.58	0.34	0.54	0.61	0.36

Catchment	Half-Record Calibration (Second Calibration Method)			Second Validation		
	Proposed Model	abcd Model	Zhang Model	Proposed Model	abcd Model	Zhang Model
3301500	0.76	0.67	0.74	0.69	0.62	0.67
4191500	0.48	0.49	0.50	0.41	0.45	0.50
5555300	0.31	0.07	0.29	0.10	0.09	0.06
5514500	0.23	0.11	0.24	-0.03	0.08	-0.10
6441500	0.31	0.36	0.25	0.16	0.20	0.09
6869500	0.35	0.37	0.22	0.51	0.18	0.17
6884400	0.40	0.40	0.31	0.37	0.46	0.44
6897500	0.42	0.38	0.33	0.51	0.57	0.69
7144780	0.32	0.34	0.13	0.15	0.21	0.10
7152000	0.48	0.38	0.54	0.49	0.43	0.59
8085500	0.35	0.34	0.34	-0.13	-0.17	0.04
7307800	0.56	0.50	0.13	0.47	0.20	0.17

A.3.2 Monthly Time Scale

Table 6.8. Calibration and Validation Results at the Monthly Time Scale (Second Analysis).

Catchment	Half-Record Calibration (Second Calibration Method)			Second Validation		
	Proposed Model	abcd Model	Zhang Model	Proposed Model	abcd Model	Zhang Model
2102000	0.79	0.76	0.70	0.82	0.84	0.86
2143040	0.08	0.06	-0.05	0.17	0.17	-0.10
2143500	0.13	0.10	0.00	0.19	0.17	0.07
2126000	0.86	0.82	0.78	0.87	0.90	0.92
2135000	0.66	0.63	0.61	0.75	0.77	0.80
2192000	0.80	0.77	0.67	0.83	0.87	0.77
2387000	0.85	0.81	0.81	0.87	0.86	0.84
2228000	0.74	0.72	0.69	0.81	0.81	0.81
2202500	0.80	0.70	0.76	0.86	0.83	0.87
2143000	0.85	0.81	0.78	0.84	0.86	0.82
2349500	0.09	0.01	-0.01	0.14	0.15	0.01
2217500	0.87	0.85	0.77	0.86	0.85	0.76
2414500	0.88	0.85	0.80	0.80	0.80	0.73
2165000	0.78	0.77	0.67	0.81	0.81	0.75
2475500	0.88	0.88	0.82	0.77	0.84	0.80
2387500	0.88	0.84	0.82	0.85	0.84	0.80
2339500	0.82	0.70	0.76	0.72	0.73	0.59
2472000	0.88	0.84	0.81	0.75	0.83	0.79
2329000	0.79	0.77	0.70	0.69	0.77	0.67
2482000	0.89	0.85	0.83	0.73	0.74	0.75
2347500	0.86	0.81	0.73	0.89	0.89	0.87
2456500	0.86	0.85	0.82	0.82	0.82	0.82
2479300	0.85	0.83	0.82	0.65	0.54	0.57
2475000	0.83	0.79	0.76	0.77	0.74	0.75
2375500	0.85	0.84	0.78	0.73	0.68	0.69
3438000	0.90	0.91	0.88	0.80	0.82	0.80
3443000	0.87	0.86	0.85	0.87	0.88	0.88
3512000	0.78	0.76	0.75	0.68	0.75	0.68

Catchment	Half-Record Calibration (Second Calibration Method)			Second Validation		
	Proposed Model	abcd Model	Zhang Model	Proposed Model	abcd Model	Zhang Model
3550000	0.88	0.84	0.68	0.79	0.80	0.26
3451500	0.87	0.85	0.82	0.89	0.89	0.86
3504000	0.84	0.85	0.83	0.83	0.86	0.85
3574500	0.84	0.82	0.81	0.83	0.85	0.79
7057500	0.70	0.77	0.74	0.66	0.75	0.69
7052500	0.87	0.89	0.84	0.80	0.86	0.81
7068000	0.79	0.88	0.84	0.65	0.77	0.73
7067000	0.81	0.89	0.84	0.68	0.74	0.71
7056000	0.91	0.92	0.88	0.87	0.88	0.83
7197000	0.24	0.00	0.24	0.20	0.05	0.38
8055500	0.60	0.68	0.77	0.33	0.55	0.33
7186000	0.76	0.80	0.77	0.80	0.86	0.81
7261000	-0.02	-0.14	-0.08	0.02	-0.06	0.01
7196500	0.77	0.74	0.68	0.73	0.70	0.76
7363500	0.84	0.78	0.74	0.78	0.74	0.72
8167500	0.90	0.86	0.80	0.86	0.85	0.69
7346000	0.07	-0.12	0.02	-0.02	-0.12	0.03
8171000	0.82	0.84	0.76	0.83	0.82	0.66
8205500	0.92	0.68	0.41	0.26	-0.01	0.72
8033500	0.68	0.70	0.75	0.64	0.67	0.64
8189500	0.87	0.73	0.80	0.15	0.33	0.30
8032000	0.68	0.77	0.68	0.59	0.65	0.53
8172000	0.90	0.88	0.81	0.81	0.79	0.72
8171300	0.08	0.06	0.11	-0.11	-0.03	-0.07
2478500	0.86	0.82	0.81	0.72	0.69	0.71
2296750	0.62	0.64	0.58	0.71	0.70	0.79
2273000	0.30	0.32	0.27	0.50	0.48	0.41
1372500	0.71	0.73	0.62	0.64	0.63	0.60
1534000	0.64	0.68	0.58	0.62	0.69	0.63
3111500	0.88	0.87	0.84	0.77	0.77	0.76
3331500	0.66	0.73	0.66	0.63	0.77	0.69
3301500	0.88	0.86	0.88	0.86	0.90	0.86
4191500	0.71	0.71	0.71	0.65	0.71	0.62

Catchment	Half-Record Calibration (Second Calibration Method)			Second Validation		
	Proposed Model	abcd Model	Zhang Model	Proposed Model	abcd Model	Zhang Model
5555300	0.34	0.31	0.33	0.14	0.35	0.26
5514500	0.10	0.18	0.17	0.03	0.09	0.07
6441500	0.80	0.62	0.83	0.10	0.33	0.24
6869500	0.70	0.81	0.67	0.68	0.58	0.58
6884400	0.71	0.76	0.79	0.68	0.86	0.72
6897500	0.54	0.73	0.59	0.65	0.87	0.79
7144780	0.36	0.37	0.33	0.31	0.74	0.35
7152000	0.67	0.62	0.61	0.52	0.74	0.55
8085500	0.78	0.79	0.71	-1.71	-2.38	-0.60
7307800	0.72	0.70	0.69	0.30	0.50	0.41

A.3.3 Annual Time Scale

Table 6.9. Calibration and Validation Results at the Annual Time Scale (Second Analysis).

Catchment	Half-Record Calibration (Second Calibration Method)			Second Validation		
	Proposed Model	abcd Model	Zhang Model	Proposed Model	abcd Model	Zhang Model
2102000	0.96	0.93	0.87	0.76	0.72	0.70
2143040	0.29	-1.36	-2.87	-0.04	0.03	-1.91
2143500	-0.34	-1.39	-0.24	0.02	-0.08	-0.24
2126000	0.93	0.94	0.89	0.89	0.83	0.81
2135000	0.87	0.73	0.72	0.63	0.64	0.62
2192000	0.93	0.82	0.78	0.52	0.37	0.68
2387000	0.95	0.94	0.93	0.89	0.84	0.86
2228000	0.71	0.47	0.54	0.55	0.51	0.48
2202500	0.66	0.55	0.56	0.59	0.10	0.02
2143000	0.97	0.85	0.80	0.73	0.79	0.75
2349500	-0.42	-1.45	-0.03	0.24	0.10	-0.05
2217500	0.88	0.80	0.73	0.66	0.56	0.66
2414500	0.90	0.82	0.75	0.65	0.64	-0.35
2165000	0.91	0.86	0.79	0.40	0.70	0.66
2475500	0.72	0.67	0.57	0.79	0.82	0.67
2387500	0.95	0.92	0.90	0.68	0.76	0.67
2339500	0.80	0.71	0.68	0.60	0.18	0.56
2472000	0.55	0.53	0.48	0.78	0.65	0.56
2329000	0.74	0.31	0.42	0.68	0.52	0.68
2482000	0.84	0.79	0.80	0.89	0.72	0.49
2347500	0.84	0.69	0.66	0.73	0.47	0.51
2456500	0.91	0.90	0.87	0.72	0.60	0.74
2479300	0.50	0.56	0.63	0.17	-1.82	-0.68
2475000	0.44	0.46	0.43	0.82	0.79	0.61
2375500	0.39	0.43	0.81	-0.21	-0.63	-0.25
3438000	0.90	0.87	0.95	0.61	0.54	0.12
3443000	0.98	0.97	0.96	0.94	0.82	0.94
3512000	0.92	0.92	0.89	0.61	0.61	0.61

Catchment	Half-Record Calibration (Second Calibration Method)			Second Validation		
	Proposed Model	abcd Model	Zhang Model	Proposed Model	abcd Model	Zhang Model
3550000	0.95	0.95	0.96	0.73	0.83	0.80
3451500	0.98	0.97	0.96	0.84	0.83	0.87
3504000	0.96	0.96	0.96	0.93	0.93	0.89
3574500	0.92	0.86	0.88	-0.58	0.00	0.39
7057500	0.60	0.45	0.82	0.10	-0.54	0.39
7052500	0.94	0.90	0.92	0.77	0.44	0.31
7068000	0.87	0.64	0.86	0.37	0.05	0.63
7067000	0.85	0.65	0.88	0.45	-0.30	0.30
7056000	0.88	0.85	0.89	0.72	0.79	-1.04
7197000	0.91	0.43	0.50	0.34	0.19	0.18
8055500	0.73	0.41	0.37	0.53	-0.06	-1.35
7186000	0.98	0.96	0.97	0.56	0.57	0.64
7261000	0.26	-0.16	-0.44	-0.45	-0.14	-0.17
7196500	0.98	0.96	0.97	0.71	0.60	0.59
7363500	0.92	0.62	0.70	0.41	0.18	0.38
8167500	0.96	0.76	0.67	0.32	0.64	0.28
7346000	0.65	0.07	0.70	-0.32	-0.25	-0.41
8171000	0.96	0.84	0.81	0.67	0.70	0.35
8205500	0.98	0.56	0.55	0.20	0.55	-1.15
8033500	0.93	0.86	0.83	0.26	-1.39	-0.17
8189500	0.76	0.69	0.66	0.29	0.26	0.46
8032000	0.95	0.89	0.91	0.17	0.18	0.46
8172000	0.95	0.84	0.77	0.43	0.57	0.53
8171300	0.77	0.61	0.79	-0.32	-0.24	-0.66
2478500	0.53	0.41	0.37	0.76	0.68	-0.96
2296750	0.79	0.57	0.65	0.59	0.26	0.33
2273000	0.65	0.50	0.56	0.52	0.31	0.32
1372500	0.79	0.86	0.82	0.83	0.71	0.61
1534000	0.92	0.90	0.98	0.91	0.88	0.71
3111500	0.97	0.95	0.95	0.81	0.73	0.79
3331500	0.93	0.87	0.89	0.56	0.66	0.63
3301500	0.89	0.82	0.89	0.81	0.76	0.82
4191500	0.98	0.94	0.98	0.81	0.77	0.68

Catchment	Half-Record Calibration (Second Calibration Method)			Second Validation		
	Proposed Model	abcd Model	Zhang Model	Proposed Model	abcd Model	Zhang Model
5555300	0.71	0.47	0.64	-0.05	0.52	0.06
5514500	0.74	0.57	0.68	0.75	0.71	0.93
6441500	0.97	0.92	0.94	0.16	0.36	-0.38
6869500	0.99	0.43	0.33	0.23	0.87	0.14
6884400	0.98	0.95	0.92	0.86	0.84	0.94
6897500	0.98	0.99	0.93	0.90	0.91	0.85
7144780	0.98	0.81	0.66	0.19	0.19	0.28
7152000	0.98	0.97	0.76	0.65	0.60	0.30
8085500	0.93	0.77	0.79	-4.38	-9.86	-6.30
7307800	0.73	0.72	0.71	0.43	0.62	0.64

**APPENDIX B:
MATLAB CODE FOR CALIBRATION AND VALIDATION**

To calibrate models with Matlab's genetic algorithm function, two types of scripts were required: (1) a script for each model to run the genetic algorithm and to define the fitness function for the genetic algorithm and (2) a master script to set the inputs for each model function and to record values obtained from the genetic algorithm. The following is a list of the tasks that these two scripts perform.

Model Function (Calibration)

- Defines the fitness function (i.e. the model structure), which is a “nested function” (i.e. sub-function)
- Runs the genetic algorithm function, which calls the fitness function
- Sets the upper and lower bounds for the genetic algorithm

Master Script (Calibration)

- Calls model file names and directories
- Sets starting time period, ending time period, and warm-up time period
- Sets general conditions for the genetic algorithm
- Sets the time scale for the model simulations
- Sets the number of times simulations are run for each catchment
- Runs models for each catchment at the specified time scale
- Records the results from the genetic algorithm for each simulation

As discussed earlier, there were two calibration approaches based on how the initial conditions were set: (1) initial conditions were set the same for all catchments and (2) the genetic algorithm calibrated the initial conditions, treating the initial conditions as parameters. The master script for both methods is identical. The model functions are similar in both conditions, except for the expression of the genetic algorithm (2 additional inputs) and the expressions for the initial conditions.

Like model calibration, two scripts are required to obtain the model validation results: (1) a script describing the structure of each model and (2) a master script that runs the first script across the calibration time period to obtain the final soil moisture and groundwater storage conditions that are used as initial conditions for the validation time period. The master script then runs the models across the validation time period and records their results for each catchment. Also, because of the two calibration methodologies, two separate sets of scripts were needed for model validation. The following is a list of the tasks that the two types of scripts perform.

Model Scripts (Validation)

- Defines the model structure
- Receives input data from the master script, including precipitation, potential evapotranspiration, streamflow, parameter values from the calibration stage, and model initial conditions
- Runs model for the specified catchment

Master Script (Validation)

- Calls model file names and directories
- Sets the starting time period, ending time period, and warm-up time period (if applicable)
- Sets the time scale for the model simulations and extracts catchment hydro-climatic data based on the specified time scale
- Extracts parameter values obtained from the calibration stage and provides them to the model scripts as input
- Sets initial conditions directly for the calibration stage (first calibration method) or sets them based on the values obtained from the calibration results (second calibration method)
- Runs the models across the calibration time period and records the final soil moisture and groundwater storage values
- Uses the final conditions obtained from the calibration stage as initial conditions for the model validation

The codes are listed in the following sections in the following order:

1. Master script for calibration
2. Model function for the abcd model (first calibration method)
3. Model function for the abcd model (second calibration method)
4. Master script for validation (first calibration method)
5. Master script for validation (second calibration method)
6. Script for the abcd model (validation based on the first calibration method)
7. Script for the abcd model (validation based on the second calibration method)

B.1 Master Script for Calibration

```
clear all; close all;
%% Input data
[~,mod_name,~]=xlsread('model_info_calib_2600.xlsx','model_names','A1:A100');
[~,mdir,~]=xlsread('model_info_calib_2600.xlsx','model_names','B1:B100');
srow=-1;%-1 is default of 1

%-1 is default of 7670 for daily and 252 for monthly.
%3653 corresponds to 12/31/1992
erow=10;

%use 2 for annual time scale. -1 is default of 24
%(first 24 data records between srow and erow)
nmonths_warm=3;
em_options=gaoptimset('PopulationSize',500,'StallGenLimit',50,'TolFun',0.0001);

%base name of output file
base_name='Final_Models\500pop_20times_calibration';
suffix_name='';

%number of times to repeat the estimation for each watershed (1 = no repetitions)
repetitions=20;

%Define Time Scale:
%daily=1   monthly=2   annual=3
tscale=3;
fitfunc=1;%1=NSE for Q, 2=NSE for Qd+Qb

%% for starting after a halt in the code
model_break=1;%which model the code stopped on
next_ws=1;%next watershed that the code halted on and didn't write

%% ----- DO NOT MODIFY BELOW THIS LINE -----
acknowledge_error=wavread('C:\Windows\Media\Windows Error.wav');
acknowledge_error= acknowledge_error*15; % Increase volume
player = audioplayer(acknowledge_error, 44100);

[n_model ~]=size(mod_name);
ws_id=load('MOPEX_list.txt');

if tscale==1
    disp('Running simulations at the daily time scale.')
elseif tscale==2
    disp('Running simulations at the monthly time scale.')
```

```

elseif tscale==3
    disp('Running simulations at the annual time scale.')
else
    disp('Incorrect value for time scale. Select either daily (1) monthly (2)
or annual (3).')
    disp('Terminating process...')
    return
end

%for i_model=1:n_model
for i_model=1:1
    cd(mdir{i_model})
    disp(['Beginning simulations for ' mod_name{i_model} ' ('
num2str(i_model) '/' num2str(n_model) ').'])
    [file_length ~]=size(ws_id);

    if i_model<model_break%fix break. set this to zero otherwise
        cd('..\')
        continue
    end

    toc2=0;
    %for ii=1:file_length
    for ii=72:-1:1
        if i_model==model_break && ii<next_ws%27 is the next round that is
missing
            continue
        end
        tic
        func_name=str2func(mod_name{i_model});

        fval_opt=100;
        para_opt=[];
        for iii=1:repetitions
            % begin cycle
            toc3=toc;
            [para fval]
=func_name(ws_id(ii),tscale,srow,erow,nmonths_warm,em_options,fitfunc);
            disp(['Cycle ' num2str(iii) '/' num2str(repetitions) ' complete.
Cycle took ' num2str(floor((toc-toc3)/60)) ' minutes and ' num2str(((toc-
toc3)/60-floor((toc-toc3)/60))*60) ' seconds.' ])
            if fval<fval_opt
                para_opt=para;
                fval_opt=fval;
                disp([' Optimal fitness updated: ' num2str(fval)])
                disp([' Optimal parameter set updated: ' num2str(para)])
            else
                disp(' Current iteration did not yield improved parameter
set.')
```

```

        if toc-toc3>120
            disp('      MEMORY FRAGMENTED!')
            disp('      RUN "PACK"...')
            for iii=1:3
                pause(1)
                commandwindow
                play(player);
            end
            return
            %keyboard
            %disp('      RESUMING EXECUTION...')
        end
    %end cycle
end

    tabname=strrep(mod_name{i_model}, '_speed', '');
    if tscale==1
        xlswrite(['..\ ' base_name '_Daily' suffix_name '.xlsx'],[fval_opt
ws_id(ii) para_opt],tabname,['A' num2str(ii)])
    elseif tscale==2
        xlswrite(['..\ ' base_name '_Monthly' suffix_name
'.xlsx'],[fval_opt ws_id(ii) para_opt],tabname,['A' num2str(ii)])
    elseif tscale==3
        xlswrite(['..\ ' base_name '_Annual' suffix_name
'.xlsx'],[fval_opt ws_id(ii) para_opt],tabname,['A' num2str(ii)])
    else
        disp('Incorrect time scale specified.')
    end

    disp(['Watershed ' num2str(ii) '/' num2str(file_length) ' processed
of Model ' num2str(i_model) '/' num2str(n_model) '.'])
    toc2=toc2+toc;
    disp(['Total elapsed time is ' num2str(floor(toc2/60)) ' minutes and
' num2str((toc2/60-floor(toc2/60))*60) ' seconds.'])
    end
    disp(['Simulations for ' mod_name{i_model} ' complete.'])
    cd('..\')

end

```

B.2 Model Function for the abcd Model (First Calibration Method)

```
function [para fval]
=abcd_constant_initial_conditions(ws_id,timescale,srow,erow,nmonths_warm,em_
ptions,fitfunc)
rs=1;
if timescale==1%daily
    nrows=7670;
    fdir=['..\..\Data\Daily\bin_speed2\' num2str(ws_id) '.bin'];
elseif timescale==2%monthly
    nrows=252;
    fdir=['..\..\Data\Monthly\bin_speed2\' num2str(ws_id) '.bin'];
elseif timescale==3%annual
    nrows=21;
    fdir=['..\..\Data\Annual\bin_speed2\' num2str(ws_id) '.bin'];
end

if srow==-1%if set to default
    srow=1;
end

if erow==-1%if set to default
    erow=nrows;
end

if nmonths_warm==-1%if set to default
    nmonths_warm=24;
end

if fitfunc==1
    [para fval] = ga(@internal_func,4,[],[],[],[],[0 1 0 0],[1 1500 1
1],[],em_options);
elseif fitfunc==2
    [para fval] = ga(@internal_func2,4,[],[],[],[],[0 1 0 0],[1 1500 1
1],[],em_options);
end

function fitness=internal_func(x)

persistent nrow nmonth_warm Qavg P Ep Qo

if rs==1
    rs=0;
    nfile = fopen(fdir);
    ndata=fread(nfile,[5 nrows], 'float32');
    nmonth_warm=nmonths_warm;
    nrow=erow-srow+1;%this prevents nrows from being called more than
once
    P=ndata(1,srow:erow)';
```



```

        Ep=ndata(2,srow:erow)';
        Qo=ndata(3,srow:erow)';
        Qavg=mean(Qo((nmonth_warm+1):nrow));
        fclose('all');
        clear nfile ndata
    end
MSE_Q=0; var_obs_Q=0;

#####INSERT PARAMETERS AND INITIAL CONDITIONS
%--parameters
a=x(1);
b=x(2);
c=x(3);
d=x(4);

%--initial storage
S_1=b;
G_1=0;

#####INSERT PARAMETERS AND INITIAL CONDITIONS END

for irow=1:nrow
    #####INSERT CODE#####
    %cycle begins

    W=P(irow)+S_1;
    yy=(W+b)/(2*a)-(((W+b)/(2*a))^2-(W*b)/a)^0.5;
    E=yy*(1-exp(-Ep(irow)/b));
    S=yy-E;

    Qd=(1-c)*(W-yy);
    R=c*(W-yy);
    G=(1/(1+d))*(R+G_1);
    Qb=d*G;

    Q=Qb+Qd;

    G_1=G;
    S_1=S;

    %For some reason this code actually is slower to run (it's not
    %that it runs too fast that the process defragments Matlab's
    %memory.

    #####INSERT CODE END#####

%----Compute fitness
%---the first 24 data records are used for warm-up

```

```

        if irow>nmonth_warm
            MSE_Q=MSE_Q+(Qo(irow)-Q)^2;
            var_obs_Q=var_obs_Q+(Qo(irow)-Qavg)^2;
        end

    end

    fitness=MSE_Q/var_obs_Q;
end

function fitness=internal_func2(x)
    %---This function is a placeholder but allows multiple performance
    %evaluation methods to be used on the same model
    %---The code should be identical to "internal_func" except for the
code in
    %the "Compute Fitness" section
end

disp('Done!')
fclose('all');
end

```

B.3 Model Function for the abcd Model (Second Calibration Method)

```
function [para fval]
=abcd_calibrated_initial_conditions(ws_id,timescale,srow,erow,nmonths_warm,em
_options,fitfunc)
rs=1;
if timescale==1%daily
    nrows=7670;
    fdir=['..\..\Data\Daily\bin_speed2\' num2str(ws_id) '.bin'];
elseif timescale==2%monthly
    nrows=252;
    fdir=['..\..\Data\Monthly\bin_speed2\' num2str(ws_id) '.bin'];
elseif timescale==3%annual
    nrows=21;
    fdir=['..\..\Data\Annual\bin_speed2\' num2str(ws_id) '.bin'];
end

if srow==-1%if set to default
    srow=1;
end

if erow==-1%if set to default
    erow=nrows;
end

if nmonths_warm==-1%if set to default
    nmonths_warm=24;
end

if fitfunc==1
    [para fval] = ga(@internal_func,6,[],[],[],[],[0 1 0 0 0 0],[1 1500 1 1 1
50],[],em_options);
elseif fitfunc==2
    [para fval] = ga(@internal_func2,6,[],[],[],[],[0 1 0 0 0 0],[1 1500 1 1
1 50],[],em_options);
end

function fitness=internal_func(x)

persistent nrow nmonth_warm Qavg P Ep Qo

if rs==1
    rs=0;
    nfile = fopen(fdir);
    ndata=fread(nfile,[5 nrows], 'float32');
    nmonth_warm=nmonths_warm;
    nrow=erow-srow+1;%this prevents nrows from being called more than
once

    P=ndata(1,srow:erow)';
```

```

        Ep=ndata(2,srow:erow)';
        Qo=ndata(3,srow:erow)';
        Qavg=mean(Qo((nmonth_warm+1):nrow));
        fclose('all');
        clear nfile ndata
    end
    MSE_Q=0; var_obs_Q=0;

    #####INSERT PARAMETERS AND INITIAL CONDITIONS
    %--parameters
    a=x(1);
    b=x(2);
    c=x(3);
    d=x(4);
    S0=x(5);

    %--initial storage
    S_1=b*S0;
    G_1=x(6);

    #####INSERT PARAMETERS AND INITIAL CONDITIONS END

    for irow=1:nrow
        #####INSERT CODE#####
        %cycle begins

        W=P(irow)+S_1;
        yy=(W+b)/(2*a)-(((W+b)/(2*a))^2-(W*b)/a)^0.5;
        E=yy*(1-exp(-Ep(irow)/b));
        S=yy-E;

        Qd=(1-c)*(W-yy);
        R=c*(W-yy);
        G=(1/(1+d))*(R+G_1);
        Qb=d*G;

        Q=Qb+Qd;

        G_1=G;
        S_1=S;

        #####INSERT CODE END#####

        %----Compute fitness
        %---the first 24 data records are used for warm-up

        if irow>nmonth_warm
            MSE_Q=MSE_Q+(Qo(irow)-Q)^2;

```

```

        var_obs_Q=var_obs_Q+(Qo(irow)-Qavg)^2;
    end

end

fitness=MSE_Q/var_obs_Q;
end

function fitness=internal_func2(x)
    %---This function is a placeholder but allows multiple performance
    %evaluation methods to be used on the same model
    %---The code should be identical to "internal_func" except for the
code in
    %the "Compute Fitness" section
end

disp('Done!')
fclose('all');
end

```

B.4 Master Script for Validation (First Calibration Method)

```
clear all; close all;
%% Input data

srow_pc=-1;
erow_pc=10;
nmonth_warm_pc=3;%use 2 for annual time scale. -1 is default of 24 (first 24
data records between srow and erow)

srow_v=11;%-1 is default of 1
erow_v=-1;%-1 is default of 7670 for daily and 252 for monthly. 3653
corresponds to 12/31/1992
nmonth_warm_v=0;

time_scale=3;

base_name='Final_Models\validation\validation_500pop_20times';%base name of
output file
suffix_name='';

%% for starting after a halt in the code
model_break=1;%which model the code stopped on
next_ws=1;%next watershed that the code halted on and didn't write

%% Load watershed names

[~,mod_name,~]=xlsread('model_info_validation.xlsx','model_names','A1:A100');
[~,mdir,~]=xlsread('model_info_validation.xlsx','model_names','B1:B100');

%% Re-adjust default parameters

if srow_v==-1%if set to default
    srow_v=1;
end

if nmonth_warm_v==-1%if set to default
    nmonth_warm_v=24;
end

if srow_pc==-1%if set to default
    srow_pc=1;
end

if nmonth_warm_pc==-1%if set to default
    nmonth_warm_pc=24;
end
```

```

%% ----- DO NOT MODIFY BELOW THIS LINE -----

[n_model ~]=size(mod_name);
%ws_id=load('MOPEX_list.txt');

if time_scale==1
    disp('Running simulations at the daily time scale.')
elseif time_scale==2
    disp('Running simulations at the monthly time scale.')
elseif time_scale==3
    disp('Running simulations at the annual time scale.')
else
    disp('Incorrect value for time scale. Select either daily (1) monthly (2)
or annual (3).')
    disp('Terminating process...')
    return
end

%% Run the models

for i_model=1:n_model
    if i_model<model_break%fix break. set this to zero otherwise
        continue
    end

    cd(mdir{i_model})

    if time_scale==1
        para_list=xlsread(['..\ ' calibration_500pop_20times_Daily'
'.xlsx'],strrep(mod_name{i_model}, '_validation', '_1500'),'A1:I72');
    elseif time_scale==2
        para_list=xlsread(['..\ ' calibration_500pop_20times_Monthly'
'.xlsx'],strrep(mod_name{i_model}, '_validation', '_1500'),'A1:I72');
    elseif time_scale==3
        para_list=xlsread(['..\ ' 500pop_20times_calibration_Annual'
'.xlsx'],strrep(mod_name{i_model}, '_validation', '_2600'),'A1:I72');
    else
        disp('ERROR!!!!')
    end

    disp(['Beginning simulations for ' mod_name{i_model} ' ('
num2str(i_model) '/' num2str(n_model) ').'])
    [file_length ~]=size(para_list(:,2));

```

```

toc2=0;
for ii=1:file_length

    if i_model==model_break && ii<next_ws%27 is the next round that is
missing
        continue
    end

    tic
    x=para_list(ii,3:end);
    ws_id=para_list(ii,2);

    %% Prepare Post Calibration
    erow=erow_pc;srow=srow_pc;nmonth_warm=nmonth_warm_pc;
    %func_name=str2func(mod_name{i_model});

    %% Post Calibration Begin

    if time_scale==1
        %-----year    month    day    P    Ep    Q    Qd    Qb    E
        %          1        2        3    4    5    6    7    8    9
        ndata= load(['..\..\..\Data\Daily\MOPEX_final2\' num2str(ws_id)
'.txt'],'-ascii');
        [nrows ~]=size(ndata);%to determine default condition (file
length)
        if erow==-1%if set to default
            erow=nrows;
        end
        clear nrows
        ndata=ndata(srow:erow,:);
        P=ndata(:,4);
        Ep=ndata(:,5);
        Qo=ndata(:,6);
        Qdo=ndata(:,7);
        Qbo=ndata(:,8);
        Eo=ndata(:,9);
        clear ndata
    elseif time_scale==2
        %Year    Month    P    Ep    Q    E    NDVI    dS    AI    Qt    Qd
        % 1        2        3    4    5    6    7    8    9    10    11
        % 12
        ndata= load(['..\..\..\Data\Monthly\MOPEX\' num2str(ws_id)
'.txt'],'-ascii');
        [nrows ~]=size(ndata);
        if erow==-1%if set to default
            erow=nrows;
        end
        clear nrows
        ndata=ndata(srow:erow,:);

```



```

P=ndata(:,3);
Ep=ndata(:,4);
Qo=ndata(:,5);
Qdo=ndata(:,11);
Qbo=ndata(:,12);
Eo=ndata(:,6);
clear ndata

elseif time_scale==3
    %Year  Month  P  Ep  Q  E  NDVI  dS  AI  Qt  Qd
Qb
12
    % 1 2 3 4 5 6 7 8 9 10 11

    ndata= load(['..\..\..\Data\Annual\MOPEX\' num2str(ws_id)
'.txt'],'-ascii');
    [nrows ~]=size(ndata);
    if erow==~-1%if set to default
        erow=nrows;
    end
    clear nrows
    ndata=ndata(srow:erow,:);
    P=ndata(:,2);
    Ep=ndata(:,3);
    Qo=ndata(:,4);
    Qdo=ndata(:,5);
    Qbo=ndata(:,6);
    Eo=ndata(:,7);
    clear ndata

else
    disp('annual data is not yet set up!');
end
[nrow ~]=size(P);

%----- Run specific model

if strcmp(mod_name{i_model},'Zhang_validation')
    S_1=x(1);G_1=0;%x(1)=S_max
    [NSE_Q NSE_Qd NSE_Qb NSE_E S_1
G_1]=Zhang_validation(x,P,Ep,Qo,Qdo,Qbo,Eo,nmonth_warm,nrow,S_1,G_1);
elseif strcmp(mod_name{i_model},'abcd_validation')
    S_1=x(2);G_1=0;%x(2)=b
    [NSE_Q NSE_Qd NSE_Qb NSE_E S_1
G_1]=abcd_validation(x,P,Ep,Qo,Qdo,Qbo,Eo,nmonth_warm,nrow,S_1,G_1);
elseif strcmp(mod_name{i_model},'M0_c1_beta_7para_validation')
    S1=x(2)*x(1);S2=(1-x(2))*x(1);G_1=0;N_1=0;%S1_max=x(2)*x(1) and
S2_max=(1-x(2))*x(1)
    [NSE_Q NSE_Qd NSE_Qb NSE_E S1 S2 G_1
N_1]=M0_c1_beta_7para_validation(x,P,Ep,Qo,Qdo,Qbo,Eo,nmonth_warm,nrow,S1,S2,
G_1,N_1);

```

```

elseif strcmp(mod_name{i_model}, 'M0_c1_beta_validation')
    S1=x(2)*x(1);S2=(1-x(2))*x(1);G_1=0;
    [NSE_Q NSE_Qd NSE_Qb NSE_E S1 S2
G_1]=M0_c1_beta_validation(x,P,Ep,Qo,Qdo,Qbo,Eo,nmonth_warm,nrow,S1,S2,G_1);
elseif strcmp(mod_name{i_model}, 'M1_c1_beta_validation')
    S1=x(2)*x(1);S2=(1-x(2))*x(1);G_1=0;
    [NSE_Q NSE_Qd NSE_Qb NSE_E S1 S2
G_1]=M1_c1_beta_validation(x,P,Ep,Qo,Qdo,Qbo,Eo,nmonth_warm,nrow,S1,S2,G_1);
elseif strcmp(mod_name{i_model}, 'Schaake_validation')
    Du_1=0;Db_1=0;%this means the soil layer is saturated (no
deficit)
    [NSE_Q NSE_Qd NSE_Qb NSE_E Du_1
Db_1]=Schaake_validation(x,P,Ep,Qo,Qdo,Qbo,Eo,nmonth_warm,nrow,Du_1,Db_1);
elseif strcmp(mod_name{i_model}, 'T_model_validation')
    S_1=x(1);G_1=0;%x(1)=phi
    [NSE_Q S_1
G_1]=T_model_validation(x,P,Ep,Qo,Qdo,Qbo,Eo,nmonth_warm,nrow,S_1,G_1);
else
    disp('Error!!!! 189')
end

%% Prepare Validation
disp(['NSE_Q (Post-Calibration)= ' num2str(NSE_Q) ' (watershed '
num2str(ii) ')'])
disp('Post Calibration Complete. Preparing for Validation')
erow=erow_v;srow=srow_v;nmonth_warm=nmonth_warm_v;

%% Validation Begin

if time_scale==1
    %-----year    month    day    P    Ep    Q    Qd    Qb    E
    %             1        2        3    4    5    6    7    8    9
    ndata= load(['..\..\..\Data\Daily\MOPEX_final2\' num2str(ws_id)
'.txt'],'-ascii');
    [nrows ~]=size(ndata);%to determine default condition (file
length)
    if erow==-1%if set to default
        erow=nrows;
    end
    clear nrow
    ndata=ndata(srow:erow,:);
    P=ndata(:,4);
    Ep=ndata(:,5);
    Qo=ndata(:,6);
    Qdo=ndata(:,7);
    Qbo=ndata(:,8);
    Eo=ndata(:,9);
    clear ndata
elseif time_scale==2
    %Year    Month    P    Ep    Q    E    NDVI    dS    AI    Qt    Qd
Qb

```

```

12          % 1      2      3      4      5      6      7      8      9     10     11
nadata= load(['..\..\..\Data\Monthly\MOPEX\' num2str(ws_id)
'.txt'],'-ascii');
[nrows ~]=size(nadata);
if erow==-1%if set to default
    erow=nrows;
end
clear nrows
nadata=nadata(srow:erow,:);
P=nadata(:,3);
Ep=nadata(:,4);
Qo=nadata(:,5);
Qdo=nadata(:,11);
Qbo=nadata(:,12);
Eo=nadata(:,6);
clear nadata

elseif time_scale==3
    %Year  Month  P    Ep    Q    E    NDVI  dS  AI  Qt  Qd
Qb
12          % 1      2      3      4      5      6      7      8      9     10     11
nadata= load(['..\..\..\Data\Annual\MOPEX\' num2str(ws_id)
'.txt'],'-ascii');
[nrows ~]=size(nadata);
if erow==-1%if set to default
    erow=nrows;
end
clear nrows
nadata=nadata(srow:erow,:);
P=nadata(:,2);
Ep=nadata(:,3);
Qo=nadata(:,4);
Qdo=nadata(:,5);
Qbo=nadata(:,6);
Eo=nadata(:,7);
clear nadata

else
    disp('annual data is not yet set up!');
end
[nrow ~]=size(P);

%----- Run specific model

%we have already calculated the initial storage values from the
%post calibration stage. we will use those values as input for the
%calibration stage

```

```

        if strcmp(mod_name{i_model},'Zhang_validation')
            [NSE_Q NSE_Qd NSE_Qb NSE_E S_1
G_1]=Zhang_validation(x,P,Ep,Qo,Qdo,Qbo,Eo,nmonth_warm,nrow,S_1,G_1);
        elseif strcmp(mod_name{i_model},'abcd_validation')
            [NSE_Q NSE_Qd NSE_Qb NSE_E S_1
G_1]=abcd_validation(x,P,Ep,Qo,Qdo,Qbo,Eo,nmonth_warm,nrow,S_1,G_1);
        elseif strcmp(mod_name{i_model},'M0_c1_beta_7para_validation')
            [NSE_Q NSE_Qd NSE_Qb NSE_E S1 S2 G_1
N_1]=M0_c1_beta_7para_validation(x,P,Ep,Qo,Qdo,Qbo,Eo,nmonth_warm,nrow,S1,S2,
G_1,N_1);
        elseif strcmp(mod_name{i_model},'M0_c1_beta_validation')
            [NSE_Q NSE_Qd NSE_Qb NSE_E S1 S2
G_1]=M0_c1_beta_validation(x,P,Ep,Qo,Qdo,Qbo,Eo,nmonth_warm,nrow,S1,S2,G_1);
        elseif strcmp(mod_name{i_model},'M1_c1_beta_validation')
            [NSE_Q NSE_Qd NSE_Qb NSE_E S1 S2
G_1]=M1_c1_beta_validation(x,P,Ep,Qo,Qdo,Qbo,Eo,nmonth_warm,nrow,S1,S2,G_1);
        elseif strcmp(mod_name{i_model},'Schaake_validation')
            [NSE_Q NSE_Qd NSE_Qb NSE_E Du_1
Db_1]=Schaake_validation(x,P,Ep,Qo,Qdo,Qbo,Eo,nmonth_warm,nrow,Du_1,Db_1);
        elseif strcmp(mod_name{i_model},'T_model_validation')
            [NSE_Q S_1
G_1]=T_model_validation(x,P,Ep,Qo,Qdo,Qbo,Eo,nmonth_warm,nrow,S_1,G_1);
        else
            disp('Error!!!! 278')
        end

        %----- Write the results to a file
        tabname=strrep(mod_name{i_model}, '_speed', '');

        tabname=strrep(tabname, '_validation', '');

        if time_scale==1
            xlswrite(['..\..\\" base_name '_Daily' suffix_name
'.xlsx'],NSE_Q,tabname,['A' num2str(ii)])
        elseif time_scale==2
            xlswrite(['..\..\\" base_name '_Monthly' suffix_name
'.xlsx'],NSE_Q,tabname,['A' num2str(ii)])
        elseif time_scale==3
            xlswrite(['..\..\\" base_name '_Annual' suffix_name
'.xlsx'],NSE_Q,tabname,['A' num2str(ii)])
        else
            disp('Incorrect time scale specified.')
        end

        %% Validation End

        disp(['Watershed ' num2str(ii) '/' num2str(file_length) ' processed
of Model ' num2str(i_model) '/' num2str(n_model) '.'])
        toc2=toc2+toc;

```

```
        disp(['Total elapsed time is ' num2str(floor(toc2/60)) ' minutes and  
' num2str((toc2/60-floor(toc2/60))*60) ' seconds.'])  
  
    end  
    disp(['Simulations for ' mod_name{i_model} ' complete.'])  
    cd('..\..\')
```

end

B.5 Master Script for Validation (Second Calibration Method)

```
clear all; close all;

%% Input data

srow_pc=-1;
erow_pc=10;

%use 2 for annual time scale. -1 is default of 24 (first 24 data records
%between srow and erow)
nmonth_warm_pc=3;

srow_v=11;%-1 is default of 1

%-1 is default of 7670 for daily and 252 for monthly.
%3653 corresponds to 12/31/1992
erow_v=-1;
nmonth_warm_v=0;

time_scale=3;

%base name of output file
base_name='Final_Models\validation\validation_500pop_20times';
suffix_name='';

%% for starting after a halt in the code
model_break=1;%which model the code stopped on
next_ws=1;%next watershed that the code halted on and didn't write

%% Load watershed names

[~,mod_name,~]=xlsread('model_info_validation.xlsx','model_names','A1:A100');
[~,mdir,~]=xlsread('model_info_validation.xlsx','model_names','B1:B100');

%% Re-adjust default parameters

if srow_v==-1%if set to default
    srow_v=1;
end

if nmonth_warm_v==-1%if set to default
    nmonth_warm_v=24;
end

if srow_pc==-1%if set to default
    srow_pc=1;
```

```

end

if nmonth_warm_pc==-1%if set to default
    nmonth_warm_pc=24;
end

%% ----- DO NOT MODIFY BELOW THIS LINE -----

[n_model ~]=size(mod_name);
%ws_id=load('MOPEX_list.txt');

if time_scale==1
    disp('Running simulations at the daily time scale.')
elseif time_scale==2
    disp('Running simulations at the monthly time scale.')
elseif time_scale==3
    disp('Running simulations at the annual time scale.')
else
    disp('Incorrect value for time scale. Select either daily (1) monthly (2)
or annual (3).')
    disp('Terminating process...')
    return
end

%% Run the models

for i_model=1:n_model
    if i_model<model_break%fix break. set this to zero otherwise
        continue
    end

    cd(mdir{i_model})

    if time_scale==1
        para_list=xlsread(['..\ '2nd_calibration_500pop_20times_Daily'
'.xlsx'],strrep(mod_name{i_model}, '_validation', '_1500'),'A1:M72');
    elseif time_scale==2
        para_list=xlsread(['..\ '2nd_calibration_500pop_20times_Monthly'
'.xlsx'],strrep(mod_name{i_model}, '_validation', '_1500'),'A1:M72');
    elseif time_scale==3
        para_list=xlsread(['..\ '2nd_calibration_500pop_20times_Annual'
'.xlsx'],strrep(mod_name{i_model}, '_validation', '_2600'),'A1:M72');
    else
        disp('ERROR!!!!')
    end
end

```

```

disp(['Beginning simulations for ' mod_name{i_model} ' ('
num2str(i_model) '/' num2str(n_model) ').'])
[file_length ~]=size(para_list(:,2));

toc2=0;
for ii=1:file_length

    if i_model==model_break && ii<next_ws%27 is the next round that is
missing
        continue
    end

    tic
    x=para_list(ii,3:end);
    ws_id=para_list(ii,2);

    %% Prepare Post Calibration
    erow=erow_pc;srow=srow_pc;nmonth_warm=nmonth_warm_pc;
    %func_name=str2func(mod_name{i_model});

    %% Post Calibration Begin

    if time_scale==1
        %-----year    month    day    P    Ep    Q    Qd    Qb    E
        %           1        2        3    4    5    6    7    8    9
        ndata= load(['..\..\..\Data\Daily\MOPEX_final2\' num2str(ws_id)
'.txt'],'-ascii');
        [nrows ~]=size(ndata);%to determine default condition (file
length)
        if erow==-1%if set to default
            erow=nrows;
        end
        clear nrows
        ndata=ndata(srow:erow,:);
        P=ndata(:,4);
        Ep=ndata(:,5);
        Qo=ndata(:,6);
        Qdo=ndata(:,7);
        Qbo=ndata(:,8);
        Eo=ndata(:,9);
        clear ndata
    elseif time_scale==2
        %Year    Month    P    Ep    Q    E    NDVI    dS    AI    Qt    Qd
        % 1        2        3    4    5    6        7        8        9    10    11
        % 12
        ndata= load(['..\..\..\Data\Monthly\MOPEX\' num2str(ws_id)
'.txt'],'-ascii');

```



```

        [nrows ~]=size(ndata);
        if erow==-1%if set to default
            erow=nrows;
        end
        clear nrow
        ndata=ndata(srow:erow,:);
        P=ndata(:,3);
        Ep=ndata(:,4);
        Qo=ndata(:,5);
        Qdo=ndata(:,11);
        Qbo=ndata(:,12);
        Eo=ndata(:,6);
        clear ndata

    elseif time_scale==3
        %Year  Month  P    Ep    Q    E    NDVI  dS  AI  Qt  Qd
Qb
        %  1      2      3      4      5      6      7      8      9      10     11
12
        ndata= load(['..\..\..\Data\Annual\MOPEX\' num2str(ws_id)
'.txt'],'-ascii');
        [nrows ~]=size(ndata);
        if erow==-1%if set to default
            erow=nrows;
        end
        clear nrow
        ndata=ndata(srow:erow,:);
        P=ndata(:,2);
        Ep=ndata(:,3);
        Qo=ndata(:,4);
        Qdo=ndata(:,5);
        Qbo=ndata(:,6);
        Eo=ndata(:,7);
        clear ndata

    else
        disp('annual data is not yet set up!');
    end
    [nrow ~]=size(P);

    %----- Run specific model

    if strcmp(mod_name{i_model},'Zhang_validation')
        S_1=x(5)*x(1);G_1=x(6);%x(1)=S_max
        [NSE_Q NSE_Qd NSE_Qb NSE_E S_1
G_1]=Zhang_validation(x,P,Ep,Qo,Qdo,Qbo,Eo,nmonth_warm,nrow,S_1,G_1);
    elseif strcmp(mod_name{i_model},'abcd_validation')
        S_1=x(2)*x(5);G_1=x(6);%x(2)=b
        [NSE_Q NSE_Qd NSE_Qb NSE_E S_1
G_1]=abcd_validation(x,P,Ep,Qo,Qdo,Qbo,Eo,nmonth_warm,nrow,S_1,G_1);

```

```

elseif strcmp(mod_name{i_model},'M0_c1_beta_7para_validation')
    S1=x(8)*x(2)*x(1);S2=x(9)*(1-x(2))*x(1);G_1=x(10);N_1=x(11);
    [NSE_Q NSE_Qd NSE_Qb NSE_E S1 S2 G_1
N_1]=M0_c1_beta_7para_validation(x,P,Ep,Qo,Qdo,Qbo,Eo,nmonth_warm,nrow,S1,S2,
G_1,N_1);
elseif strcmp(mod_name{i_model},'M0_c1_beta_validation')
    S1=x(7)*x(2)*x(1);S2=x(8)*(1-x(2))*x(1);G_1=x(9);
    [NSE_Q NSE_Qd NSE_Qb NSE_E S1 S2
G_1]=M0_c1_beta_validation(x,P,Ep,Qo,Qdo,Qbo,Eo,nmonth_warm,nrow,S1,S2,G_1);
    %disp(['S1_calibration=' num2str(S1) ' S2_calibration='
num2str(S2) ' G_calibration=' num2str(G_1)])
elseif strcmp(mod_name{i_model},'M1_c1_beta_validation')
    S1=x(7)*x(2)*x(1);S2=x(8)*(1-x(2))*x(1);G_1=x(9);
    [NSE_Q NSE_Qd NSE_Qb NSE_E S1 S2
G_1]=M1_c1_beta_validation(x,P,Ep,Qo,Qdo,Qbo,Eo,nmonth_warm,nrow,S1,S2,G_1);
else
    disp('Error!!!! 189')
end

%% Prepare Validation
NSE_Q1=NSE_Q;
disp(['NSE_Q (Post-Calibration)= ' num2str(NSE_Q1) ' (watershed '
num2str(ii) ')'])
disp('Post Calibration Complete. Preparing for Validation')
erow=erow_v;srow=srow_v;nmonth_warm=nmonth_warm_v;

%% Validation Begin

if time_scale==1
    %-----year    month    day    P    Ep    Q    Qd    Qb    E
    %          1        2        3    4    5    6    7    8    9
    ndata= load(['..\..\..\Data\Daily\MOPEX_final2\' num2str(ws_id)
'.txt'],'-ascii');
    [nrows ~]=size(ndata);%to determine default condition (file
length)
    if erow==-1%if set to default
        erow=nrows;
    end
    clear nrow
    ndata=ndata(srow:erow,:);
    P=ndata(:,4);
    Ep=ndata(:,5);
    Qo=ndata(:,6);
    Qdo=ndata(:,7);
    Qbo=ndata(:,8);
    Eo=ndata(:,9);
    clear ndata
elseif time_scale==2
    %Year    Month    P    Ep    Q    E    NDVI    dS    AI    Qt    Qd
    Qb

```

```

12          % 1      2      3      4      5      6      7      8      9     10     11
nadata= load(['..\..\..\Data\Monthly\MOPEX\' num2str(ws_id)
'.txt'],'-ascii');
[nrows ~]=size(nadata);
if erow==-1%if set to default
    erow=nrows;
end
clear nrows
nadata=nadata(srow:erow,:);
P=nadata(:,3);
Ep=nadata(:,4);
Qo=nadata(:,5);
Qdo=nadata(:,11);
Qbo=nadata(:,12);
Eo=nadata(:,6);
clear nadata

elseif time_scale==3
    %Year  Month  P    Ep    Q    E    NDVI  dS  AI  Qt  Qd
Qb
12          % 1      2      3      4      5      6      7      8      9     10     11
nadata= load(['..\..\..\Data\Annual\MOPEX\' num2str(ws_id)
'.txt'],'-ascii');
[nrows ~]=size(nadata);
if erow==-1%if set to default
    erow=nrows;
end
clear nrows
nadata=nadata(srow:erow,:);
P=nadata(:,2);
Ep=nadata(:,3);
Qo=nadata(:,4);
Qdo=nadata(:,5);
Qbo=nadata(:,6);
Eo=nadata(:,7);
clear nadata

else
    disp('annual data is not yet set up!');
end
[nrow ~]=size(P);

%----- Run specific model

%we have already calculated the initial storage values from the
%post calibration stage. we will use those values as input for the
%calibration stage

```

```

        if strcmp(mod_name{i_model},'Zhang_validation')
            [NSE_Q NSE_Qd NSE_Qb NSE_E S_1
G_1]=Zhang_validation(x,P,Ep,Qo,Qdo,Qbo,Eo,nmonth_warm,nrow,S_1,G_1);
            elseif strcmp(mod_name{i_model},'abcd_validation')
                [NSE_Q NSE_Qd NSE_Qb NSE_E S_1
G_1]=abcd_validation(x,P,Ep,Qo,Qdo,Qbo,Eo,nmonth_warm,nrow,S_1,G_1);
            elseif strcmp(mod_name{i_model},'M0_c1_beta_7para_validation')
                [NSE_Q NSE_Qd NSE_Qb NSE_E S1 S2 G_1
N_1]=M0_c1_beta_7para_validation(x,P,Ep,Qo,Qdo,Qbo,Eo,nmonth_warm,nrow,S1,S2,
G_1,N_1);
            elseif strcmp(mod_name{i_model},'M0_c1_beta_validation')
                %disp(['S1_validation=' num2str(S1) ' S2_validation='
num2str(S2) ' G_validation=' num2str(G_1)])
                [NSE_Q NSE_Qd NSE_Qb NSE_E S1 S2
G_1]=M0_c1_beta_validation(x,P,Ep,Qo,Qdo,Qbo,Eo,nmonth_warm,nrow,S1,S2,G_1);
            elseif strcmp(mod_name{i_model},'M1_c1_beta_validation')
                [NSE_Q NSE_Qd NSE_Qb NSE_E S1 S2
G_1]=M1_c1_beta_validation(x,P,Ep,Qo,Qdo,Qbo,Eo,nmonth_warm,nrow,S1,S2,G_1);
            else
                disp('Error!!!! 189')
            end

%----- Write the results to a file
tabname=strrep(mod_name{i_model}, '_speed', '');

tabname=strrep(tabname, '_validation', '');

if time_scale==1
    xlswrite(['..\..\\" base_name '_Daily' suffix_name '.xlsx'],[NSE_Q
NSE_Q1],tabname,['A' num2str(ii)])
elseif time_scale==2
    xlswrite(['..\..\\" base_name '_Monthly' suffix_name
'.xlsx'],[NSE_Q NSE_Q1],tabname,['A' num2str(ii)])
elseif time_scale==3
    xlswrite(['..\..\\" base_name '_Annual' suffix_name
'.xlsx'],[NSE_Q NSE_Q1],tabname,['A' num2str(ii)])
else
    disp('Incorrect time scale specified.')
end

%% Validation End

disp(['Watershed ' num2str(ii) '/' num2str(file_length) ' processed
of Model ' num2str(i_model) '/' num2str(n_model) '.'])
toc2=toc2+toc;
disp(['Total elapsed time is ' num2str(floor(toc2/60)) ' minutes and
' num2str((toc2/60-floor(toc2/60))*60) ' seconds.'])

end

```

```
disp(['Simulations for ' mod_name{i_model} ' complete.'])
cd('..\..\')
end
```

B.6 Script for the abcd Model (Validation based on the First Calibration Method)

```
function [NSE_Q NSE_Qd NSE_Qb NSE_E S_1
G_1]=abcd_validation_constant_initial_conditions(x,P,Ep,Qo,Qdo,Qbo,Eo,nmonth_
warm,nrow,S_1,G_1)

MSE_Q=0; var_obs_Q=0;
MSE_Qd=0; var_obs_Qd=0;
MSE_Qb=0; var_obs_Qb=0;
MSE_E=0; var_obs_E=0;

%set up initial matrices
Qavg=mean(Qo((nmonth_warm+1):nrow));
Qdavg=mean(Qdo((nmonth_warm+1):nrow));
Qbavg=mean(Qbo((nmonth_warm+1):nrow));
Eavg=mean(Eo((nmonth_warm+1):nrow));

W(nrow)=0;
y(nrow)=0;
E(nrow)=0;
S(nrow)=0;
Q(nrow)=0;
Qb(nrow)=0;
Qd(nrow)=0;
G(nrow)=0;
R(nrow)=0;

%--parameters
a=x(1);
b=x(2);
c=x(3);
d=x(4);

%--initial storage (set by input)
%S_1=b;
%G_1=0;

#####INSERT PARAMETERS AND INITIAL CONDITIONS END

for irow=1:nrow
#####INSERT CODE#####
%cycle begins

W(irow)=P(irow)+S_1;
y(irow)=(W(irow)+b)/(2*a)-(((W(irow)+b)/(2*a))^2-((W(irow)*b)/a))^0.5;
E(irow)=y(irow)*(1-exp(-Ep(irow)/b));
```

```

S(irow)=y(irow)-E(irow);

Qd(irow)=(1-c)*(W(irow)-y(irow));
R(irow)=c*(W(irow)-y(irow));
G(irow)=(1/(1+d))*(R(irow)+G_1);
Qb(irow)=d*G(irow);

Q(irow)=Qb(irow)+Qd(irow);

G_1=G(irow);
S_1=S(irow);

#####INSERT CODE END#####

%----Compute fitness
if irow>nmonth_warm
    %----Q
    MSE_Q=MSE_Q+(Qo(irow)-Q(irow))^2;
    var_obs_Q=var_obs_Q+(Qo(irow)-Qavg)^2;
    %----Qd
    MSE_Qd=MSE_Qd+(Qdo(irow)-Qd(irow))^2;
    var_obs_Qd=var_obs_Qd+(Qdo(irow)-Qdavg)^2;
    %----Qb
    MSE_Qb=MSE_Qb+(Qbo(irow)-Qb(irow))^2;
    var_obs_Qb=var_obs_Qb+(Qbo(irow)-Qbavg)^2;
    %----E (as an additional check)
    MSE_E=MSE_E+(Eo(irow)-E(irow))^2;
    var_obs_E=var_obs_E+(Eo(irow)-Eavg)^2;
end
end
NSE_Q=1-MSE_Q/var_obs_Q;
NSE_Qd=1-MSE_Qd/var_obs_Qd;
NSE_Qb=1-MSE_Qb/var_obs_Qb;
NSE_E=1-MSE_E/var_obs_E;

```

B.7 Script for the abcd Model (Validation based on the Second Calibration Method)

```
function [NSE_Q NSE_Qd NSE_Qb NSE_E S_1
G_1]=abcd_validation_calibrated_initial_conditions(x,P,Ep,Qo,Qdo,Qbo,Eo,nmont
h_warm,nrow,S_1,G_1)

MSE_Q=0; var_obs_Q=0;
MSE_Qd=0; var_obs_Qd=0;
MSE_Qb=0; var_obs_Qb=0;
MSE_E=0; var_obs_E=0;

%set up initial matrices
Qavg=mean(Qo((nmonth_warm+1):nrow));
Qdavg=mean(Qdo((nmonth_warm+1):nrow));
Qbavg=mean(Qbo((nmonth_warm+1):nrow));
Eavg=mean(Eo((nmonth_warm+1):nrow));

%--parameters

a=x(1);
b=x(2);
c=x(3);
d=x(4);

%--initial storage
%S_1=x(2)*x(5);
%G_1=x(6);

#####INSERT PARAMETERS AND INITIAL CONDITIONS END

for irow=1:nrow
#####INSERT CODE#####
%cycle begins

W=P(irow)+S_1;
yy=(W+b)/(2*a)-(((W+b)/(2*a))^2-(W*b)/a)^0.5;
E=yy*(1-exp(-Ep(irow)/b));
S=yy-E;

Qd=(1-c)*(W-yy);
R=c*(W-yy);
G=(1/(1+d))*(R+G_1);
Qb=d*G;

Q=Qb+Qd;

G_1=G;
```



```

S_1=S;

%For some reason this code actually is slower to run (it's not
%that it runs too fast that the process defragments Matlab's
%memory.

#####INSERT CODE END#####

%----Compute fitness
if irow>nmonth_warm
    %----Q
    MSE_Q=MSE_Q+(Qo(irow)-Q)^2;
    var_obs_Q=var_obs_Q+(Qo(irow)-Qavg)^2;
    %----Qd
    MSE_Qd=MSE_Qd+(Qdo(irow)-Qd)^2;
    var_obs_Qd=var_obs_Qd+(Qdo(irow)-Qdavg)^2;
    %----Qb
    MSE_Qb=MSE_Qb+(Qbo(irow)-Qb)^2;
    var_obs_Qb=var_obs_Qb+(Qbo(irow)-Qbavg)^2;
    %----E (as an additional check)
    MSE_E=MSE_E+(Eo(irow)-E)^2;
    var_obs_E=var_obs_E+(Eo(irow)-Eavg)^2;
end
end
NSE_Q=1-MSE_Q/var_obs_Q;
NSE_Qd=1-MSE_Qd/var_obs_Qd;
NSE_Qb=1-MSE_Qb/var_obs_Qb;
NSE_E=1-MSE_E/var_obs_E;

```

REFERENCES

- Alley, W. M. (1984). On the treatment of evapotranspiration, soil moisture accounting, and aquifer recharge in monthly water balance models. *Water Resources Research*, 20(8), 1137-1149.
- Alley, W. M. (1985). Water balance models in one-month-ahead streamflow forecasting. *Water Resources Research*, 21(4), 597-606.
- Arnell, N. W. (1999). A simple water balance model for the simulation of streamflow over a large geographic domain. *Journal of Hydrology*, 217(3), 314-335.
- Block, P. J., Souza Filho, F. A., Sun, L., & Kwon, H. H. (2009). A Streamflow Forecasting Framework using Multiple Climate and Hydrological Models1. *JAWRA Journal of the American Water Resources Association*, 45(4), 828-843.
- Brutsaert, W. (2005). *Hydrology: an introduction*: Cambridge University Press.
- Budyko, M. (1974). Climate and Life, 508. *Academic, San Diego, Calif.*
- Dripps, W., & Bradbury, K. (2007). A simple daily soil–water balance model for estimating the spatial and temporal distribution of groundwater recharge in temperate humid areas. *Hydrogeology Journal*, 15(3), 433-444.
- Duan, Q., Schaake, J., Andreassian, V., Franks, S., Goteti, G., Gupta, H., . . . Hay, L. (2006). Model Parameter Estimation Experiment (MOPEX): An overview of science strategy and major results from the second and third workshops. *Journal of Hydrology*, 320(1), 3-17.

- Duan, Q., Sorooshian, S., & Gupta, V. (1992). Effective and efficient global optimization for conceptual rainfall-runoff models. *Water Resources Research*, 28(4), 1015-1031.
- Duan, Q., Sorooshian, S., & Gupta, V. K. (1994). Optimal use of the SCE-UA global optimization method for calibrating watershed models. *Journal of Hydrology*, 158(3), 265-284.
- Dunne, T., & Leopold, L. (1978). *Water in Environmental Planning*. New York.
- Eckhardt, K. (2005). How to construct recursive digital filters for baseflow separation. *Hydrological Processes*, 19(2), 507-515.
- Farnsworth, R., Thompson, E., & Peck, E. (1982). Evaporation atlas for the contiguous 48 United States. National Oceanic and Atmospheric Administration, National Weather Service: NOAA technical report NWS.
- Fernandez, W., Vogel, R., & Sankarasubramanian, A. (2000). Regional calibration of a watershed model. *Hydrological Sciences Journal*, 45(5), 689-707.
- Fu, B. (1981). On the calculation of the evaporation from land surface. *Sci. Atmos. Sin*, 5(1), 23-31.
- Green, W. H., & Ampt, G. (1911). Studies on soil physics, 1. The flow of air and water through soils. *J. Agric. Sci*, 4(1), 1-24.
- Jakeman, A., & Hornberger, G. (1994). Reply [to “Comment on ‘How much complexity is warranted in a rainfall-runoff model?’ by AJ Jakeman and GM Hornberger”]. *Water Resources Research*, 30(12), 3567-3567.

- Kuczera, G. (1983). Improved parameter inference in catchment models: 2. Combining different kinds of hydrologic data and testing their compatibility. *Water Resources Research*, 19(5), 1163-1172.
- Li, W., & Sankarasubramanian, A. (2012). Reducing hydrologic model uncertainty in monthly streamflow predictions using multimodel combination. *Water Resources Research*, 48(12).
- Linsley, R. K., Franzini, J. B., Freyberg, D. L., & Tchobanoglous, G. (1992). *Water-resources engineering*: McGraw-Hill New York et al.
- Makhlouf, Z., & Michel, C. (1994). A two-parameter monthly water balance model for French watersheds. *Journal of Hydrology*, 162(3), 299-318.
- Martinez, G. F., & Gupta, H. V. (2010). Toward improved identification of hydrological models: A diagnostic evaluation of the “abcd” monthly water balance model for the conterminous United States. *Water Resources Research*, 46(8).
- Nash, J., & Sutcliffe, J. (1970). River flow forecasting through conceptual models part I—A discussion of principles. *Journal of Hydrology*, 10(3), 282-290.
- Palmer, W. C. (1965). *Meteorological drought*: US Department of Commerce, Weather Bureau Washington, DC, USA.
- Pitman, W. (1973). *A mathematical model for generating monthly river flows from meteorological data in South Africa*: University of the Witwatersrand, Department of Civil Engineering, Hydrological Research Unit.

- Pitman, W. (1978). Flow generation by catchment models of differing complexity—A comparison of performance. *Journal of Hydrology*, 38(1), 59-70.
- Potter, N., Zhang, L., Milly, P., McMahon, T., & Jakeman, A. (2005). Effects of rainfall seasonality and soil moisture capacity on mean annual water balance for Australian catchments. *Water Resources Research*, 41(6).
- Sankarasubramanian, A., & Vogel, R. M. (2002). Annual hydroclimatology of the United States. *Water Resources Research*, 38(6), 19-11-19-12.
- Schaake, J. C., Koren, V. I., Duan, Q. Y., Mitchell, K., & Chen, F. (1996). Simple water balance model for estimating runoff at different spatial and temporal scales. *Journal of Geophysical Research: Atmospheres (1984–2012)*, 101(D3), 7461-7475.
- Sivapalan, M., Blöschl, G., Zhang, L., & Vertessy, R. (2003). Downward approach to hydrological prediction. *Hydrological Processes*, 17(11), 2101-2111.
- Snyder, W. M. (1963). A Water Yield Model Derived from Monthly Runoff Data.
- Soil Survey Staff. (2013). U.S. General Soil Map (STATSGO). Retrieved 4/10/2013
<http://sdmdataaccess.nrcs.usda.gov/>
- Stanton, J. S., Qi, S. L., Ryter, D. W., Falk, S. E., Houston, N. A., Peterson, S. M., . . . Christenson, S. C. (2011). Selected Approaches to Estimate Water-Budget Components of the High Plains, 1949 through 1949 and 2000 through 2009. *US Geological Survey, Reston, VA, Scientific Investigations Report, 5183*.
- Thomas, H. (1981). Improved methods for national water assessment. *Report WR15249270, US Water Resource Council, Washington, DC*.

- Thomas, H., Marin, C., Brown, M., & Fiering, M. (1983). Methodology for water resource assessment, report to US Geological Survey. *Rep. NTIS*, 84-124163.
- Thornthwaite, C., & Mather, J. (1955). *The Water Balance* (Vol. 8). Centerton, NJ: Drexel Institute of Technology-Laboratory of Climatology.
- Thornthwaite, C., & Mather, J. (1957). Instructions and tables for computing potential evapotranspiration and the water balance.
- Thornwaite, C. (1944). Report of the Committee on Transpiration and Evaporation. *Trans. Amer. Geophys. Union*, 25, 683-693.
- Thornwaite, C. (1948). An approach toward a rational classification of climate. *Geographical review*, 38(1), 55-94.
- US Geological Survey. (2011). Gap Analysis Program (GAP).
<http://dingo.gapanalysisprogram.com/landcoverv2/>
- US Geological Survey. (2014a). *U.S. Geological Survey Water-Data Report WDR-US-2013, site 02143500*. Retrieved from <http://wdr.water.usgs.gov/wy2013/pdfs/02143500.2013.pdf>.
- US Geological Survey. (2014b). *U.S. Geological Survey Water-Data Report WDR-US-2013, site 08171300*. Retrieved from <http://wdr.water.usgs.gov/wy2013/pdfs/08171300.2013.pdf>.
- USDA, S. (1972). National Engineering Handbook, Section 4: Hydrology. *Washington, DC*.
- Vandewiele, G., & Elias, A. (1995). Monthly water balance of ungauged catchments obtained by geographical regionalization. *Journal of Hydrology*, 170(1), 277-291.

- Vandewiele, G., Xu, C.-Y., & Win, N.-L. (1992). Methodology and comparative study of monthly water balance models in Belgium, China and Burma. *Journal of Hydrology*, 134(1), 315-347.
- Walter, M. T. (2005a). Infiltration Excess Overland Flow. 2014, from http://soilandwater.bee.cornell.edu/research/VSA/processes/processes_infil.html
- Walter, M. T. (2005b). Saturation Excess Overland Flow. 2014, from http://soilandwater.bee.cornell.edu/research/VSA/processes/processes_sat.html
- Wang, D., & Tang, Y. (2014). A Commonality of Hydrologic Models Across Temporal Scales. (submitted).
- Wang, G., Xia, J., & Chen, J. (2009). Quantification of effects of climate variations and human activities on runoff by a monthly water balance model: A case study of the Chaobai River basin in northern China. *Water Resources Research*, 45(7).
- Wang, Q., Pagano, T., Zhou, S., Hapuarachchi, H., Zhang, L., & Robertson, D. (2011). Monthly versus daily water balance models in simulating monthly runoff. *Journal of Hydrology*, 404(3), 166-175.
- Xu, C.-Y., & Singh, V. (1998). A review on monthly water balance models for water resources investigations. *Water Resources Management*, 12(1), 20-50.
- Zhang, K. (2010). Remote Sensing (RS) GIMMS NDVI Based Daily ET and Monthly PET for Continental US (CONUS) from 1983 to 2006. from Numerical Terradynamic Simulation Group, University of Montana ftp://ftp.ntsg.umt.edu/pub/data/CONUS_ET/

Zhang, L., Potter, N., Hickel, K., Zhang, Y., & Shao, Q. (2008). Water balance modeling over variable time scales based on the Budyko framework—Model development and testing. *Journal of Hydrology*, 360(1), 117-131.